



Room 14-0551
77 Massachusetts Avenue
Cambridge, MA 02139
Ph: 617.253.5668 Fax: 617.253.1690
Email: docs@mit.edu
<http://libraries.mit.edu/docs>

DISCLAIMER OF QUALITY

Due to the condition of the original material, there are unavoidable flaws in this reproduction. We have made every effort possible to provide you with the best copy available. If you are dissatisfied with this product and find it unusable, please contact Document Services as soon as possible.

Thank you.

Author miss-numbered some pages.
Page numbers for page 103 & 104
are repeated. Numbering goes back
to normal at page 150. Author
skipped pages 151-152.

Distal Hydrogen-Bonding Effects and Cofacial Bimetallic Salen Architectures for Oxygen Activation Chemistry

Jenny Yue-fon Yang

B. S., University of California, Berkeley (2001)

Submitted to the Department of Chemistry
In Partial Fulfillment of the Requirements

For the Degree of

DOCTOR OF PHILOSOPHY IN INORGANIC CHEMISTRY

at the

MASSACHUSETTS INSTITUTE OF TECHNOLOGY

April 2007

[June 2007]

© 2007 Massachusetts Institute of Technology. All rights reserved.

Signature of Author: _____

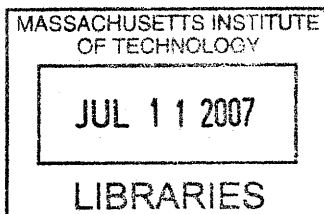
Department of Chemistry
April, 2007

Certified by: _____

Daniel G. Nocera
W. M. Keck Professor of Energy and Professor of Chemistry
Thesis Supervisor

Accepted by: _____

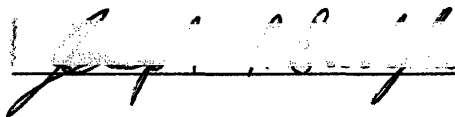
Robert W. Field
Haslam and Dewey Professor of Chemistry
Chairman, Department Committee on Graduate Studies



ARCHIVED

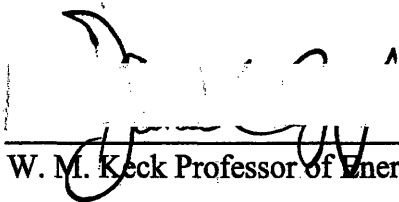
This doctoral thesis has been examined by a Committee of the Department of Chemistry as follows:

Professor Joseph P. Sadighi



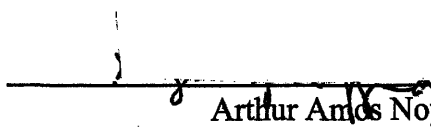
Professor of Chemistry
Chairman

Professor Daniel G. Nocera



W. M. Keck Professor of Energy and Professor of Chemistry
Thesis Supervisor

Professor Stephen J. Lippard



Arthur Amos Noyes Professor of Chemistry

To my family

Distal Hydrogen-Bonding Effects and Cofacial Bimetallic Salen Architectures for Oxygen Activation Chemistry

By Jenny Yue-fon Yang

Submitted to the Department of Chemistry
on April 18, 2007 in partial fulfillment of
the requirements for the degree of
Doctor of Philosophy in Inorganic Chemistry

Abstract

Two distinct structural scaffolds elaborated from Schiff-base macrocycles were designed to study the proton-coupled electron transfer chemistry of O—O bond forming and activation chemistry. The “Hangman” architecture is composed of hydrogen-bonding functionalities poised over a redox active manganese salophen or salen platform. The complexes proved to be proficient catalase mimics (disproportionation of hydrogen peroxide to water and oxygen). Detailed spectroscopic, computational, and structure-function relationship studies elucidated the key redox, steric, and secondary coordination sphere effects for optimal catalytic ability. The incorporation a chiral backbone into the macrocycle led to catalysts that perform enantioselective epoxidation of unfunctionalized olefins. A macrocycle with an amide, imine, and bisphenolic functionalities was also incorporated as the redox platform in the Hangman framework; the manganese complex also performed catalytic oxygen atom transfer to olefins. The second framework, dubbed “Pacman”, is composed of two salen platforms linked cofacially by rigid pillars xanthene or dibenzofuran. A series of bimetallic complexes, including chromium, iron, manganese, cobalt, copper, and zinc were generated. Mossbauer spectroscopy was used in the characterization of the iron salen complexes, which were also examined for photolytic oxidation chemistry.

Thesis supervisor: Daniel G. Nocera
W. M. Keck Professor of Energy and Professor of Chemistry

Table of contents

| | |
|--|-----------|
| Title page | 1 |
| Thesis Committee | 2 |
| Dedication | 3 |
| Abstract | 5 |
| | |
| Table of contents | 7 |
| List of Figures | 12 |
| List of Schemes | 17 |
| List of Charts | 19 |
| List of Tables | 20 |
| List of abbreviations | 23 |
| | |
| Chapter 1 Introduction | 25 |
| 1. Proton-Coupled Electron Transfer in Nature | 26 |
| 2. Proton-Coupled Electron Transfer in Synthetic Systems | 27 |
| 3. Photolytic Generation of Metal Oxo Species | 29 |
| 4. Schiff-base Macrocycles as Redox Platforms | 20 |
| 5. References | 32 |
| | |
| Chapter 2 Hangman Salophen Mediated Activation of O—O Bonds: Mechanistic Insights | 39 |
| 1. Motivation and Specific Aims | 40 |
| 2. Background | 40 |
| 3. Results and Discussion | 42 |
| 3.1. Synthesis | 42 |
| 3.2. Stop-Flow Spectroscopy | 43 |
| 3.3. Decomposition in the Presence of Hydrogen Peroxide | 47 |
| 3.4. Mechanistic Implications | 47 |
| 3.5. Generation of Manganese Salophen Oxo with Hydrogen Peroxide | 50 |
| 4. Concluding Remarks | 53 |

Contents

| | | |
|--|---|------------|
| 5. | Experimental | 53 |
| 5.1 | General Methods | 53 |
| 5.2. | Physical Methods | 54 |
| 5.3. | Synthesis | 54 |
| 5.4. | Stop-Flow Kinetic Studies | 58 |
| 5.5. | Hydrogen Peroxide Disproportionation Reactions | 59 |
| 5.6. | Independent Generation of High-Valent Mn(V) oxo | 60 |
| 6. | References and Notes | 62 |
| Chapter 3 Synthesis of Enantiopure Manganese Hangman Salens and Their Epoxidation Activity | | 65 |
| 1. | Motivation and Specific Aims | 66 |
| 2. | Background | 66 |
| 3. | Results and Discussion | 67 |
| 3.1. | Ligand Design | 67 |
| 3.2. | Synthesis of Hangman Salen Ligands (HSX*) | 68 |
| 3.3. | Synthesis of Benzoic Acid Functionalized Hangman Salen Ligands (H _{ph} SX*) | 72 |
| 3.4. | Epoxidation Activity of Manganese Hangman Salens | 75 |
| 3.5. | Design of Sterically Protected Hangman Salens | 75 |
| 3.6. | Synthesis of Mn[HSX* ^t Bu]Cl and Mn[H _{ph} SX* ^t Bu]Cl | 77 |
| 3.7. | Epoxidation Activity of Sterically Protected Manganese Hangman Salens | 78 |
| 3.8. | Mechanistic Implications | 79 |
| 4. | Concluding remarks | 80 |
| 5. | Experimental Section | 81 |
| 5.1. | Materials | 81 |
| 5.2. | Physical Measurements | 82 |
| 5.3. | Synthesis | 82 |
| 5.4. | Epoxidation of 1,2-Dihydronaphthalene | 97 |
| 5.5. | X-Ray Crystal Data Collection and Refinement Parameters | 98 |
| 6. | References | 102 |
| Chapter 4 Catalase Activity and Epoxidation of Functionalized Olefins by Manganese Hangman Salens | | 105 |

Contents

| | | |
|---|--|------------|
| 1. | Motivation and Specific Aims | 106 |
| 2. | Background | 106 |
| 3. | Results and Discussion | 107 |
| 3.1. | Synthesis | 107 |
| 3.2. | Catalase Activity of Manganese Hangman Salen Complexes | 109 |
| 3.3. | Mechanistic Insights | 111 |
| 3.4. | Synthesis of Methyl Esters of Sterically Protected Manganese Hangman Salen Complexes | 113 |
| 3.5. | Catalase Activity of Sterically Protected Manganese Hangman Salen Complexes | 114 |
| 3.6. | Mechanistic Insights into Steric Protection | 115 |
| 3.7. | Density Functional Theory of Manganese Hydroperoxide Hangman Salen Complexes | 116 |
| 3.8. | Acid to Metal Distance Effects | 119 |
| 3.9. | Synthesis of Dibenzofuran Analogues of Manganese Hangman Salens | 119 |
| 3.10. | Density Functional Theory of Dibenzofuran Analogues of Manganese Hangman Salens | 121 |
| 3.11. | Catalase Activity: Acid to Metal Distance Effects | 122 |
| 3.12. | Epoxidation of Functionalized Olefins | 124 |
| 4. | Conclusions and Future Work | 126 |
| 5. | Experimental Section | 128 |
| 5.1. | Materials | 128 |
| 5.2. | Physical Measurements | 129 |
| 5.1. | Synthesis | 129 |
| 5.2. | Hydrogen Peroxide Disproportionation Reactions | 143 |
| 5.1. | Epoxidation of Functionalized Olefins | 144 |
| 5.2. | Density Functional Theory Calculations | 145 |
| 7. | References | 148 |
| Chapter 5 Synthesis of Amido-Imine Macrocyclic Ligands | | 153 |
| 1. | Motivation and Specific Aims | 154 |
| 2. | Background | 154 |
| 3. | Results and Discussion | 155 |

Contents

| | | |
|--|--|------------|
| 3.1. | Synthetic Attempts towards a Hangman Salen Bearing a Single Functionalized Xanthene Scaffold | 155 |
| 3.2. | Design and Synthesis of Amido-Imine Macrocycles and Manganese Complexes | 156 |
| 3.2. | Epoxidation Activity of Manganese Complexes | 158 |
| 4. | Concluding Remarks | 158 |
| 5. | Experimental Section | 159 |
| 5.1. | Materials | 159 |
| 5.2. | Physical Methods | 159 |
| 5.3. | Synthesis | 160 |
| 5.3. | Epoxidation Measurements | 167 |
| 6. | References | 168 |
| Chapter 6 Synthesis of Cofacial Pacman Salen Architectures and Their Iron Complexes | | 171 |
| 1. | Motivation and Specific Aims | 172 |
| 2. | Background | 172 |
| 3. | Results and Discussion | 174 |
| 3.1. | Ligand Design | 174 |
| 3.2. | Synthesis of DiSalen Xanthene Ligand (DSX) | 175 |
| 3.3. | Synthesis of DiSalen Dibenzofuran Ligand (DSD) | 178 |
| 3.4. | Synthesis of Ferric Chloride Complexes | 180 |
| 3.5. | Synthesis of Diiron μ -oxo Complexes | 181 |
| 3.6. | Synthesis of Ferrous Complexes | 182 |
| 3.7. | ^{57}Fe Mössbauer Spectroscopy of Iron Complexes | 183 |
| 3.8. | Photolysis Studies of Iron Complexes | 186 |
| 4. | Concluding remarks | 187 |
| 5. | Experimental Section | 188 |
| 5.1. | Materials | 188 |
| 5.2. | Physical Measurements | 188 |
| 5.3. | Synthesis | 189 |
| 5.4. | Photolysis Studies | 195 |
| 5.5. | X-Ray Crystal Data Collection and Refinement Parameters | 196 |
| 6. | References | 201 |

| | |
|--|------------|
| Chapter 7. Synthesis of Bimetallic Cofacial Pacman Salens | 207 |
| 1. Motivation and Specific Aims | 208 |
| 2. Background | 208 |
| 3. Results and Discussion | 209 |
| 3.1. Ligand Characteristics and Synthesis | 209 |
| 3.2. Synthesis of Chromium Pacman Complexes | 209 |
| 3.3. Epoxide Ring Opening with Chromium Pacman Complexes | 210 |
| 3.4. Synthesis of Copper Pacman Complexes | 210 |
| 3.5. Synthesis of Manganese, Cobalt, and Zinc Pacman Complexes | 211 |
| 4. Concluding Remarks and Future Work | 212 |
| 5. Experimental Section | 212 |
| 5.1. Materials | 212 |
| 5.2. Physical Measurements | 213 |
| 5.3. Synthesis | 213 |
| 5.4. Epoxide Ring Opening Studies | 217 |
| 6. References | 219 |
| Appendix | 221 |
| A. Reaction Setup for Measuring Catalase Activity | 222 |
| B. Alternative Synthetic Procedures | 223 |
| B.1. From Chapter 3 | 223 |
| B.2. From Chapter 5 | 225 |
| C. Density Functional Theory Calculations | 228 |
| C.1. Input File and Output Coordinates for the hydroperoxide complex of Mn(HSX*) | 228 |
| C.2. Input File and Output Coordinates for the hydroperoxide complex of Mn(H _{ph} SX*) with carboxylic acid dimers. | 233 |
| C.3. Input File and Output Coordinates for the hydroperoxide complex of Mn(HSD*) | 239 |
| C.4. Input File and Output Coordinates for the hydroperoxide complex of Mn(H _{ph} SD*) | 244 |
| Acknowledgements | 249 |
| Biographical note | 252 |
| Curriculum vitae | 253 |

List of Figures

Chapter 1

- Figure 1.1. Representation of the active sites (a) peroxidases, (b) catalases, and (c) cytochrome P450 monooxygenases highlighting the proposed roles distal residues play in O—O bond cleavage.
- Figure 1.2. Proposed catalytic cycle of the catalase-like disproportionation of hydrogen peroxide by iron (HPX-CO₂H) and epoxidation by manganese (HPX-CO₂H).
- Figure 1.3. Proposed catalytic cycle for the photolytic oxidation catalysis performed by diiron Pacman porphyrin complexes, and summary of substrates and turnover numbers observed.

Chapter 2

- Figure 2.1. Reaction profiles of O₂ evolution over time from the dismutation of H₂O₂ from manganese Hangman salophen catalysts with X = OMe (□), Br (◇), H (○), *t*-Butyl (Δ), and NO₂ (●).
- Figure 2.2. (a) Stopped-flow UV-vis spectra obtained from reaction of *m*-CPBA (3.3×10^{-4}) with 4.0×10^{-5} M **1** (red solid line) ca. 3 s post injection in 1:1 MeOH:MeCN at -20 °C. (b) UV-vis spectrum obtained from a solution of 5.0×10^{-5} M **1** in MeOH:MeCN at room temperature (red solid line). UV-vis spectrum obtained from a solution of 5.0×10^{-5} M **1** in 1:1 MeOH:MeCN at room temperature in the presence of benzoic acid (5.0×10^{-3} M) (black dotted line).
- Figure 2.3. (a) Absorption spectra obtained from spectral global analysis of a stopped-flow reaction of 4.0×10^{-5} M **1** and 3.3×10^{-4} M *m*-CPBA in 1:1 MeOH:MeCN at -20 °C. Formation of Mn(V) oxo (green solid line) is immediately followed by a bleach, likely to a Mn^{III} decay product (red solid line) over 800 s. (b) Calculated concentrations of the colored species with respect to time by spectral global analysis by Jake Soper.
- Figure 2.4. Observation of a common oxidized Hangman salophen intermediate by treating Mn[HSX(OMe)-COOH]Cl (**1**) with three different oxidants: (a) hydrogen peroxide, (b) *m*-CPBA, (c) iodosylbenzene.

- Figure 2.5. Studying high-valent Mn-salophens: (a) comparison of the UV-Vis spectra of Mn-oxo complexes derived from Mn[salophen(*t*-bu)] and Mn[salophen(OMe)], respectively; (b) comparison of the UV-Vis spectra of Mn(V)-nitrido complexes derived from Mn[salophen(*t*-bu)] and Mn[salophen(OMe)], respectively.
- Figure 2.6. Reaction of Mn-oxo with a reductant leads to the regeneration of the Mn(III) starting material.

Chapter 3

- Figure 3.1. Potential approaches of an olefin to Jacobsen's Catalyst. The high valent oxo bound to the manganese (not shown) is perpendicular to and coming out of the page.
- Figure 3.2. Thermal ellipsoid plot of 5-(boronic acid)-2,7-di-*tert*-butyl-9,9-dimethyl-9H-xanthene-4-carboxylic acid methyl ester (**3**). Thermal ellipsoids are drawn at the 50% probability level.
- Figure 3.3. Thermal ellipsoid plot of 2,7-di-*tert*-butyl-5-(3-formyl-4-hydroxyphenyl)-9,9-dimethyl-9H-xanthene-4-carboxylic acid (**5**). Thermal ellipsoids are drawn at the 50% probability level.
- Figure 3.4. Thermal ellipsoid plot of 4-Bromo-2,7-di-*tert*-butyl-9,9-dimethyl-5-(4-hydroxyborane)-9H-xanthene (**19**). Thermal ellipsoids are drawn at the 50% probability level.

Chapter 4

- Figure 4.1. Turnover number (TON) of hydrogen peroxide dismutation catalyzed by manganese compounds [Mn(5-phsalen)Cl] (**13**) (**13*** in the presence of 2 equivalents of benzoic acid), Mn[HSX*-COOH]Cl, Mn[HSX*-COOMe]Cl (**9**), Mn[H_{ph}SX*-COOH]Cl and Mn[H_{ph}SX*-COOMe]Cl (**10**) after 1 hour.
- Figure 4.2. Oxygen release from hydrogen peroxide dismutation catalyzed by manganese compounds Mn(5-phsalen)Cl] (**13**) (□), **13*** (*in the presence of 2 equivalents of benzoic acid) (◇), Mn[HSX*-COOH]Cl (●), Mn[HSX*-COOMe]Cl (**9**) (×), Mn[H_{ph}SX*-COOH]Cl (◆), and Mn[H_{ph}SX*-COOMe]Cl (**10**) (○) over 1 hour. Inset shows reaction profile for the first five minutes excluding the methyl ester compounds **9** and **10**.

Contents

- Figure 4.3. Turnover number (TON) of hydrogen peroxide dismutation catalyzed by manganese compounds Mn(salen)Cl, Mn(salen)Cl in the presence of 2 equivalents of benzoic acid), Mn[HSX*^tBu-COOH]Cl, Mn[HSX*^tBu-COOMe]Cl (**18**), Mn[H_{ph}SX*^tBu -COOH]Cl and Mn[H_{ph}SX*^tBu-COOMe]Cl (**19**) after 1 hour.
- Figure 4.4. Energy minimized structure obtained from DFT of the hydroperoxide complexes of Mn(HSX*-COOH), showing one of the carboxylic acids is hydrogen bonded to the oxygen on the xanthene scaffold, while the other is hydrogen bonded to the hydroperoxide.
- Figure 4.5. Energy minimized structure obtained from DFT of the hydroperoxide complexes of Mn(H_{ph}SX*-COOH) showing the two carboxylic acids span the face of the salen macrocycle to make a -(COOH)₂- dimer that interacts with the hydroperoxide via a hydrogen bond.
- Figure 4.6. Energy minimized structure obtained from DFT of the hydroperoxide complexes of Mn(H_{ph}SX*-COOH) with the xanthenes splayed away from each other, precluding formation of the -(COOH)₂- dimer. Each of the carboxylic acids has a hydrogen-bonding interaction with the hydroperoxide.
- Figure 4.7. Energy-minimized structures obtained from DFT of the hydroperoxide complex Mn[HSD*^tBu]OOH.
- Figure 4.8. Energy-minimized structures obtained from DFT of the hydroperoxide complex Mn[HphSD*^tBu]OOH.

Chapter 5

- Figure 5.1. Equilibrium representing the exchange reaction that produces symmetric impurities when salens containing two unique phenolate arms undergo hydrolysis. The two unique salicylaldehyde components are represented in blue (dashed) and red (solid).
- Figure 5.2. ¹H NMR of compound **17**.
- Figure 5.3. ¹H NMR spectra of compound **19**.

Chapter 6

- Figure 6.1. Variable temperature ¹H NMR spectra of DiSalen Xanthene ligand (**4**) from room temperature (20 °C) to -60 °C, taken in 10 °C intervals.

- Figure 6.2. X-Ray crystal structure of DiSalen Xanthene (**8**). Crystals were grown from slow evaporation of a pentane-dichloromethane solution. Carbons are depicted as gray, oxygens as red, and nitrogens as blue. H atoms are omitted for clarity.
- Figure 6.3. X-Ray crystal structure of DSD impurity. Crystals were grown out of a pentane-dichloromethane solution. Carbons are depicted as gray.
- Figure 6.4. X-Ray crystal structure of the unpillared $\text{Fe}_2(\text{salen})_2\text{O}$ (**15**). Crystals were grown from a pentane-dichloromethane solution. The angle of the Fe-O-Fe bond is $165.2(7)^\circ$, and the salens are by rotated 124.5° with respect to each other.
- Figure 6.5. Infrared spectra displaying the fingerprint region of Fe_2DSXO (**13**), Fe_2DSDO (**14**), and $\text{Fe}_2(\text{salen})_2\text{O}$ (**15**), highlighting the imine (C=N) and Fe-O-Fe bond stretch.
- Figure 6.6. Fitted ^{57}Fe Mössbauer spectra of (a) $\text{Fe}_2\text{DSXCl}_2$ (**10**), (b) $\text{Fe}_2\text{DSDCl}_2$ (**11**), (c) $\text{Fe}(\text{salen})\text{Cl}$ (**12**) at 4.2 K. Gray dots represent the experimental data points and the black solid line represents the fit. The vertical axis is an arbitrary transmission scale.
- Figure 6.7. Fitted ^{57}Fe Mössbauer spectra of (a) Fe_2DSXO (**13**), (b) Fe_2DSDO (**14**), (c) $\text{Fe}_2(\text{salen})_2\text{O}$ (**15**) at 4.2 K. Gray dots represent the experimental data points and the black solid line represents the fit. The vertical axis is an arbitrary transmission scale.
- Figure 6.8. Fitted ^{57}Fe Mössbauer spectra of (a) Fe_2DSX (**16**), (b) Fe_2DSD (**17**), (c) $\text{Fe}(\text{salen})$ (**18**) at 4.2 K. Gray dots represent the experimental data points and the solid black line represents the fit. The vertical axis is an arbitrary transmission scale.
- Figure 6.9. UV-vis absorption profiles of 30 μmol solutions of $\text{Fe}_2\text{DSXCl}_2$ (**13**) (---), $\text{Fe}_2\text{DSDCl}_2$ (**14**) (···), and $\text{Fe}_2(\text{salen})_2\text{O}$ (**15**) (—) in acetonitrile. The spectra is scaled to molar absorbtivity.
- Figure 6.10. X-Ray crystal structure of 4,6-(4,4,5,5-Tetramethyl-[1,3,2]dioxaborolan-2-yl)-dibenzofuran (**6**).

Chapter 7

- Figure 7.1. EPR spectra of compound **11** taken a chloroform-ethanol frozen solution at 4.5 K.

Appendix

Figure A.1. Reaction setup for measuring catalase activity.

List of Schemes

Chapter 1

Scheme 1.1. Hangman Architecture

Chapter 2

Scheme 2.1. Synthesis

Scheme 2.1. Proposed catalytic cycle for iron Hangman porphyrin and manganese Hangman salophen compounds. The porphyrin compounds are indicated in green, and the salophen in black. The catalase reaction is represented in blue. The stop-flow kinetic studies were performed using the red reagents, as well as the rates that can be determined using the double-mixing setup.

Chapter 3

Scheme 3.1. Synthesis

Scheme 3.2. Synthesis

Scheme 3.3. Synthesis

Scheme 3.4. Synthesis

Scheme 3.5. Synthesis

Scheme 3.6. Synthesis

Scheme 3.7. Synthesis

Scheme 3.8. Proposed catalytic cycle for substrate oxidation by a Hangman catalyst, highlighting the potential interaction of the carboxylic acid functionality with the external oxidant O-X

Chapter 4

Scheme 4.1. Synthesis

Scheme 4.2. Synthesis

Scheme 4.3. Proposed catalytic cycle for the dismutation of hydrogen peroxide by manganese salens, highlighting substrate assembly by the hanging groups to facilitate oxidation

Contents

Scheme 4.4. Synthesis

Scheme 4.5. Synthesis

Scheme 4.1. Proposed interaction between a functionalized olefin and the high valent metal oxo of a Hangman salen complex

Scheme 4.1. Synthesis

Chapter 5

Scheme 5.1. Synthesis

Scheme 5.2 Synthesis

Scheme 5.3 Synthesis

Chapter 6

Scheme 6.1. Proposed catalytic cycle in the photocatalytic oxidation chemistry of diiron μ -oxo Pacman porphyrin complexes.

Scheme 6.2 Synthesis

Scheme 6.3 Synthesis

Chapter 7

Scheme 7.1. Proposed bimetallic intermediate in the nucleophilic epoxide ring opening reactions catalyzed by metallosalens.

Appendix

Scheme B2.1. Synthesis

List of Charts

Chapter 1

- Chart 1.1. Porphyrins and Schiff-base Macrocycles

Chapter 2

- Chart 2.1. Hangman Salophen Architecture and PCET
Chart 2.2. Manganese Hangman Salophens
Chart 2.3. Manganese Salophens

Chapter 3

- Chart 3.1. Jacobsen's Catalyst and Epoxidation
Chart 3.2. Hangman Salens
Chart 3.3. Sterically Protected Hangman Salens

Chapter 4

- Chart 4.1. Dibenzofuran Analogues of Hangman Salens

Chapter 5

- Chart 5.1. Hangman Salen Architecture and Salient Features

Chapter 6

- Chart 6.1. Xanthene and Dibenzofuran Pillared Pacman Salen Ligands
Chart 6.2. Iron Complexes

Chapter 7

- Chart 7.1. Summary of Pacman Ligands and Prepared Complexes

List of Tables**Chapter 2**

- Table 2.1. Redox potential of manganese (HSX) chloride compounds with varying X functionalities in the 5 and 5' position, observed LMCT band in the UV-visible spectrum, and the amount of time after injection that half of 4388 equivalents of H₂O₂ was measured to be consumed by monitoring the amount of oxygen evolved
- Table 2.2. Rates of the formation of Mn(V) oxo intermediates and their decay for a series of Mn[salophen(X)] peroxyacid complexes
- Table 2.3. Stability of Methoxy-Substituted Manganese Salophen Complexes
- Table 2.4. Stopped-Flow Kinetic Studies on the Formation of Mn(V)-oxo Intermediates

Chapter 3

- Table 3.1. Turnover numbers (TON) for epoxidation of 1,2-dihydronaphthalene in dichloromethane
- Table 3.2. Crystal data and structure refinement for 5-(boronic acid)-2,7-di-*tert*-butyl-9,9-dimethyl-9H-xanthene-4-carboxylic acid methyl ester (**3**).
- Table 3.3. Crystal data and structure refinement 2,7-di-*tert*-butyl-5-(3-formyl-4-hydroxy-phenyl)-9,9-dimethyl-9H-xanthene-4-carboxylic acid (**5**).

Chapter 4

- Table 4.1. Observed turnover number (TON) and initial rate constant (k_i) for Catalase-like H₂O₂ disproportionation catalyzed by manganese catalysts in 2: 1 dichloromethane/methanol at 25° C.
- Table 4.2. Total bond energies of calculated manganese Hangman salen compounds.
- Table 4.3. Observed Turnover Number (TON) for H₂O₂ Disproportionation by Manganese Hangman Catalysts over one hour.

Contents

Table 4.4 Analysis of products and turnover numbers (TON) for epoxidation reactions as determined using GC/MS with 4-acetoxystyrene (R = H) and 2,2-dimethyl-propionic acid 4-vinyl-phenyl ester (R = *t*-bu) over 1 and 3 hours, using sodium hypochlorite as the oxidant.

Table 4.5 Selected bond distance parameters from DFT calculated energy minimized structures of the hydroperoxide complexes of manganese Hangman salen compounds.

Chapter 6

Table 6.1. Summary of Mössbauer parameters for compounds **10 - 18** recorded at 4.2 K. δ is relative to elemental iron. All samples were measured in the solid state (powdered). Γ is the half-width at half-maximum of the peaks, and the value presented is the same for both peaks.

Table 6.2 Crystal data and structure refinement for DSX (**4**).

Table 6.3 Crystal data and structure refinement for 4,6-(4,4,5,5-Tetramethyl-[1,3,2]dioxaborolan-2-yl)-dibenzofuran (**6**).

Table 6.4 Crystal data and structure refinement for structure shown in Figure 6.3.

Table 6.5 Crystal data and structure refinement for structure shown in Figure 6.4.

Appendix

Table C.1 Cartesian coordinates from the DFT calculated energy minimized structure of the hydroperoxide complex of Mn(HSX*). The structure is shown in Figure 4.4.

Table C.2 Cartesian coordinates from the DFT calculated energy minimized structure of the hydroperoxide complex of Mn(H_{ph}SX*) with the xanthenes oriented so the carboxylic acids can form a hydrogen bonded dimer. The structure is shown in Figure 4.5.

Table C.3 Cartesian coordinates from the DFT calculated energy minimized structure of the hydroperoxide complex of Mn(HSD*). The structure is shown in Figure 4.7.

Contents

Table C.4 Cartesian coordinates from the DFT calculated energy minimized structure of the hydroperoxide complex of Mn(H_{ph}SD*). The structure is shown in Figure 4.8.

List of Abbreviations

| | |
|--------------|------------------------------------|
| Ac | acetate |
| ADF | Amsterdam Density Functional |
| anal | analytical |
| bn | benzyl |
| BSA | bovine serum albumin |
| Bu | butyl |
| C | Celsius |
| calcd | calculated |
| CcO | Cytochrome <i>c</i> Oxidase |
| cm | centimeter |
| Cy | cyclohexane |
| DCC | 3-dicyclohexylcarbodiimide |
| DFT | Density functional theory |
| DMAP | 4-dimethylaminopyridine |
| DME | dimethoxyethane |
| DMF | dimethylformamide |
| DMS | dimethyl sulfide |
| DMSO | dimethyl sulfoxide |
| dppf | (diphenylphosphino)ferrocene |
| ee | enantiomeric excess |
| EPR | electron paramagnetic spectroscopy |
| ΔE_Q | quadrupole splitting value |
| ESI | electrospray ionization |
| Et | ethyl |
| exec | excitation |
| FG | functional group |
| FT | fourier transform |
| g | gram |
| GC | gas chromatography |
| GGA | generalized gradient approximation |
| HRMS | high resolution mass spectroscopy |
| Hz | hertz |
| init | initial |
| <i>i</i> -Pr | <i>iso</i> -propyl |
| IR | infrared |
| K | Kelvin |
| kJ | kilojoule |

Contents

| | |
|----------------|----------------------------------|
| LMCT | ligand to metal charge transfer |
| lwp | long wavelength pass |
| M | molar |
| max | maximum |
| Mb | myoglobin |
| <i>m</i> -CPBA | <i>m</i> -chloroperbenzoic acid |
| mg | milligram |
| Me | methyl |
| MeCN | acetonitrile |
| mL | milliliter |
| MeOH | methanol |
| MHz | megahertz |
| mm | millimeter |
| mM | milimolar |
| mmol | milimol |
| MS | mass spectroscopy |
| nm | nanometer |
| NMR | nuclear magnetic resonance |
| OAT | oxygen atom transfer |
| OEC | Oxygen Evolving Complex |
| OMe | methoxy |
| PCET | proton-coupled electron transfer |
| Ph | phenyl |
| PSII | Photosystem II |
| ROS | reactive oxygen species |
| S | spin state |
| SOD | Superoxide dismutase |
| t | temperature |
| T | time |
| <i>t</i> -Bu | <i>tert</i> -butyl |
| THF | tetrahydrofuran |
| TON | turnover number |
| TMP | tetramesitylporphyrin |
| TS | transition state |
| UV-vis | ultraviolet-visible |
| v | volume |

Chapter 1

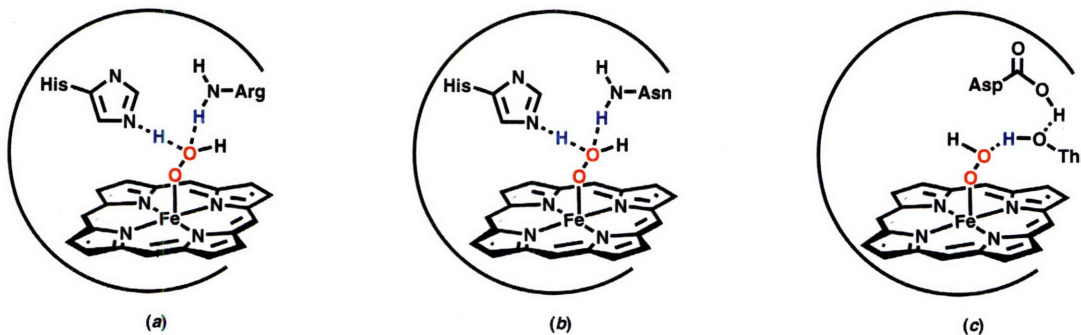
Introduction

1.1 Proton Coupled Electron Transfer in Nature

The principal theme of the research presented is the elucidation of mechanistic details in the coupled transport of both protons and electrons in bond-making and bond-breaking catalysis.¹⁻⁴ This is a recurring theme throughout a broad range of natural systems that encompass a diverse range of reactivity. Consummate examples are the four electron oxidation of water to oxygen by Photosystem II (PSII),⁵⁻⁹ and its microscopic reverse, the reduction of oxygen to water by cytochrome *c* oxidase (CcO),¹⁰⁻¹⁷ which highlights our interests in O—O bond chemistry.

While electron transfer at active sites is typically regulated via a transition metal platform or cluster, proton transfer is mediated through non-covalent hydrogen-bonding interactions in the secondary coordination sphere. A prototypical example of the dual importance of electron and proton control by structure and function can be found in heme-dependent hydroperoxidases.¹⁸⁻²² A ferric protoporphyrin IX prosthetic group is found at the active site of peroxidases, catalases, and the cytochrome P450 monooxygenases, as shown in Figure 1.1. Structurally oriented acidic or basic amino acid residues and/or locally hydrogen bonded water assist O—O bond cleavage of hydrogen peroxide in peroxidases and catalases, and oxygen in the cytochrome P450 monooxygenases. These interactions on the distal oxygen, frequently characterized as the “pull effect”,¹⁸⁻²² promote heterolytic bond cleavage to form the two electron oxidized Compound I intermediate,²⁰⁻²⁴ as opposed to the one electron oxidized Compound II

Figure 1.1 Representation of the active sites (a) peroxidases, (b) catalases, and (c) cytochrome P450 monooxygenases highlighting the proposed roles distal residues play in O-O bond cleavage. Adapted from reference 67.



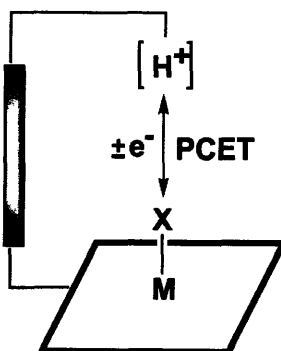
species that results from homolytic bond cleavage. The reactivity of the of Compound I species in these subclasses then diverge; peroxidases tend to behave as one electron oxidants,^{22,25,26} while catalases are selective in their reactivity towards the two electron oxidation of hydrogen peroxide,^{22,26-28} and cytochrome P450 monooxygenases perform two electron oxygen atom transfer chemistry to a variety of substrates.¹⁹ The tuned microenvironment guides proton and electron delivery within the active site, assisting in O—O bond activation, and the subsequent chemistry of the oxidizing intermediate.

The importance of this microenvironment has successfully been demonstrated by modifying natural enzymes. By adjusting the distance and position of distal residue(s) over the heme environment in the oxygen carrier myoglobin (Mb), peroxidase, catalase, or enantioselective monooxygenase activity is observed.^{18,29-47} Additionally, the effect of the redox environment has been studied independently by inserting unnatural redox cofactors to generate artificial metalloenzymes.⁴⁸⁻⁶⁴ Alternatively, these individual factors can be analyzed in greater detail using a synthetic system which incorporates the key factors that mediate reactivity in the natural systems we are targeting.

1.2 Proton Coupled Electron Transfer in Synthetic Systems

The complexity of tuning the precise factors which dictate PCET in biological systems has led to the use of molecular models to elucidate important non-covalent interactions in oxidation catalysis. A minimalist secondary coordination sphere is constructed onto a ligand platform which can support metals in a wide range of oxidation states, as shown in Scheme 1.1. This Hangman architecture in effect “hangs” an acid-base functional group over the redox platform using a rigid scaffold.⁶⁵ Synthetic methods can be used to tune the redox properties of the metal, while the scaffold can be modified to specify the spatial

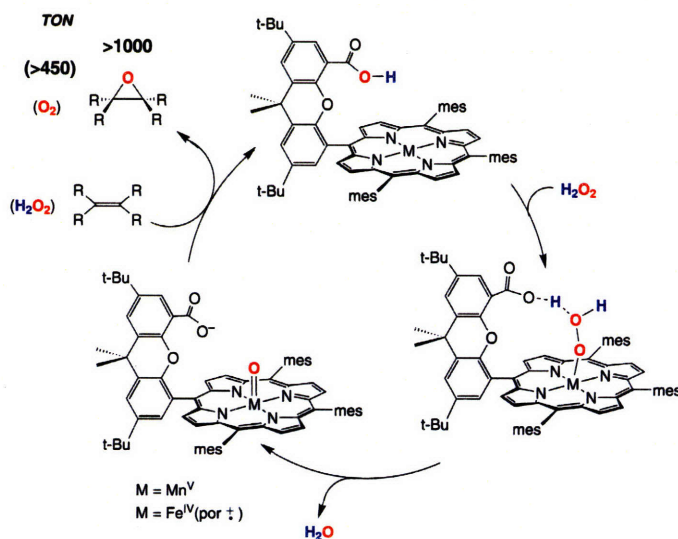
Scheme 1.1



location and pK_a of the distal group. This allows structure-function relationships to be probed using more direct methods.

The initial redox platform incorporated into this architecture was a porphyrin macrocycle with a carboxylic acid functionality (HPX-CO₂H), as shown in Figure 1.2.⁶⁵⁻⁶⁸ The iron porphyrin platform faithfully reproduces many of the essential features of heme-dependent hydroperoxidases, including a ferric hydroperoxide and Compound I and Compound II type intermediates. Additionally, crystallographic characterization of the ferric hydroxide complex reveals a water molecule oriented by the acid and bound hydroxide. This is reminiscent of water molecules situated by distal amino acid residues in heme peroxidases.⁶⁶ The effect of the hanging group is highlighted in the reactivity of the Hangman complexes. The iron Hangman complexes are effective catalase mimics, generating turnover numbers (TON) more than two orders of magnitude over the unfunctionalized redox platform (Figure 1.2).^{67,68} Stop-flow spectroscopic studies of the reaction using the oxidant *m*-CPBA found the presence of the hanging group both accelerated peroxy acid ligation and exclusively favored the proton-coupled two-electron O—O bond heterolysis to form a Compound I-like intermediate, as opposed to a less oxidizing Compound II-like intermediate.⁶⁹ In the presence of olefin substrate and

Figure 1.2. Proposed catalytic cycle of the catalase-like disproportionation of hydrogen peroxide by iron (HPX-CO₂H), and epoxidation by manganese (HPX-CO₂H). Adapted from reference 67.

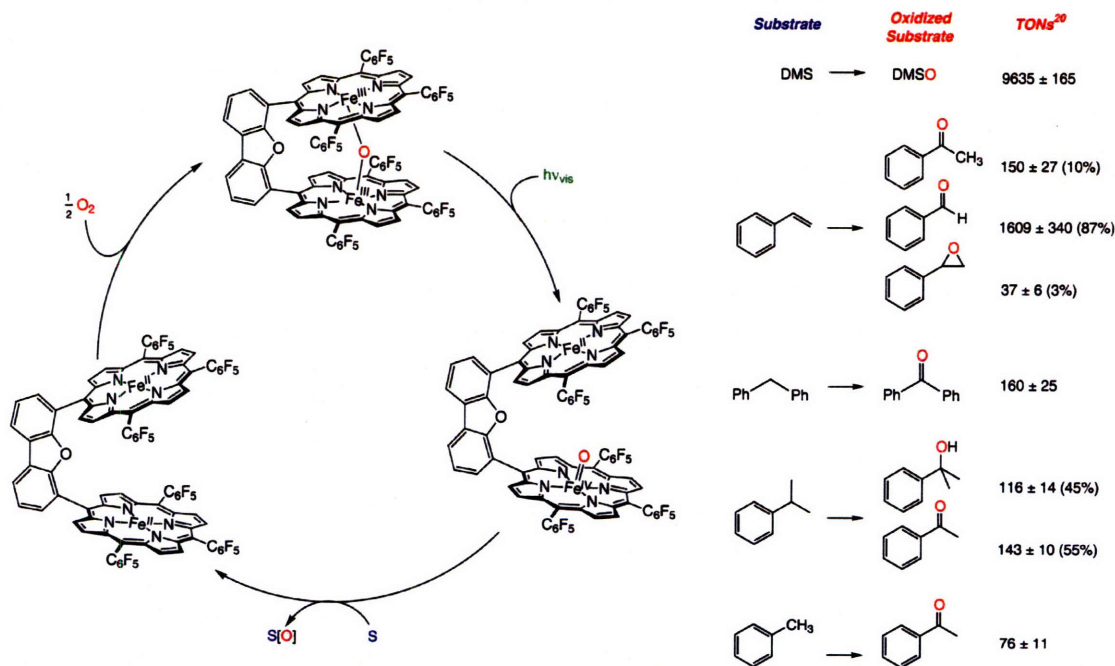


hydrogen peroxide, the manganese Hangman complexes catalyzed epoxidation at improved TON over the manganese porphyrin lacking the hanging group.⁶⁷ In both cases, the exceptional improvement in catalytic activity due to the hanging acid group is due to the proton mediated formation of the more oxidizing high valent M=O species.

1.3 Photolytic Generation of Metal Oxo Species

In Nature, O—O bond formation is performed by the oxygen evolving complex (OEC) in Photosystem II. In the proposed mechanism, O—O bond formation is initiated via a nucleophilic hydroxide or water attack onto an electrophilic manganese oxo.^{6,9} Initially, we are interested in studying the formation and electrophilic character of high valent metal oxo species. Both of these factors can be probed by their reaction with a variety of electron rich substrates. (Analogous to the use of olefin epoxidation in investigating high valent oxo formation in the manganese hangman porphyrins described above.) This approach has been successful in the cofacial bimetallic “pacman” porphyrin system that has also been explored in this research program.⁷⁰⁻⁷⁷ The Fe—O bond in diiron μ -oxo pacman porphyrin complexes can be photolytically cleaved to expose an iron(IV) oxo

Figure 1.3. Proposed catalytic cycle for the photolytic oxidation catalysis performed by diiron pacman porphyrin complexes, and summary of substrates and turnover numbers observed.⁷⁸⁻⁸²

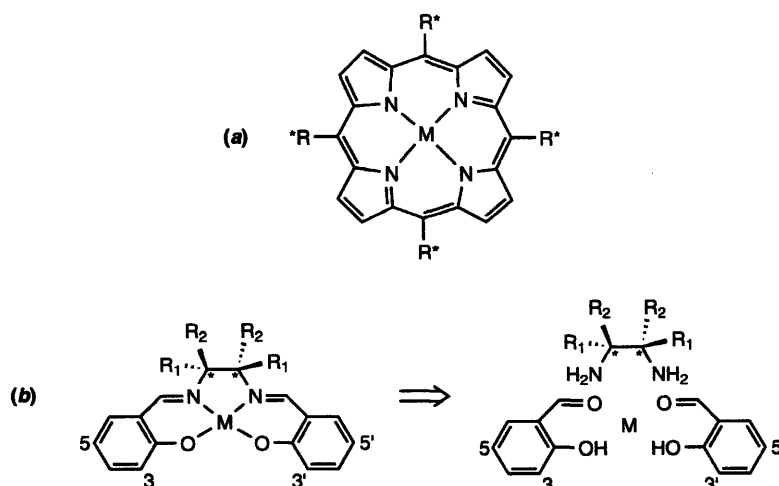


capable of oxidation chemistry.⁷⁸⁻⁸² Detailed mechanistic studies resulted in ligand architecture modifications that dramatically increased turnover numbers.^{81,82} This was coupled with the use of electron withdrawing groups on the porphyrin to increase the electrophilic nature of the iron oxo intermediate and thus the ability to oxidize more difficult substrates, as shown in Figure 1.3. The photolytic generation of a high valent metal oxo from a thermally inert diiron μ -oxo complex to perform oxidation chemistry using molecular oxygen as the oxidant was an additional avenue of reactivity that we were interested in expanding.

1.4 Schiff-base Macrocycles as Redox Platforms

The use of porphyrin macrocycles to support the redox platform in Hangman and Pacman porphyrin architectures was very successful in producing effective catalysts for oxidation chemistry. Furthermore, modulating functional groups around the porphyrin platform allowed tuning of the steric, redox, and photophysical properties in order to expand the scope of substrate and catalytic conditions. While synthetic preparation of variously functionalized porphyrins is well established, most procedures still require lengthy, multi-step synthesis, particularly in order to allow attachment to the xantheno and dibenzofuran spacers in constructing the Hangman and Pacman ligands. Alternatively, the replacement of the porphyrins with Schiff-base macrocycles as the redox platform in our architectures engenders several advantages. Firstly, they are easily assembled via condensation of two salicylaldehydes with a diamine, as shown in the retrosynthesis in Chart 1.1b. Secondly, a large variety of functionalized salicylaldehydes exists commercially and in the literature,

Chart 1.1



and can typically be prepared in one or two steps.⁸³⁻⁸⁷ The 3 and 5 positions are highlighted in Chart 1.1b as they are activated and thus the easiest positions to functionalize. Combined with the scope of aliphatic and aromatic diamines that can be used, this constitutes a modular approach to a wide range of macrocycles with tunable steric and redox properties. Additionally, given the rich oxidation chemistry displayed by the porphyrin hangman and pacman complexes, one of the features that would be appealing to add to the catalytic chemistry is enantioselectivity. Although some metalloporphyrins catalysts have, through elaborate synthetic pathways, incorporated asymmetric functional groups to promote chiral induction of substrates, the enantiomeric excess (*ee*) of the products tend to be poor, and the scope of substrates limited.⁸⁸⁻⁹⁵ This is partly due to the lack of sp^3 carbons near the metal center; addition of chiral functionalities has to occur on the perimeter of the macrocycle (Chart 1.1a). As shown in Chart 1.1.b, an aliphatic diamine provides a location for enantioselective induction proximate to the reactive metal center. Macrocycles of this type have already demonstrated excellent stereochemical communication to a wide variety of substrates in organic transformations.⁹⁶⁻¹⁰⁵ We are interested in integrating these features into the catalysts that we have studied thus far.

References

1. Chang, C. J.; Chang, M. C. Y.; Damrauer, N. H.; Nocera, D. G. *Biophys. Biochim. Acta* **2004**, *1655*, 13-28.
2. Stubbe, J.; Nocera, D. G.; Yee, C. S.; Chang, M. C. Y. *Chem. Rev.* **2003**, *103*, 2167-2202.
3. Cukier, R. I.; Nocera, D. G. *Annu. Rev. Phys. Chem.* **1998**, *49*, 337-369.
4. Dempsey, J. L.; Esswein, A. J.; Manke, D. R.; Rosenthal, J.; Soper, J. D.; Nocera, D. G. *Inorg. Chem.* **2005**, *44*, 6879-6892.
5. Yachandra, V. K.; Sauer, K.; Klein, M. P. *Chem. Rev.* **1996**, *96*, 2927-2950.
6. Tommos, C.; Babcock, G. T. *Acc. Chem. Res.* **1998**, *31*, 18-25.
7. Yocum, C. G.; Pecoraro, V. L. *Curr. Opin. Chem. Biol.* **1999**, *3*, 182-187.
8. Dismukes, G. C. *Science* **2001**, *292*, 447-448.
9. Vrettos, J. S.; Limburg, J.; Brudvig, G. W. *Biochim. Biophys. Acta* **2001**, *1503*, 229-245.
10. Babcock, G. T.; Wikström, M. *Nature* **1992**, *356*, 301-309.
11. Ramirez, B. E.; Malmström, B. G.; Winkler, J. R.; Gray, H. B. *Proc. Natl. Acad. Sci. U. S. A.* **1995**, *92*, 11949-11951.
12. Ferguson-Miller, S.; Babcock, G. T. *Chem. Rev.* **1996**, *96*, 2889-2907.
13. Michel, H.; Behr, J.; Harrenga, A.; Kannt, A. *Annu. Rev. Biophys. Biomol. Struct.* **1998**, *27*, 329-356.
14. Gennis, R. B. *Proc. Natl. Acad. Sci. U.S.A.* **1998**, *95*, 12747-12749.
15. Brzezinski, P. *Biochim. Biophys. Acta* **2000**, *1458*, 1-5.
16. Wikström, M. *Biochim. Biophys. Acta* **2000**, *1458*, 188-198.
17. Schultz, B. E.; Chan, S. I. *Annu. Rev. Biophys. Biomol. Struct.* **2000**, *30*, 23-65.
18. Ozaki, S.-I.; Roach, M. P.; Matsui, T.; Watanabe, Y. *Acc. Chem. Res.* **2001**, *34*, 818-825.
19. *Cytochrome P-450 Structure, Mechanism, and Biochemistry*; P. R. Ortiz de Montellano, Ed.; Plenum Press: New York, 1986.
20. Sono, M.; Roach, M. P.; Coulter, E. D.; Dawson, J. H. *Chem. Rev.* **1996**, *96*, 2841-2887.
21. Dawson, J. H. *Science* **1988**, *240*, 433-439.
22. Dunford, H. B. *Heme Peroxidases*; Wiley: New York, 1999.

23. Suslick, K. S. "Shape-Selective Oxidation by Metalloporphyrins" In *The Porphyrin Handbook*; Kadish, K. M.; Smith, K. M.; Guilard, R., Eds.; Academic Press: San Diego, 2000; Vol. 4, pp 41-63.
24. Watanabe, Y. "High-Valent Intermediates" In *The Porphyrin Handbook*; Kadish, K. M.; Smith, K. M.; Guilard, R., Eds.; Academic Press: San Diego, 2000; Vol. 4, pp 97-117.
25. Hiner, A. N. P.; Raven, E. L.; Thorneley, R. N. F.; Garcia-Canovas, F.; Rodriguez-Lopez, J. N. *J. Inorg. Biochem.* **2002**, *91*, 27-34.
26. Jones, P. *J. Biol. Chem.* **2001**, *276*, 13791-13796.
27. Nicolls, P.; Fita, I.; Lowen, P. C. "Enzymology and Structure of Catalases" In *Advances in Inorganic Chemistry*; Academic Press: New York, 2001; Vol. 51, pp 51-106.
28. Sivaraja, M.; Goodin, D. B.; Smith, M.; Hoffman, B. M. *Science* **1989**, *245*, 738-740.
29. Adachi, S.-I.; Nagano, S.; Ishimori, K.; Watanabe, Y.; Morishima, I. *Biochemistry*, **1993**, *32*, 241-252.
30. Rao, S. I.; Wilks, A.; Ortiz de Montellano, P. R. *J. Biol. Chem.* **1993**, *268*, 803-809.
31. Levinger, D. C.; Stevenson, J.-A.; Wong, L.-L. *J. Chem. Soc., Chem. Commun.* **1995**, 2305-2306.
32. Ozaki, S.-I.; Matsui, T.; Watanabe, Y. *J. Am. Chem. Soc.* **1996**, *118*, 9784-9785.
33. Nagano, S.; Tanaka, M.; Ishimori, K.; Watanabe, Y.; Morishima, I. *Biochemistry*, **1996**, *35*, 14251-14258.
34. Ozaki, S.-I.; Matsui, T.; Watanabe, Y. *J. Am. Chem. Soc.* **1997**, *119*, 6666-6667.
35. Matsui, T.; Ozaki, S.-I.; Watanabe, Y. *J. Biol. Chem.* **1997**, *272*, 32735-32738.
36. Murakami, T.; Moishima, I.; Matsui, T.; Ozaki, S.-I.; Watanabe, Y. *J. Chem. Soc., Chem. Commun.* **1998**, 773-774.
37. Murakami, T.; Morishima, I.; Matsui, T.; Ozaki, S.-I. Hara, I.; Yang, H.-J.; Watanabe, Y. *J. Am. Chem. Soc.* **1999**, *121*, 2007-2011.
38. Wan, L.; Twitchett, M. B.; Eltis, L. D.; Mauk, A. G.; Smith, M. *Proc. Natl. Acad. Sci. U.S.A.* **1998**, *95*, 12835-12831.
39. Ozaki, S.-I.; Yang, H.-J.; Matsui, T.; Goto, Y.; Watanabe, Y. *Tetrahedron: Asymmetry* **1999**, *10*, 183-192.
40. Matsui, T.; Ozaki, S.-I.; Liong, E.; Phillips Jr., G. N.; Watanabe, Y. *J. Biol. Chem.* **1999**, *274*, 2838-2844.
41. Matsui, T.; Ozak, S.-I.; Watanabe, Y. *J. Am. Chem. Soc.* **1999**, *121*, 9952-9957.

42. Sigman, J. A.; Kwok, B. C.; Lu, Y. *J. Am. Chem. Soc.* **2000**, *122*, 8192-8196.
43. Ozaki, S.-I.; Hara, I.; Matsui, T.; Watanabe, Y. *Biochemistry* **2001**, *40*, 1044-1052.
44. Kato, S.; Yang, H.-J.; Ueno, T.; Ozaki, S.-I.; Phillips Jr., G. N.; Fukuzumi, S.; Watanabe, Y. *J. Am. Chem. Soc.* **2002**, *124*, 8506-8507.
45. Yang, H.-J.; Matsui, T.; Ozaki, S.-I.; Kato, S.; Ueno, T.; Phillips Jr., G. N.; Fukuzumi, S.; Watanabe, Y. *Biochemistry*, **2003**, *42*, 10174-10181.
46. Kato, S.; Ueno, T.; Fukuzumi, S.; Watanabe, Y. *J. Biol. Chem.* **2004**, *279*, 52376-52381.
47. Pfister, T. D.; Ohki, T.; Ueno, T.; Hara, I.; Adachi, S.; Makino, Y.; Ueyama, N.; Lu, Y.; Watanabe, Y. *J. Biol. Chem.* **2005**, *280*, 12858-12866.
48. KiNello, R. K.; Dolphin, D. H. *J. Biol. Chem.* **1981**, *256*, 6903-6912.
49. Hayashi, T.; Tomokuni, T.; Mizutani, T.; Hisaeda, Y.; Ogoshi, H. *Chem. Lett.* **1998**, 1229-1230.
50. Ryabov, A. D.; Goral, V. N.; Gorton, L.; Csöregi, E. *Chem. Eur. J.* **1999**, *5*, 961-967.
51. Hamachi, I.; Shinkai, S. *Eur. J. Org. Chem.* **1999**, *1999*, 539-549.
52. Hayashi, T.; Hitomi, Y.; Kaimura, A.; Tomokuni, A.; Mizutani, T. Hisaeda, Y.; Ogoshi, H. *Coord. Chem. Rev.* **1999**, *190-192*, 961-974.
53. Monzani, E.; Alzuet, G.; Casella, L.; Redaelli, C.; Bassani, C.; Sanangelantoni, A. M.; Gullotti, M.; Gioia, L. D.; Santagostini, L.; Chillemi, F. *Biochemistry* **2000**, *39*, 9571-8582.
54. Hayashi, T.; Hitomi, Y.; Ando, T.; Mizutani, T.; Hisaeda, Y.; Kitagawa, S.; Ogoshi, H. *J. Am. Chem. Soc.* **1999**, *121*, 7747-7750.
55. Lu, Y.; Berry, S. M.; Pfister, T. D. *Chem. Rev.* **2001**, *101*, 3047-3080.
56. Hayashi, T.; Hisaeda, Y. *Acc. Chem. Res.* **2002**, *35*, 35-43.
57. Hayashi, T.; Matsuda, T.; Hisaeda, Y. *Chem. Lett.* **2003**, *32*, 496-497.
58. Ohashi, M.; Koshiyama, T.; Ueno, T.; Yanase, M.; Fujii, H.; Watanabe, Y. *Angew. Chemie. Int. Ed.* **2003**, *42*, 1005-1008.
59. Sato, H.; Hayashi, T.; Ando, T.; Hisaeda, Y.; Ueno, T.; Watanabe, Y. *J. Am. Chem. Soc.* **2004**, *126*, 436-437.
60. Ueno, T.; Ohashi, M.; Kono, M.; Kondo, K.; Suzuki, A.; Yamane, T.; Watanabe, Y. *Inorg. Chem.* **2004**, *43*, 2852-2858.
61. Hayashi, T.; Nakagawa, T.; Harada, K.; Matsuo, T.; Hitomi, Y.; Hisaeda, Y. *Chem Lett.* **2004**, *33*, 1512-1513.

62. Ueno, T.; Koshiyama, T.; Ohashi, M.; Kondo, K.; Kono, M.; Suzuki, A.; Yamane, T.; Watanabe, Y. *J. Am. Chem. Soc.* **2005**, *127*, 6556-6562.
63. Sato, H.; Wantanbe, M.; Hisaeda, Y.; Hayashi, T. *J. Am. Chem. Soc.* **2005**, *127*, 56-57.
64. Ueno, T.; Koshiyama, T.; Abe, S.; Yokoi, N.; Ohashi, M.; Nakajima, H.; Watanabe, Y. *J. Organomet. Chem.* **2007**, *692*, 142-147.
65. Chang, C. J.; Yeh, C.-Y.; Nocera, D. G. *J. Org. Chem.* **2002**, *67*, 1403-1406.
66. Yeh, C.-Y.; Chang, C. J.; Nocera, D. G. *J. Am. Chem. Soc.* **2001**, *123*, 1513-1514.
67. Chang, C. J.; Chng, L. L.; Nocera, D. G. *J. Am. Chem. Soc.* **2003**, *125*, 1866-1876.
68. Chng, L. L.; Chang, C. J.; Nocera, D. G. *Org. Lett.* **2003**, *5*, 2421-2424.
69. Soper, J. D.; Kryatov, S. V.; Rybak-Akimova, E. V.; Nocera, D. G. *J. Am. Chem. Soc.* **2007**, *ASAP*, DOI: 10.1021/ja0683032.
70. Deng, Y.; Chang, C. J.; Nocera, D. G. *J. Am. Chem. Soc.* **2000**, *122*, 410-411.
71. Chng, L. L.; Chang, C. J.; Nocera, D. G. *J. Org. Chem.* **2003**, *68*, 4075-4078.
72. Chang, C. J.; Deng, Y.; Heyduk, A. F.; Chang, C. K.; Nocera, D. G. *Inorg. Chem.* **2000**, *39*, 959-966.
73. Chang, C. J.; Deng, Y.; Peng, S.-M.; Lee, G.-H.; Yeh, C.-Y.; Nocera, D. G. *Inorg. Chem.* **2002**, *41*, 3008-3016.
74. Chang, C. J.; Loh, Z.-H.; Deng, Y.; Nocera, D. G. *Inorg. Chem.* **2003**, *42*, 8262-8269.
75. Chang, C. J.; Deng, Y.; Shi, C.; Chang, C. K.; Anson, F. C.; Nocera, D. G. *J. Chem. Soc., Chem. Commun.* **2000**, 1355-1356.
76. Loh, Z.-H.; Miller, S. E.; Chang, C. J.; Carpenter, S. D.; Nocera, D. G. *J. Phys. Chem. A* **2002**, *106*, 11700-11708.
77. Chang, C. J.; Loh, Z.-H.; Shi, C.; Anson, F. C.; Nocera, D. G. *J. Am. Chem. Soc.* **2004**, *126*, 10013-10020.
78. Pistorio, B. J.; Chang, C. J.; Nocera, D. G. *J. Am. Chem. Soc.* **2002**, *124*, 7884-7885.
79. Chang, C. J.; Baker, E. A.; Pistorio, B. J.; Deng, Y.; Loh, Z.-H.; Miller, S. E.; Carpenter, S. D.; Nocera, D. G. *Inorg. Chem.* **2003**, *41*, 3102-3109.
80. Hodgkiss, J. M.; Chang, C. J.; Pistorio, B. J.; Nocera, D. G. *Inorg. Chem.* **2003**, *42*, 8270-8277.
81. Rosenthal, J.; Pistorio, B. J.; Chng, L. L.; Nocera, D. G. *J. Org. Chem.* **2005**, *70*, 1885-1888.

82. Rosenthal, J.; Lockett, T. D.; Hodgkiss, J. M.; Nocera, D. G. *J. Am. Chem. Soc.* **2006**, *128*, 6546-6547.
83. Zhang, W.; Loebach, J. L.; Wilson, D. R.; Jacobsen, E. N. *J. Am. Chem. Soc.* **1990**, *112*, 2081-2083.
84. Jacobsen, E. N.; Zhang, W.; Muci, A. R.; Ecker, J. R.; Deng, L. *J. Am. Chem. Soc.* **1991**, *113*, 7063-7064.
85. Jacobsen, E. N. Asymmetric Catalytic Epoxidation of Unfunctionalized Olefins. In *Catalytic Asymmetric Synthesis*, 1st Eds; Ojima, I; Wiley-VCH: New York, 1993; Chapter 4.2.
86. Katsuki, T. *Coord. Chem. Rev.* **1995**, *140*, 189-214.
87. Katsuki, T. *J. Mol. Cat. A* **1996**, *113*, 87-107.
88. Groves, J. T.; Myers, R. S. *J. Am. Chem. Soc.* **1983**, *105*, 5791-5796.
89. Groves, J. T.; Viski, P. *J. Org. Chem.* **1990**, *55*, 3628-3634.
90. Mansuy, D.; Battoni, P.; Renaud, J.-P.; Guerin, P. *J. Chem. Soc., Chem. Commun.* **1985**, 155-156.
91. Naruta, Y.; Tani, F.; Ishihara, N.; Maruyama, K. *J. Am. Chem. Soc.* **1991**, *113*, 6865-6872.
92. Collman, J. P.; Zhang, X.; Hembre, R. T.; Brauman, J. I. *J. Am. Chem. Soc.* **1990**, *112*, 5356-5357.
93. Konishi, K.; Oda, K.-L.; Nishida, K.; Aida, T.; Inoue, S. *J. Am. Chem. Soc.* **1992**, *114*, 1313-1317.
94. O'Malley, S.; Kodadek, T. *J. Am. Chem. Soc.* **1989**, *111*, 9116-9117.
95. Halterman, R. L.; Jan, S.-T. *J. Org. Chem.* **1991**, *56*, 5253-5254.
96. Lin, G.-Q.; Li, Y.-M.; Chan, A. S. C. Asymmetric Oxidations. In *Principles and Applications of Asymmetric Synthesis*; Wiley-Interscience: New York, 2001, Chapter 4.
97. Jacobsen, E. N. Transition Metal-Catalyzed Oxidations: Asymmetric Epoxidation. In *Comprehensive Organometallic Chemistry*, 2nd Eds; Wilkinson, G; Stone, F. G. A.; Abel, E. W.; Hegedus, L. S.; Pergamon: New York, 1995; page 1097-1135.
98. Williams, J. M. J. Epoxidation of Alkenes. In *Catalysis in Asymmetric Synthesis*; Sheffield Academic Press: Sheffield, 1999, Chapter 4.
99. Jacobsen, E. N.; Wu, M. H. Epoxidation of Alkenes other than Allylic Alcohols. In *Comprehensive Asymmetric Catalysis*, Vol 2; Pfaltz, A.; Jacobsen, E. N.; Yamamoto H.; Springer: Berlin, Heidelberg, New York, 1999; Chapter 18.2.
100. Larrow, J. F.; Jacobsen, E. N. *Topics Organomet. Chem.* **2004**, *6*, 123-152.

101. Shyu, H.-L.; Wei, H.-H.; Lee, G.-H.; Wang, Y. *J. Chem. Soc., Dalton Trans.* **2000**, 915-918.
102. Sivasubramanian, V. K.; Ganesan, M.; Rajagopal, S.; Ramaraj, R. *J. Org. Chem.* **2002**, *67*, 1506-1514.
103. Tokunaga, M.; Larrow, J. F.; Kakiuchi, F.; Jacobsen, E. N. *Science* **1997**, *277*, 936-938.
104. Jacobsen, E. N.; Wu, M. H. Ring Opening of Epoxides and Related Reactions. In *Comprehensive Asymmetric Catalysis*, Vol 2; Pfaltz, A.; Jacobsen, E. N.; Yamamoto H.; Springer: Berlin, Heidelberg, New York, 1999: Chapter 35.
105. Jacobsen, E. N. *Acc. Chem. Res.* **2000**, *33*, 421-431.

Chapter 2

Hangman Salophen Mediated Activation of O—O Bonds: Mechanistic Insights

Portions of the work presented in this chapter have been published:

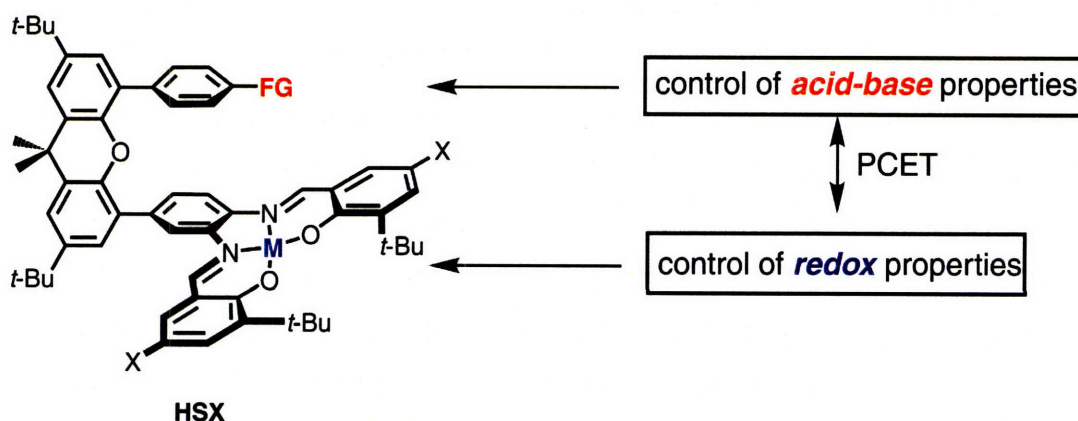
Liu, S.-Y.; Soper, J. D.; Yang, J. Y.; Rybak-Akimova, E. V.; Nocera, D. G. *Inorg. Chem.* **2006**, *45*, 7572-7574.

2.1. Motivation and Specific Aims

The Hangman ligand architecture, which incorporates an acid functionalized scaffold over a metal-ligand platform, is expanded by replacing the previously studied porphyrin ligand platform with a salophen macrocycle. This modification permits a more facile synthetic introduction of functional groups to the phenolic arms of the salophen, thereby permitting the steric and redox environment of the metal center to be varied more easily. The manganese Hangman salophen compounds are successful catalase mimics, and their reactivity can be tuned by varying the redox properties of the salophen macrocycle. In order to determine the basis for the enhanced activity for the dismutation of hydrogen peroxide, stopped-flow spectroscopic techniques using the peroxyacid *m*-CPBA to probe intermediates in the catalytic cycle and the kinetics of their formation. This includes heterolysis of the O—O bond to form a putative Mn(V) oxo. Stopped-flow studies help define the electronic effects that perturb the kinetics of the Mn(V) oxo formation. Conditions to independently generate the Mn(V) salophen oxo using hydrogen peroxide have also been discovered. By comparing our results to those of manganese salophen platforms lacking the acid functionalized scaffold and Hangman porphyrins, insight into the mechanism of catalase activity by manganese salophens is gained.

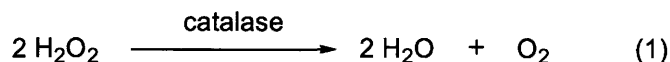
2.2. Background

Chart 2.1



Expanding upon the work on the Hangman Porphyrin ligand, HPX¹⁻⁴ (discussed in Chapter 1), a series of Hangman Salophen compounds were assembled (HSX, shown in Chart 2.1).⁵ The modular synthesis of salophen compounds allows for easy synthetic

modification in the functionalities of the 5 and 5' position along the phenolic arms (indicated by X) of the macrocycle. This position exerts a particularly strong influence on the redox properties of the metal center.⁶ Within the HSX framework, PCET catalysis was explored in the activation of O—O bonds by studying the disproportionation of H₂O₂.



This catalase reaction is an important PCET process that is catalyzed by a variety of enzymes.⁷⁻¹¹ In the case of manganese(III) chloride HSX compounds where X = *tert*-butyl, the turnover number (TON) for oxygen production upon addition of hydrogen peroxide is dramatically higher with the acid functionalized xanthene (4372 TON/hour) compared to the ester analogue (98 TON/hour), which lacks the acidic proton. The control experiment with the redox only manganese salophen platform (lacking the xanthene scaffold) shows a similarly low activity (86 TON/hour).⁵ Thus, an enhancement of catalase activity is observed by positioning a carboxylic acid group over a redox platform. This enhanced reactivity is also observed for iron(III) Hangman porphyrin compounds when compared to iron(III) tetramesityl porphyrin (TMP).³ While similar reactivity is also observed for Hangman salophen and porphyrin platforms, the former is synthetically much easier to modify. The meso-positions of the porphyrins are not available for modification because they are needed to incorporate steric protection to prevent formation of inactive diiron μ -oxo dimers.¹² To this end, a series of HSX analogs

Table 2.1. Redox potential of manganese (HSX) chloride compounds with varying X functionalities in the 5 and 5' position, observed LMCT band in the UV-visible spectrum, and the amount of time after injection that half of 4388 equivalents of H₂O₂ was measured to be consumed by monitoring the amount of oxygen evolved.^{5,13}

| X | E _{1/2} (Mn ^{II} /Mn ^{III}) | λ_{max} (nm) | t (50%) (sec) |
|-----------------|---|-----------------------------|---------------|
| OMe | -0.36 | 511 | 560 |
| Br | -0.5 | 490 | 860 |
| H | 0.0 | 486 | 970 |
| <i>t</i> -Bu | 0.14 | 476 | 1760 |
| NO ₂ | 0.44 | 460 | - |

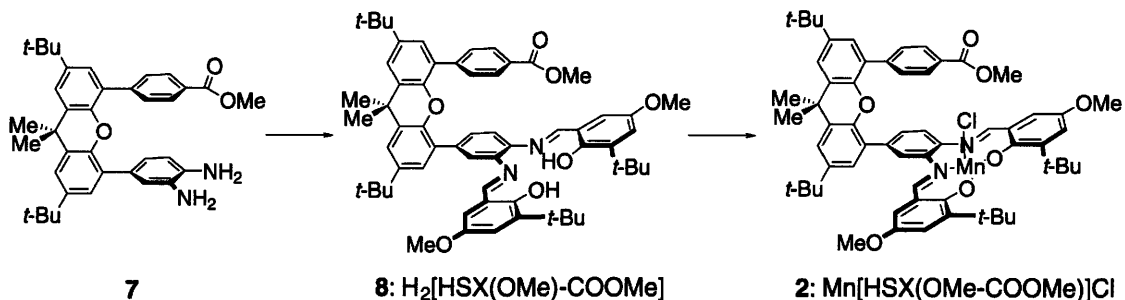
with X = OMe, Br, H, *t*-Bu, and NO₂ were synthesized. This family of manganese(III) Hangman salophen compounds shows an increase in oxidation potential as the electron with-drawing ability of groups in the 5 and 5' position (shown in Table 2.1) is increased.^{5,13} The redox potential of the manganese(II/III) couple can be varied from 0.37 V, with the introduction of electron donating methoxy groups to 0.44 V with the introduction of electron withdrawing nitro groups.^{5,13} The electronic perturbation of substituent groups is reflected in a low energy absorption band,¹⁴ which exhibits a red-shift from 511 nm to 460 nm along the series of increasing electron-donating ability of the substituent. This trend is consistent with a salophen ligand-to-metal charge transfer parentage of the absorption band. Variations in redox potential and electron density at the metal site are directly correlated with the rate of catalase activity as measured by the rate of H₂O₂ consumption (shown in Table 2.1 and Figure 2.1). We can also measure reactivity by comparing the amount of time it takes for half of the H₂O₂ equivalents to be dismutated into oxygen and water. We can also measure reactivity by comparing the amount of time it takes for half of the H₂O₂ equivalents to be dismutated into oxygen and water. The Hangman salophen with X = NO₂ displays very little reactivity and only achieves a TON of 81, or 2% conversion over the hour the reaction was monitored, whereas the methoxy substituted congener is the most successful catalase mimic. There is only a moderate correlation between the initial rates of reaction and the σ_p^+ constant and the sensitivity parameter ($\rho = -0.3$) is quite low, which suggests there are little changes in the transition state of the rate-limiting step of the reaction.¹³ It is likely that under the biphasic reaction conditions used in these studies, the diffusion of H₂O₂ is an important factor in the rate-determining step for the initial reactivity and this result in the low observed ρ value.

2.3. Results and Discussion

2.3.1. Synthesis

The compounds that are the focus of this Chapter are shown in Chart 2.2. The acid functionalized manganese Hangman salophen (**1**) was synthesized as described previously.⁵ The synthesis of the corresponding methyl ester is outlined in Scheme 2.1. The functionalized xanthene precursor **7**⁵ was condensed with two equivalents of 3-*tert*-butyl-2-hydroxy-5-methoxy-benzaldehyde to give the ligand **8**, which was refluxed with

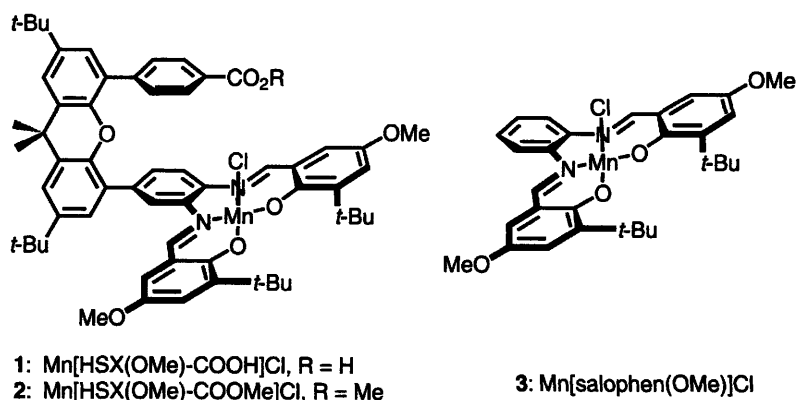
Scheme 2.1



manganese(II) acetate in air, followed by an aqueous sodium chloride wash to give the Mn(III) complex **2**. Manganese salophen complex **3** was synthesized for the purposes of performing control experiments; it was prepared by the stepwise condensation of two equivalents of 3-*tert*-butyl-2-hydroxy-5-methoxybenzaldehyde with 1,2-phenylenediamine followed by the same metalation procedure described for **2**.

2.3.2. Stopped-flow Spectroscopy

Chart 2.2



In order to understand the role the hanging functionality may play in the catalase activity of manganese salophens, stopped-flow kinetic studies were used to provide spectroscopic evidence of intermediates and their rates of their formation. The stopped-flow spectroscopic experiments were conducted by postdoctoral associate Jake Soper on the acid (**1**) and ester (**2**) functionalized manganese Hangman salophens, substituted with methoxy in the 5 and 5' position as shown in Chart 2.2. The unfunctionalized manganese salophen (**3**) was also investigated to provide a side by side comparison to the Hangman compounds. The experiments were performed using *m*-CPBA as the oxygen atom source instead of hydrogen peroxide, which would continue to react with the oxidizing

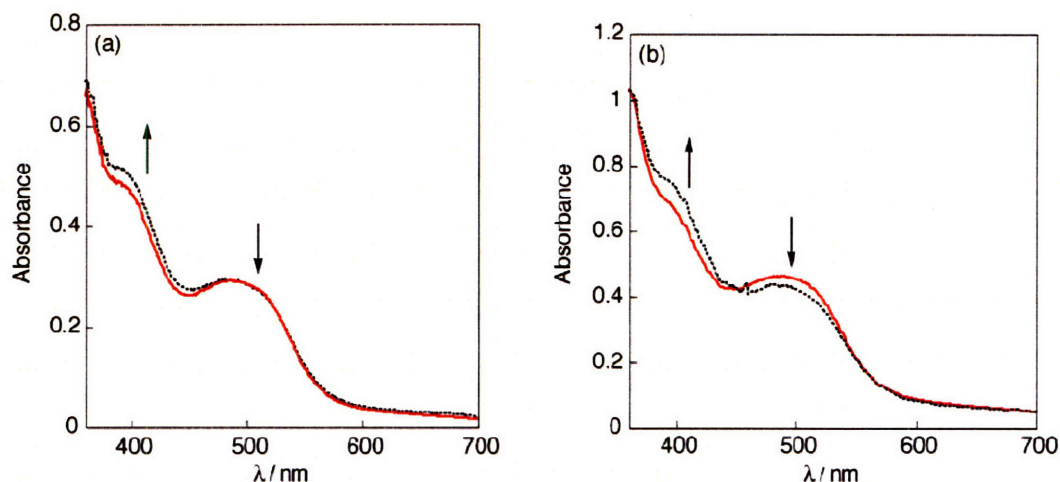


Figure 2.2. (a) Stopped-flow UV-vis spectra obtained from reaction of *m*-CPBA (3.3×10^{-4}) with 4.0×10^{-5} M **1** (red solid line) ca. 3 s post injection in 1:1 MeOH:MeCN at -20 °C. (b) UV-vis spectrum obtained from a solution of 5.0×10^{-5} M **1** in MeOH:MeCN at room temperature (red solid line). UV-vis spectrum obtained from a solution of 5.0×10^{-5} M **1** in 1:1 MeOH:MeCN at room temperature in the presence of benzoic acid (5.0×10^{-3} M) (black dotted line).

intermediate and complicate kinetic studies. The use of *m*-CPBA arrests the catalase cycle after formation of the high valent manganese species, enabling detection of the first two intermediates at the Hangman salophen platform.

The initial stage of the reaction upon addition of *m*-CPBA to **1** is characterized by small changes in the stopped-flow UV-vis spectrum (Figure 2.2a), suggesting a simple ligand substitution by the perbenzoate at the Mn(III) center. This substitution reaction was modeled by the addition of benzoic acid to **1**. The benzoate substrate circumvents the possibility of O—O bond cleavage, therefore allowing the substitution reaction to be isolated. The small spectral shifts observed for perbenzoate substitution are captured with the benzoate model (Figure 2.2b). Global fitting of the transient spectra indicates that ligand substitution is complete in 3 s at -20 °C.

The appearance of the Mn(III) perbenzoate complex (Figure 2.3a, black dotted line) is immediately followed by a subsequent reaction that generates a species with the spectrum shown by the green line in Figure 2.3a. The spectrum does not depend on the nature of the oxidant; a similar spectrum is obtained with the same isosbestic points when *m*-CPBA is replaced by the two-electron oxidant, iodosylbenzene. These results lead us to assign

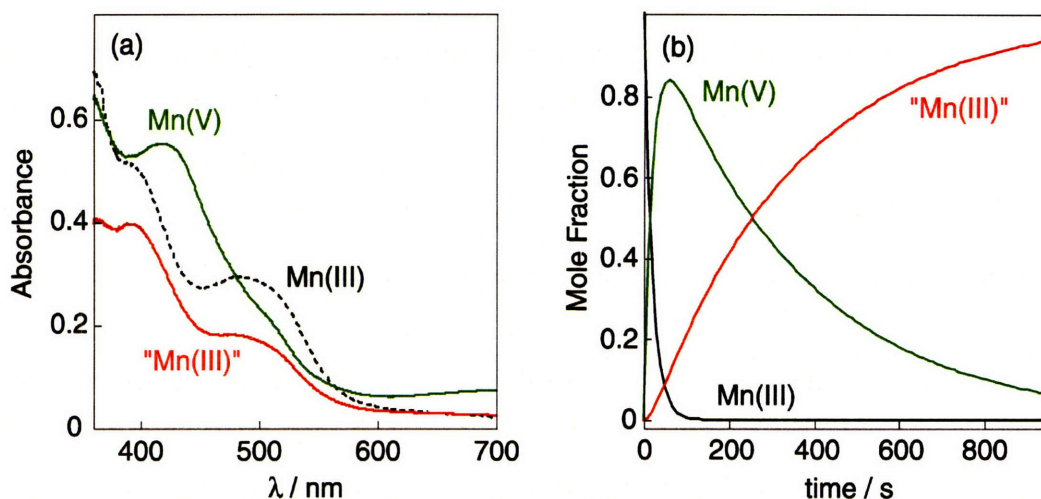


Figure 2.3. (a) Absorption spectra obtained from spectral global analysis of a stopped-flow reaction of 4.0×10^{-5} M **1** and 3.3×10^{-4} M *m*-CPBA in 1:1 MeOH:MeCN at -20 °C. Formation of Mn(V) oxo (green solid line) is immediately followed by a bleach, likely to a Mn^{III} decay product (red solid line) over 800 s. (b) Calculated concentrations of the colored species with respect to time by spectral global analysis by Jake Soper.

this intermediate to the Mn(V) oxo salphen. Several observations support this assignment. First, the transient spectrum is reminiscent to that of structurally similar, crystallographically characterized Mn(V) oxo complexes of bis-amido bis-alkoxo redox platforms.¹⁵ Moreover, the spectral features in Figure 2.3a (green line) concur with those of other (non-oxo) multiply bonded Mn(V) ligand salphen species. The corresponding nitrido complex, Mn[salphen(OMe)]N complex was also synthesized and isolated. The crystal structure of the compound is similar to other Mn(V) nitrido complexes featuring a formal Mn—N triple bond ($d(\text{Mn}-\text{N}) = 1.523(3) \text{ \AA}$).¹⁶ The absorption spectrum of the Mn(V) complex shows a pronounced absorption band at $\lambda_{\text{max}} = 459 \text{ nm}$, similar to 420 nm feature that dominates the absorption spectrum of Figure 2.3a (green line). The electron-donating methoxy group on the salphen platform of the Mn(V) oxo species impart sufficient stability¹⁷ that it is observed as a stopped-flow transient. The reactive high-valent oxo intermediate eventually disappears 60-800 seconds after substrate injection as evidenced by the decrease of the absorption profile across the entire spectral range (360 - 700 nm). The final spectrum, shown by the red line in Figure 2.3a, strongly resembles the Mn(III) starting material, though the product was not unequivocally identified.

Table 2.2. Rates of the formation of Mn(V) oxo intermediates and their decay for a series of Mn[salophen(X)] peroxyacid complexes^a



| Entry | Mn-Complex | K_1 (s ⁻¹) | k_2 (s ⁻¹) |
|-------|---|------------------------------|------------------------------|
| 1 | Mn[HSX(OMe)-COOH] (1) | $2.3 \pm 0.6 \times 10^{-2}$ | $3.6 \pm 0.3 \times 10^{-3}$ |
| 2 | Mn[HSX(OMe)-COOMe] (2) | $2.8 \pm 0.8 \times 10^{-2}$ | $2.5 \pm 0.3 \times 10^{-3}$ |
| 3 | Mn[salophen(OMe)] (3) | $2.1 \pm 0.5 \times 10^{-2}$ | $4.1 \pm 0.3 \times 10^{-3}$ |
| 4 | Mn[HSX(OMe)-COOH] (1) ^b | $2.9 \pm 0.6 \times 10^{-2}$ | $5.5 \pm 0.5 \times 10^{-3}$ |

^a Rate constants determined with global analysis using A to B to C kinetic model. All reactions at -20 °C in 1:1 MeOH: MeCN with [Mn(III)] = 4.0×10^{-5} M and [*m*-CPBA] = 3.3×10^{-4} M.

^b [*m*-CPBA] = 13×10^{-4} M

The rate constants for the O—O bond heterolysis to produce the Mn(V) oxo salophen and its subsequent decay were obtained from global analysis of the full-spectral stopped-flow data (360 - 700 nm). The data were modeled with a consecutive unimolecular kinetic model in which the A → B phase represents the heterolytic O—O bond cleavage to furnish the Mn(V) oxo transient, and the B → C phase corresponds to the decay of the transient to the final Mn(III) species. Figure 2.3b illustrates the calculated concentrations of each of the manganese species with respect to time according to this kinetic model, and Table 2.2 provides the rate constants that yields the best fit for the kinetics model.

We note several features of the kinetics analysis: (1) Both the growth of the Mn(V) transient spectrum and the decay of the Mn(III) reactant are simultaneously fit well by a first-order exponential equation indicating heterolytic cleavage to generate Mn(V) oxo occurs without intermediates. This result is consistent with the heterolysis of O—O bonds of peroxides at Fe(III) heme centers to form Compound I.¹⁸⁻²⁰ (2) The production of the Mn(V) oxo intermediate is independent of the presence of the hanging acid-base group (entry 1 vs. 3 in Table 2.2) or intramolecular proton inventory (entry 1 vs. entry 2 in Table 2.2). (3) The rate of the O—O bond heterolysis appears to be independent of the initial concentration of the *m*-CPBA oxidant (Table 2.2, entry 1 vs. entry 4) though an

increase in *m*-CPBA concentration results in a slightly enhanced decay of the Mn(V) oxo intermediate (Table 2.2, k_2 in entry 1 vs. entry 4).

2.3.3. Decomposition in the Presence of Hydrogen Peroxide

To address the role of the intramolecular acid on enhancing TON, **1** was monitored by post-doctoral fellow Shih-Yuan Liu in the presence of H₂O₂ (30% aqueous solution in MeOH) in homogeneous solution conditions. The UV-vis absorption spectrum shows that the Mn(III) starting material gradually decomposes over time. Kinetics experiments show that the decomposition of **1** is first order with respect to the Mn(III) complex and H₂O₂, and zero order with respect to water. As shown by the rate constants in Table 2.3, the Hangman architecture improves the kinetic stability of the salophen catalyst against oxidative degradation by ~1 order of magnitude. This increased stability is expected to account for the higher TONs listed in Table 2.3 for the Hangman salophen system.

Table 2.3. Stability of Methoxy-Substituted Manganese Salophen Complexes

| Mn-complex | Yield of O ₂ / TON ^a | k_{obs} (s ⁻¹) |
|-----------------------------------|--|-------------------------------------|
| Mn[HSX(OMe)-COOH]Cl (1) | 4500 | 2.9×10^{-4} |
| Mn[HSX(OMe)-COOMe]Cl (2) | 550 | 1.3×10^{-3} |
| Mn[salophen(OMe)]Cl (3) | 100 ^b | 2.3×10^{-3} |

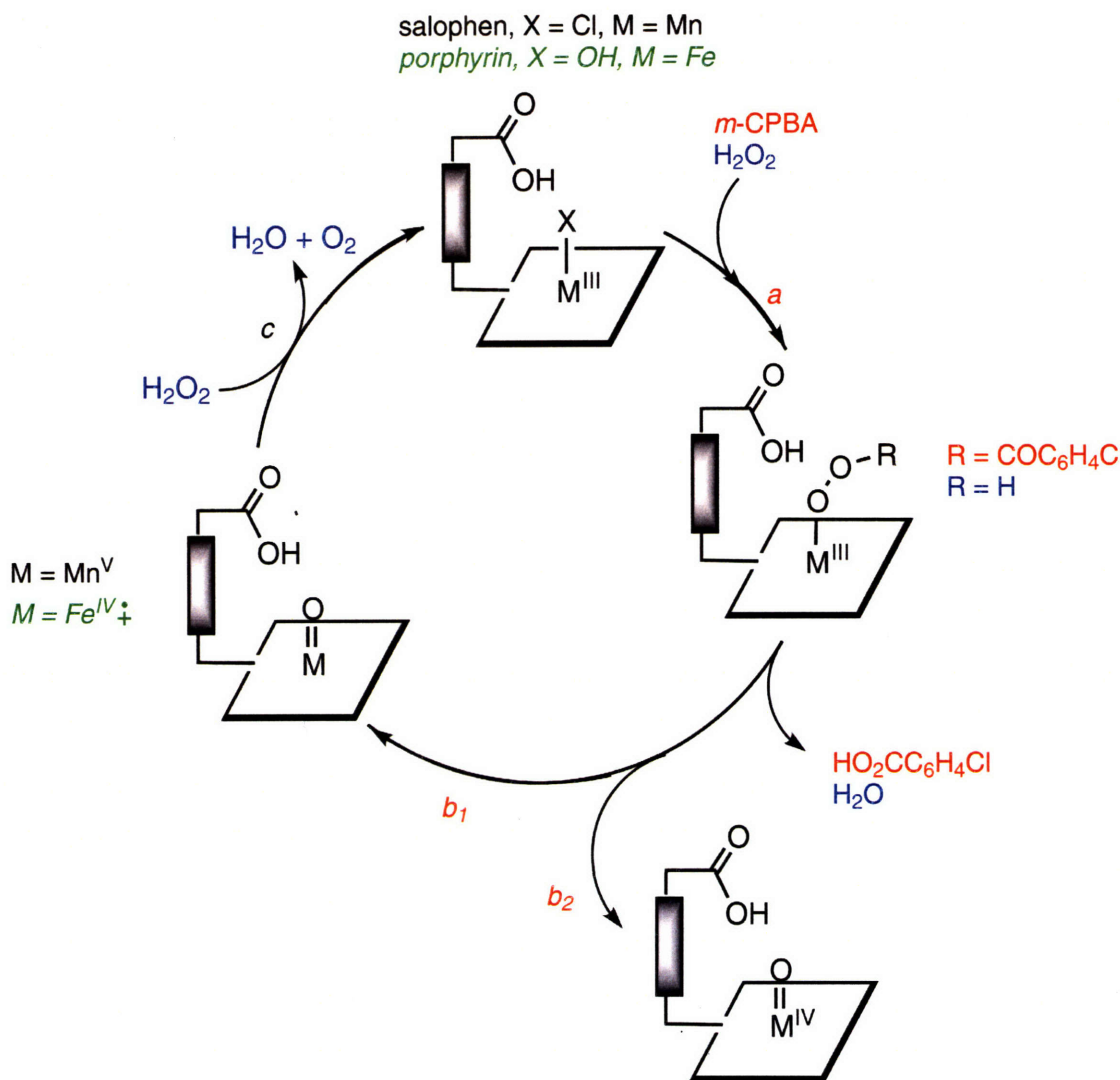
^a Yield of O₂ measured in TON after 1 hr of reaction time

^b In the presence of 1 equivalent of benzoic acid

2.3.4. Mechanistic Implications

The results of the stopped-flow studies on the manganese Hangman salophen compounds contrast with the results of the analogous studies on iron Hangman porphyrin compounds, which also display high catalase activity. Despite what superficially appears to be the same enhancement of catalytic activity by the same structural modification (addition of a proximate carboxylic acid group by the rigid xanthene scaffold), it appears the reasons behind the "Hangman effect" are different for the porphyrin and salophen ligand systems. Addition of *m*-CPBA to the Fe(III) porphyrin hydroxide complex, tetramesityl porphyrin

Scheme 2.2. Proposed catalytic cycle for iron Hangman porphyrin and manganese Hangman salophen compounds. The porphyrin compounds are indicated in green, and the salophen in black. The catalase reaction is represented in blue. The stopped-flow kinetic studies were performed using the red reagents, as well as the rates that can be determined using the double-mixing setup.



(TMP), and the two Fe(III) Hangman porphyrins functionalized with the acid and ester group also undergo substitution to form the Fe(III) acylperoxo complex (shown as reaction *a* in Scheme 2.2).²¹ However, the substitution rate increases along the following trend: TMP < HPX-CO₂Me < HPX-CO₂H, which suggest the hydrogen-bonding microenvironment for the Hangman porphyrin complexes assists in the ligand substitution.²¹ This contrasts with the manganese salophen compounds, which undergo ligand substitution at very close to the same rate for the Hangman compounds and the

unfunctionalized salophen (Table 2.2). The formation of the acyl peroxy porphyrin complex is followed by cleavage of the O—O to form a metal oxo, shown as reaction *b* in Scheme 2.2. As discussed in Chapter 1, the two electron oxidation of Fe(III) heme in hydroperoxidase enzymes to generate a ferryl Fe(IV) oxo with an associated radical that resides on the ligand is commonly referred to as Compound I (reaction *b*₁).²²⁻²⁶ This is coupled with the delivery of a proton from a precisely positioned acid/base residue in the active-site cavity to the distal oxygen of a Fe(III) hydroperoxide complex, which contributes a "pull" effect that facilitates two electron heterolytic bond cleavage.^{22-25,27-32} Alternatively, homolytic cleavage of the O—O results in the one electron oxidation of the metal to generate the less oxidizing Fe(IV) oxo, commonly called Compound II (reaction *b*₂).^{33,34} In the Hangman porphyrin compounds, the acid group impacts the ratio of productive two electron heterolytic O—O bond cleavage to form the high-valent Compound I like oxidant, as opposed to homolytic cleavage to form a Fe(IV)=O, or by favoring reaction *b*₁ over reaction *b*₂.²¹ However, the hanging group does not affect the rate of formation of the Compound I like species.²¹ On the other hand, the acid group in the Hangman salophen compounds does not appear to have the same effect; heterolytic cleavage to form the Mn(V)=O occurs at close to the same rate and quantity for the Hangman compounds as for the unfunctionalized salophens; the lower valent Mn(IV) oxo is not observed (product from *b*₂). It has been noted that Mn(III) Schiff-base compounds are less prone to homolytic cleavage and one electron oxidation to form the less active metal oxo species.^{35,36} Therefore these studies suggest that the "Hangman effect" that we see for the manganese Hangman salophens does not affect the rate or reactivity in the first two steps of the catalase cycle (substitution of the peroxy species, followed by O—O bond cleavage to form the high valent metal oxo species).

Using stopped-flow spectroscopic methods to investigate the kinetics of the next step (reaction *c*, oxidation of hydrogen peroxide by the putative Mn(V) oxo to form oxygen and water) is considerably more difficult. It would require a triple-mixing experiment in order to add hydrogen peroxide to the premixed manganese salophen and *m*-CPBA solution. Alternatively, monitoring the decay of the Mn(III) salophen in solution in the presence of hydrogen peroxide indicates that the acid group may protect the compound from oxidative damage. The greater stability of the manganese Hangman salophen

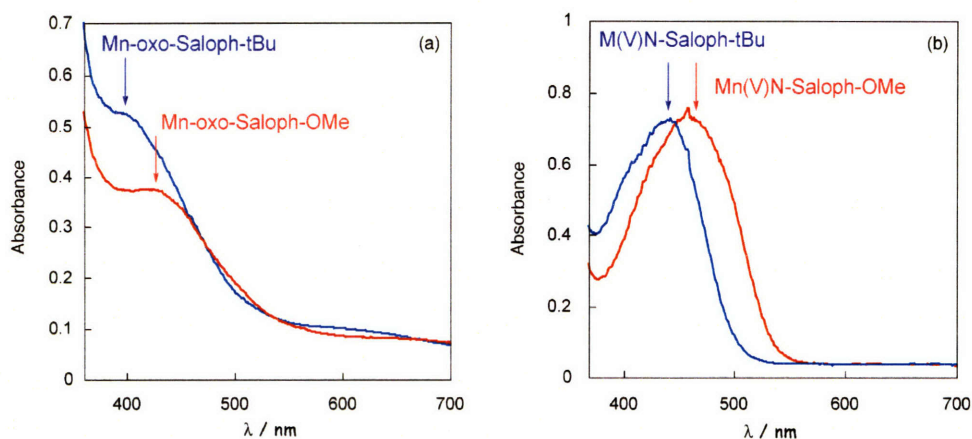


Figure 2.5. UV-vis of high-valent Mn-salophens: (a) comparison of the spectra of Mn-oxo complexes derived from Mn[salophen(*t*-bu)] and Mn[salophen(OMe)], respectively; (b) comparison of the spectra of Mn(V)-nitrido complexes derived from Mn[salophen(*t*-bu)] and Mn[salophen(OMe)], respectively.

(Chart 2.3). These complexes were synthesized stepwise by condensing the appropriately functionalized salicylaldehydes with 1,2-phenylenediamine followed by reflux with manganese acetate in air. Workup with aqueous sodium chloride gives chloride as the counteranion.

As can be seen from Figure 2.5a, the absorption maxima of the high-valent Mn-oxo complexes exhibit a red shift along the series from $X = t\text{-Bu} < X = \text{OMe}$.⁴¹ Interestingly, this spectral feature concurs with that of the corresponding high-valent Mn(V)-nitrido

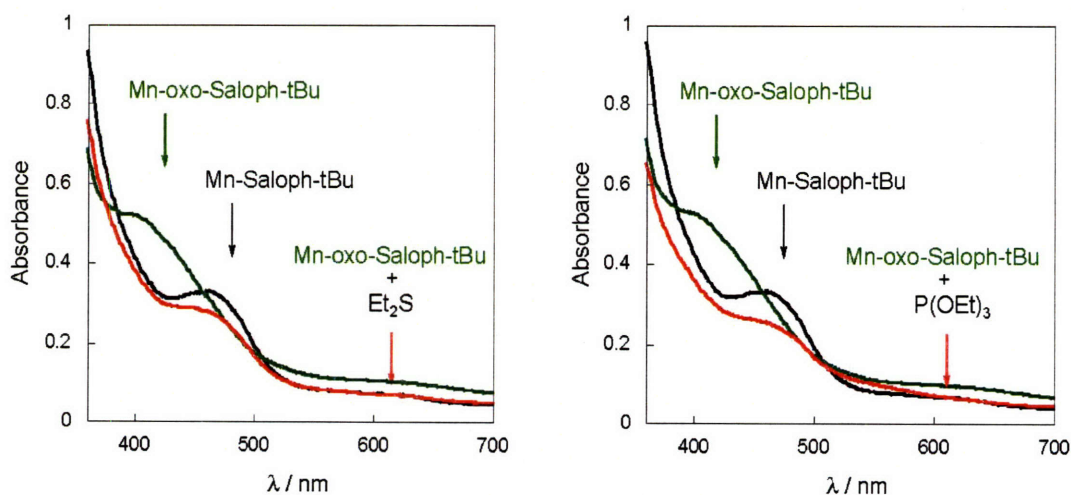


Figure 2.6. Reaction of Mn-oxo with a reductant leads to the regeneration of the Mn(III) starting material.

salophen species (Figure 2.5b). Thus, for both high-valent Mn-salophen complexes (oxo and nitrido) the observed spectral trends are consistent with a salophen ligand-to-metal charge transfer parentage of the absorption band.

Upon standing, the high-valent Mn[salophen(X)]O intermediates decompose gradually. On the other hand, treatment of Mn[salophen(*t*-Bu)]O with reducing substrates such as Et₂S immediately produces a spectrum that strongly resembles the starting material Mn(III)[salophen(*t*-Bu)]Cl (**4**) (Figure 2.6a). Similar spectral shifts are observed when Et₂S is replaced with another reducing substrate, P(OEt)₃ (Figure 2.6b). These results in total support our assignment of the primary oxidation intermediate as a Mn(V) oxo species.

Ivan V. Korendovych from Elena Rybak-Akimova's group at Tufts carried out stopped-flow kinetic studies on the reactions of Mn[salophen(X)]Cl complexes with H₂O₂. The formation of the Mn(V) oxo species was observed to be first order in the Mn-complex and first order in H₂O₂. Furthermore, the experiments established that the rate of Mn(V) oxo formation at -50 °C is slightly enhanced when the redox platform contains π-donating, albeit σ-withdrawing substituents (Table 2.4, entries 3-4 vs. entries 1-2). We have also studied the kinetics of the Mn(V) oxo formation over a temperature range of 40K (233 - 273 K). As can be seen from Table 2.4, the resulting activation entropies are consistent with a bimolecular transition state. Furthermore, the activation parameters for the formation of the Mn(V) oxo are independent of substituent effects. These results are consistent with a rate-limiting coordination of the H₂O₂ oxidant.

Table 2.4. Stopped-Flow Kinetic Studies on the Formation of Mn(V) oxo Intermediates^a

| Entry | Compound | λ (nm) | k ₁ (223 K) ^b s ⁻¹ | ΔH ^{‡,b} kcal/mol | ΔS ^{‡,b} e.u. |
|-------|----------------------|--------|--|-------------------------------|---------------------------|
| 1 | 3 (X = H) | 400 | 0.61 (3) | 9.6 (2) | - 18 (1) |
| 2 | 4 (X = <i>t</i> -Bu) | 420 | 0.75 (8) | 11 (1) | - 10 (5) |
| 3 | 5 (X = OMe) | 440 | 1.4 (2) | 8.6 (7) | - 20 (3) |
| 4 | 6 (X = Br) | 410 | 2.14 (3) | 8.8 (7) | - 19 (3) |

^a Mn[salophen(X)]Cl = 2.5 x 10⁻⁵ M, [H₂O₂] = 0.17 M, [NaOH] = 2.5 x 10⁻⁴ M

2.4. Concluding Remarks

We have successfully captured the active site of catalase enzymes by designing synthetic Hangman constructs that precisely position an acid-base functionality from a xanthene spacer over the face of salophen redox cofactors. In these systems, the distal function of the enzymes is faithfully modeled by the acid-base hanging group⁵ allowing us to compare the chemistry of model catalase systems to their biological counterparts. Using stopped-flow methods and *m*-CPBA as opposed to H₂O₂ as the peroxide substrate allows the reaction to be arrested after O—O bond heterolysis, and allowing the Mn(V) oxo to build-up and be detected with facility. This intermediate is often cited as the active catalyst in model⁴² and enzymatic systems, but its characterization heretofore has remained elusive.^{43,44} In accordance with theoretical predictions of the salen catalase models,^{45,46} the stopped-flow results show that the rate for the production of the high-valent oxo at the salen platform is independent of the distal acid-base functional group. Instead, the role of the hanging group appears to stabilize the catalyst against oxidative degradation.

Additionally, we have established reaction conditions to generate the Schiff base-derived Mn(V) oxo that is capable of reacting with reducing substrates. Stopped-flow kinetic data of an electronically diverse set of Mn-salophen complexes are consistent with a mechanism involving a rate-limiting coordination of the oxidant to generate the Mn(V) oxo intermediates.

2.5. Experimental

2.5.1. General Methods

Dichloromethane and diethyl ether were passed through a neutral alumina column under argon before usage. NaOCl (13% in water) and hydrogen peroxide (30% solution) were used as received from Alfa Aesar. The purchased hydrogen peroxide was volumetrically determined to be 10.4 M (32%) via its decomposition to oxygen gas over manganese dioxide. Methyl alcohol (anhydrous), ethyl alcohol (anhydrous), 1,2-phenylenediamine, ammonium hydroxide (28% NH₃ in water), 3-*tert*-butyl-2-hydroxybenzaldehyde, diethyl sulfide, and triethyl phosphate were used as received from Aldrich. Manganese(II)

acetate tetrahydrate (99+%) was used as received from Strem. 4-[2,7-Di-*tert*-butyl-5-(4,5-diamino-cyclohexa-1,3-dienyl)-9,9-dimethyl-9H-xanthen-4-yl]-cyclohexa-1,3-dienecarboxylic acid methyl ester (**7**)⁵ and 3-*tert*-butyl-2-hydroxy-5-methoxy-benzaldehyde,⁴⁷ and Mn(salophen)Cl (X = OMe (**3**), *t*-Bu (**4**), Br (**6**))⁴⁸ was prepared according to literature procedures. The compound Mn[HSX(OMe)-COOH]Cl (**1**) was synthesized and characterized according to published procedures and recrystallized from CH₂Cl₂/Et₂O before usage.⁵

2.5.2. Physical Measurements

¹H-NMR and ¹³C NMR spectra were recorded at the MIT Department of Chemistry Instrumentation Facility (DCIF) on a Varian Inova 500 spectrometer. ¹H NMR chemical shifts are quoted in ppm relative to tetramethylsilane and spectra have been internally calibrated to the monoprotio impurity of the deuterated solvent used. Spectra were recorded at 20 °C unless otherwise stated.

UV-Visible absorption spectra were recorded on a Spectral Instruments 440 spectrophotometer. IR absorption spectra were recorded on a Perkin-Elmer 2000 FT-IR spectrophotometer.

2.5.3. Synthesis

2.5.3.1. H₂[HSX(OMe)-COOMe] (**8**)

The synthesis was accomplished as described in Scheme 2. A vial containing a stirbar was charged with 4-[2,7-di-*tert*-butyl-5-(4,5-diamino-cyclohexa-1,3-dienyl)-9,9-dimethyl-9H-xanthen-4-yl]-cyclohexa-1,3-dienecarboxylic acid methyl ester (**7**) (21.0 mg, 0.0373 mmol) and 3-*tert*-butyl-2-hydroxy-5-methoxy-benzaldehyde (16.0 mg, 0.078 mmol). Ethanol (0.5 mL) was added, and the vial was sealed with a Teflon cap, and the reaction mixture was allowed to stir at 100 °C for 24 hours. The desired product precipitated out of solution as a red-orange solid and was collected on a glass frit after filtering and copious washing with EtOH. The resulting material was purified by column chromatography (silica gel, pentane: dichloromethane 1: 1) to elute the desired product as a yellow solid (24 mg, 69%). ¹H NMR (500 MHz, CD₂Cl₂, δ): 13.50 (s, 1H), 13.41 (s, 1H), 8.75 (s, 1H), 7.97 (s, 1H), 7.67 (d, *J* = 8.0 Hz, 2H), 7.53 (d, *J* = 2.5 Hz, 1H), 7.52

(d, $J = 2.5$ Hz, 1H), 7.38 (d, $J = 8.0$ Hz, 2H), 7.32 (dd, $J = 8.5$ Hz, $J = 2.0$ Hz, 1H), 7.31 (d, $J = 2.5$ Hz, 1H), 7.25 (d, $J = 2.5$ Hz, 1H), 7.22 (d, $J = 2.0$ Hz, 1H), 7.18 (d, $J = 8.0$ Hz, 1H), 7.06 (d, $J = 3.0$ Hz, 1H), 7.02 (d, $J = 3.0$ Hz, 1H), 6.97 (d, $J = 3.0$ Hz, 1H), 6.58 (d, $J = 3.0$ Hz, 1H), 3.85 (s, 3H), 3.78 (s, 3H), 3.51 (s, 3H), 1.76 (s, 6H), 1.46 (s, 9H), 1.43 (s, 9H), 1.39 (s, 9H), 1.37 (s, 9H). ^{13}C NMR (125 MHz, CD_2Cl_2 , δ): 167.0, 164.8, 164.3, 155.9, 155.8, 152.1, 151.9, 146.5, 146.4, 146.3, 146.1, 143.4, 142.1, 142.0, 139.72, 139.70, 138.3, 131.2, 130.9, 130.1, 129.4, 129.3, 129.0, 128.9, 128.5, 126.4, 126.3, 123.1, 122.7, 121.6, 120.1, 120.0, 119.8, 119.3, 118.8, 112.7, 112.5, 56.24, 56.20, 52.3, 35.7, 35.51, 35.49, 35.08, 35.05, 32.1, 31.85, 31.80, 29.61, 29.60. FTIR (thin film) 2958, 2870, 1719, 1611, 1577, 1445, 1393, 1362, 1333, 1279, 1234, 1211, 1151, 1061. HRMS (ESI) Calcd for $\text{C}_{61}\text{H}_{70}\text{N}_2\text{O}_7$: $([\text{M} + \text{H}]^+) = 943.5256$. Found 943.5237.

2.5.3.2. **Mn[HSX(OMe)-COOMe]Cl (2)**

The synthesis was accomplished as described in Scheme 2. A vial containing a stirbar was charged with $\text{H}_2[\text{HSX}(\text{OMe})\text{-COOMe}]$ (**8**) (21.0 mg, 0.0222 mmol) and $\text{Mn}(\text{OAc})_2 \cdot 4\text{H}_2\text{O}$ (6.0 mg, 0.025 mmol). Ethanol (1.0 mL) was added, followed by CH_2Cl_2 (0.2 mL) and the reaction mixture was stirred at room temperature for 24 h. The dark brown reaction mixture was diluted with CH_2Cl_2 . The organic extract was washed with brine, dried over Na_2SO_4 , and concentrated under vacuum. The crude material was purified by column chromatography ($\text{CH}_2\text{Cl}_2/\text{Et}_2\text{O}$ gradient), and the desired product was obtained as a brown solid (22 mg, 96%). HRESI-MS $([\text{M} - \text{Cl}]^+) \text{C}_{61}\text{H}_{68}\text{N}_2\text{O}_7\text{MnCl}$ m/z , Calcd. 995.4402, Found 995.4436.

2.5.3.3. **$\text{H}_2[\text{salophen}(\text{OMe})]$**

A vial containing a stirbar was charged with 1,2-phenylenediamine (0.108 g, 1.00 mmol) and 3-*tert*-butyl-2-hydroxy-5-methoxybenzaldehyde (0.416 g, 2.00 mmol). Ethanol (4.0 mL) was added, the vial was sealed with a Teflon cap, and the reaction mixture was stirred at 100 °C for 21 hours. The desired product precipitated out of solution as a red-orange solid and was collected on a glass frit after filtering and copious washing with ethanol (0.369 g, 76%). ^1H NMR (500 MHz, CD_2Cl_2 , δ): 13.42 (s, 2H), 8.66 (s, 2H), 7.37 (dd, $J = 5.5$ Hz, 3.0 Hz, 2H), 7.29 (dd, $J = 5.5$ Hz, 3.0 Hz, 2H), 7.03 (d, $J = 3.0$ Hz, 2H), 6.77 (d, $J = 3.0$ Hz, 2H), 3.78 (s, 6H), 1.42 (s, 18H). ^{13}C NMR (125 MHz, CD_2Cl_2 , δ):

164.8, 155.8, 152.1, 143.0, 139.8, 128.2, 120.1 (2x), 119.0, 112.5, 56.2, 35.5, 29.5. FTIR (thin film) $\nu = 2954, 1617, 1595, 1571, 1448, 1428, 1333, 1206, 1150, 1060 \text{ cm}^{-1}$. HRESI-MS ($[M + Na]^+$) $C_{30}H_{36}N_2O_4$ m/z , Calcd. 511.2567, Found 511.2584.

2.5.3.4. **Mn[salophen(OMe)]Cl (3)**

A vial containing a stirbar was charged with H_2 [salophen(OMe)] (0.070 g, 0.143 mmol) and manganese (II) acetate tetrahydrate (0.039 g, 0.158 mmol). Ethanol (1.6 mL) was added, and the reaction mixture was stirred at room temperature for 21 hours. The dark brown reaction mixture was diluted with dichloromethane. The organic extract was washed with brine. The desired product precipitated out of solution as a brown solid and was collected on a glass frit after filtering and copious washings with diethyl ether (0.072 g, 87%). HRESI-MS ($[M - Cl]^+$) $C_{30}H_{34}N_2O_4MnCl$ m/z , Calcd. 541.1894, Found 541.1870.

2.5.3.5. **H_2 [salophen], X = H**

A vial containing a stirbar was charged with 1,2-phenylenediamine (108 mg, 1.00 mmol) and 3-*tert*-butyl-2-hydroxy-benzaldehyde (356 mg, 2.00 mmol). Ethanol (4.0 mL) was added, the vial was sealed with a Teflon cap, and the reaction mixture was stirred at 100 °C for 21 hours. The desired ligand precipitated from solution as an orange solid and was collected on a glass frit after filtering and copious washings with EtOH (287 mg, 67%). 1H NMR (500 MHz, CD_2Cl_2): 13.80 (s, 2H), 8.69 (s, 2H), 7.41-7.36 (m, 4H), 7.31-7.29 (m, 4H), 6.88 (t, $J = 7.5$ Hz, 2H), 1.42 (s, 18H). ^{13}C NMR (125 MHz, CD_2Cl_2): 165.0, 161.2, 143.1, 138.2, 131.3, 131.1, 128.2, 120.1, 119.7, 118.8, 35.3, 29.6. FTIR (thin film) 2959, 2943, 2908, 2867, 1610, 1571, 1427, 1391, 1363, 1311, 1275, 1194, 1146, 1107, 1087. HRMS (ESI) Calcd for $C_{28}H_{33}N_2O_2$: $[M + H]^+ = 429.25365$. Found 429.25349.

2.5.3.6. **Mn[salophen]Cl, X = H (5)**

A vial containing a stirbar was charged with the ligand H_2 [salophen], X = H (60.0 mg, 0.131 mmol) and $Mn(OAc)_2 \cdot 4H_2O$ (36.0 mg, 0.144 mmol). Ethanol (1.6 mL) was added, and the reaction mixture was stirred at room temperature for 21 hours. The dark brown reaction mixture was diluted with CH_2Cl_2 . The organic extract was washed with brine, dried over Na_2SO_4 , and concentrated to dryness. The crude material was purified by

column chromatography (CH₂Cl₂/Et₂O/MeOH gradient), and the desired final product Mn[salophen]Cl, X = H was obtained as a brown solid (60 mg, 84%). HRMS (ESI) Calcd for C₂₈H₃₀MnN₂O₂Mn: [M - Cl]⁺ = 481.16823. Found 481.16650.

2.5.3.7. Mn(V)[salophen]N, X = OMe

A vial containing a stirbar was charged with Mn(salophen)Cl, X = OMe (**3**) (25 mg, 0.043 mmol) in 0.6 mL MeOH. Under vigorous stirring at room temperature, ammonium hydroxide (41 μ L, 0.65 mmol; 16M in water) was added dropwise followed by NaOCl (130 μ L, 0.26 mmol; 2.0 M in water). CH₂Cl₂ was added, followed by water to form a biphasic mixture. The brown organic phase was washed with water (\times 3), dried over Na₂SO₄, and concentrated to dryness. The crude material was purified by flash chromatography (CH₂Cl₂ as eluent) to furnish the desired product as a brown solid (16.1 mg, 67%). The UV-vis spectrum of Mn(V)[salophen]N, X = OMe is shown in red in Figure 3b (5.0×10^{-5} M Mn(V)[salophen]N, X = OMe in 1:1 MeOH:MeCN at room temperature). ¹H NMR (500 MHz, CD₂Cl₂): 8.84 (s, 2H), 7.85 (dd, *J* = 6.0 Hz, 3.0 Hz, 2H), 7.40 (dd, *J* = 6.0 Hz, 3.0 Hz, 2H), 7.21 (d, *J* = 3.5 Hz, 2H), 6.71 (d, *J* = 3.5 Hz, 2H), 3.81 (s, 6H), 1.48 (s, 18H). ¹³C NMR (125 MHz, CD₂Cl₂): 166.6, 158.4, 150.4, 145.7, 143.9, 128.0, 126.4, 119.3, 115.6, 110.6, 56.1, 36.3, 29.9. FTIR (thin film) 2944, 1602, 1582, 1534, 1458, 1427, 1411, 1387, 1359, 1312, 1212, 1191, 1059, 1040. HRMS (ESI) Calcd for C₃₀H₃₄MnN₃O₄: [M + H]⁺ = 555.1930. Found 555.1911.

2.5.3.8. Mn(V)[salophen]N, X = *t*-Bu

A vial containing a stirbar was charged with Mn[salophen]Cl, X = *t*-bu (**4**) (25 mg, 0.040 mmol) in 0.6 mL MeOH. Under vigorous stirring at room temperature, ammonium hydroxide (41 μ L, 0.65 mmol; 16M in water) was added dropwise followed by NaOCl (130 μ L, 0.26 mmol; 2.0 M in water). CH₂Cl₂ was added, followed by water to form a biphasic mixture. The dark organic phase was washed with water (\times 3), dried over Na₂SO₄ and concentrated to dryness. The crude material was purified by flash chromatography (pentane:CH₂Cl₂ = 2:1 as eluent) to furnish the desired product as a greenish solid (19.5 mg, 81%). The UV-vis spectrum of Mn(V)[salophen]N, X = *t*-Bu, is shown in blue in Figure 3b (5.0×10^{-5} M Mn(V)[salophen]N, X = *t*-Bu in 1:1 MeOH:MeCN at room temperature). ¹H NMR (500 MHz, CD₂Cl₂): 8.89 (s, 2H), 7.86

(dd, $J = 6.5$ Hz, 3.5 Hz, 2H), 7.61 (d, $J = 2.5$ Hz, 2H), 7.40 (dd, $J = 6.5$ Hz, 3.5 Hz, 2H), 7.27 (d, $J = 2.5$ Hz, 2H), 1.51 (s, 18H), 1.35 (s, 18H). ^{13}C NMR (125 MHz, CD_2Cl_2): 168.6, 159.5, 145.8, 141.5, 139.0, 133.1, 128.8, 128.0, 119.8, 115.6, 36.4, 34.5, 31.5, 30.0. FTIR (thin film) 2954, 2909, 2867, 1605, 1579, 1527, 1488, 1463, 1422, 1387, 1359, 1258, 1197, 1179, 1046. HRMS (ESI) Calcd for $\text{C}_{36}\text{H}_{47}\text{MnN}_3\text{O}_2$: $[\text{M} + \text{H}]^+ = 608.30433$. Found 608.30316.

2.5.4. Stopped-flow Kinetic Studies

2.5.4.1. General Considerations

All solutions were prepared and handled in an inert atmosphere (argon-filled glove box), unless otherwise noted. Kinetics measurements were made using a Hi-Tech Scientific (Salisbury, Wiltshire, U.K.) SF-43 multi-mixing anaerobic cryogenic stopped-flow instrument equipped with a Hi-Tech Scientific Kinetascan diode array rapid scanning unit. Full-spectra kinetics data were fitted globally with the commercially available software Specfit32 with IS-2 Rapid Scanning Kinetic Software (Hi-Tech Scientific).

2.5.4.2. Materials

MeOH (anhydrous) was used as received (Burdick & Jackson). All other solvents were purchased from VWR Scientific Products, passed through an M. Braun, Inc. purification system and sparged with N_2 to remove trace O_2 prior to use. 3-Chloroperoxybenzoic acid (*m*-CPBA) was purchased from Aldrich (77%) and purified by washing with pH 7.40 phosphate buffer and recrystallized from pentane to remove 3-chlorobenzoic acid. Purity (>95%) was determined by ^1H NMR.

2.5.4.3. Stopped-Flow Experiments

In a representative procedure, a gas-tight syringe was charged with 8.0×10^{-5} M (1) in 1: 1 MeOH: MeCN (25 mL, 2.0 μmol). A second gas-tight syringe was charged with 6.6×10^{-4} M *m*-CPBA in a 1: 1 MeOH: MeCN (25 mL, 17 μmol). The solutions were loaded into the stopped-flow spectrophotometer and triggered by simultaneous injection of a 0.1 mL of each solution to make the reactant concentrations 4.0×10^{-5} M and 3.3×10^{-4} M in manganese and *m*-CPBA, respectively. The solutions were cooled to -20 °C prior to

mixing and maintained at that temperature in a chilled heptane bath throughout the reaction. The reaction was monitored by UV-vis spectroscopy. Spectra (350-700 nm) were acquired for 100 s at 0.5 second intervals. Figure 2.2a shows the absorption spectrum of the Mn(III) substitution of the axial chloride ligand of the reactant by the *m*-CPBA substrate. The spectral changes associated with the addition of the non-reactive benzoate, which serves as a model for the substitution reaction, are shown in Figure 2.2b.

Conditions to obtain spectra in Figure 2.2a.

Stopped-flow UV-vis spectra obtained from reactions of *m*-CPBA (3.3×10^{-4}) with 4.0×10^{-5} M **1** (red solid line) ca. 3 s post injection in 1: 1 MeOH: MeCN at 20 °C.

Conditions to obtain spectra in Figure 2.2b

UV-vis spectrum obtained from a solution of 5.0×10^{-5} M **1** in 1: 1 MeOH: MeCN at room temperature (red solid line). UV-vis spectrum obtained from a solution of 5.0×10^{-5} M **1** in 1:1 MeOH:MeCN at room temperature in the presence of benzoic acid (5.0×10^{-3} M) (black dotted line).

Conditions to obtain spectra in Figure 2.3a

Absorption spectra obtained from spectral global analysis of a stopped-flow reaction of 4.0×10^{-5} M **1** and 3.3×10^{-4} M *m*-CPBA in 1:1 MeOH:MeCN at -20 °C over 800 s.

2.5.5. Hydrogen Peroxide Disproportionation Reactions

Dismutation reactions were performed at room temperature in a sealed (PTFE septum) 3 mL reaction vial equipped with a magnetic stirbar and a capillary gas delivery tube linked to a graduated burette filled with water. The reaction vial was charged with a stock solution of the corresponding catalyst in CH_2Cl_2 (1.0 mL). MeOH (0.5 mL) was added followed by H_2O_2 (790 μL , 8.22 mmol; 10.4 M (30% aqueous solution), and the reaction mixture was stirred vigorously. The time was set to zero immediately after the addition of H_2O_2 . The progress of the reaction was monitored volumetrically, and the amount of produced O_2 (*n*) was calculated through the gas equation $pV=nRT$, assuming that $p = 1$ atm.

The amount of catalyst used to obtain the results of Table 2.2: Mn[HSX(OMe)-COOH]Cl (1.0 mg, 0.00098 mmol; from a 1.0 mg/mL CH₂Cl₂ stock solution) to give 106 cm³ of O₂ in 1 hr; Mn[HSX(OMe-COOMe)]Cl (1.0 mg, 0.00097 mmol; from a 1.0 mg/mL CH₂Cl₂ stock solution) to give 13.0 cm³ of O₂ in 1 hr; and Mn[salophen(OMe)]Cl (0.56 mg, 0.00098 mmol) and benzoic acid (1.2 mg, 0.00098 mmol) in 10.0 mL CH₂Cl₂) to give 2.5 cm³ of O₂ in 1 hr.

2.5.6. UV-Vis Kinetics of Mn[HSX(OMe)]Cl (1) Decomposition in the Presence of H₂O₂.

Kinetic studies were performed in a sealed quartz cuvette at room temperature. The cuvette was charged with a stock solution of 1 (2.6×10^{-5} M) in MeOH (3.0 mL). H₂O₂ was added (50 μ L; 32% aqueous solution; $d = 1.1126$ g/mL), thereby generating a 2.5×10^{-5} M, 0.17 M, and 0.69 M solution of 1, H₂O₂, and H₂O, respectively. The time was set to zero immediately after addition of H₂O₂. The first spectrum was taken 30 seconds after injection of H₂O₂. The progress of the reaction was monitored by UV-vis spectroscopy at two minute intervals. The decrease in absorbance at 500 nm was fitted to an exponential function, and k_{obs} was determined to be 2.9×10^{-4} s⁻¹.

2.5.7. Independent Generation of High-Valent Mn(V) oxo

Conditions to obtain the spectra in Figure 3a

Absorption spectra from a stopped-flow reaction of 2.5×10^{-5} M Mn[HSX(OMe)-COOH]Cl with 1.7×10^{-1} M H₂O₂ in 2.5×10^{-4} M NaOH solution in MeOH at -50 °C. Formation of Mn-oxo (green) is observed at ~ 96 s post-injection.

Conditions to obtain the spectra in Figure 3b

Absorption spectra from spectral global analysis of a stopped-flow reaction of 4.0×10^{-5} M Mn[HSX(OMe)-COOH]Cl with 3.3×10^{-4} M m-CPBA in 1: 1 MeOH: MeCN at -20 °C. The calculated Mn-oxo intermediate at ~ 60 s post-injection is shown in green.

Conditions to obtain the spectra in Figure 3c

Absorption spectra from a reaction of 5.0×10^{-5} M Mn[HSX(OMe)-COOH]Cl with iodosylbenzene (50 equiv.) in 1: 1 MeOH: MeCN at room temperature. Formation of Mn-oxo (green) is observed 28 min post-addition. Due to insolubility of iodosylbenzene, the reaction solution was filtered through an acrodisc prior to measurement.

Conditions to obtain the spectra in Figure 4a

Absorption spectrum from a reaction of 2.5×10^{-5} M Mn[salophen(X)]Cl with 3.5×10^{-2} M H₂O₂ in 2.5×10^{-4} M NaOH solution in MeOH at room temperature. Formation of Mn[salophen(*t*-Bu)]O (blue) is observed 10 s post-injection. Formation of Mn[salophen(OMe)]O (red) is observed 10 s post-injection.

Conditions to obtain the spectra in Figure 3, left

Absorption spectrum from a reaction of 2.5×10^{-5} M Mn[salophen(*t*-Bu)]Cl with 3.5×10^{-2} M H₂O₂ in 2.5×10^{-4} M NaOH solution in MeOH (3.0 mL) at room temperature. Formation of Mn[salophen(*t*-Bu)]O (green) is observed 10 s post-injection. Et₂S (100 mL, 0.937 mmol) is added at 50 s post-injection of H₂O₂. Formation of Mn[salophen(*t*-Bu)]Cl starting material (red) is observed 20 s post-injection of Et₂S.

Conditions to obtain the spectra in Figure 3, right

Absorption spectrum from a reaction of 2.5×10^{-5} M Mn[salophen(*t*-Bu)]Cl with 3.5×10^{-2} M H₂O₂ in 2.5×10^{-4} M NaOH solution in MeOH (3.0 mL) at room temperature. Formation of Mn[salophen(*t*-Bu)]O (green) is observed 10 s post-injection. P(OEt)₃ (100 mL, 0.584 mmol) is added at 50 s post-injection of H₂O₂. Complete re-formation of Mn[salophen(*t*-Bu)]Cl starting material (red) is observed 760 s post-injection of P(OEt)₃.

References and Notes

1. Yeh, C.-Y.; Chang, C. J.; Nocera, D. G. *J. Am. Chem. Soc.* **2001**, *123*, 1513-1514.
2. Chang, C. J.; Yeh, C.-Y.; Nocera, D. G. *J. Org. Chem.* **2002**, *67*, 1403-1406.
3. Chang, C. J.; Chng, L. L.; Nocera, D. G. *J. Am. Chem. Soc.* **2003**, *125*, 1866-1876.
4. Chng, L. L.; Chang, C. J.; Nocera, D. G. *Org. Lett.* **2003**, *5*, 2421-2424.
5. Liu, S.-Y.; Nocera, D. G. *J. Am. Chem. Soc.* **2005**, *127*, 5278-5279.
6. Palucki, M.; Finney, N. S.; Pospisil, P. J.; Güler, M. L.; Ishida, T.; Jacobsen, E. N. *J. Am. Chem. Soc.* **1998**, *120*, 948-954.
7. Law, N. A.; Caudle, M. T.; Pecoraro, V. L. In *Manganese Redox Enzymes and Model Systems: Properties, Structure, and Reactivity*; Pecoraro, V. L., Ed.; Academic Press: San Deigo, CA, 1999; Vol. 46.
8. Nicholls, P.; Fita, I.; Loewen, P.C. *Adv. Inorg. Chem.* **2001**, *51*, 51-106.
9. Yodar, D. W.; Hwang, J.; Penner-Hahn, J. E. In *Metal Ions in Biological Systems*; Sigel, A.; Sigel, H., Eds.; Marcel Dekker: New York, 1999; Vol. 37.
10. Christianson, D. W. *Prog. Biophys. Mol. Biol.* **1997**, *67*, 217.
11. Wu, A. J.; Penner-Hahn, J. E.; Pecoraro, V. L. *Chem. Rev.* **2004**, *104*, 903-938.
12. Rosenthal, J.; Chng, L. L.; Friedman, S. P.; Nocera, D. G. *in press*.
13. Liu, S.-Y.; Yang, J. Y., Nocera, D. G. *unpublished work*.
14. Feth, M.P.; Bolm, C.; Hildebrand, J. P.; Köhler, M.; Beckmann, O.; Bauer, M.; Ramamonjisoa, R.; Bertagnolli, H. *Chem.-Eur. J.* **2003**, *9*, 1348-1359.
15. McDonnell, F. M.; Fackler, N. L. P.; Stern, C.; O'Halloran, T. V. *J. Am. Chem. Soc.* **1994**, *116*, 7431-7432.
16. Du Bois, J.; Hong, J.; Carreira, E. M.; Day, M. W. *J. Am. Chem. Soc.* **1996**, *118*, 915-916.
17. Feichtinger, D.; Plattner, D. *Chem. Eur. J.* **2001**, *7*, 591-599.
18. Davydov, R.; Makris, T. M.; Kofman, V.; Werst, D. E.; Sligar, S. G.; Hoffman, B. M. *J. Am. Chem. Soc.* **2001**, *123*, 1403-1415.
19. Ogliaro, F.; de Visser, S. P.; Cohen, S.; Sharma, P. K.; Shaik S. *J. Am. Chem. Soc.* **2002**, *124*, 2806-2817.
20. Groves, J. T.; Watanabe, Y. *J. Am. Chem. Soc.* **1988**, *110*, 8443-8452.
21. Soper, J. D.; Kryatov, S. V.; Rybak-Akimova, E. V.; Nocera, D. G. *J. Am. Chem. Soc.* **2007**, *ASAP*, DOI: 10.1021/ja0683032.
22. *Cytochrome P-450 Structure, Mechanism, and Biochemistry*; Ortiz de Montellano, P. R., Ed.; Plenum Press: New York, 1986.

23. Sono, M.; Roach, M. P.; Coulter, E. D.; Dawson, J. H. *Chem. Rev.* **1996**, *96*, 2841-2887.
24. Dunford, H. B. *Heme Peroxidases*; Wiley: New York, 1999.
25. Watanabe, Y. In *The Porphyrin Handbook*; Kadish, K. M.; Smith, K. M.; Guillard, R., Eds.; Academic Press: San Diego, 2000; Vol. 4, pp 97-117.
26. Newcomb, M.; Zhang, R.; Chandrasena, R. E. P.; Halgrimson, J. A.; Horner, J. H.; Makris, T. M.; Sligar, S. G. *J. Am. Chem. Soc.* **2006**, *128*, 4580-4581.
27. Suslick, K. S. In *The Porphyrin Handbook*; Kadish, K. M.; Smith, K. M.; Guillard, R., Eds.; Academic Press: San Diego, 2000; Vol. 4, pp 41-63.
28. Rodriguez-Lopez, J. N.; Lowe, D. J.; Hernandez-Ruiz, J.; Hiner, A. N. P.; Garcia-Canovas, F.; Thorneley, R. N. F. *J. Am. Chem. Soc.* **2001**, *123*, 11838-11847.
29. Veitch, N. C.; Smith, A. T. In *Advances in Inorganic Chemistry*; Academic Press: New York, 2001; Vol. 51, pp 107-162.
30. Newcomb, M.; Chandrasena, R. E. P. *Biochem. Biophys. Res. Commun.* **2005**, *338*, 394-403.
31. Davydov, R.; Chemerisov, S.; Werst, D. E.; Rajh, T.; Matsui, T.; Ikeda-Saito, M.; Hoffman, B. M. *J. Am. Chem. Soc.* **2004**, *126*, 15960-15961.
32. Hiner, A. N. P.; Raven, E. L.; Thorneley, R. N. F.; Garcia-Canovas, F.; Rodriguez-Lopez, J. N. *J. Inorg. Biochem.* **2002**, *91*, 27-34.
33. Hersleth, H.-P.; Ryde, U.; Rydberg, P.; Gorbitz, C. H.; Andersson, K. K. *J. Inorg. Biochem.* **2006**, *100*, 460-476.
34. Behan, R. K.; Green, M. T. *J. Inorg. Biochem.* **2006**, *100*, 448-459.
35. Khavrutskii, I. V.; Musaev, D. G.; Morokuma, K. *Inorg. Chem.* **2005**, *44*, 206-315.
36. Yang, J. Y.; Nocera, D. G. *submitted for publication*.
37. Zhang, W.; Loebach, J. L.; Wilson, D. R.; Jacobsen, E. N. *J. Am. Chem. Soc.* **1990**, *112*, 2081-2083.
38. Irie, R.; Noda, K.; Ito, Y.; Matsumoto, N.; Katsuki, T. *Tetrahedron Lett.* **1990**, *31*, 7345-7348.
39. Jacobsen, E. N.; Wu, M. H. In *Comprehensive Asymmetric Catalysis*, Jacobsen, E. N., Pfaltz, A., Yamamoto, H., Eds.; Springer: New York, 1999; pp 649-677.
40. Lin, G.-Q.; Li, Y.-M.; Chan, A. S. C. In *Principles and Applications of Asymmetric Synthesis*; Wiley-Interscience: New York, 2001; pp 237-241.
41. A similar trend is observed for Hangman Mn-salophen complexes, see reference 5.
42. McGarrigle E. M.; Gilheany, D. G. *Chem. Rev.* **2005**, *105*, 1563-1602.
43. Sabater, M. J.; Alvaro, M.; Garcia, H.; Palomares, E.; Scaiano, J. C. *J. Am. Chem. Soc.* **2001**, *123*, 7074-7080.

44. Srinivasan, K.; Michaud, P.; Kochi, J. K. *J. Am. Chem. Soc.* **1986**, *108*, 2309-2320.
45. Abashkin, Y. G.; Burt, S. K. *Inorg. Chem.* **2005**, *44*, 1425-1432.
46. Abashkin Y. G.; Burt, S. K. *J. Phys. Chem. B* **2004**, *108*, 2708-2711.
47. Larrow, J. R.; Jacobsen, E. N.; Gao, Y.; Hong, Y.; Nie, X.; Zepp, C. M. *J. Org. Chem.* **1994**, *59*, 1939-1942.
48. Liu, S.-Y.; Nocera, D. G. *Tetrahedron Lett.* **2006**, *47*, 1923-1926.

Chapter 3

Synthesis of Enantiopure Manganese Hangman Salens and Their Epoxidation Activity

Portions of the work presented in this chapter have been published:

Yang, J. Y.; Bachmann, J.; Nocera, D. G. *J. Org. Chem.* **2006**, *71*, 8706-8714.

3.1. Motivation and Specific Aims

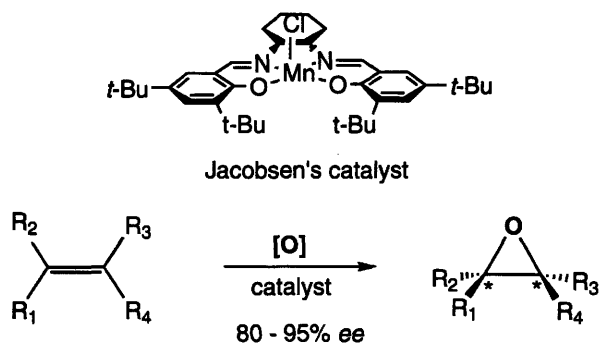
The Hangman salen system described in Chapter 2 permitted the study of redox effects on the catalase activity, and the stopped-flow detection of intermediates in the first two steps of the catalase cycle and the kinetics of their formation, including a putative Mn(V) oxo species. We wished to extend the reactivity of the Hangman salen framework to oxygen atom transfer (OAT) chemistry. In addition, we sought to modify the ligand framework to incorporate a chiral functionality to see if we can add the feature of enantioselectivity to OAT transformations. A synthetic strategy for the construction of chiral salen ligands bearing two rigid xanthene spacers functionalized with carboxylic acid groups is presented. Suzuki cross-coupling methodology is used to furnish the appropriately functionalized xanthene spacers to a salicylaldehyde, which is subsequently condensed with (1*R*,2*R*)-(-)-1,2-diaminocyclohexane to produce salen ligands featuring an expandable molecular cleft capable of multiple hydrogen bonding interactions, in addition to metallosalen oxidation chemistry. Within this functionalized Hangman framework, the stereochemistry of the cyclohexane backbone of the salen platform is revealed in the epoxidation of 1,2-dihydronaphthalene by the metal oxo.

3.2. Background

Catalytic oxygen atom transfer chemistry to olefins using first row metallosalen compounds was first explored by Kochi^{1,2} and Burrows³ using achiral salen ligands. Shortly thereafter, Katuski⁴ and Jacobsen⁵ independently synthesized manganese salen complexes incorporating chiral functionalities into the ligand that were capable of epoxidizing a wide range of olefins with very high selectivity. Manganese salen catalysts have been optimized to synthesize *cis*-disubstituted,^{6,7} *trans*-disubstituted,^{8,9} trisubstituted,¹⁰ and even some monosubstituted¹¹ epoxides with high enantioselectivity. Prior to this, the most selective epoxidation catalyst had been titanium tartrate, which is limited in substrate scope to allylic alcohols.¹² The broad substrate scope of manganese salens and modular synthesis led to a rapid expansion to catalyst variants.^{5,13-19}

The most commonly used and commercially available catalyst is manganese [(1,2-cyclohexanediamino-*N,N'*-bis(3,5-di-*tert*-butylsalicylidene)] chloride (shown in Chart

Chart 3.1



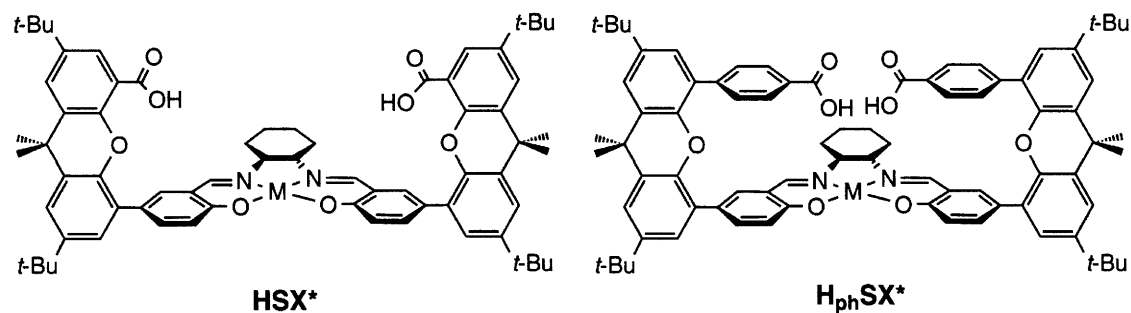
3.1), which combines the key electronic and steric features necessary for high selectivity with synthetic accessibility and substrate generality.^{6,13-20} It is frequently employed on both a laboratory and industrial scale and its synthesis has been commercialized on a multi-hundred kilogram scale.^{21,22} The widespread use of this catalyst has been fueled by its ease of use and economical cost. This has mediated one of the catalyst's shortcomings; decomposition under the oxidizing conditions typically limits the catalyst to double digit turnover numbers (TON). Depending on the substrate, the TON can be as low ten.⁵ Given the remarkable ability for the manganese Hangman porphyrins (HPX) to enhance the epoxidation of olefins by an order of magnitude over the unmodified platform using the mild oxidant hydrogen peroxide, we set out to unite the enantioselective OAT chemistry of a salen framework with the PCET-mediated catalysis afforded by a Hangman framework.

3.3. Results and Discussion

3.3.1. Ligand Design

We wished to incorporate the highly successful chiral 1,2-diaminocyclohexane bridge into our Hangman architecture. This objective precluded the use of Hangman salophen platforms of the type presented in Chapter 2, because the ligand bridge lacks the sp^3 carbons that can impart chirality. Simply replacing the 1,2-phenylenediamine backbone is not prudent; attachment of the xanthene scaffold on a cyclohexane backbone would dynamically shift the ligand geometry as it transitioned through chair and boat conformers. Additionally, forming a bond between the aryl-carbon on the xanthene to the aliphatic-carbon bond on the cyclohexanediamine is synthetically more challenging relative to aryl-aryl bond coupling. Therefore, we sought to adjust the attachment point of

Chart 3.2



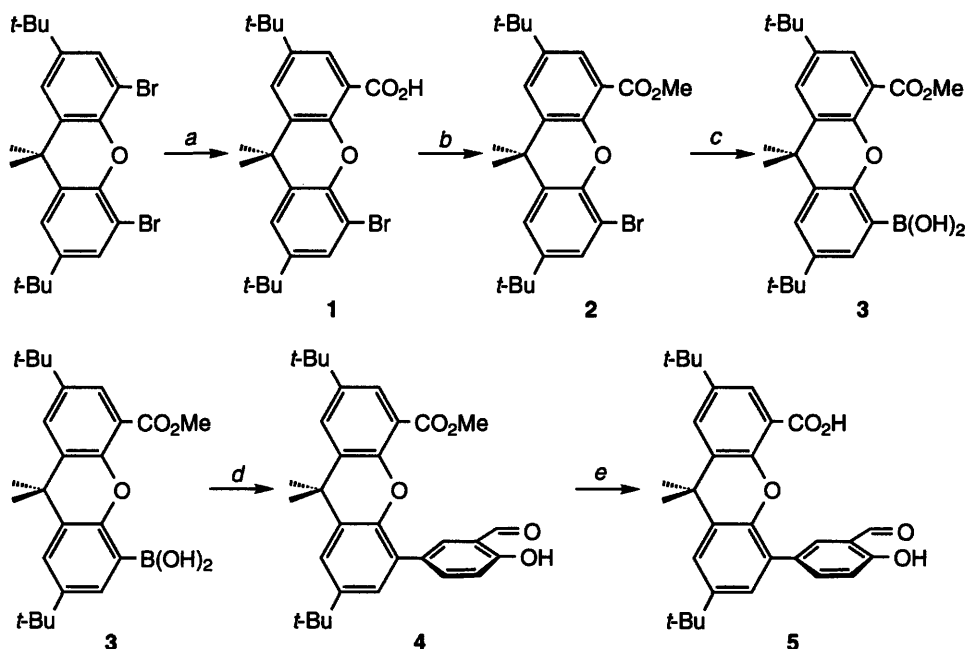
the functionalized xanthene to the 5 and 5' position on the phenolic arms of the macrocycle.

The two imine bonds on a salen are prone to hydrolysis²³⁻²⁶ and exchange²⁷ which makes it difficult to synthesize salens composed of two uniquely functionalized salicylaldehydes, since they can easily disproportionate in the presence of trace water to form a mixture of symmetric and asymmetric salens.^{28,29} (This issue is discussed further in Chapter 5). To circumvent this problem, we construct the symmetric salen complex using two equivalents of the functionalized salicylaldehyde per 1,2-cyclohexanediamine bridge. The (1*R*,2*R*)-(-)-1,2-diaminocyclohexane enantiomer was targeted owing to its lower cost. As the role of the acid-to-metal distance is unclear, we set out to synthesize the two variants, named HSX* and H_{ph}SX*, shown in Chart 3.2. The synthesis and OAT chemistry of these compounds is described below.

3.3.2. Synthesis of Hangman Salen Ligands (HSX*)

Scheme 3.1 illustrates our initial attempts to synthesize **5**, the precursor to synthesis of the HSX* ligand. We followed established methods to functionalize the xanthene bridge selectively with a carboxylic acid (**1**) from the commercially available xanthene dibromide.^{30,31} The methyl ester (**2**) derivative is obtained directly by protection of **1** upon refluxing methanol with a catalytic amount of sulfuric acid.³¹ We initially focused on obtaining **5** by replacing the bromide in **1** with a boronic acid in order to establish a site for subsequent cross-coupling with 5-bromosalicylaldehyde. This was achieved using palladium catalyzed cross-coupling conditions with bis(pinacolato)diboron,³² but the reaction and the subsequent Suzuki coupling only proceeded when the acid is protected

Scheme 3.1

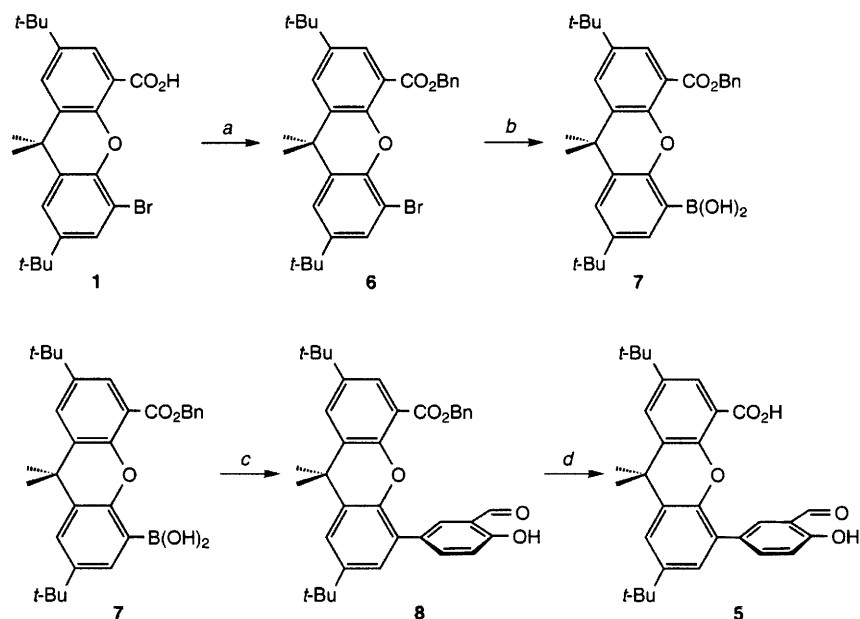


(a) *i*) phenyllithium, THF, *ii*) CO₂(g), (b) H₂SO₄, MeOH, (c) bis(pinacolato)diboron, Pd(dppf)Cl₂, KOAc, DMSO, (d) 5-bromosalicylaldehyde, Pd(dppf)Cl₂, Na₂CO₃, DME: H₂O (9: 1), (e) BBr₃, CH₂Cl₂

by an ester functionality. Methyl ester **2** was used to obtain the boronic ester which is hydrolyzed to the boronic acid upon recrystallization to generate precursor **3** in 43% yield. X-ray quality crystals confirmed the structure, shown in Figure 3.2 in the Experimental Section. **3** is then coupled to 5-bromosalicylaldehyde to afford precursor **4** in 40% yield.^{33,34} The two coupling steps provided product for a combined 17% yield. However, it was found that the methyl ester proved difficult to deprotect to achieve the desired precursor **5**. Very little or no reaction was observed upon refluxing with a variety of weak bases; the harsher reagent boron tribromide successfully gave the acid with a modest 28% yield.

Alternatively, the benzyl ester protecting group on the acid was also used as shown in Scheme 3.2. The benzyl ester **6** can be made in quantitative yield from the previously described precursor **1** using benzyl alcohol and 3-dicyclohexylcarbodiimide with a catalytic amount of 4-dimethylaminopyridine.³⁵ Following the otherwise analogous synthetic route of replacing the bromide on the benzyl ester protected xanthene with a boronic acid followed by Suzuki coupling to 5-bromosalicylaldehyde to give **8** also

Scheme 3.2

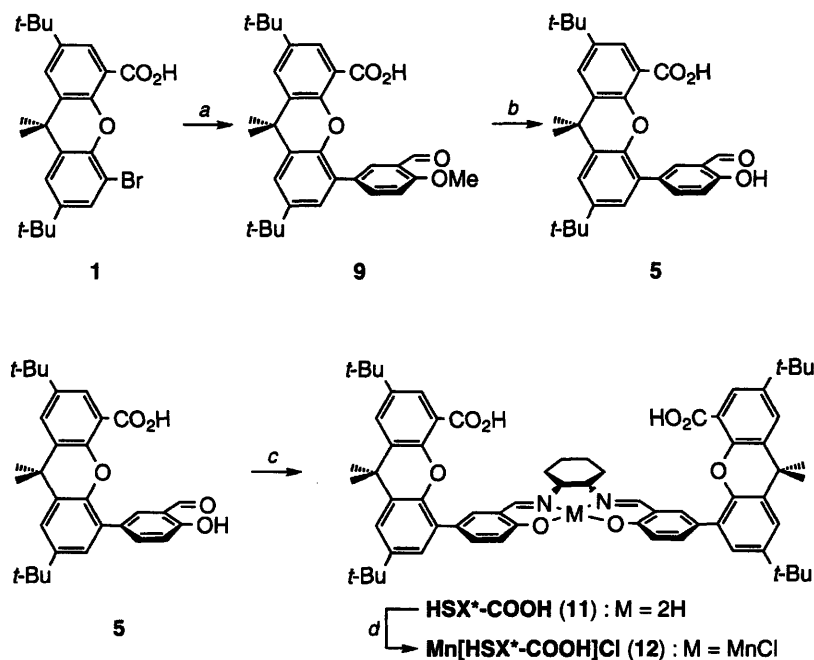


(a) benzyl alcohol, DCC, DMAP, CH₂Cl₂, (b) bis(pinacolato)diboron, Pd(dppf)Cl₂, KOAc, DMSO, (c) 5-bromosalicylaldehyde, Pd(dppf)Cl₂, Na₂CO₃, DME: H₂O (9:1), (d) H₂, Pd on charcoal, ethyl acetate

resulted in a modest combined yield of 19% in the successive palladium catalyzed cross-coupling steps. Although the benzyl ester was easier to cleave using hydrogen gas over activated palladium on charcoal, the overall yield along this synthetic pathway was not favorable. We therefore sought an alternative synthetic pathway to the Hangman salen ligand HSX*.

Scheme 3.3 outlines the synthetic strategy that successfully delivers the HSX* ligand in good yield. With the appropriately functionalized xanthene precursor **1** in hand, the construction of the salen macrocycle begins with the catenation of 3-formyl-4-ethoxyphenyl boronic acid to the remaining bromide of **1**. Effectively the site of boronic acid and bromide functionalization on the xanthene and salicylaldehyde has been inverted from that of Scheme 3.1 and Scheme 3.2. This important modification provides a better nucleophilic site for the Suzuki cross-coupling step than the boronic acid functionalized xanthene and consequently delivered **9** in good yield. Subsequent deprotection of the methyl ether by treatment with boron tribromide^{36,37} yields the appropriate xanthene functionalized salicylaldehyde derivatives **5**. The construction of the salen ring is

Scheme 3.3

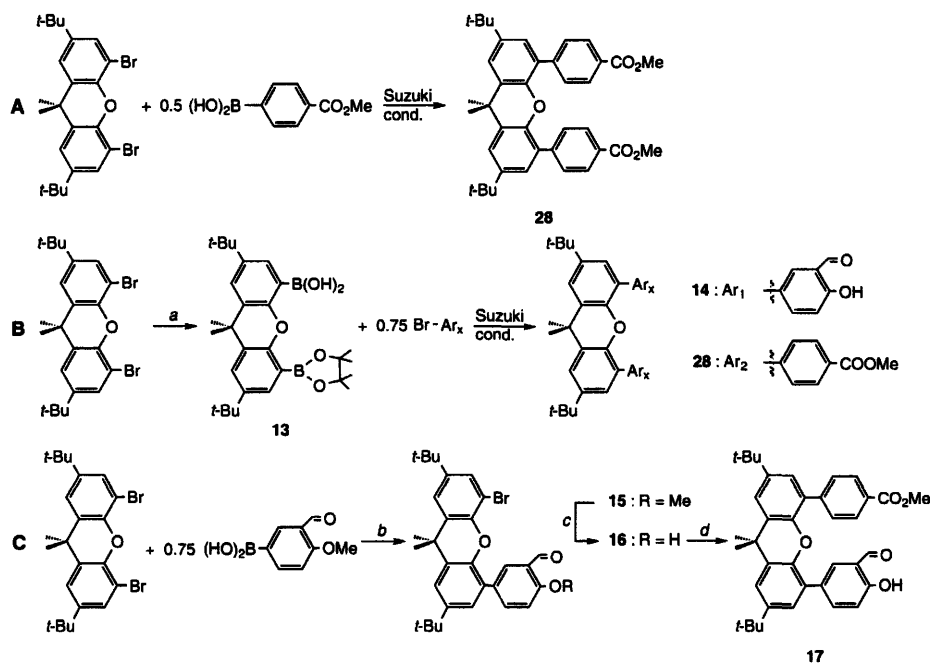


(a) 3-formyl-4-methoxyphenylboronic acid, Na_2CO_3 , $\text{Pd}(\text{PPh}_3)_4$, $\text{DMF}:\text{H}_2\text{O}$ (9:1), (b) BBr_3 , CH_2Cl_2 , (c) (1*R*,2*R*)-(-)-1,2-diaminocyclohexane, EtOH , (d) (i) $\text{Mn}(\text{OAc})_2(\text{H}_2\text{O})_4$, (ii) $\text{NaCl}(\text{aq})$

completed with the condensation, in high yield, of **5** with 0.5 equivalents of (1*R*,2*R*)-(-)-1,2-diaminocyclohexane to produce the desired Hangman salen ligand **11**. Mass spectral evidence shows no evidence of any singly condensed diamine product and the ^1H NMR integrations are consistent with two functionalized xanthenes to one cyclohexanediamine bridge. Analogous porphyrins ligands bearing two xanthene bridges possess two different atropisomers (xanthenes facing each other across the macrocycle as opposed to the xanthenes being one-up and one-down) that can be independently identified by ^1H NMR spectroscopy. For these porphyrin ligands, no exchange is observed between the two atropisomers in solution at room temperature.^{38,39} In contrast, the ^1H NMR for the HSX^* and $\text{H}_{\text{ph}}\text{SX}^*$ ligands at room temperature show only one set of well-resolved ligand peaks, suggesting there is either one atropisomer in solution, or exchange between the two is extremely rapid. The metallated salen **12** is synthesized by refluxing the ligand with manganese(II) acetate in air, followed by an aqueous sodium chloride solution workup, which provides the chloride salt.

3.3.3. Synthesis of Benzoic Acid Functionalized Hangman Salen Ligands ($H_{ph}SX^*$)

Scheme 3.4



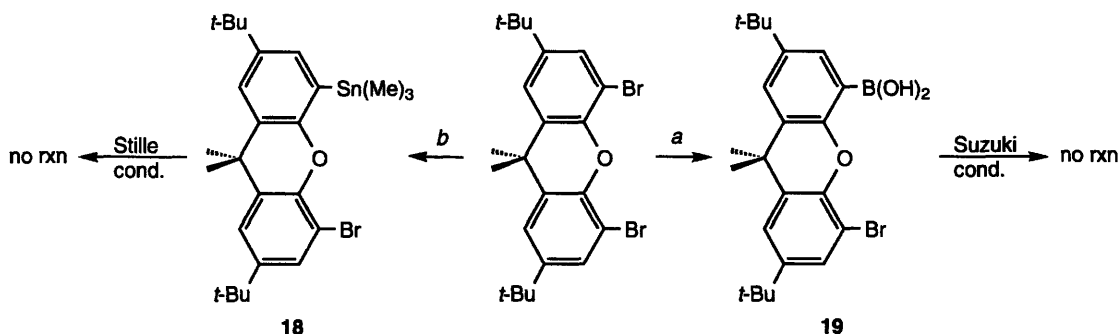
(a) bis(pinacolato)diboron, $\text{Pd}(\text{dppf})\text{Cl}_2$, KOAc, DMSO, (b) 3-formyl-4-methoxyphenylboronic acid, Na_2CO_3 , $\text{Pd}(\text{PPh}_3)_4$, DMF: H_2O (9:1), (c) BBr_3 , CH_2Cl_2 , (d) 4-methoxycarbonylphenylboronic acid, Na_2CO_3 , $\text{Pd}(\text{dppf})\text{Cl}_2$, DME: H_2O (3: 1)

In order to assemble the benzoic acid functionalized Hangman salen ligand ($H_{ph}SX^*$), we targeted the synthesis of precursor **25** (shown in Scheme 3.6). The selective functionalization of the 4 and 5 positions of the xanthene spacer with a benzoic acid and a salicylaldehyde functionality, respectively, was required. In order to attach these two aryl groups, we once again looked to palladium-catalyzed cross-coupling methods.

The most straightforward attempt to achieve this selective functionalization is described in Scheme 3.4. Xanthene dibromide was first allowed to react with one equivalent with of 4-methoxycarbonylphenylboronic acid as shown in route A under Suzuki coupling conditions. However, this did not result in the mono-functionalized xanthene spacer; the product consisted only of the symmetric doubly functionalized benzoic acid (**28**). The next attempt (route B) began with the boronic acid/ester group on the xanthenes, effectively reversing the electrophile/nucleophile groups for the coupling reaction.

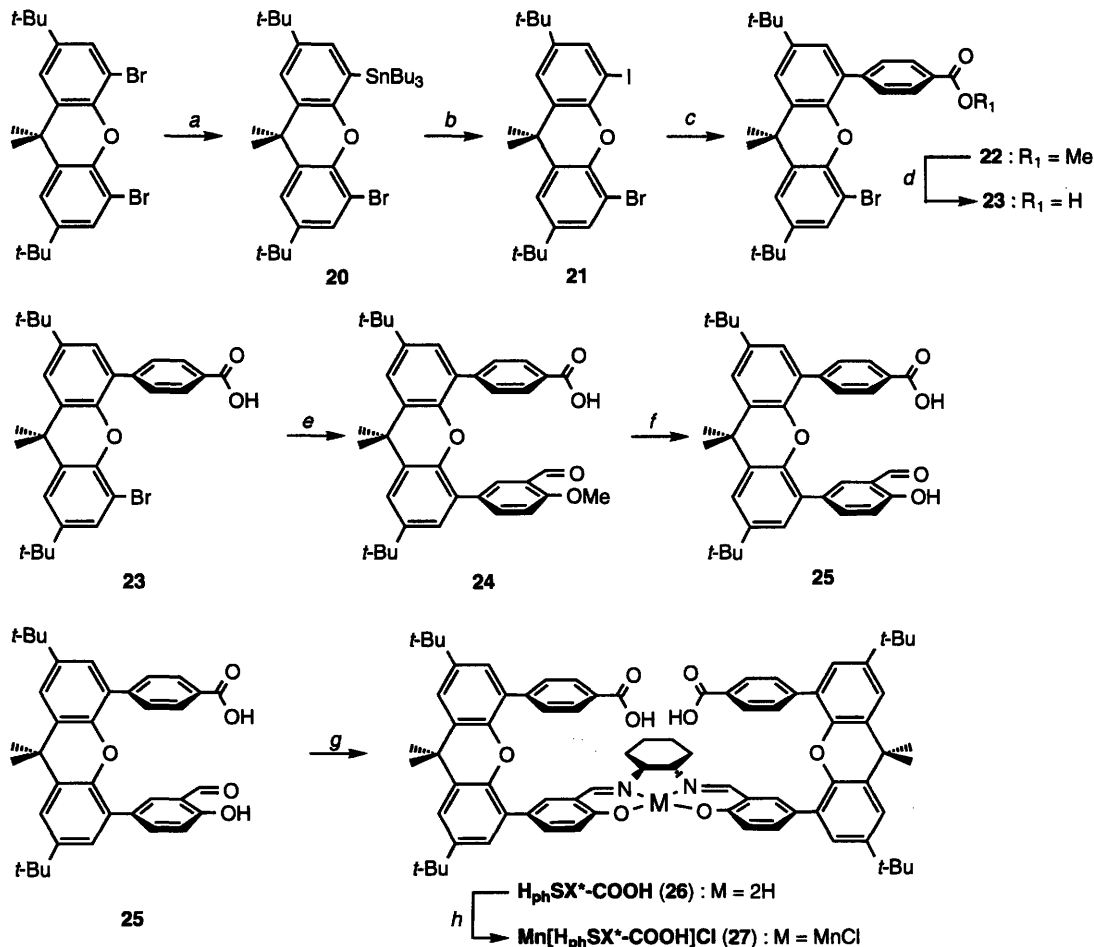
Reaction with less than one equivalent of 5-bromosalicylaldehyde and methyl-4-bromobenzoate resulted primarily in the bis-coupled products **14** and **28**. The highest yield for a monocatenated product was obtained by coupling the xanthene dibromide with 0.75 equivalents of 3-formyl-4-methoxyphenylboronic acid, which only provided 5% yield of **15**. Upon deprotection of the methyl ether via boron tribromide, we obtain **16**, which can be subsequently coupled under Suzuki conditions with methoxycarbonylphenylboronic acid to give **17** for an overall yield of less than 3%. From the resulting predominant biscoupled products in this series of reactions, it is apparent that the initial coupling to the xanthene bromo or boronic acid group activates the other aryl carbon site palladium-catalyzed Suzuki coupling that we employ, thus resulting in impractical yields for the overall synthesis.

Scheme 3.5



We therefore sought to begin our synthesis with differentially functionalized xanthenes as starting synthons, thereby introducing the selectivity before addition of the benzoic acid and salicylaldehyde to the xanthene framework, as shown in Scheme 3.5. We xanthene dibromide was treated with one equivalent of phenyllithium, followed by addition of triisopropyl borate and hydrolysis. The resulting product (**19**) could be purified via column chromatography. However, **19** was completely unreactive to the aryl boronic acids and aryl bromides that we tested under a variety of Suzuki- coupling conditions. Attempts were made to promote coupling using conditions described to couple the generally more difficult aryl chlorides.⁴⁰⁻⁴⁴ Notwithstanding, precursor **19** was found to be completely inert to palladium-catalyzed cross-coupling conditions. In the same vein, we isolated the alkyltin and bromo functionalized xanthene **18** was isolated by using trimethyltin chloride following treatment with phenyllithium. Stille-coupling conditions⁴⁵

Scheme 3.6



(a) *i*) phenyllithium, THF, *ii*) $\text{Sn}(n\text{-Bu})_3\text{Cl}$, (b) I_2 , CH_2Cl_2 , (c) 4-bromobenzoic acid methyl ester, CsF, $\text{Pd}(\text{PPh}_3)_4$, DME, (d) NaOH, THF/ H_2O , (e) 3-formyl-4-methoxyphenylboronic acid, Na_2CO_3 , $\text{Pd}(\text{PPh}_3)_4$, DMF: H_2O (9:1), (f) BBr_3 , CH_2Cl_2 , (g) (1*R*,2*R*)-(-)-1,2-diaminocyclohexane, EtOH, (h) *i*) $\text{Mn}(\text{OAc})_2(\text{H}_2\text{O})_4$, *ii*) $\text{NaCl}(\text{aq})$

were attempted in an effort to attach a salicylaldehyde to the aryl tin site, but this strategy also proved fruitless. It is not entirely clear why a xanthene functionalized with both nucleophilic and electrophilic group would be unreactive to aryl-aryl bond coupling. However, it appears from the attempts outlined in Scheme 3.4 that there are non-trivial electronic effects between the two aryl carbons that are the site of functionalization. The oxygen on the xanthene may effectively neutralize the nucleophilic or electrophilic nature of the functionalized aryl carbons, limiting their ability to react with the palladium catalyst.

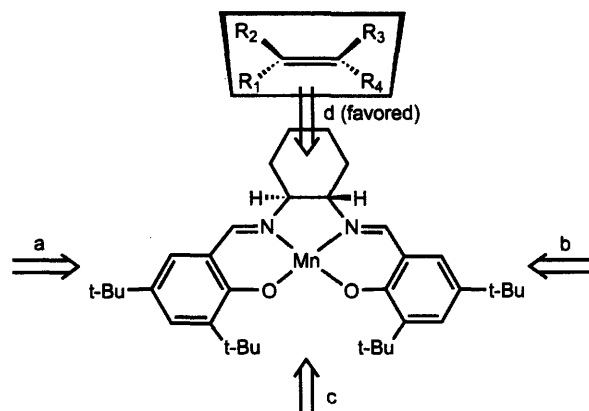
Ultimately, the selective aryl coupling to the xanthene was achieved by an alternative route, described in Scheme 3.6.⁴⁶ The unreactive alkyltin and bromo functionalized xanthene (**20**) was treated with elemental iodine to give **21**. This allows the more reactive aryl iodide to be selectively coupled to 4-bromobenzoic acid methyl ester using the catalyst tetrakis(triphenylphosphine)palladium to give the benzoic acid methyl ester functionalized xanthene **22**, which can be deprotected to the acid by refluxing in base to give **23**. The bromo site on **23** can then be coupled to 3-formyl-4-methoxyphenyl boronic acid to give **24**, respectively. Deprotection of the methyl ether using boron tribromide furnishes the salen precursors **25**, which can be condensed with half an equivalent of (1*R*,2*R*)-(-)-1,2-diaminocyclohexane to give the targeted benzoic acid and ester functionalized Hangman ligand. Manganese ion is inserted into the salen core by refluxing the ligand with an excess of manganese acetate in air, followed by workup with a saturated aqueous sodium chloride solution to give **27** in 93% yield.

3.3.4. Epoxidation Activity of Manganese Hangman Salens

We tested the epoxidation of the prochiral olefin 1,2-dihydronaphthalene by Mn(HSX*-COOH)Cl (**12**) using sodium hypochlorite as the oxygen atom transfer source, and conditions found to be optimal for previously studied manganese salen compounds.⁴⁷ We were pleased to find that our modified chiral salen macrocycle transfers stereochemical information in the oxygen atom transfer reaction to the prochiral substrate. The epoxide product was resolved with 23% enantiomeric excess (*ee*) as determined by chiral GC, and demonstrates communication with the chiral backbone and substrate despite the xanthene functionalizations situated at the 5 and 5' position of the macrocycle. Whereas this *ee* does not compete with the best salen epoxidation catalysts, it is on par with the “introductory” *ees* observed for first generation catalysts, such as salen macrocycles unfunctionalized in the 3 and 3' positions.¹⁵ However, we feel that we can improve on this by making a minor modification on the ligand macrocycle.

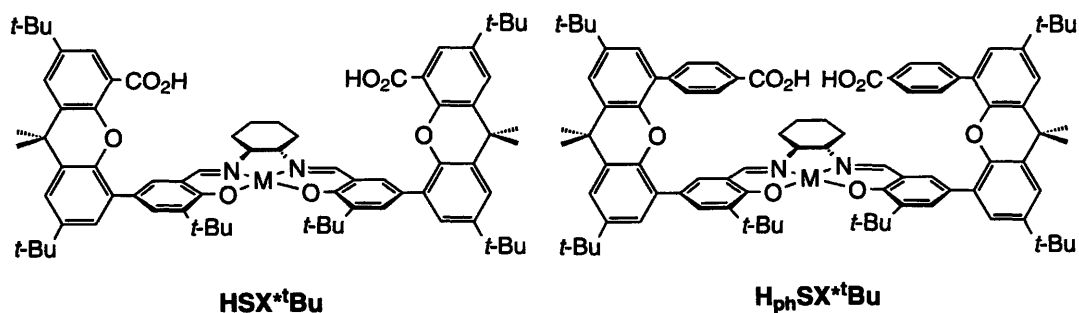
3.3.5. Design of Sterically Protected Hangman Salens

Figure 3.1. Potential approaches of an olefin to Jacobsen's Catalyst. The high valent oxo bound to the manganese (not shown) is perpendicular to and coming out of the page. Figure is adapted from reference 19.



The high selectivity that has been the centerpiece of Jacobsen's catalyst is believed to be enforced by sterically encumbering functionalities incorporated in the macrocycle. Figure 3.1 shows the potential directions substrate can approach the high valent Mn(oxo), the catalytic oxidant. *T*-Butyl group in the 5 and 5' position blocks approaches a and b, while the *tert*-butyl groups in the 3 and 3' position deter approach c. This favors the unencumbered approach a, which maximizes substrate communication with the chiral diamine, orienting the substrate for high resulting enantioselectivity upon oxygen atom transfer.^{13-15,19,48,49} With this in mind, changes in the site of functionalization around the macrocycle was considered with the goal of optimizing the enantiomeric selectivity within this Hangman framework. Although determining the optimal routes in the initial Hangman synthesis was not as straightforward as we had hoped, the modular nature of salen ligands allowed us to more easily revise the ligand to add the bulky substituents at

Chart 3.3

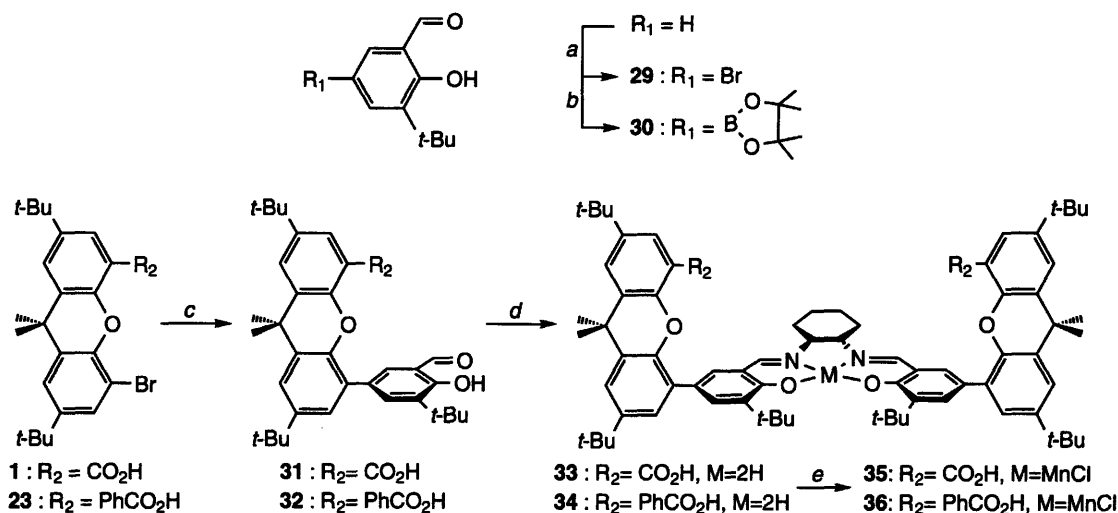


the desired 3 and 3' position. As described below, we were indeed able to quickly access the HSX^tBu and $\text{H}_{\text{ph}}\text{SX}^t\text{Bu}$ ligands shown in Chart 3.3.

3.3.6. Synthesis of $\text{Mn}[\text{HSX}^t\text{Bu}]\text{Cl}$ and $\text{Mn}[\text{H}_{\text{ph}}\text{SX}^t\text{Bu}]\text{Cl}$

The synthesis of the Hangman family of salens substituted with *tert*-butyl groups in the 3 and 3' positions is presented in Scheme 3.7. The ligand construction again begins with the commercially available 4,5-dibromo-2,7-di-*tert*-butyl-9,9-dimethylxanthene to give the functionalized precursors **1** and **22**, as described earlier in this Chapter. Synthesis of the precursor boronic ester **29**, which installs the *tert*-butyl groups on the salicylaldehyde prior to insertion into the ligand, required a two-step procedure. Firstly, the commercially available 3-*tert*-butyl-2-hydroxybenzaldehyde was functionalized with a bromo group in the 5 position (**28**) as described in the literature.⁵⁰ The bromo was then replaced with a boronic ester functionality by palladium catalyzed cross coupling methods⁵¹ to give **29**. Synthon **29** serves as a good nucleophilic substrate for the conversion of xanthene precursors **1** and **22** to **31** and **32**, respectively.³⁴ Hangman ligands **33** and **34** are provided by the condensation of **31** and **32** with 0.5 equivalent of (1*R*,2*R*)-(-)-1,2-diaminocyclohexane. The amount of product depends critically on the stoichiometry of

Scheme 3.7



(a) Br_2 , HOAc, (b) bis(pinacolato)diboron, KOAc, $\text{Pd}(\text{PCy}_3)_2$, (c) 3-*t*-Butyl-2-hydroxy-5-(4,4,5,5-tetramethyl-[1,3,2]dioxaborolan-2-yl)-benzaldehyde, Na_2CO_3 , $\text{Pd}(\text{PPh}_3)_4$, DMF/ H_2O , (d) (1*R*,2*R*)-(-)-1,2-diaminocyclohexane, EtOH, (e) *i\text{Mn}(\text{OAc})_2(\text{H}_2\text{O})_4, EtOH, *ii*) aq. NaCl*

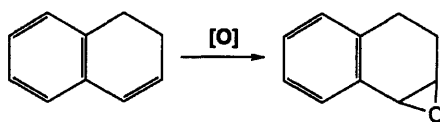
(1*R*,2*R*)-(-)-1,2-diaminocyclohexane. If more than 0.5 equivalent is used, varying amounts of product with an incompletely formed macrocycle is obtained; only one imine forms to make an —(ONN)— tridentate sparingly soluble ligand impurity. This unintended product can be identified by ¹H NMR and mass spectrometry. When 0.5 equivalent of (1*R*,2*R*)-(-)-1,2-diaminocyclohexane is employed, ¹H NMR integrations of **33** and **34** establish the presence of one cyclohexanediimine per two xanthene scaffolds.

Manganese acetate is again an efficient metalation agent for **33** and **34**. The oxidized Mn(III) products **35** and **36** are obtained when the metalation is performed in air followed by a workup with aqueous sodium chloride.

3.3.7. Epoxidation Activity of Sterically Protected Manganese Hangman Salens

To investigate whether the presence of the acid Hangman moiety in conjunction with 3 and 3' substitution leads to better yields as well as enantioselectivity, a comparative study was undertaken of the epoxidation of the prochiral olefin, 1,2-dihydronaphthalene by **35** and **36** versus the unsubstituted Hangman salens, Mn(HSX*^tBu-COOH)Cl and Mn(H_{ph}SX*^tBu-COOH)Cl, and the non-Hangman catalyst (1*R*,2*R*)-(-)[1,2-cyclohexanediamino-*N,N'*-bis(3,5-di-*tert*-butylsalicylidene)]manganese(III) chloride (Jacobsen's catalyst).⁴⁷ Table 3.1 lists the TONs measured by GC/MS for the various catalysts and oxidants. Unlike the Hangman porphyrin complexes, hydrogen peroxide is limited in its utility as an oxidant owing to its proclivity to disproportionate.^{52,53} Hence low TONs are observed for hydrogen peroxide as an oxidant even when diluted solutions are added via a syringe pump to high concentrations of substrate to reduce the amount of available hydrogen peroxide in solution. Conversely, the more commonly used oxidants, sodium hypochlorite (NaOCl) under biphasic reaction conditions of dichloromethane and water, and iodosobenzene (PhIO) in dichloromethane, results in higher TONs, but are commensurate with the unmodified platform. The reactions using hydrogen peroxide and iodosobenzene as the oxidant were also performed in the presence of one equivalent of *N*-methylimidazole, as that has been shown to sometimes favorably affect overall activity and catalyst stability. For the oxidants or conditions that we tried, we did not see any significant improvement in TONs in the Hangman complexes, although both acid functionalized Hangman complexes **35** and **36** give products with a considerably

Table 3.1. Turnover numbers (TON) for epoxidation of 1,2-dihydronaphthalene in dichloromethane



| Oxidant | t (hrs) | Catalyst | | |
|--|---------|--------------------------|----------------|-------------------------------|
| | | Mn(salen)Cl ^a | Mn(HSX*-'Bu)Cl | Mn(H _{ph} SX*-'Bu)Cl |
| NaOCl | 3 | 21 | 12 | 29 |
| NaOCl | 24 | 76 | 59 | 69 |
| PhIO | 3 | 22 | 28 | 25 |
| PhIO | 24 | 89 | 79 | 85 |
| PhIO ^b | 3 | 24 | 31 | 25 |
| PhIO ^b | 24 | 80 | 75 | 85 |
| H ₂ O ₂ | 4 | 3 | 2 | 2 |
| H ₂ O ₂ ^b | 4 | 6 | 9 | 4 |

^a salen = (1*R*, 2*R*)-(-)-[1,2-cyclohexanediamino-*N,N'*-bis(3,5-di-*tert*-butylsalicylidene)].

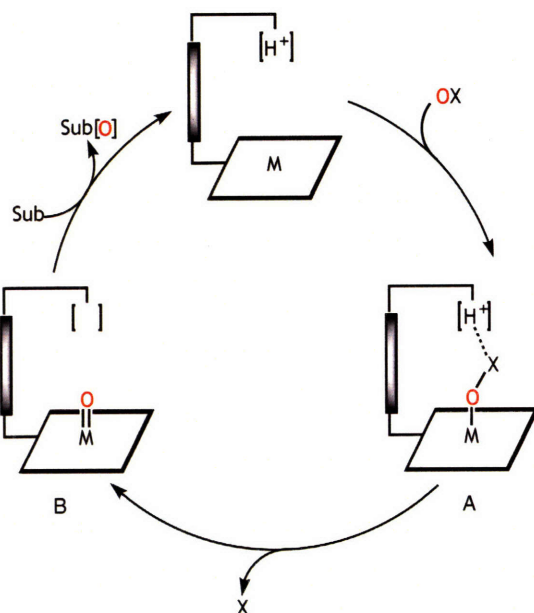
^b With 1 equivalent of *N*-methylimidazole.

improved 53% *ee*, demonstrating that the functionalities at the 3 and 3' positions on the salicylaldehyde are a critical element for good enantioselectivity by maximizing stereochemical communication between the manganyl oxo and substrate.^{13-15,19,49,54}

3.3.8. Mechanistic Implications

Mn(V) oxo is believed to be the enantioselective oxidant in manganese salen epoxidation reactions.¹ This manganyl oxo is formed by the activation of the O—X bond (intermediate A in Scheme 3.8) of various oxidants.⁵⁵ Computational⁵⁶ studies performed on the O—O bond cleavage of acylperoxo manganese salen complexes in acidic and neutral media identify the proton as a means to promote O—O bond heterolysis, and prevent O—O bond homolysis to produce the less reactive Mn(IV) oxo. Such acid-base induced bond activation chemistry, classically known as the “pull effect” in heme oxidations,⁵⁷⁻⁶¹ is responsible for the enhanced olefin epoxidation observed in Hangman porphyrin complexes.^{31,62} We did not see an increase in TON for our Hangman salen

Scheme 3.8



compounds with iodosylbenzene and hypochlorite as the oxidant. We can therefore infer that the acid group does not have any effect on cleaving the O—I or O—Cl bond, respectively, to form B in Scheme 3.8. Using hydrogen peroxide as the oxidant, excess equivalents successfully compete with substrate upon formation of B, and the catalase activity mentioned in Chapter 2 (and Chapter 4, *vide infra*) predominates. Hence, olefins are a poor probe for Mn(V) oxo formation with H₂O₂ as an oxidant. We also tried to probe Mn(V) oxo formation with hydrogen peroxide using more electron rich substrates such as sulfides or phosphates, but they are easily oxidized in the presence of oxidant without any catalyst.

3.4. Concluding Remarks

We have developed a versatile methodology to install Hangman scaffolds on salen macrocycles while maintaining the ligand's chiral framework. Two functionalized xanthene scaffolds form a symmetric molecular cleft, which can be structurally tuned with spacers appended to the xanthene scaffold. Epoxidation studies using prochiral substrates such as 1,2-dihydronaphthalene demonstrated asymmetric induction with an introductory *ee* of 23%. Addition of *tert*-butyl groups on the macrocycle confers an improved 53% enantioselectivity by promoting substrate interaction with the chiral cyclohexanediamine backbone of the salen macrocycle. The turnover number (TON) for

epoxidation was also determined using hydrogen peroxide, sodium hypochlorite, and iodosylbenzene as oxidants. We did not see any enhancement in TON for our Hangman compounds, indicating either that the acid-hanging group does not facilitate formation of the oxidizing intermediate (Mn(V) oxo) or that oxygen atom transfer to the olefin is the rate-determining step in the epoxidation reaction.

3.5. Experimental Section

3.5.1. Materials

Silica gel 60 (70 - 230 and 230 - 400 mesh) was used for column chromatography. Analytical thin layer chromatography was performed using F254 silica gel (pre-coated sheets, 0.2 mm thick). Solvents for synthesis were reagent grade or better and used as received from Aldrich or dried according to standard methods.⁶³ 4,5-Dibromo-2,7-di-*tert*-butyl-9,9-dimethylxanthene, boron tribromide (1.0 M in dichloromethane), (1*R*,2*R*)-(-)-1,2-diaminocyclohexane, manganese(II) acetate tetrahydrate, 5-bromosalicylaldehyde, 4-dimethylaminopyridine, 3-dicyclohexylcarbodiimide, 3-*tert*-butyl-2-hydroxybenzaldehyde, 1,2-dihydronaphthalene, dodecane, and N-methylimidazole were used as received from Aldrich. Iodosobenzene was used as received from TCI America. Bis(pinacolato)diboron, 3-formyl-4-methoxyphenylboronic acid, and 4-methoxycarbonylphenylboronic acid were used as received from Frontier Scientific. Sodium carbonate, potassium acetate, dichloro[1,1'-bis(diphenylphosphino)ferrocene]palladium(II) dichloromethane adduct, tetrakis(triphenylphosphine)palladium, bis(tricyclohexylphosphine)palladium(0), trimethyltin chloride, tri(*n*-butyl)tin chloride, tri(*i*-propyl)borate, and (1*R*, 2*R*)-(-)-[1,2-cyclohexanediamino-*N,N'*-bis(3,5-di-*tert*-butylsalicylidene)]manganese(III) chloride were used as received from Strem Chemicals. Phenyllithium (1.6- 1.7 M in cyclohexane) and 30% aqueous solution of hydrogen peroxide were used as received from Alfa Aesar.

The following compounds were obtained using published protocols and their purity confirmed by ¹H NMR: 4-hydroxycarbonyl-5-bromo-2,7-di-*tert*-butyl-9,9-dimethylxanthene (1),^{31,39} 4-methoxycarbonyl-5-bromo-2,7-di-*tert*-butyl-9,9-dimethylxanthene (2),³¹ 4-bromo-2,7-di-*tert*-butyl-5-iodo-9,9-dimethyl-9H-xanthene 4-(5-bromo-2,7-di-*tert*-butyl-9,9-dimethyl-9H-xanthen-4-yl)-benzoic acid methyl ester

(**22**),⁴⁶ and bromo-3-*tert*-butylsalicylaldehyde (**1**).⁶⁴ An optimized synthesis for 4,5-di(5-salicylaldehyde)-2,7-di-*tert*-butyl-9,9-dimethylxanthene (**14**) will be presented in Chapter 5.

3.5.2. Physical Measurements

¹H NMR, ¹³C NMR and ¹¹B NMR spectra were collected in CDCl₃ or C₄D₈O (Cambridge Isotope Laboratories) at 25 °C unless otherwise noted. Spectra were taken on an Inova 500 or Mercury 300 Spectrometer housed in the MIT Department of Chemistry Instrumentation Facility (DCIF). All chemical shifts are reported using the standard δ notation in parts-per-million relative to tetramethylsilane. The ¹H NMR and ¹³C NMR spectra have been internally calibrated to the monoproton impurity of the deuterated solvent used. Boron trifluoride etherate was used as the standard for the ¹¹B NMR. High-resolution mass spectral analyses were carried out by the MIT DCIF on a Bruker APEXIV47e.FT-ICR-MS using an Apollo ESI source.

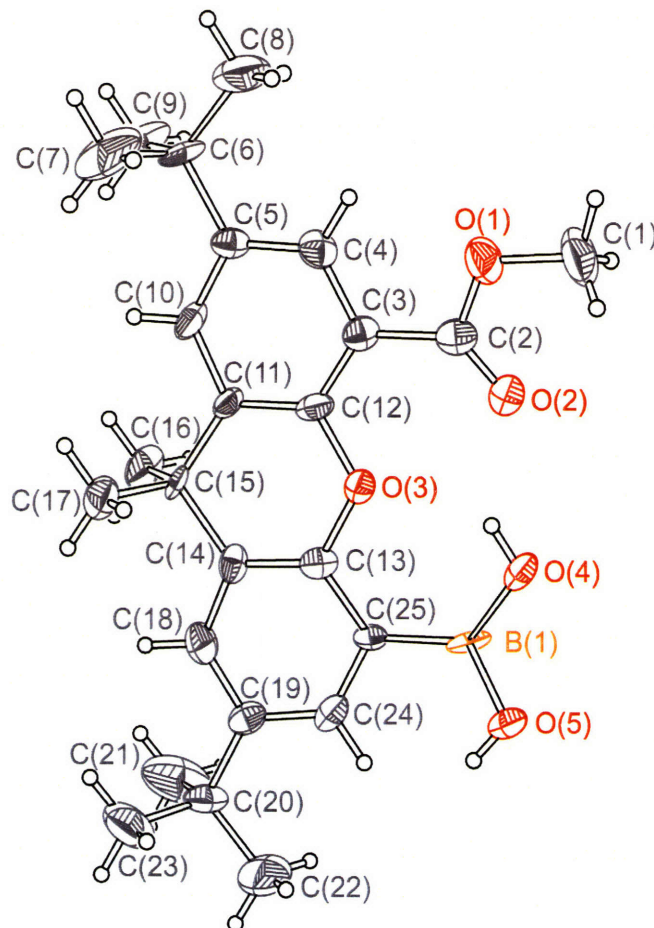
3.5.3. Synthesis

3.5.3.1. 5-(Boronic acid)-2,7-di-*tert*-butyl-9,9-dimethyl-9H-xanthene-4-carboxylic acid methyl ester (**3**)

Under nitrogen, 4-methoxycarbonyl-5-bromo-2,7-di-*tert*-butyl-9,9-dimethylxanthene (**2**) (1.00 g, 2.18 mmol), bis(pinacolato)diboron (0.830 g, 3.27 mmol), potassium acetate (0.747 g, 7.63 mmol), dichloro[1,1'-bis(diphenylphosphino)ferrocene]-palladium(II) dichloromethane adduct (0.159 g, 0.218 mmol) was added to 10 mL of anhydrous dimethylsulfoxide and heated to 90 °C for 36 hours. Upon cooling, 60 mL of benzene was added and the solution was washed with 3 \times 100 mL of deionized water. The organic layer was dried over MgSO₄ and reduced by rotary evaporation to obtain a black crude product which was taken up in 200 mL of hexane and filtered; this was repeated three times. The combined filtrates were reduced by rotary evaporation and the resulting solid was recrystallized in hot isopropyl alcohol to yield the product as a white crystalline solid upon cooling (0.398 g, 43% yield). X-ray quality crystals were grown from isopropyl alcohol; the structure is shown in Figure 3.2. ¹H NMR (500 MHz, CDCl₃, δ): 7.56 (d, J = 2.5 Hz, 1H), 7.51 (d, J = 2.5 Hz, 1H), 7.48 (m, 2H), 3.95 (s, 3H) 1.62 (s, 6H) 1.41 (bs, 2H), 1.34 (s, 9H), 1.33 (s, 9H). ¹³C NMR (500 MHz, CDCl₃, δ): 166.7, 152.6, 149.1,

145.8, 145.0, 135.5, 131.4, 128.6, 128.0, 127.4, 126.2, 125.5, 116.2, 64.3, 52.8, 34.5, 33.0, 32.9, 31.7, 31.5, 24.9. HRESI-MS ($[M + H]^+$) $C_{25}H_{34}O_5B$ m/z , Calcd. 425.2495, Found 425.2494. Subsequent synthetic procedure to bring **3** to **4** and then **5** as shown in Scheme 3.1 can be found in Appendix B.

Figure 3.2. Thermal ellipsoid plot of 5-(boronic acid)-2,7-di-*tert*-butyl-9,9-dimethyl-9H-xanthene-4-carboxylic acid methyl ester (**3**). Thermal ellipsoids are drawn at the 50% probability level.



3.5.3.2. 5-Bromo-2,7-di-*tert*-butyl-9,9-dimethyl-9H-xanthene-4-carboxylic acid benzyl ester (**6**)

4-Hydroxycarbonyl-5-bromo-2,7-di-*tert*-butyl-9,9-dimethylxanthene (**1**) (0.500 g, 1.12 mmol), 4-dimethylaminopyridine (0.013 g, 0.107 mmol), and benzyl alcohol (0.12 mL, 1.12 mmol) was added to 50 mL of dry dichloromethane and the solution was cooled to 0 °C in an ice water bath. To this, 1.22 mL of a 1.0 M solution of 3-

dicyclohexylcarbodiimide in dichloromethane (1.22 mmol) was added and the reaction stirred at 0 °C for 10 minutes than warmed to room temperature. Upon stirring for an addition 6 hours at room temperature, the solution was again cooled to 0 °C, filtered, and washed with a minimal amount of cold dichloromethane (about 6 mL). The filtrate was reduced by rotary evaporation; the crude product was purified by column chromatography (silica gel, 9:1 hexane: ethyl acetate) to elute the product as a pale yellow oil that solidified under vacuum overnight. (0.599 g, 99% yield). ¹H NMR (500 MHz, CDCl₃, δ): 7.71 (d, *J* = 2.5 Hz, 1H), 7.54 (m, 3H), 7.45 (d, *J* = 2.4 Hz, 1H), 7.38 (m, 2H), 7.33 (m, 2H) 5.50 (s, 2H), 1.65 (s, 6H), 1.34 (s, 9H), 1.33 (s, 9H). ¹³C NMR (500 MHz, CDCl₃, δ): 167.1, 147.4, 147.3, 145.7, 145.3, 136.5, 131.1, 130.7, 128.74, 128.72, 128.68, 128.3, 126.7, 126.6, 121.7, 119.7, 110.5, 67.3, 35.4, 34.79, 34.76, 32.2, 31.6, 20.8. HRESI-MS ([M + Na]⁺) C₃₁H₃₅O₃BrNa *m/z*, Calcd. 557.16406, Found 557.1641.

3.5.3.3. 2,7-Di-*tert*-butyl-9,9-dimethyl-5-(4,4,5,5-tetramethyl-[1,3,2]dioxaborolan-2-yl)-9H-xanthene-4-carboxylic acid benzyl ester (7)

Under nitrogen, 5-bromo-2,7-di-*tert*-butyl-9,9-dimethyl-9H-xanthene-4-carboxylic acid benzyl ester (6) (0.500 g, 0.93 mmol), potassium acetate (0.321 g, 3.27 mmol), bis(pinacolato)diboron (0.355 g, 1.40 mmol), and dichloro[1,1'-bis(diphenylphosphino)ferrocene]palladium(II) dichloromethane adduct (0.068 g, 0.093 mmol) was added to 5 mL of anhydrous dimethylsulfoxide and heated to 90 °C for 24 hours. Upon cooling, 25 mL of benzene was added and the solution was washed with 3 × 50 mL of water and dried with MgSO₄. The solvent was removed by rotary evaporation and the resulting crude black oil was put under vacuum overnight to give a crude black solid. The solid was stirred in 100 mL of hexane and filtered; this procedure was repeated three times. The combined filtrate was rotary evaporated to reveal a semicrystalline colorless solid, which was used in the next step without further purification.

3.5.3.4. 2,7-Di-*tert*-butyl-5-(3-formyl-4-hydroxy-phenyl)-9,9-dimethyl-9H-xanthene-4-carboxylic acid benzyl ester (8)

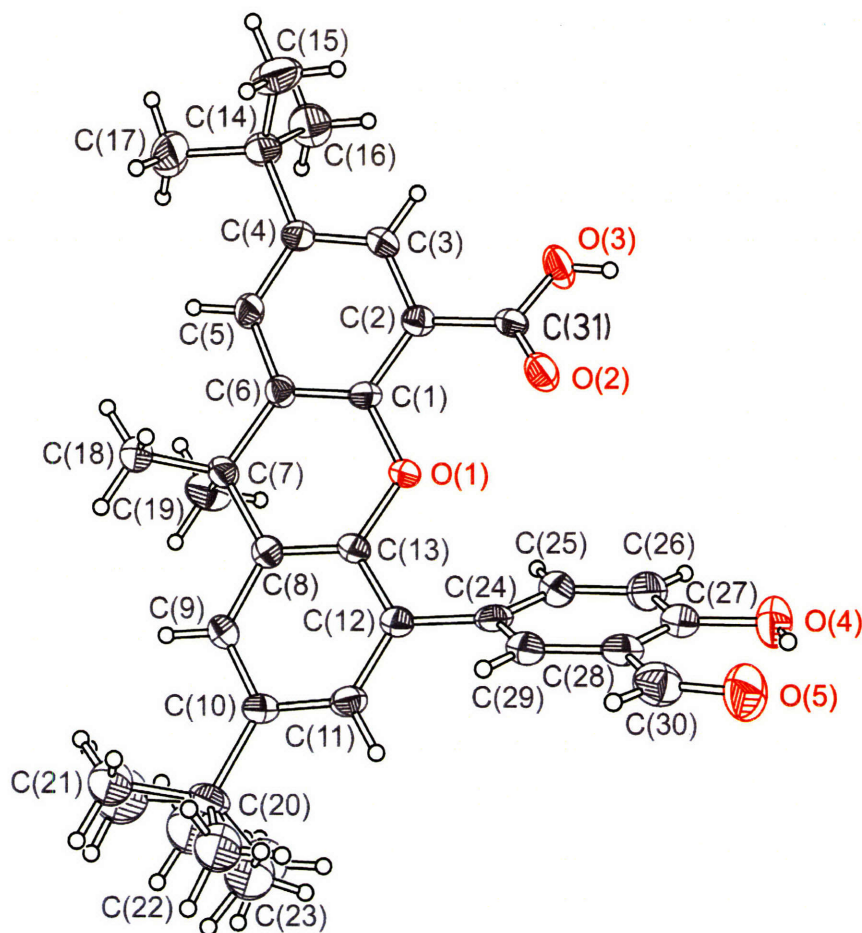
Under nitrogen, 2,7-di-*tert*-butyl-9,9-dimethyl-5-(4,4,5,5-tetramethyl-[1,3,2]dioxaborolan-2-yl)-9H-xanthene-4-carboxylic acid benzyl ester (7) (0.307 g, 0.61 mmol) is added to 5-bromosalicylaldehyde (0.123 g, 0.61 mmol), sodium carbonate

(0.094 g, 0.91 mmol), dichloro[1,1'-bis(diphenylphosphino)ferrocene]palladium(II) dichloromethane adduct (0.027 g, 0.034 mmol), 9 mL of 1,2-dimethoxyethane and 3 mL of deionized water and heated to 90 °C for 48 hours. Upon cooling, 50 mL of dichloromethane was added and the solution was washed with 2 × 50 mL of deionized water. The combined aqueous layers were extracted with 20 mL of dichloromethane, and the combined organic layers were dried with MgSO₄. Upon solvent removal by rotary evaporation the crude solid was purified by column chromatography (silica gel, 8:2 hexane: ethyl acetate) to elute the desired product as a colorless solid (0.102 g, 29%). ¹H NMR (500 MHz, CDCl₃, δ): 11.03 (s, 1H), 9.96 (s, 1H), 7.91 (d, *J* = 2.5 Hz, 1H), 7.72 (dd, *J* = 8.5 Hz, 2 Hz, 1H), 7.58 (m, 2H), 7.46 (d, *J* = 2 Hz, 1H), 7.24 (m, 4H), 7.15 (m, 2H), 7.00 (2, *J* = 8.5 Hz, 1H), 5.06 (s, 2H), 1.71 (s, 6H), 1.37 (s, 9H), 1.33 (s, 9H). HRESI-MS ([M + Na]⁺) C₃₈H₄₀O₅Na *m/z*, Calcd. 599.2768, Found 599.2781. Synthetic procedure to deprotect **8** to give **5** can be found in Appendix B.

3.5.3.5. 2,7-Di-*tert*-butyl-5-(3-formyl-4-methoxy-phenyl)-9,9-dimethyl-9H-xanthene-4-carboxylic acid (**9**)

Under nitrogen, a mixture of 4-hydroxycarbonyl-5-bromo-2,7-di-*tert*-butyl-9,9-dimethylxanthene (**1**) (0.150 g, 0.338 mmol), 3-formyl-4-methoxyphenylboronic acid (0.067 g, 0.371 mmol), sodium carbonate (0.052 g, 0.507 mmol), tetrakis(triphenylphosphine)palladium (0.015 g, 0.020 mmol), DMF (9 mL), and deionized water (1 mL) was heated to 90 °C for 36 hours. Upon cooling, 10 mL of water was added and the mixture was extracted with 3 × 25 mL of dichloromethane. The organic portions were combined and dried over MgSO₄ and the solvent removed by rotary evaporation. The crude solid was purified by column chromatography (silica gel, 8:2 pentane: ethyl acetate) to elute the colorless product (0.108 g, 64% yield). ¹H NMR (500 MHz, CDCl₃, δ): 10.55 (s, 1H), 8.03 (d, *J* = 2.5 Hz, 1H), 7.98 (d, *J* = 2.5 Hz, 1H), 7.70 (dd, *J* = 8.5 Hz, 2 Hz, 1 H), 7.68 (d, *J* = 2.5 Hz, 1H), 7.49 (d, *J* = 2.5 Hz, 1H), 7.21 (d, *J* = 2 Hz, 1H), 7.15 (d, *J* = 8.5 Hz, 1H), 4.02 (s, 3H), 1.73 (s, 6H), 1.37 (s, 9H), 1.34 (s, 9H). ¹³C NMR (500 MHz, CDCl₃, δ): 190.1, 167.8, 161.7, 148.3, 147.1, 146.3, 144.7, 137.6, 134.2, 131.3, 130.1, 130.0, 129.3, 128.21, 128.16, 126.4, 124.8, 122.1, 116.9, 112.2, 56.0, 35.1, 34.83, 34.80, 32.0, 31.7, 31.5. HRESI-MS ([M - H]⁻) C₃₂H₃₅O₅ *m/z*, Calcd. 499.2490, Found 499.2482.

Figure 3.3. Thermal ellipsoid plot of 2,7-di-*tert*-butyl-5-(3-formyl-4-hydroxyphenyl)-9,9-dimethyl-9H-xanthene-4-carboxylic acid (**5**). Thermal ellipsoids are drawn at the 50% probability level.



3.5.3.6. 2,7-Di-*tert*-butyl-5-(3-formyl-4-hydroxy-phenyl)-9,9-dimethyl-9H-xanthene-4-carboxylic acid (**5**)

2,7-Di-*tert*-butyl-5-(3-formyl-4-methoxy-phenyl)-9,9-dimethyl-9H-xanthene-4-carboxylic acid (**9**) (0.545 g, 1.11 mmol) was added to 20 mL of dry dichloromethane and cooled to 0 °C. A solution of boron tribromide (3 mL, 1.0 M in dichloromethane) was added and upon stirring for 3 hours, 20 mL of water was added. The organic layer was separated, washed with 10 mL of water, and dried over MgSO₄. The solvent was evaporated and the residue was purified by column chromatography (silica gel, 98:2 dichloromethane: methanol) to elute the product (0.330 g, 62% yield). X-ray quality crystals were grown by slow evaporation of a saturated dichloromethane solution. The

structure is shown in Figure 3.3. ^1H NMR (500 MHz, CDCl_3): δ = 11.13 (s, 1H), 9.97 (s, 1H), 8.02 (d, J = 2.5 Hz, 1H), 7.79 (d, J = 2.5 Hz, 1H), 7.71 (d, J = 2.5 Hz, 1H), 7.69 (d, J = 2.5 Hz, 1H), 7.50 (d, J = 2.5 Hz, 1H), 7.23 (d, J = 2.5 Hz, 1H), 7.13 (d, J = 8.5, 1H), 1.74 (s, 6H), 1.39 (s, 9H), 1.38 (s, 9H). ^{13}C NMR (500 MHz, CDCl_3 , δ): 198.0, 169.8, 160.8, 147.0, 146.4, 145.7, 145.3, 138.7, 136.0, 130.6, 130.4, 130.1, 127.5, 126.4, 125.9, 125.8, 122.2, 121.5, 120.5, 117.5, 44.9, 35.1, 34.8, 34.7, 32.2, 31.7, 31.6. HRESI-MS ($[\text{M} - \text{H}]^-$) $\text{C}_{31}\text{H}_{33}\text{O}_5$ m/z , Calcd. 485.2323, Found 485.2234.

3.5.3.7. $\text{H}_2(\text{HSX}^*-\text{COOH})$ (11)

A mixture of 2,7-di-*tert*-butyl-5-(3-formyl-4-hydroxy-phenyl)-9,9-dimethyl-9H-xanthene-4-carboxylic acid (**5**) (0.100 g, 0.206 mmol) was combined with (1*R*,2*R*)-(-)-1,2-diaminocyclohexane (0.012 g, 0.103 mmol) in 4 mL of absolute ethanol and refluxed for 12 hours. Upon cooling the solvent was removed by rotary evaporation and the resulting yellow solid was washed with 1 mL of cold methanol and dried under vacuum to yield 0.100 g of product (92% yield). ^1H NMR (500 MHz, CDCl_3 , δ): 8.63 (s, 2H), 7.90 (d, J = 2 Hz, 2H), 7.76 (d, J = 2.5 Hz, 2H), 7.58 (d, J = 2.5 Hz, 2H), 7.38 (m, 4H), 7.23 (d, J = 2 Hz, 2H), 6.95 (d, J = 8.5 Hz, 2H), 3.60 (d, J = 9.5 Hz, 2H), 2.07 (d, J = 11.5 Hz, 2H), 1.95 (d, J = 9.5 Hz), 1.76 (s, 6H), 1.73 (m, 2H), 1.68 (s, 2H), 1.61 (s, 6H), 1.36 (s, 18H), 1.35 (s, 18H). HRESI-MS ($[\text{M} - \text{H}]^-$) $\text{C}_{68}\text{H}_{77}\text{N}_2\text{O}_8$ m/z , Calcd. 1049.5676, Found 1049.5676. Anal. Calcd for $\text{C}_{68}\text{H}_{78}\text{N}_2\text{O}_8$: C, 77.68; H, 7.48; N, 2.61. Found: C, 77.61; H, 7.56; N, 2.61.

3.5.3.8. $\text{Mn}(\text{HSX}^*-\text{COOH})\text{Cl}$ (12)

$\text{H}_2(\text{HSX}^*-\text{COOH})$ (**11**) (0.100 g, 0.095 mmol) and manganese(II) acetate tetrahydrate (0.035 g, 0.143 mmol) was added to 8 mL of ethanol and refluxed for 3 hours in air. Upon cooling 1 mL of an aqueous saturated sodium chloride solution was added and after stirring for 5 minutes an additional 10 mL of water was added. The mixture was then extracted with 2×6 mL of dichloromethane. The combined organic portions were then washed with 5 mL of water and dried over MgSO_4 . The solvent was removed by rotary evaporation to yield the brown product (0.101 g, 93% yield). HRESI-MS ($[\text{M} - \text{Cl}]^-$) $\text{C}_{68}\text{H}_{76}\text{MnN}_2\text{O}_8$ m/z , Calcd. 1103.4977, Found 1103.4931. Anal. Calcd for $\text{C}_{68}\text{H}_{76}\text{ClMnN}_2\text{O}_8 \cdot 2\text{H}_2\text{O}$: C, 69.46; H, 6.86; N, 2.38. Found: C, 69.65; H, 6.67; N, 2.21.

3.5.3.9. 2,7-Di-tert-butyl-9,9-dimethyl-4-dihydroxyborane-5-(4,4,5,5-tetramethyl-[1,3,2]dioxaborolan-2-yl)-9H-xanthene (13)

Under nitrogen, a mixture of 4,5-dibromo-2,7-di-tert-butyl-9,9-dimethylxanthene (2.00 g, 4.17 mmol), bis(pinacolato)diboron (3.17 g, 12.5 mmol), potassium acetate (2.86 g, 29.2 mmol), dichloro[1,1'-bis(diphenylphosphino)ferrocene]palladium(II) dichloromethane adduct (0.305 g, 0.41 mmol), and anhydrous dimethyl sulfoxide (25 ml) was heated to 90 °C for 48 hours. Upon cooling, the mixture was extracted with 4 × 100 mL of dichloromethane. The organic portions were combined and washed with 4 × 100 mL of water and dried over MgSO₄ and the solvent removed by rotary evaporation. 500 mL of hexanes was stirred into the residue and filtered. The filtrate was reduced by rotary evaporation to give a crude solid, which was recrystallized by hot isopropyl alcohol to give the colorless product (0.622 g, 30 %). Upon recrystallization, the monoboronic acid and mono-ester is typically the pure product. ¹H NMR (300 MHz, CDCl₃, δ): 7.86 (d, *J* = 2.7 Hz, 1H), 7.72 (d, *J* = 2.4 Hz, 1H), 7.55 (d, *J* = 2.4 Hz, 1H), 7.47 (d, *J* = 2.7 Hz, 1H), 1.63 (s, 6H), 1.42 (s, 12H), 1.36 (s, 9H), 1.35 (s, 9H).

3.5.3.10. 5-(5-Bromo-2,7-di-tert-butyl-9,9-dimethyl-9H-xanthen-4-yl)-2-methoxybenzaldehyde (15)

Under nitrogen, 3-formyl-4-methoxyphenylboronic acid (0.409 g, 1.56 mmol), 4,5-dibromo-2,7-di-tert-butyl-9,9-dimethylxanthene (1.00 g, 2.08 mmol), sodium carbonate (0.321 g, 0.321 mmol), and dichloro[1,1'-bis(diphenylphosphino)ferrocene]palladium(II) dichloromethane adduct (0.076 g, 0.104 mmol) was added to 18 mL of dimethoxyethane and 6 mL of deionized water, degassed prior to use. This was heated to 90 °C for 12 hours. Upon cooling, the mixture was extracted with 4 × 75 mL of dichloromethane. The organic portions were combined and washed with 2 × 25 mL of water and dried over MgSO₄. The solvent removed by rotary evaporation and the residue was purified by column chromatography (silica gel, 7: 3 hexane: dichloromethane) to elute the product (0.040 g, 5 % yield). ¹H NMR (500 MHz, CDCl₃, δ): 10.56 (s, 1H), 8.16 (d, *J* = 2.5 Hz, 1H), 8.04 (dd, *J* = 9 Hz, 2 Hz, 1H), 7.44 (d, *J* = 2 Hz, 1H), 7.43 (d, *J* = 2 Hz, 1H), 7.38 (d, *J* = 2 Hz, 1H), 7.30 (d, *J* = 2 Hz, 1H), 7.12 (d, *J* = 9 Hz, 1H), 4.02 (s, 3H), 1.71 (s, 6H), 1.39 (s, 9H), 1.33 (s, 9H). ¹³C NMR (500 MHz, CDCl₃, δ): 190.0, 161.2, 146.9, 146.2, 145.4, 145.3, 138.4, 131.3, 130.7, 130.5, 129.9, 128.5, 127.7, 126.0, 124.5, 122.1,

121.9, 111.3, 110.2, 56.0, 35.5, 34.8, 34.7, 32.4, 31.7, 31.75, 31.72, 31.6. HRESI-MS ($[M + Na]^+$) $NaC_{31}H_{35}BrO_3$ m/z , Calcd. 557.1662 Found 557.1662.

3.5.3.11. 5-(5-Bromo-2,7-di-*tert*-butyl-9,9-dimethyl-9H-xanthen-4-yl)-2-hydroxy-benzaldehyde (16)

Under nitrogen, 5-(5-bromo-2,7-di-*tert*-butyl-9,9-dimethyl-9H-xanthen-4-yl)-2-methoxybenzaldehyde (**15**) (0.040 g, 0.074 mmol) was added to dry dichloromethane (10 mL) and the solution was cooled in an ice bath. Boron tribromide was added (1.4 mL, 1.0 M in dichloromethane) and the solution was warmed to room temperature and for 12 hours. The solution was washed with 3×6 mL of saturated sodium carbonate solution followed by brine and dried using $MgSO_4$. The solvent was removed by rotary evaporation to give the product as a colorless oil (0.037 g, 97%). Synthetic procedure to take **16** to **17** can be found in Appendix B.

3.5.3.12. (5-Bromo-2,7-di-*tert*-butyl-9,9-dimethyl-9H-xanthen-4-yl)-trimethylstannane (18)

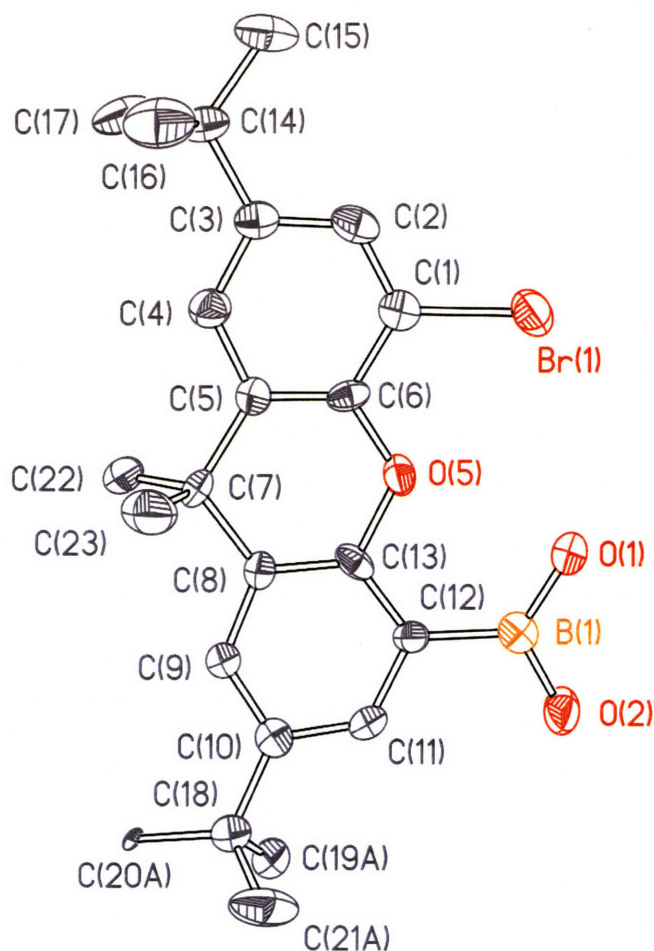
4,5-Dibromo-2,7-di-*tert*-butyl-9,9-dimethylxanthene (1.00 g, 2.08 mmol) was added to 12 mL of dry tetrahydrofuran and cooled to $-78^\circ C$ in a dry ice/acetone bath. Phenyllithium (1.7 mL, 1.8 M in cyclohexane) was added dropwise and the mixture was stirred for one hour and then warmed to room temperature. Trimethyltin chloride was added and stirred an additional hour. The solution was reduced by rotary evaporation to an oil, and purified by column chromatography (silica gel, pentane) to elute the product (0.446g, 38% yield). 1H NMR (500 MHz, $CDCl_3$, δ): 7.46 (d, $J = 2$ Hz, 1H), 7.36 (m, 3H), 1.66 (s, 6H), 1.37 (s, 9H), 1.34 (s, 9H).

3.5.3.13. 4-Bromo-2,7-di-*tert*-butyl-9,9-dimethyl-5-(4-hydroxyborane)-9H-xanthene (19)

4,5-Dibromo-2,7-di-*tert*-butyl-9,9-dimethylxanthene (2.00 g, 4.16 mmol) was added to 40 mL of dry tetrahydrofuran under nitrogen and cooled to $-78^\circ C$ in a dry ice/acetone bath. Phenyllithium (2.4 mL, 1.8 M in cyclohexane) was added dropwise and the reaction was stirred for one hour and then warmed to room temperature. Tri-*i*-propylborate (0.95 mL 4.15 mmol) was added and the reaction stirred for an additional hour. 20 mL of dilute HCL was then added slowly and the organic solvent was removed

by rotary evaporation. The remaining aqueous solution was filtered, and the colorless precipitate was recrystallized from hot methanol, and further purified by column chromatography (silica gel, 8: 2 hexane: ethyl acetate) to elute the product (1.440 g, 78 % yield). ^1H NMR (300 MHz, CDCl_3 , δ): 7.87 (d, $J = 2.5$ Hz, 1H), 7.55 (d, $J = 2.5$ Hz, 1H), 7.47 (d, $J = 2.5$ Hz, 1H), 7.39 (d, $J = 2.5$ Hz, 1H), 6.09 (bs, 2H), 1.66 (s, 6H), 1.37 (s, 9H), 1.34 (s, 9H). ^{13}C NMR (500 MHz, CDCl_3 , δ): 153.19, 147.52, 146.31, 144.63, 132.51, 131.55, 128.61, 128.25, 126.42, 122.38, 109.73, 35.24, 35.82, 34.72, 32.56, 31.72, 31.58. ^{11}B NMR (500 MHz, CDCl_3 , δ): 28.42.

Figure 3.4. Thermal ellipsoid plot of 4-Bromo-2,7-di-*tert*-butyl-9,9-dimethyl-5-(4-hydroxyborane)-9H-xanthene (**19**). Thermal ellipsoids are drawn at the 50% probability level.



3.5.3.14. (5-Bromo-2,7-di-*tert*-butyl-9,9-dimethyl-9H-xanthen-4-yl)-tributylstannane (**20**)

4,5-Dibromo-2,7-di-*tert*-butyl-9,9-dimethylxanthene (5.00 g, 10.42 mmol) was added to 80 mL of dry tetrahydrofuran and cooled to -78° C in a dry ice/acetone bath. Phenyllithium (6.5 mL, 1.8 M in cyclohexane) was added dropwise and the mixture was stirred for one and a half hours and then warmed to room temperature. Tri(*n*-butyl)tin chloride was added and the reaction stirred an additional hour. The reaction was then reduced by rotary evaporation to an oil, to which 10 mL of pentane was added and the resulting solution filtered. The filtrate was reduced to oil and purified by column chromatography (silica gel, pentane) to elute the product as colorless oil (3.12 g, 60% yield). ¹H NMR (500 MHz, CDCl₃, δ): 7.46 (d, *J* = 2 Hz, 1H), 7.37 (m, 2H), 7.35 (d, *J* = 2 Hz, 1H), 1.66 (s, 6H), 1.61 (q, *J* = 8 Hz, 6H), 1.40 (m, 6H), 1.37 (s, 9H), 1.34 (s, 9H), 1.28 (t, *J* = 8 Hz, 6H), 0.91 (t, *J* = 8 Hz, 9H). ¹³C NMR (500 MHz, CDCl₃, δ): 152.48, 146.36, 145.92, 145.78, 132.37, 131.48, 128.57, 128.45, 127.51, 123.31, 122.32, 109.80, 35.55, 34.71, 32.92, 31.82, 31.63, 29.54, 27.65, 13.98, 10.19. HRESI-MS ([M + Na]⁺) C₃₅H₅₅O₃BrOSn *m/z*, Calcd. 713.2355, Found 713.2352.

3.5.3.15. 4-(5-Bromo-2,7-di-*tert*-butyl-9,9-dimethyl-9H-xanthen-4-yl)-benzoic acid (23)

A solution of 4-(5-bromo-2,7-di-*tert*-butyl-9,9-dimethyl-9H-xanthen-4-yl)-benzoic acid methyl ester (22) (0.414 g, 0.773 mmol) in 10 mL of THF was refluxed with 5 mL of saturated sodium hydroxide in water for 2 hours. The mixture was neutralized with aqueous HCl and extracted with 3 × 25 mL of dichloromethane. The combined organic layers were dried with MgSO₄ and the solvent removed by rotary evaporation to yield the colorless product (0.334 g, 83.1% yield). ¹H NMR (500 MHz, CDCl₃, δ): 8.07 (d, *J* = 6.0 Hz, 2H), 7.65 (d, *J* = 6.0 Hz, 2H), 7.48 (s, 1H), 7.36 (s, 1H), 7.30 (s, 1H), 7.22 (s, 1H), 1.63 (s, 6H), 1.28 (m, 18H). ¹³C NMR (500 MHz, CDCl₃, δ): 172.6, 147.1, 146.3, 145.5, 145.4, 144.0, 131.4, 130.6, 130.2, 130.1, 128.6, 128.3, 128.0, 126.3, 122.9, 121.8, 110.4, 35.6, 34.83, 34.79, 35.4, 31.7, 31.6. HRESI-MS ([M + H]⁺) C₃₀H₃₃O₃Br *m/z*, Calcd. 521.1686, Found 521.1679.

3.5.3.16. 4-[2,7-Di-*tert*-butyl-5-(3-formyl-4-methoxy-phenyl)-9,9-dimethyl-9H-xanthen-4-yl]-benzoic acid (24)

Under nitrogen, a mixture of 4-(5-bromo-2,7-di-*tert*-butyl-9,9-dimethyl-9H-xanthen-4-yl)-benzoic acid (23) (0.300 g, 0.575 mmol), 3-formyl-4-methoxyphenylboronic acid

(0.114 g, 0.633 mmol), sodium carbonate (0.089 g, 0.864 mmol), tetrakis(triphenylphosphine)palladium (0.025 g, 0.034 mmol), DMF (9 mL), and deionized water (1 mL) was heated to 90 °C for 36 hours. Upon cooling, the mixture was extracted with 3 × 100 mL of dichloromethane. The organic portions were combined and dried over MgSO₄ and the solvent removed by rotary evaporation. The crude solid was purified by column chromatography (silica gel, 98:2 dichloromethane: methanol) to elute the colorless product (0.323 g, 97.3% yield). ¹H NMR (500 MHz, CDCl₃, δ): 10.41 (s, 1H), 7.87 (s, 1H), 7.82 (s, 1H), 7.74 (d, *J* = 1.25 Hz, 1H), 7.49 (d, *J* = 2.5 Hz, 1 H), 7.45 (d, *J* = 2.5 Hz, 1 H), 7.43 (dd, *J* = 6 Hz, 2.5 Hz, 1H), 7.36 (d, *J* = 8 Hz, 2H), 7.18 (dd, *J* = 8 Hz, 2 Hz, 2H), 6.68 (d, *J* = 8.5 Hz, 1H), 3.96 (s, 3H), 1.75 (s, 6H), 1.37 (s, 9H), 1.36 (s, 9H). ¹³C NMR (500 MHz, CDCl₃, δ): 189.9, 171.9, 161.1, 146.0, 145.94, 145.88, 145.5, 137.4, 135.3, 130.9, 130.5, 130.0, 129.8, 129.7, 128.3, 128.2, 128.1, 127.0, 125.73, 125.70, 124.4, 122.7, 121.9, 111.0, 55.8, 35.4, 34.8, 31.83, 31.79, 31.77, 29.9, 27.5. HRESI-MS ([M + Na]⁺) C₃₈H₄₀O₅Na *m/z*, Calcd. 599.2768, Found 599.2757.

3.5.3.17. 4-[2,7-Di-*tert*-butyl-5-(3-formyl-4-hydroxy-phenyl)-9,9-dimethyl-9H-xanthen-4-yl]-benzoic acid (25)

4-[2,7-Di-*tert*-butyl-5-(3-formyl-4-methoxy-phenyl)-9,9-dimethyl-9H-xanthen-4-yl]-benzoic acid (24) (0.300 g, 0.520 mmol) was added to 10 mL of dichloromethane and cooled to 0 °C. A solution of boron tribromide (1.6 mL, 1.0 M in dichloromethane) was added and upon stirring for 2 hours, 6 mL of water was added. The organic layer was separated, washed with 10 mL of water, and dried over MgSO₄. The solvent was evaporated and the residue was purified by column chromatography (silica gel, 98:2 dichloromethane: methanol) to elute the product (0.181 g, 62% yield). ¹H NMR (500 MHz, C₄D₈O δ): 9.45 (s, 1H), 7.74 (d, *J* = 8 Hz, 1H), 7.68 (d, *J* = 8 Hz, 1H), 7.54 (d, *J* = 2 Hz, 2H), 7.45 (m, 4H), 7.31 (d, *J* = 8 Hz, 1H), 7.23 (dd, *J* = 10.5, 1.5 Hz, 1H), 6.73 (d, *J* = 8.5 Hz, 1H), 1.36 (s, 18H). ¹³C NMR (500 MHz, C₄D₈O, δ): 196.9, 167.5, 161.7, 146.74, 146.66, 143.6, 138.6, 135.5, 133.0, 132.9, 132.5, 131.6, 131.5, 130.7, 130.6, 130.3, 130.1, 129.4, 129.3, 129.0, 126.7, 126.5, 123.3, 122.8, 121.8, 117.7, 36.1, 35.4, 32.0, 25.8, 25.6, 25.3, 25.2. HRESI-MS ([M - H]⁻) C₃₇H₃₇O₅ *m/z*, Calcd. 561.2646, Found 561.2646.

3.5.3.18. H₂(H_{ph}SX*-COOH) (26)

A mixture of 4-[2,7-di-*tert*-butyl-5-(3-formyl-4-hydroxy-phenyl)-9,9-dimethyl-9H-xanthen-4-yl]-benzoic acid (**25**) (0.025 g, 0.044 mmol) was combined with (1*R*,2*R*)-(-)-1,2-diaminocyclohexane (0.003 g, 0.022 mmol) in 5 mL of absolute ethanol and refluxed for 15 hours. Upon cooling the solvent was removed by rotary evaporation and the resulting yellow solid was washed with 0.5 mL of cold methanol and dried under vacuum to yield the product as a dull yellow solid (0.026 g, 97 % yield). ¹H NMR (500 MHz, CDCl₃, 25 °C, δ): 7.91 (m, 4H), 7.47 (d, *J* = 7 Hz, 2H), 7.68 (m, 4H), 7.55 (d, *J* = 7 Hz, 2H), 7.39 (m, 4H), 7.19 (m, 2H), 7.11 (s, 2H), 7.10 (s, 2H), 3.54 (bs, 2H), 2.33 (bs, 4H), 2.05 (bs, 4H), 1.72 (s, 12H), 1.35 (s, 18H), 1.30 (s, 18H). HRESI-MS ([M - H]⁻) C₈₀H₈₅N₂O₈ *m/z*, Calcd. 1201.6311, Found 1201.6329.

3.5.3.19. Mn(H_{ph}SX*-COOH)Cl (**27**)

H₂(H_{ph}SX*-COOH) (**26**) (0.010 g, 0.008 mmol) and manganese(II) acetate tetrahydrate (0.003 g, 0.012 mmol) was added to 3 mL of ethanol and refluxed for 4 hours in air. Upon cooling 0.5 mL of an aqueous saturated sodium chloride solution was added and the mixture was extracted with 2 × 15 mL of dichloromethane. The combined organic portions were then washed with 15 mL of water and dried over MgSO₄. The solvent was removed by rotary evaporation to yield the brown product (0.010 g, 93% yield). HRESI-MS ([M - Cl]⁻) C₈₀H₈₄MnN₂O₈ *m/z*, Calcd. 1255.5603, Found 1255.5605. Anal. Calcd for C₈₀H₈₄ClMnN₂O₈: C, 74.37; H, 6.55; N, 2.17. Found: C, 74.21; H, 6.72; N, 2.10.

3.5.3.20. 2,7-Di-*tert*-butyl-9,9-dimethyl-4,5-di-(4-benzoic acid methyl ester)-9H-xanthene (**28**)

28 was the major product of reaction A under several Suzuki coupling conditions shown in Scheme 3.4. Characterization data: ¹H NMR (500 MHz, CDCl₃, δ): 7.72 (d, *J* = 8.5 Hz, 4H), 7.48 (d, *J* = 2 Hz, 2H), 7.28 (d, *J* = 8.5 Hz, 4H), 7.19 (d, *J* = 2 Hz, 2H), 3.96 (s, 6H), 1.75 (s, 6H), 1.36 (s, 18H). ¹³C NMR (500 MHz, CDCl₃, δ): 167.1, 145.9, 143.0, 130.8, 129.7, 129.1, 128.6, 128.4, 125.7, 122.3, 52.2, 35.5, 34.8, 31.8, 31.6. HRESI-MS ([M + Na]⁺) NaC₃₉H₄₂O₅ *m/z*, Calcd. 613.2924, Found 521.1679.

3.5.3.21. 3-*tert*-Butyl-2-hydroxy-5-(4,4,5,5-tetramethyl-[1,3,2]dioxaborolan-2-yl)-benzaldehyde (**30**)

Under nitrogen, a mixture of 5-bromo-3-*tert*-butylsalicylaldehyde (**29**) (1.00 g, 3.89 mmol), bis(pinacolato)diboron (1.087 g, 4.28 mmol), potassium acetate (0.572 g, 5.83 mmol), and bis(tricyclohexylphosphine)palladium(0) (0.130 g, 0.194 mmol) was combined with 24 mL of dry dioxane and heated to 85 °C for 36 hours. Upon cooling, 20 mL of water was added and the mixture was extracted with 4 × 50 mL benzene. The organic portions were combined and dried over MgSO₄. The solvent was removed by rotary evaporation and the residue was purified by column chromatography (silica gel, 7:3 hexane: dichloromethane) to give the desired product (0.715 g, 60.4%). ¹H NMR (500 MHz, CDCl₃, 25 °C): δ = 12.00 (s, 1H), 9.90 (s, 1H), 7.93 (s, 1H), 7.91 (s, 1H), 1.43 (s, 9H), 1.35 (s, 12H). ¹³C NMR (500 MHz, CDCl₃, δ): 197.72, 163.81, 140.21, 140.18, 137.62, 120.61, 84.15, 35.04, 30.40, 29.44, 25.08. HRESI-MS ([M + H]⁺) calcd for C₁₇H₂₆BO₄ *m/z*, 305.1933, found 305.1922.

3.5.3.22. 2,7-Di-*tert*-butyl-5-(3-*tert*-butyl-5-formyl-4-hydroxy-phenyl)-9,9-dimethyl-9H-xanthene-4-carboxylic acid (**31**)

Under nitrogen, 4-hydroxycarbonyl-5-bromo-2,7-di-*tert*-butyl-9,9-dimethylxanthene (**1**) (0.400 g, 0.898 mmol), 3-*tert*-butyl-2-hydroxy-5-(4,4,5,5-tetramethyl-[1,3,2]dioxaborolan-2-yl)-benzaldehyde (**30**) (0.300 g, 0.988 mmol), sodium carbonate (0.139 g, 1.35 mmol) and tetrakis(triphenylphosphine)palladium(0) (0.062 g, 0.053 mmol) were combined with 18 mL of DMF and 2 mL of deionized water and the mixture was heated to 90 °C for 36 hours. Upon cooling 30 mL of dichloromethane was added and the solution was washed with 10 mL of water. The aqueous layer was then extracted with 2 × 10 mL dichloromethane and the combined organic portions were dried over MgSO₄. The solvent was removed by rotary evaporation and the residue was purified by column chromatography (silica gel, 3:7 diethyl ether: pentane) to give the desired product (0.265 g, 54%). ¹H NMR (500 MHz, CDCl₃, 25 °C): δ = 11.92 (s, 1H), 9.95 (s, 1H), 8.06 (d, *J* = 2 Hz, 1H), 7.71 (d, *J* = 2 Hz, 1H), 7.63 (d, *J* = 2 Hz, 1H), 7.57 (d, *J* = 2 Hz, 1H), 7.51 (d, *J* = 2 Hz, 1H), 7.24 (d, *J* = 2 Hz, 1H), 1.76 (s, 6H), 1.48 (s, 9H), 1.40 (s, 9H), 1.37 (s, 9H). ¹³C NMR (500 MHz, CDCl₃, δ): 197.29, 165.26, 161.25, 148.08, 147.57, 146.93, 144.52, 139.44, 135.25, 132.60, 131.19, 130.14, 129.00, 128.73, 128.54, 128.33, 126.68, 122.34, 120.88, 116.29, 35.32, 35.16, 34.91, 32.11, 31.72, 31.52, 29.32. HRESI-MS ([M + H]⁺) calcd for C₃₅H₄₃O₅ *m/z*, 543.3105, found 543.3109.

3.5.3.23. 4-[2,7-Di-*tert*-butyl-5-(3-*tert*-butyl-5-formyl-4-hydroxy-phenyl)-9,9-dimethyl-9H-xanthen-4-yl]-benzoic acid (32)

Under nitrogen, 4-(5-bromo-2,7-di-*tert*-butyl-9,9-dimethyl-9H-xanthen-4-yl)-benzoic acid (**22**) (0.312 g, 0.598 mmol), 3-*tert*-butyl-2-hydroxy-5-(4,4,5,5-tetramethyl-[1,3,2]dioxaborolan-2-yl)-benzaldehyde (**30**) (0.200 g, 0.657 mmol), sodium carbonate (0.092 g, 0.897 mmol), and tetrakis(triphenylphosphine)palladium(0) (0.041 g, 0.036 mmol) were added to 18 mL DMF and 2 mL deionized water. The mixture was heated to 90 °C for 36 hours. Upon cooling 30 mL of dichloromethane was added and the solution was washed with 10 mL of water. The aqueous layer was then extracted with 2 × 15 mL dichloromethane and the combined organic portions were dried over MgSO₄. The solvent was removed by rotary evaporation and the residue was purified by column chromatography (silica gel, 2:8 ethyl acetate: pentane) to give the desired product (0.273 g, 68% yield). ¹H NMR (500 MHz, CDCl₃, 25 °C): δ = 11.72 (s, 1H), 9.36 (s, 1H), 7.80 (d, *J* = 8 Hz, 2H), 7.50 (m, 2H), 7.48 (d, *J* = 2 Hz, 1H), 7.32 (d, *J* = 8 Hz, 2H), 7.22 (*J* = 2 Hz, 1H), 7.20 (m, 2H) 1.78 (s, 6H), 1.45 (s, 9H), 1.40 (s, 9H), 1.38 (s, 9H). ¹³C NMR (500 MHz, CDCl₃, δ): 196.78, 170.83, 160.39, 145.95, 145.89, 145.78, 145.72, 143.74, 138.02, 135.02, 135.33, 133.63, 130.69, 130.38, 129.75, 129.62, 128.90, 128.69, 128.20, 127.69, 125.59, 122.75, 121.90, 120.39, 35.39, 35.08, 34.81, 31.14, 31.80, 31.77, 29.45. HRESI-MS ([M + H]⁺) calcd for C₄₁H₄₇O₅ *m/z*, 619.3418, found 619.3414.

3.5.3.24. H₂[HSX*^{*t*}Bu-COOH] (33)

2,7-Di-*tert*-butyl-5-(3-*tert*-butyl-5-formyl-4-hydroxy-phenyl)-9,9-dimethyl-9H-xanthen-4-carboxylic acid (**31**) (0.100 g, 0.184 mmol) was added to (1*R*,2*R*)-(-)-1,2-diaminocyclohexane (0.010 g, 0.092 mmol) to 6 mL of absolute ethanol. The mixture was heated to reflux for 12 hours. Upon cooling, the solvent was removed by rotary evaporation and the residue was washed with 1 mL of cold methanol and then dried under vacuum to give the bright yellow product (0.105 g, 98%). ¹H NMR (500 MHz, CDCl₃, 25°C): δ = 8.61 (s, 2H), 7.66 (s, 2H), 7.58 (bs, 2H), 7.51 (s, 2H), 7.46 (d, *J* = 2 Hz, 2H), 7.41 (d, *J* = 2 Hz, 2H), 7.31 (d, *J* = 2 Hz, 2H), 3.16 (bs, 2H), 2.97 (m, 2H), 2.31 (m, 2H), 1.83 (s, 12H), 1.52 (s, 18H), 1.50 (s, 4H), 1.39 (18H), 1.35 (18H). HRESI-MS ([M - H]⁻) calcd for C₇₆H₉₃N₂O₈ *m/z*, 1161.6926, found 1161.6884.

3.5.3.25. H₂[H_{ph}SX*^{*t*}Bu-COOH] (34)

4-[2,7-Di-*tert*-butyl-5-(3-*tert*-butyl-5-formyl-4-hydroxy-phenyl)-9,9-dimethyl-9H-xanthen-4-yl]-benzoic acid (**32**) (0.050 g, 0.081 mmol) was added to (1*R*,2*R*)-(-)-1,2-diaminocyclohexane (0.005 g, 0.040 mmol) to 5 mL of absolute ethanol. The mixture was refluxed for 12 hours. Upon cooling, the solvent was removed by rotary evaporation and the residue was washed with 1 mL of cold methanol and dried under vacuum to give the yellow product (0.051 g, 96%). ¹H NMR (500 MHz, CDCl₃, 25°C): δ = 7.82 (m, 6H), 7.49 (d, *J* = 2 Hz, 2H), 7.43 (d, *J* = 2 Hz, 2H), 7.34 (m, 6H), 7.22 (m, 4H), 6.92 (s, 2H), 3.74 (m, 2H), 3.66 (bs, 2H), 3.51 (bs, 2H), 2.02 (bs, 4H), 1.76 (s, 12H), 1.56 (s, 18H), 1.39 (s, 18H), 1.38 (s, 18H). HRESI-MS ([M + H]⁺) calcd for C₃₈H₁₀₃N₂O₈ *m/z*, 1315.7709, found 1315.7704.

3.5.3.26. Mn[HSX*^tBu-COOH]Cl (**35**)

H₂[HSX*^tBu-COOH] (**33**) (0.105 g, 0.093 mmol) was added to manganese(II) acetate tetrahydrate (0.033 g, 0.140 mmol) in 6 mL of absolute ethanol and the solution was refluxed in air for 2 hours. Upon cooling, 1 mL of an aqueous saturated sodium chloride solution was added and the mixture was stirred for 10 minutes and then extracted with 3 × 10 mL of dichloromethane. The organic layers were combined and washed with 10 mL of water and then dried over MgSO₄. The solvent was removed by rotary evaporation to leave the brown product (0.112 g, 99%). HRESI-MS ([M - Cl]⁺) calcd for C₇₆H₉₂ClMnN₂O₈ *m/z*, 1215.6229, found 1215.6241. Anal. Calcd for C₇₆H₉₂ClMnN₂O₈: C, 72.91; H, 7.41; N, 2.24. Found: C, 72.84; H, 7.46; N, 2.35.

3.5.3.27. Mn[H_{ph}SX*^tBu-COOH]Cl (**36**)

H₂[H_{ph}SX*^tBu-COOH] (**34**) (0.025 g, 0.019 mmol) was combined with manganese(II) acetate tetrahydrate (0.007 g, 0.028 mmol) in 3 mL of absolute ethanol and refluxed in air for 2 hours. Upon cooling, 0.5 mL of an aqueous saturated sodium chloride solution was added and the mixture was stirred for 10 minutes and then extracted with 3 × 10 mL of dichloromethane. The organic layers were combined and washed with 5 mL of water and dried over MgSO₄. The solvent was removed by rotary evaporation to give the brown product (0.027 g, 100%). HRESI-MS ([M - Cl]⁺) calcd for C₈₈H₁₀₀MnN₂O₈ *m/z*, 1367.6860, found 1367.7056. Anal. Calcd for C₈₈H₁₀₀ClMnN₂O₈: C, 75.27; H, 7.18; N, 2.00. Found: C, 75.15; H, 7.38; N, 2.13.

3.5.4. Epoxidation of 1,2-Dihydronaphthalene

For the determination of *ee*, the epoxidation method and conditions are modified from previous epoxidation studies using manganese salen complexes.⁴⁷ 5 mL of a 0.05 M solution of Na₂HPO₄ was added to 12.5 mL of commercial bleach (Clorox). The pH of this solution (~55 mM in NaOCl) was adjusted to pH 12 by the dropwise addition of 1.0 M NaOH solution and cooled to 0 °C. 4.5 mL of this prepared bleach solution was added to a pre-cooled 0 °C solution of 1,2-dihydronaphthalene (100 mg, 0.77 mmol) and Mn[HSX*-COOH]Cl (**12**) (85 mg, 0.077 mmol, 10% catalyst loading) in 2 mL of dichloromethane. 4.8 mL of the prepared bleach solution was added to a pre-cooled 0 °C solution of 1,2-dihydronaphthalene (104 mg, 0.800 mmol) and Mn[HSX*^tBu-COOH]Cl (**35**) (10 mg, 0.008 mmol, 1% catalyst loading) in 8 mL of dichloromethane. 3.6 mL of the prepared bleach solution was added to a pre-cooled 0 °C solution of 1,2-dihydronaphthalene (78 mg, 0.600 mmol) and Mn[H_{ph}SX*^tBu-COOH]Cl (**36**) (8.4 mg, 0.006 mmol, 1% catalyst loading) in 6 mL of dichloromethane. Upon stirring for 12 hours, the layers were separated and the aqueous layer was extracted with 2 × 6 mL of dichloromethane. The combined organic layers were washed with 10 mL of water and 10 mL of a saturated sodium chloride solution and dried over MgSO₄. After solvent removal by rotary evaporation the crude product was purified to by column chromatography (silica gel, 98:2 pentane:ethyl acetate) to yield the epoxide product. The *ee* was determined by use of a chiral GC calibrated using a pure racemic epoxide sample. The *ee* measurements were performed using a chiral GC housed in Professor Timothy Jamison's laboratory and the experiment was assisted by graduate students Chudi Ndubaku and Ryan Moslin.

The data from Table 3.1 was determined as followed: 0.2 mM solutions of the catalyst (1*R*, 2*R*)-(-)-[1,2-cyclohexanediamino-*N,N'*-bis(3,5-di-*tert*-butylsalicylidene)] manganese(III) chloride (1.3 mg in 10 mL of dichloromethane), Mn[HSX*^tBu-COOH]Cl (**35**) (2.5 mg in 10 mL of dichloromethane), and [H_{ph}SX*^tBu-COOH]Cl (**36**) (2.8 mg in 10 mL of dichloromethane) were prepared. A 20 mM solution of 1,2-dihydronaphthalene and 10 mM dodecane (65 mg of 1,2-dihydronaphthalene and 43 mg of dodecane in 25 mL) was prepared. For NaOCl as the oxidant, the oxidant solution was prepared by mixing 2 mL of 0.05 M NaHPO₄ and 5 mL of commercial bleach (Clorox) and 0.1 mL of 1 M

NaOH solution and then cooled to 0 °C. 1.5 mL of this solution was added to 0.5 mL of each catalyst solution and 0.5 mL of the 1,2-dihydronaphthalene/dodecane solution, pre-cooled to 0 °C. For PhIO as the oxidant, 4.0 mg of PhIO was added to 0.5 mL of each catalyst solution with 0.5 mL of the 1,2-dihydronaphthalene/dodecane solution. For the trial with an equivalent of *N*-methylimidazole, 10 µL of a 0.0104 M solution (42.7 mg in 50 mL of dichloromethane) of *N*-methylimidazole was added to each reaction. For H₂O₂, the oxidant solution was prepared by diluting 1 mL of 30% H₂O₂ solution with 9 mL of H₂O. A 40 mM solution of 1,2-dihydronaphthalene and 10 mM of dodecane was prepared (130 mg 1,2-dihydronaphthalene and 43 mg of dodecane in 25 mL of dichloromethane). 0.5 mL of this was added to 0.5 mL of each catalyst solution. The diluted solution of H₂O₂ was added over 3 hours. Upon completion of the oxidant addition, the reaction was stirred for an additional hour before being sampled. The concentration of the substrate and epoxide product was determined by GC/MS with dodecane as the internal standard to determine the turnover numbers (TON). The GC/MS spectra were taken on an Agilent Technologies 6890N Network housed at the MIT DCIF.

3.5.5. X-Ray Crystal Data Collection and Refinement Parameters

Data collection and reduction

Crystals were coated with Paratone N oil and mounted on a glass fiber. X-ray diffraction data were collected at –80 °C on a Siemens three-circle diffractometer equipped with a CCD detector, using the Mo K α radiation, selected by a graphite monochromator. The data were integrated to *hkl*-intensity and the final unit cell calculated using the SAINT v.4.050 program from Siemens. Solution and refinement were performed with the SHELXTL v.5.03 suite of programs developed by G. M. Sheldrick and Siemens Industrial Automation, 1995. No absorption correction was performed. The structure was solved by direct methods; the least-squares refinement converged normally (with hydrogen atoms placed at calculated positions using a standard riding model and refined isotropically).

Table 3.2. Crystal data and structure refinement for 5-(boronic acid)-2,7-di-*tert*-butyl-9,9-dimethyl-9H-xanthene-4-carboxylic acid methyl ester (**3**).

| | | |
|--|--|-----------------------------|
| Identification code | 030780a | |
| Empirical formula | C ₂₅ H ₃₃ BO ₅ | |
| Formula weight | 424.32 | |
| Temperature | 467(2) K | |
| Wavelength | 0.71073 Å | |
| Crystal system | Triclinic | |
| Space group | $P\bar{1}$ | |
| Unit cell dimensions | $a = 9.157(7)$ Å | $\alpha = 77.035(14)^\circ$ |
| | $b = 11.143(10)$ Å | $\beta = 83.053(17)^\circ$ |
| | $c = 12.500(11)$ Å | $\gamma = 79.421(18)^\circ$ |
| Volume | 1217.6(18) Å ³ | |
| Z | 2 | |
| Density (calculated) | 1.157 Mg/m ³ | |
| Absorption coefficient | 0.078 mm ⁻¹ | |
| $F(000)$ | 456 | |
| Crystal size | 0.20 × 0.17 × 0.04 mm ³ | |
| Θ range for data collection | 2.26 to 24.69° | |
| Index ranges | $-8 \leq h \leq 7, -11 \leq k \leq 12, -5 \leq \ell \leq 14$ | |
| Reflections collected | 2658 | |
| Independent reflections | 2654 [$R_{\text{int}} = 0.0508$] | |
| Completeness to $\Theta = 24.69^\circ$ | 63.9 % | |
| Absorption correction | None | |
| Refinement method | Full-matrix least-squares on F^2 | |
| Data / restraints / parameters | 2654 / 0 / 291 | |
| Goodness-of-fit on F^2 | 1.083 | |
| Final R indices [$I > 2\sigma(I)$] | $R_1 = 0.0970, wR_2 = 0.1710$ | |
| R indices (all data) | $R_1 = 0.1935, wR_2 = 0.2057$ | |
| Largest diff. peak and hole | 0.201 and -0.212 e/Å ³ | |

Table 3.3. Crystal data and structure refinement 2,7-di-*tert*-butyl-5-(3-formyl-4-hydroxyphenyl)-9,9-dimethyl-9H-xanthene-4-carboxylic acid (**5**).

| | | |
|--|--|----------------------------|
| Identification code | 03084a | |
| Empirical formula | C ₃₁ H ₃₄ O ₅ | |
| Formula weight | 486.58 | |
| Temperature | 467(2) K | |
| Wavelength | 0.71073 Å | |
| Crystal system | Triclinic | |
| Space group | $P\bar{1}$ | |
| Unit cell dimensions | $a = 9.7828(9)$ Å | $\alpha = 78.978(2)^\circ$ |
| | $b = 9.8015(9)$ Å | $\beta = 82.309(2)^\circ$ |
| | $c = 15.2502(14)$ Å | $\gamma = 68.047(2)^\circ$ |
| Volume | 1336.8(2) Å ³ | |
| Z | 2 | |
| Density (calculated) | 1.209 Mg/m ³ | |
| Absorption coefficient | 0.081 mm ⁻¹ | |
| $F(000)$ | 520 | |
| Crystal size | 0.34 × 0.31 × 0.15 mm ³ | |
| θ range for data collection | 2.27 to 24.73° | |
| Index ranges | $-11 \leq h \leq 7, -11 \leq k \leq 9, 18 \leq \ell \leq 18$ | |
| Reflections collected | 6974 | |
| Independent reflections | 4471 [$R_{\text{int}} = 0.0274$] | |
| Completeness to $\theta = 24.73^\circ$ | 97.6 % | |
| Absorption correction | None | |
| Refinement method | Full-matrix least-squares on F^2 | |
| Data / restraints / parameters | 4471 / 0 / 334 | |
| Goodness-of-fit on F^2 | 1.021 | |
| Final R indices [$I > 2\sigma(I)$] | $R_1 = 0.0720, wR_2 = 0.1568$ | |
| R indices (all data) | $R_1 = 0.1084, wR_2 = 0.1738$ | |
| Largest diff. peak and hole | 0.476 and -0.284 e/Å ³ | |

Table 3.4. Crystal data and structure refinement 4-bromo-2,7-di-tert-butyl-9,9-dimethyl-5-(4-hydroxyborane)-9H-xanthene (**19**)

| | | |
|-----------------------------------|--|------------------------------|
| Identification code | 003321m | |
| Empirical formula | $C_{23.50} H_{31} B Br Cl O_3$ | |
| Formula weight | 487.65 | |
| Temperature | 193(2) K | |
| Wavelength | 0.71073 Å | |
| Crystal system | Monoclinic | |
| Space group | $P2_1/n$ | |
| Unit cell dimensions | $a = 17.9609(11)$ Å | |
| | $b = 15.4003(9)$ Å | $\beta = 108.9950(10)^\circ$ |
| | $c = 18.3354(11)$ Å | |
| Volume | $4795.5(5)$ Å ³ | |
| Z | 8 | |
| Density (calculated) | 1.351 Mg/m ³ | |
| Absorption coefficient | 1.847 mm ⁻¹ | |
| F(000) | 2024 | |
| Crystal size | $0.42 \times 0.40 \times 0.38$ mm ³ | |
| Theta range for data collection | 1.77 to 23.27°. | |
| Index ranges | $-10 \leq h \leq 19, -17 \leq k \leq 17, -20 \leq l \leq 18$ | |
| Reflections collected | 21429 | |
| Independent reflections | 6890 [R(int) = 0.1133] | |
| Completeness to theta = 23.27° | 99.9 % | |
| Absorption correction | None | |
| Refinement method | Full-matrix least-squares on F ² | |
| Data / restraints / parameters | 6890 / 0 / 577 | |
| Goodness-of-fit on F ² | 0.894 | |
| Final R indices [I > 2σ(I)] | R1 = 0.0568, wR2 = 0.1082 | |
| R indices (all data) | R1 = 0.1263, wR2 = 0.1249 | |

References

1. Srinivasan, K.; Michaud, P.; Kochi, J. K. *J. Am. Chem. Soc.* **1986**, *108*, 2309-2320.
2. Samsel, E. G.; Srinivasan, K.; Kochi, J. K. *J. Am. Chem. Soc.* **1985**, *107*, 7606-7616.
3. Yoon, H.; Burrows, C. J. *J. Am. Chem. Soc.* **1988**, *110*, 4087-4089.
4. Irie, R.; Noda, K.; Ito, Y.; Matsumoto, N.; Katsuki, T. *Tetrahedron Lett.* **1990**, *31*, 7345-7348.
5. Zhang, W.; Loebach, J. L.; Wilson, D. R.; Jacobsen, E. N. *J. Am. Chem. Soc.* **1990**, *112*, 2081-2083.
6. Lee, N. H.; Mcu, A. R.; Jacobsen, E. N. *Tetrahedron Lett.* **1991**, *32*, 5055-5058.
7. Deng, L.; Jacobsen, E. N. *J. Org. Chem.* **1992**, *57*, 4320-4323.
8. Chang, S.; Lee, N. H.; Jacobsen, E. N. *J. Org. Chem.* **1993**, *58*, 6939-6941.
9. Chang, S.; Galvin, J. M.; Jacobsen, E. N. *J. Am. Chem. Soc.* **1994**, *116*, 6937-6938.
10. Brandes, B. D.; Jacobsen, E. N. *J. Org. Chem.* **1994**, *59*, 4378-4380.
11. Palucki, M.; Pospisil, P. J.; Zhang, W.; Jacobsen, E. N. *J. Am. Chem. Soc.* **1994**, *116*, 9333-9334.
12. Katsuki, T.; Sharpless, K. B. *J. Am. Chem. Soc.* **1980**, *102*, 5974-5978.
13. Lin, G.-Q.; Li, Y.-M.; Chan, A. S. C. Asymmetric Oxidations. In *Principles and Applications of Asymmetric Synthesis*; Wiley-Interscience: New York, 2001, Chapter 4.
14. Jacobsen, E. N. Asymmetric Catalytic Epoxidation of Unfunctionalized Olefins. In *Catalytic Asymmetric Synthesis*, 1st Eds; Ojima, I; Wiley-VCH: New York, 1993; Chapter 4.2.
15. Jacobsen, E. N. Transition Metal-Catalyzed Oxidations: Asymmetric Epoxidation. In *Comprehensive Organometallic Chemistry*, 2nd Eds; Wilkinson, G; Stone, F. G. A.; Abel, E. W.; Hegedus, L. S.; Pergamon: New York, 1995; page 1097-1135.
16. Katsuki, T. *Coord. Chem. Rev.* **1995**, *140*, 189-214.
17. Williams, J. M. J. Epoxidation of Alkenes. In *Catalysis in Asymmetric Synthesis*; Sheffield Academic Press: Sheffield, 1999, Chapter 4.
18. Katsuki, T. *J. Mol. Cat. A* **1996**, *113*, 87-107.
19. Jacobsen, E. N.; Wu, M. H. Epoxidation of Alkenes other than Allylic Alcohols. In *Comprehensive Asymmetric Catalysis*, Vol 2; Pfaltz, A.; Jacobsen, E. N.; Yamamoto H.; Springer: Berlin, Heidelberg, New York, 1999; Chapter 18.2.
20. Larrow, J. F.; Jacobsen, E. N. *Topics Organomet. Chem.* **2004**, *6*, 123-152.

21. Larrow, J. F.; Jacobsen, E. N.; Gao, Y.; Hong, Y.; Nie, X.; Zepp, C. M. *J. Org. Chem.* **1994**, *59*, 1939-1942.
22. Larrow, J. F.; Jacobsen, E. N. *Org. Synth.*, **1997**, *97*, 1-6.
23. Koehler, K.; Sandstrom, W.; Cordes, E. H. *J. Am. Chem. Soc.* **1964**, *86*, 2413-2419.
24. Toth, G.; Pinter, I.; Messmer, A. *Tetrahedron Lett.* **1974**, 735-738.
25. Layer, R. W. *Chem. Rev.* **1963**, *63*, 489-510.
26. Rowan, S. J.; Cantrill, S. J.; Cousins, G. R. L.; Sanders, J. K. M.; Stoddart, J. F. *Angew. Chemie. Int. Ed.* **2002**, *41*, 898-952.
27. Akin, S.; Taniguchi, T.; Dong, W.; Masubuchi, S.; Naebeshima, T. *J. Org. Chem.* **2005**, *70*, 1704-1711.
28. Sasaki, I.; Pujol, D.; Gaudemer, A. *Inorg. Chim. Acta* **1987**, *134*, 53-57.
29. Daly, A. M.; Dalton, C. T.; Renehan, M. F.; Gilheany, D. G. *Tetrahedron Lett.* **1999**, *40*, 3617-3620.
30. Malaise, G.; Barloy, L.; Osborn, J. A. *Tetrahedron Lett.* **2001**, *42*, 7417-7419.
31. Chang, C. J.; Chng, L. L.; Nocera, D. G. *J. Am. Chem. Soc.* **2003**, *125*, 1866-1876.
32. Ishiyama, T.; Murata, M.; Miyaura, N. *J. Org. Chem.* **1995**, *60*, 7508-7510.
33. Deng, Y.; Chang, C. K.; Nocera, D. G. *Angew. Chemie. Int. Ed.* **2000**, *39*, 1066-1068.
34. Miyaura, N.; Suzuki, A. *Chem. Rev.* **1995**, *95*, 2457-2483.
35. Neises, B.; Andries, T.; Steglich, W. *J. Chem. Soc., Chem. Commun.* **1982**, 1132-1133.
36. Kende, A. S.; Rizzi, J. P. *Tetrahedron Lett.* **1981**, *22*, 1779-1982.
37. Brooks, P. R.; Wirtz, M. C.; Vetelino, M. G.; Rescek, D. M.; Woodworth, G. F.; Morgan, B. P.; Coe, J. W. *J. Org. Chem.* **1999**, *64*, 9719-9712.
38. Chang, C. J.; Yeh, C.-Y.; Nocera, D. G. *J. Org. Chem.* **2002**, *67*, 1403-1406.
39. Ships, G., Jr.; Rebek, J., Jr. *Tetrahedron Lett.* **1994**, *35*, 6823-6825.
40. Littke, A. F.; Fu, G. C. *Angew. Chemie. Int. Ed.* **2002**, *41*, 4176-4211.
41. Wolfe, J. F.; Buchwald, S. L. *Angew. Chemie. Int. Ed.* **1999**, *38*, 2413-2416.
42. Wolfe, J. P.; Tomori, H.; Sadighi, J. P.; Yin, J.; Buchwald, S. L. *J. Org. Chem.* **2000**, *65*, 1158-1174.
43. Wolfe, J. P.; Singer, R. A.; Yang, B. H.; Buchwald, S. L. *J. Am. Chem. Soc.* **1999**, *121*, 9950-9561.
44. Aranyos, A.; Old, D. W.; Kiyomori, A.; Wolfe, J. P.; Sadighi, J. P.; Buchwald, S. L. *J. Am. Chem. Soc.* **1999**, *121*, 4369-4378.
45. Littke, A. F.; Fu, G. C. *Angew. Chemie. Int. Ed.* **1999**, *38*, 2411-2413.

46. Liu, S.-Y.; Nocera, D. G. *J. Am. Chem. Soc.* **2005**, *127*, 5278-5279.
47. Zheng, W.; Jacobsen, E. N. *J. Org. Chem.* **1991**, *56*, 2296-2298.
48. Hosoya, N.; Hatayama, A.; Yania, K.; Fujii, H.; Irie, R.; Katuski, T. *Synlett*, **1993**, 641-645.
49. Brandes, B. D.; Jacobsen, E. N. *J. Org. Chem.* **1994**, *59*, 4378.
50. Cavazzini, M.; Manfredi, A.; Montanari, F.; Quici, S.; Pozzi, G. *Eur. J. Org. Chem.* **2001**, 4639-4649.
51. Ishiyama, T.; Ishida, K.; Miyaura, N. *Tetrahedron* **2001**, *57*, 9813-9816.
52. Irie, R.; Hosoya, N.; Katsuki, T. *Synlett* **1994**, *1994*, 255-256.
53. McGarrigle, E. M.; Gilheany, D. C. *Chem. Rev.* **2005**, *105*, 1563-1602.
54. Hosoya, N.; Hatayama, A.; Yania, K.; Fujii, H.; Irie, R.; Katuski, T. *Synlett*, **1993**, 641-645.
55. Allain, E. J.; Hager, L. P.; Deng, L.; Jacobsen, E. N. *J. Am. Chem. Soc.* **1993**, *115*, 4415-4416.
56. Khavrutskii, I. V.; Musaev, D. G.; Morokuma, K. *Inorg. Chem.* **2005**, *44*, 206-315.
57. Sono, M.; Roach, M. P.; Coulter, E. D.; Dawson, J. H. *Heme-containing Oxygenases*; *Chem. Rev.* **1996**, *96*, 2841-2887.
58. Watanabe, Y. In *The Porphyrin Handbook*; Kadish, K. M.; Smith, K. M.; Guillard, R., Eds.; Academic Press: San Diego, 2000; Vol. 4, pp 97-117.
59. Veitch, N. C.; Smith, A. T. In *Advances in Inorganic Chemistry*; Academic Press: New York, 2001; Vol. 51, pp 107-162.
60. Poulos, T. L. In *Advances in Inorganic Biochemistry*; Eichhorn, G. L.; Marzilli, L. G., Eds.; Elsevier: New York, 1988; Vol. 7, pp 1-36.
61. Dawson, J. H. *Science* **1988**, *240*, 433-439.
62. Soper, J. D.; Kryatov, S. V.; Rybak-Akimova, E. V.; Nocera, D. G. *J. Am. Chem. Soc.* **2007**, *ASAP*, DOI: 10.1021/ja0683032.
63. Armarego, W. L. F.; Perrin, D. D. *Purification of Laboratory Chemicals*; 4th ed.; Butterworth-Heinmann: Oxford, 1966.
64. Cavazzini, M.; Manfredi, A.; Montanari, F.; Quici, S.; Pozzi, G. *Eur. J. Org. Chem.* **2001**, *24*, 4639-4649.

Chapter 4

Catalase Activity and Epoxidation of Functionalized Olefins by Manganese Hangman Salens

Portions of the work presented in this chapter have been published:

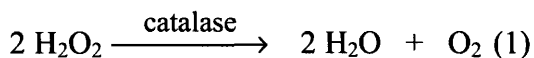
Yang, J. Y.; Bachmann, J.; Nocera, D. G. *J. Org. Chem.* **2006**, *71*, 8706-8714.

4.1. Motivation and Specific Aims

The ability of the Hangman salen platform to support multielectron chemistry mediated by proton-coupled electron transfer (PCET) is established by their proclivity to promote the catalytic disproportionation of hydrogen peroxide to oxygen and water (Chapter 2) and OAT (Chapter 3) via a high-valent metal oxo. The stopped-flow spectroscopic studies discussed in Chapter 2 afforded kinetic information on the reaction with the first equivalent of hydrogen peroxide to produce the oxidizing species in the manganese Hangman salophen complexes. Although the second step of the catalase reaction, the oxidation of the second equivalent of hydrogen peroxide by the Mn(V) oxo, is difficult to probe directly, it has been examined computationally. The modular nature of the salen Hangman ligand permits these computational predictions to be examined experimentally by correlating catalytic efficiency with structural features, such as the addition of steric parameters around the ligand macrocycle and changes in the acid-to-metal distance within the molecular cleft. The interplay of experiment with computation in further elucidating the mechanism of catalase activity by salen active sites is examined in this Chapter.

4.2. Background

The penchant to be highly effective mimics of the catalase enzyme (see equation 1) is a characteristic shared by the manganese Hangman salophen complexes studied in Chapter 2,^{1,2} and the previously studied iron Hangman porphyrin complexes.^{3,4} The hanging group in the Hangman ligand construct mediates proton-coupled electron transfer (PCET) activation that is at the core of bond-making and -breaking reactions in Nature.⁵⁻⁸ In these systems, the hanging acid-base functional group controls the secondary coordination sphere for substrate assembly and activation, distilling the essential components of their enzymatic counterparts.⁹ We were compelled to expand our knowledge of the catalase reaction,



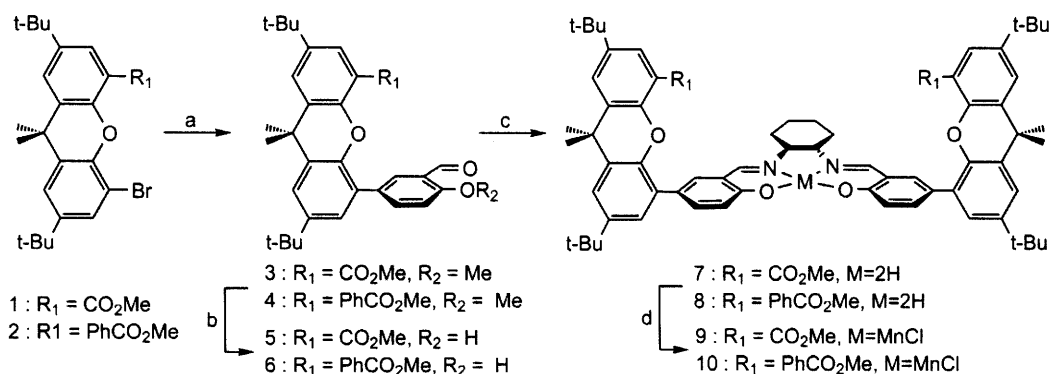
and specifically with salen as catalase mimics because of the efficacy of manganese salen complexes as therapeutic agents of reactive oxygen species (ROS) in biological

systems.¹⁰ Increased formation of ROS has been associated with a number of pathological processes, including inflammatory, ischemic and neurodegenerative diseases.¹¹ Oxidative stress and tissue damage is thought to occur if the amount of ROS generated exceeds the capabilities of existing natural antioxidants to neutralize them.¹² Preventing this damage has prompted the search for low molecular weight, non-toxic, synthetic compounds that can catalytically reduce ROS to serve as antioxidant therapeutics.^{11,13} The discovery of nonpeptidyl macrocyclic manganese compounds that are competent superoxide dismutase (SOD) mimics^{14,15} (dismutate superoxide to hydrogen peroxide and oxygen) has resulted in the screening of many different manganese compounds for SOD and/or catalase activity.¹⁶ (Not all SOD mimics are good catalase mimics; the production of cytotoxic hydrogen peroxide from the dismutation of superoxide makes both abilities equally important as a ROS scavenger).¹⁷ Currently, the patented salen complexes manganese bis(salicylidene)-1,2-ethylenediamine chloride (EUK-8), and manganese bis(3-methoxysalicylidene)-1,2-ethylenediamine chloride (EUK-134)¹⁸ have displayed extremely high SOD *and* catalase activity, and has already demonstrated success in removing cytotoxic amounts of hydrogen peroxide in animal¹⁹⁻²³ and human tissue,²⁴ preventing damage by endotoxic shock,²⁰ stroke,²² and UV-light,²⁴ as well as extending the life of a multicellular organism (the nematode *Caenorhabditis elegans*).²⁵ Both compounds are presently in clinical trials for their antioxidant capabilities.²⁶ The success of these compounds has prompted many structure-reactivity^{10,27} and computational^{28,29} investigations aimed at elucidating key intermediates and steps in the catalytic cycle and apply this knowledge to rationally design better catalysts. To this end, the Hangman salen platform with its modular synthesis makes it an ideal venue in which to define the structural and electronic properties of salen complexes that are critical to enhanced ROS activity.

4.3. Results and Discussion

4.3.1. Synthesis

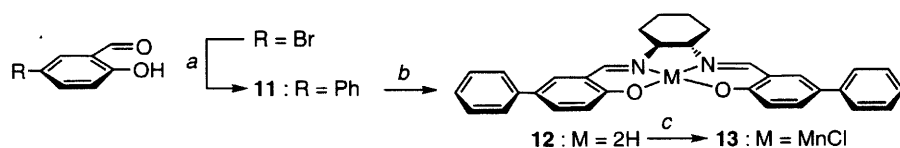
Scheme 4.1



(a) 3-formyl-4-methoxyphenylboronic acid, Na₂CO₃, Pd(PPh₃)₄, DMF: H₂O (9:1), (b) BBr₃, CH₂Cl₂, (c) (1*R*,2*R*)-(-)-1,2-diaminocyclohexane, EtOH, (d) *i*) Mn(OAc)₂(H₂O)₄, *ii*) NaCl(aq)

The synthesis of acid functionalized compounds Mn[HSX*-COOH]Cl and Mn[H_{ph}SX*-COOH]Cl is described in Chapter 3. To serve as control compounds, we also synthesized the analogous methyl esters Mn[HSX*-COOMe]Cl and Mn[H_{ph}SX*-COOMe]Cl, as shown in Scheme 4.1. The methyl ester functionalized xanthene precursors **1**^{3,30} and **2**¹ are Suzuki coupled³¹ with 3-formyl-4-methoxyphenylboronic acid to give **3** and **4**. The methyl ethers on **3** and **4** are deprotected using boron tribromide.^{32,33} Boron tribromide is also known to deprotect methyl esters,³⁴ however, **5** and **6** can be isolated by reducing the reaction time to selectively cleave the methyl ether while leaving the ester intact in the major product. Condensation of **5** and **6** with 0.5 equivalents of (1*R*,2*R*)-(-)-1,2-diaminocyclohexane provides the ligands **7** and **8** respectively; they are metallated using manganese acetate with an aqueous sodium chloride workup, as described for their acid functionalized analogues in Chapter 3 to give **9** and **10**.

Scheme 4.2



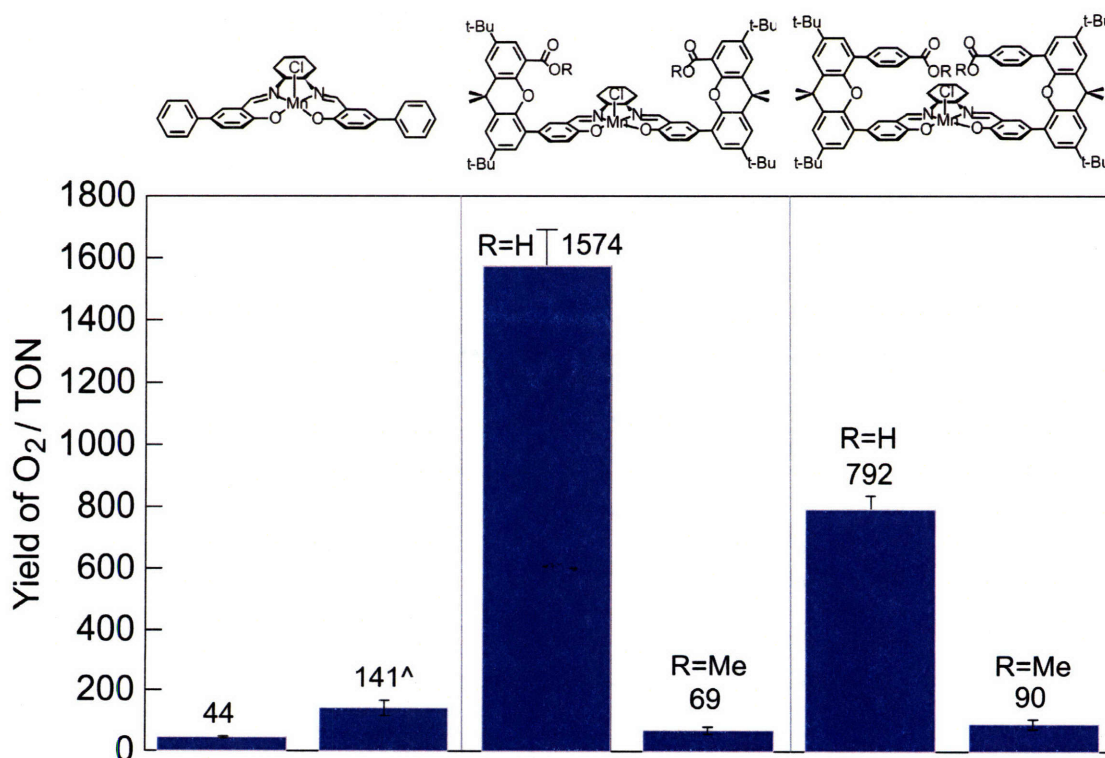
(a) phenylboronic acid, Na₂CO₃, Pd(dppf)Cl₂, DME: H₂O (3: 1), (b) (1*R*,2*R*)-(-)-1,2-diaminocyclohexane, EtOH, (c) Mn(OAc)₂(H₂O)₄, *ii*) NaCl(aq)

To generate a redox- only control compound that lacks the functionalized xanthenes, we synthesized the salen ligand (*R,R*)-*N,N'*-Bis(5-phenylsalicylidene)-1,2-cyclohexanediamine (**12**) (see Scheme 4.2), which is functionalized with phenyl groups in the 5 and 5' positions. The functionalized salicylaldehyde 4-hydroxy-biphenyl-3-carbaldehyde (**11**) can be synthesized by Suzuki coupling³¹ 5-bromosalicylaldehyde to phenylboronic acid and the synthesis of the ligand (**12**) followed standard condensation conditions. Manganese ion may be inserted into the salen core by refluxing the ligand with an excess of manganese acetate in air, followed by workup with a saturated aqueous sodium chloride solution to give Mn[5-phsalen]Cl (**13**).

4.3.2. Catalase Activity of Manganese Hangman Salen Complexes

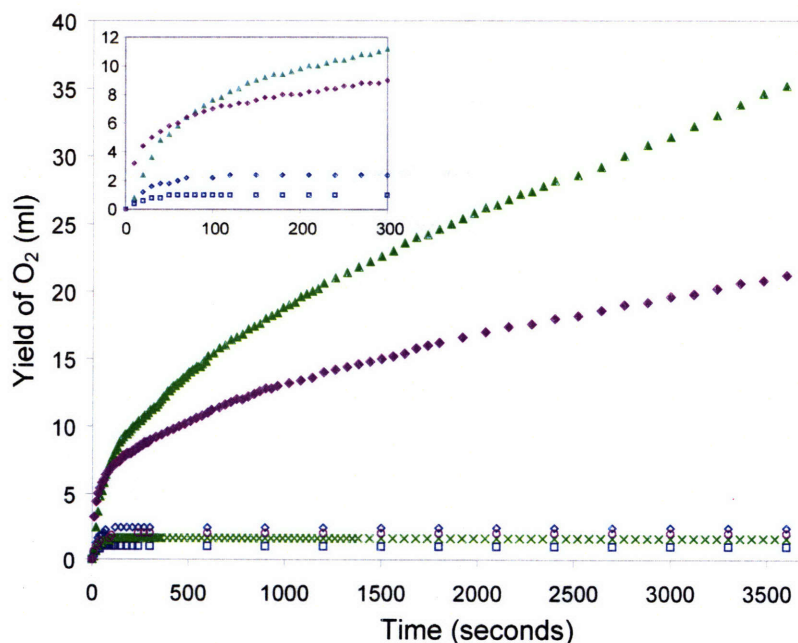
The acid-functionalized Mn[HSX*-COOH]Cl and Mn[H_{ph}SX*-COOH]Cl comprise a structurally homologous series of doubly-bridged Hangman constructs in which the acid

Figure 4.1. Turnover number (TON) of hydrogen peroxide dismutation catalyzed by manganese compounds [Mn(5-phsalen)Cl] (**13**) (**13*** in the presence of 2 equivalents of benzoic acid), Mn[HSX*-COOH]Cl, Mn[HSX*-COOMe]Cl (**9**), Mn[H_{ph}SX*-COOH]Cl and Mn[H_{ph}SX*-COOMe]Cl (**10**) after 1 hour.



group can be differentially extended over the face of the salen. We examined the activity of Mn[HSX*-COOH]Cl and Mn[H_{ph}SX*-COOH]Cl and their corresponding methyl ester analogues **9** and **10** towards the disproportionation of hydrogen peroxide in biphasic dichloromethane/methanol, under similar conditions to those used in the prior catalase studies. Figure 4.1 shows the turnover numbers (TON) for oxygen production by Mn[HSX*-COOH]Cl and Mn[H_{ph}SX*-COOH]Cl, and control systems in which (i) a proton is absent from the hanging group (**9** and **10**) and (ii) the salen platform is unmodified [Mn(5-phsalen)Cl] (**13**). The presence of the acid-base hanging group results in a dramatic increase in catalase-type reactivity. Whereas high TON can be achieved with Mn[HSX*-COOH]Cl and Mn[H_{ph}SX*-COOH]Cl, relatively low TONs are observed when the carboxylic acid functionality is replaced by an ester (**9** and **10**). Similarly, control experiments with the redox-only manganese salen complex **13** shows low activity for disproportionation. The addition of an external H⁺ source (benzoic acid) enhances TON of the parent salen complex, but the activity remains far inferior to that of

Figure 4.2. Oxygen release from hydrogen peroxide dismutation catalyzed by manganese compounds Mn(5-phsalen)Cl] (**13**) (□), **13*** (*in the presence of 2 equivalents of benzoic acid) (◇), Mn[HSX*-COOH]Cl (●), Mn[HSX*-COOMe]Cl (**9**) (×), Mn[H_{ph}SX*-COOH]Cl (◆), and Mn[H_{ph}SX*-COOMe]Cl (**10**) (○) over 1 hour. Inset shows reaction profile for the first five minutes excluding the methyl ester compounds **9** and **10**.



Mn[HSX*-COOH]Cl and Mn[H_{ph}SX*-COOH]Cl, which manages the proton by intramolecular transfer from the hanging functional group. The superior activity of Mn[HSX*-COOH]Cl and Mn[H_{ph}SX*-COOH]Cl is reflected in the activity profiles shown in Figure 4.2. Both Mn[HSX*-COOH]Cl and Mn[H_{ph}SX*-COOH]Cl exhibit similar reactivity profiles. Initial turnover frequencies are the similar for both catalysts but Mn[HSX*-COOH]Cl appears to be more robust over time and hence exhibits higher overall activity.

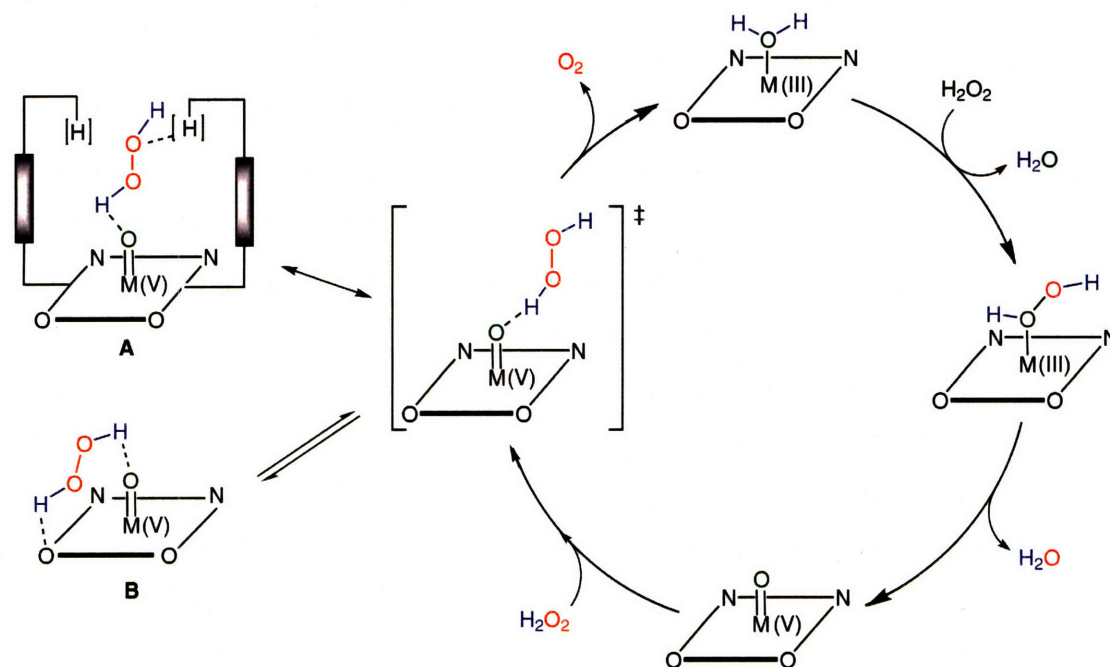
4.3.3. Mechanistic Insights

The dismutation of hydrogen peroxide by manganese salens^{28,29} is believed to proceed via the same “ping-pong” mechanism that has been proposed for the catalase enzyme.³⁵ In this mechanism (outlined in Scheme 4.3), the first molecule of hydrogen peroxide binds to the Mn(III) metal site and oxidizes it to Mn(V) oxo, releasing a molecule of water. A second molecule of hydrogen peroxide is then oxidized by the Mn(V) oxo forming oxygen and water while the metal is reduced back to the Mn(III) resting state. Although each step in this proposed catalytic cycle is not understood in detail, recent experimental and theoretical investigations have provided valuable insight into the potential intermediates and their kinetic and energetic parameters.

In Chapter 2, we replaced H₂O₂ by acyl peroxide to permit the catalase cycle at the Hangman salophen platform to be arrested; upon proton transfer, the acyl peroxide coordinated to the Mn(III) center furnishes a high-valent Mn(V) oxo intermediate, isolating the first step of the cycle.² The stopped-flow studies reveal that this step, however, is not rate-determining and for this reason we believe the acid-to-metal distance is less crucial for the first step in of the catalase cycle in the Hangman systems. A theoretical study of manganese salen oxidation to from Mn(V) oxo by hydrogen peroxide supports this observation. Abashkin and Burt found that O—O bond cleavage, oxidation of the Mn, and water molecule formation is an efficient intramolecular one-step reaction with the low calculated TS barrier of 3.6 kcal/mol.²⁸

Instead, subsequent oxidation of the second molecule of hydrogen peroxide by the Mn(V) oxo appears to be rate-determining.^{28,29} The hydrogen peroxide can approach the terminal oxo in two different orientations, and it is this orientation that is critical to the second step

Scheme 4.3



in the catalytic cycle. A top-side approach forms the end-on assembly shown in the transition state, and provides a low energy pathway towards oxidation of the hydrogen-bonded peroxide. Following a singlet reaction channel with this assembly, (spin ground-state of the resting catalyst), the activation barrier for protonation of the metal oxo by the hydrogen peroxide (to form water and release oxygen) is a modest 11.7 kcal/mol.²⁹ We believe the hanging acid group in the molecular cleft is beneficial to promoting the formation of the end-on intermediate via a hydrogen bonding network, shown as intermediate A in Scheme 4.3.

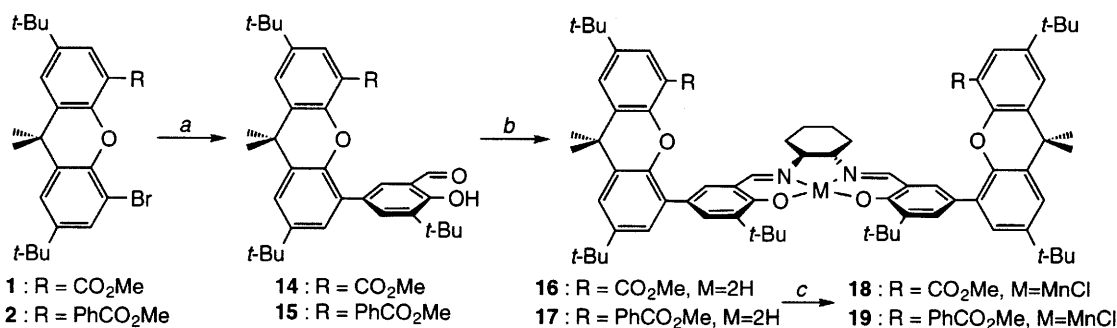
If the hydrogen peroxide instead approaches the Mn(V) oxo in a side-on fashion, it can form productive hydrogen-bonds with the phenolic oxygen as well as the metal oxo to give intermediate B. Both protons on the hydrogen peroxide are necessary to protonate the metal oxo and form water; therefore the hydrogen-bond with the phenolic oxygen must be broken in order to return to the Mn(III) resting state and complete the catalytic cycle. The effect of this high activation barrier is that B is a kinetically stable intermediate which limits the overall catalytic activity by temporarily deactivating the catalyst.²⁹ It is proposed that addition of steric blocking groups in the 3 and 3' position, ortho to the phenols, can prevent the side-on approach and formation of the hydrogen-

bond to the phenolic oxygen to form intermediate B. This would provide our catalysts with a further bias for intermediate A versus intermediate B, and should show enhanced catalytic activity as a result. Engineering our catalyst to enforce the ideal intermediate geometry is particularly important since in the absence of any of these features both intermediates are almost energetically equal, with intermediate B only 1.8 kcal/mol lower in energy than the end-on assembly.²⁹ As we have already synthesized the analogous manganese Hangman salens that are functionalized with *tert*-butyl groups in the 3 and 3' position, we are well situated to test this hypothesis.

4.3.4. Synthesis of Methyl Esters of Sterically Protected Manganese Hangman Salens

The synthesis of acid functionalized compounds $\text{Mn}[\text{HSX}^t\text{Bu-COOH}]\text{Cl}$ and $\text{Mn}[\text{H}_{\text{ph}}\text{SX}^t\text{Bu-COOH}]\text{Cl}$ is described in Chapter 3. The methyl ester analogues were synthesized as described in Scheme 4.4 to serve as proton-absent control catalysts. The two precursors **1**^{3,30} and **2**¹ were synthesized stepwise as previously described. They were Suzuki-coupled³¹ with 3-*tert*-butyl-2-hydroxy-5-(4,4,5,5-tetramethyl-[1,3,2]dioxaborolan-2-yl)-benzaldehyde (synthesis described previously, compound **16** in Chapter 3) to give **14** and **15**, which is then condensed with 0.5 equivalents of (1*R*,2*R*)-(-)-1,2-diaminocyclohexane. The manganese chloride ion was inserted similarly to the procedure previously described in this Chapter, using manganese(II) acetate as the metal

Scheme 4.4



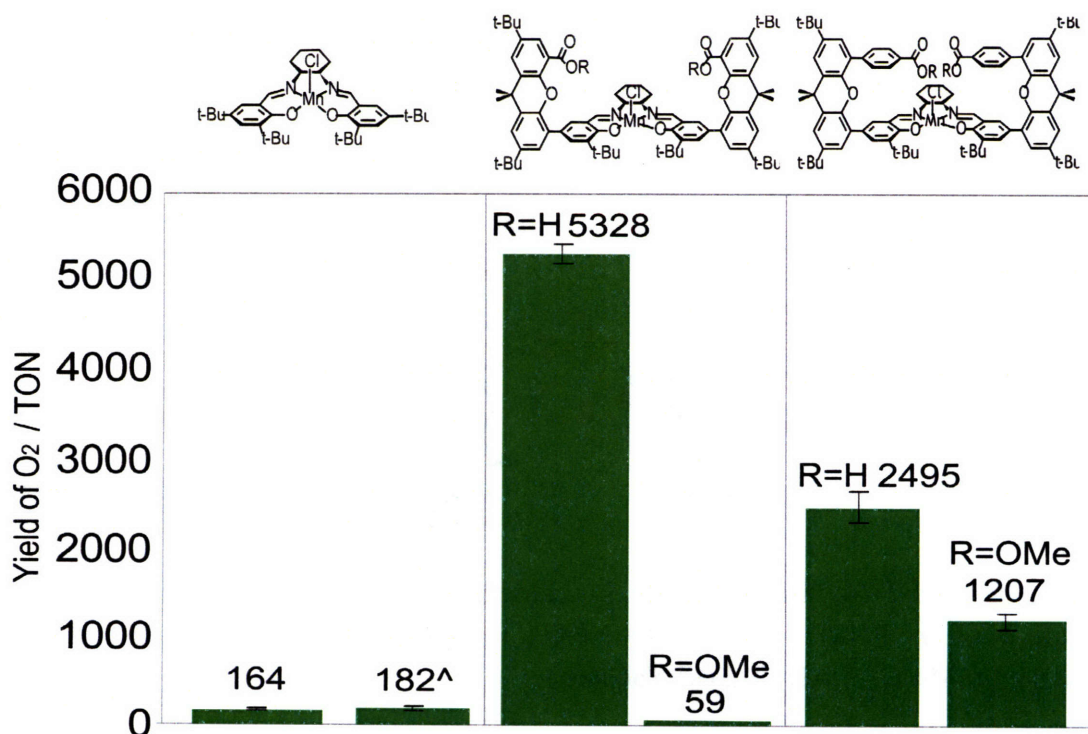
(a) 3-*tert*-butyl-2-hydroxy-5-(4,4,5,5-tetramethyl-[1,3,2]dioxaborolan-2-yl)-benzaldehyde, Na₂CO₃, Pd(PPh₃)₄, DMF: H₂O (9:1), (b) (1*R*,2*R*)-(-)-1,2-diaminocyclohexane, EtOH, (c) Mn(OAc)₂(H₂O)₄, (ii) NaCl(aq)

precursor to give the methyl-ester-functionalized manganese Hangman **18** and **19**.

4.3.5. Catalase Activity of Sterically Protected Manganese Salen Complexes

Hangman complexes $\text{Mn}(\text{HSX}^t\text{Bu-COOH})\text{Cl}$ and $\text{Mn}(\text{H}_{\text{ph}}\text{SX}^t\text{Bu-COOH})\text{Cl}$ were examined for their catalytic activity. Figure 4.3 shows the turnover numbers (TON) for hydrogen peroxide dismutation by the Hangman systems over the course of one hour. These results are compared to two controls: a manganese salen lacking a xanthene scaffold but with the *tert*-butyl groups in the 3 and 3' position and the analogous Hangman platform functionalized with methyl esters. The unsubstituted control, [(1,2-cyclohexanediamino-*N,N'*-bis(3,5-di-*tert*-butylsalicylidene))] manganese chloride, demonstrates negligible TONs, even with the addition of two equivalents of benzoic acid to serve as an intermolecular proton source. Conversely, Hangman platforms show high TONs, but only if a proton is present on the hanging group; $\text{Mn}(\text{HSX}^t\text{Bu-COOH})\text{Cl}$ exhibits TONs that are appreciably higher than $\text{Mn}(\text{HSX}^t\text{Bu-COOMe})\text{Cl}$ (**18**), where the

Figure 4.3 Turnover number (TON) of hydrogen peroxide dismutation catalyzed by manganese compounds $\text{Mn}(\text{salen})\text{Cl}$, $\text{Mn}(\text{salen})\text{Cl}$ in the presence of 2 equivalents of benzoic acid), $\text{Mn}[\text{HSX}^t\text{Bu-COOH}]\text{Cl}$, $\text{Mn}[\text{HSX}^t\text{Bu-COOMe}]\text{Cl}$ (**18**), $\text{Mn}[\text{H}_{\text{ph}}\text{SX}^t\text{Bu-COOH}]\text{Cl}$ and $\text{Mn}[\text{H}_{\text{ph}}\text{SX}^t\text{Bu-COOMe}]\text{Cl}$ (**19**) after 1 hour.



acid functionality has been replaced by an ester. The activity of Mn(H_{ph}SX*^tBu-COOH)Cl, with the acid extended from the xanthene with a phenylene group, also demonstrates increased activity with respect to its methyl ester analogue Mn(H_{ph}SX*^tBu-COOMe)Cl (**19**), albeit to a lesser extent. We note that the activity of **19** is complicated by ester hydrolysis. Oxygen evolution is initially slow and ceases within 15 minutes of hydrogen peroxide addition. At this point, a marked increase in activity is observed and TONs are obtained that are higher than expected from the initial rate. Mass spectrometry of Mn-containing species obtained from quenched reaction mixtures (~20 min) reveals the presence of manganese salen complexes with the methyl ester deprotected. Deprotection of methyl esters to give the acid derivative with hydrogen peroxide is possible owing to the high p*K*_a of the conjugate acid. Moreover it has been shown that HOO⁻ can nucleophilically cleave the methyl ester in some cases.³⁶ The oxygen evolution profiles for the catalysts tested are shown in Figure 4.4.

4.3.6. Mechanistic Insights into Steric Protection

The effect of substitution at the 3 and 3' positions is revealed by comparison of the activity of Mn(HSX*-COOH)Cl and Mn(H_{ph}SX*-COOH)Cl to Mn(HSX*^tBu-COOH)Cl and Mn(H_{ph}SX*^tBu-COOH)Cl, respectively. An approximately three-fold increase in the catalase activity is observed upon substitution of the *tert*-butyl groups. The overall TONs are closely tied with the reaction rates in the first two minutes of the reaction. The initial rate constants (*k*_{init}) for H₂O₂ consumption by the four acid functionalized manganese Hangman complexes are listed in Table 1. Mn(HSX*^tBu-COOH)Cl and Mn(H_{ph}SX*^tBu-

Table 4.1. Observed turnover number (TON) and initial rate constant (*k*_i) for Catalase-like H₂O₂ disproportionation catalyzed by manganese catalysts in 2: 1 dichloromethane/methanol at 25 °C.

| Catalyst | <i>k</i> _i (M ⁻¹ s ⁻¹) |
|--|--|
| Mn(HSX*-COOH)Cl | 6 |
| Mn(HSX* ^t Bu-COOH)Cl ^a | 14 |
| Mn(H _{ph} SX-COOH*)Cl | 5 |
| Mn(H _{ph} SX* ^t Bu-COOH)Cl | 10 |

^a Similar numbers were obtained using 2: 1 THF/methanol as the solvent.

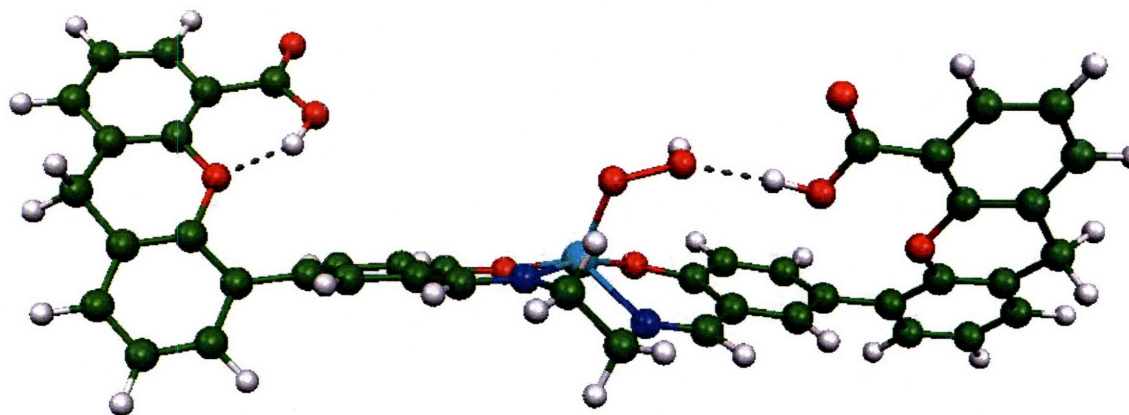
COOH)Cl display k_{init} that are roughly double that of their respective unsubstituted congeners. Though the reactions are run under biphasic conditions with methanol serving as a phase transfer reagent between dichloromethane/catalyst solution and the aqueous hydrogen peroxide phase, reaction rates and TON are not limited by the biphasic nature of the reaction. Dissolution of the more soluble Mn(HSX*^tBu-COOH)Cl in tetrahydrofuran and methanol yields a homogenous reaction mixture. Addition of the aqueous hydrogen peroxide to this solution results in TONs that are commensurate with those obtained under the biphasic conditions

We believe that it is the confluence of the hydrogen-bonding scaffold of the Hangman platform and the steric blocking groups in the 3 and 3' position of Mn(HSX*^tBu-COOH)Cl and Mn(H_{ph}SX*^tBu-COOH)Cl that keeps the system on cycle and leads to the enhanced rates and TONs for catalase activity.

4.3.7. Density Functional Theory on Manganese Hydroperoxide Hangman Salen Complexes

Scheme 4.3 presents the possibility that the acid group of the Hangman scaffold enhances catalase activity by pre-assembling intermediate A, which rapidly disproportionates to bring the catalyst back to its resting state. The {Mn(V) oxo-H₂O₂} assembly is expected to be sensitive to the positioning of the acid-base group over the face of the salen platform. Energy minimized geometry optimizations were performed on our two acid

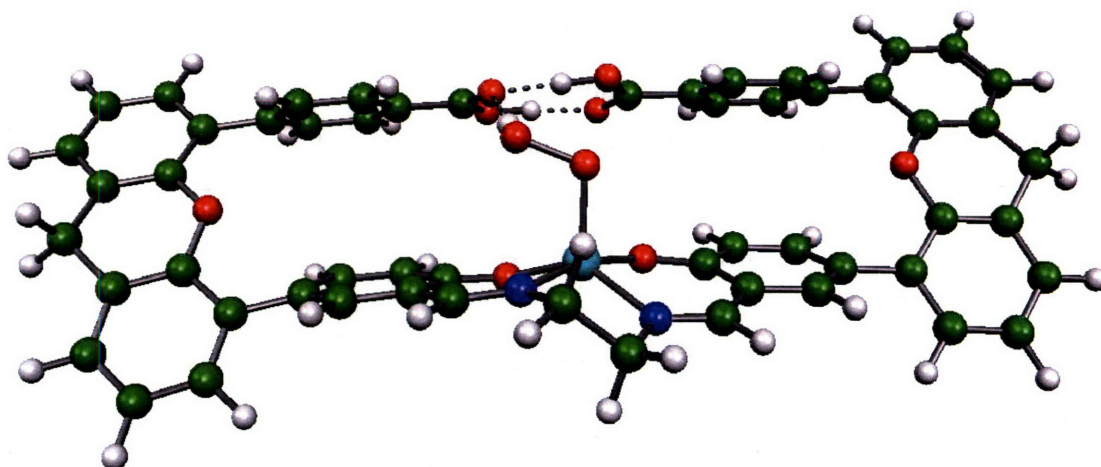
Figure 4.4. Energy minimized structure obtained from DFT of the hydroperoxide complexes of Mn(HSX*^t-COOH), showing one of the carboxylic acids is hydrogen bonded to the oxygen on the xanthene scaffold, while the other is hydrogen bonded to the hydroperoxide.



functionalized manganese Hangman salen ligands using the Amsterdam Density Functional (ADF) program. In order to simplify the calculations, the methyl and *tert*-butyl groups on the xanthene were excluded, and the cyclohexanediamine bridge was replaced with ethylenediamine. The complexes were modeled with a hydroperoxide bound axial to the manganese. The geometric parameters are listed in Table 4.3 later in this Chapter, and the input file and optimized coordinates in the converged calculations are listed in Appendix C.

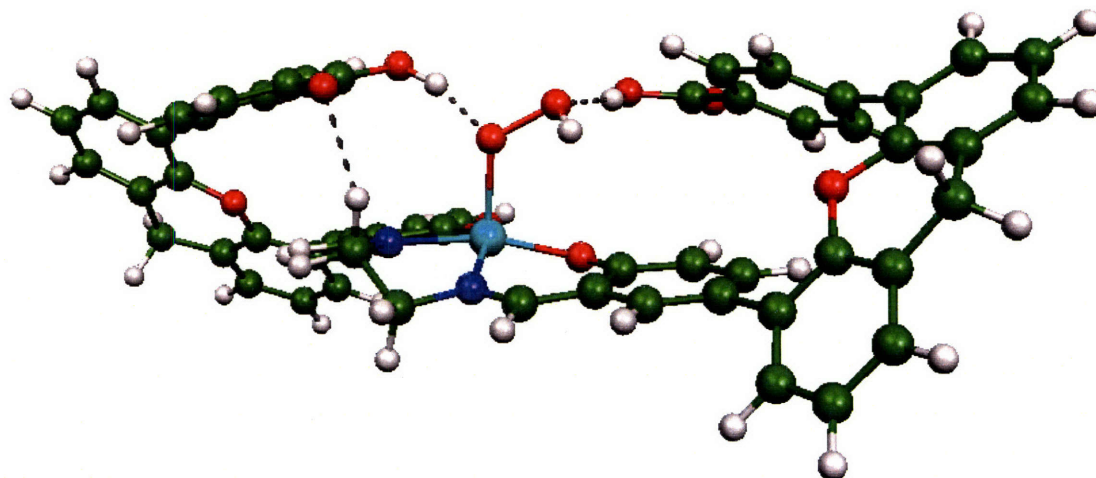
For $\text{Mn}[\text{HSX}^*-\text{COOH}]\text{OOH}$, the geometry optimized structure is shown in Figure 4.6. Whereas one carboxylic acid can hydrogen-bond with the unbound oxygen on the hydroperoxide at an acid-to-metal distance of $\sim 5 \text{ \AA}$, the other forms an unconstructive intramolecular hydrogen-bond with the oxygen on the xanthene. To form this intramolecular hydrogen bond, the xanthene tilts appreciably toward the plane of the macrocycle ring presumably driven by the stabilization incurred from the formation of the six-membered ring. This intramolecular bond has been observed in porphyrin xanthene complexes in the absence of substrate.³⁷ Hence, only one hanging group need be involved for substrate assembly, even when two are available.

Figure 4.5. Energy minimized structure obtained from DFT of the hydroperoxide complexes of $\text{Mn}(\text{H}_{\text{ph}}\text{SX}^*-\text{COOH})$ showing the two carboxylic acids span the face of the salen macrocycle to make a $-(\text{COOH})_2-$ dimer that interacts with the hydroperoxide via a hydrogen bond.



The hydrogen bond network is structurally different for the phenyl-spaced system. Two analogous energy-minimized calculation of the hydroperoxide bound $\text{Mn}(\text{H}_{\text{ph}}\text{SX}^*-$

Figure 4.6. Energy minimized structure obtained from DFT of the hydroperoxide complexes of $\text{Mn}(\text{H}_{\text{ph}}\text{SX}^*-\text{COOH})$ with the xanthenes splayed away from each other, precluding formation of the $-(\text{COOH})_2-$ dimer. Each of the carboxylic acids has a hydrogen-bonding interaction with the hydroperoxide.



COOH) were performed. The first revealed that the addition of the phenylene spacer permits the two acids to comfortably span the distance above the salen platform to form an intramolecular carboxylic acid dimer (Figure 4.7). An alternative structure was explored by tilting the xanthene scaffolds away from each other so that while both carboxylic acids can still form productive hydrogen bonds with the bound hydroperoxide, they are not facing each other and thus cannot form a $-(\text{COOH})_2-$ dimer (Figure 4.8). The structure is destabilized by 44 kJ/mol relative to that of the $-(\text{COOH})_2-$ dimer (Table 4.2) showing that formation of the dimer confers significant stabilization to $\text{Mn}(\text{H}_{\text{ph}}\text{SX}^*-\text{COOH})$. The formation of this stabilizing intramolecular hydrogen bond is likely accompanied by a decrease in the acidity of the proton over the reactive cleft. Accordingly, substrate assembly will be diminished due to the reduced ability to form additional hydrogen bonds, thus accounting for the lower catalase activity of the benzoic

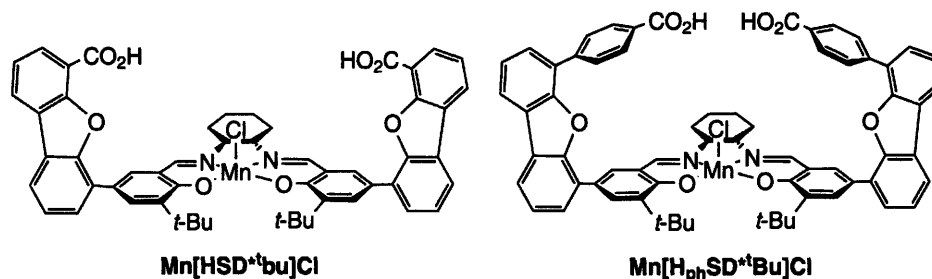
Table 4.2 Total bond energies of calculated manganese Hangman salen compounds.

| Compound | Total Energy (kJ/mol) |
|--|-----------------------|
| $\text{Mn}(\text{HSX}^*)-\text{OOH}$ | -56695.92 |
| $\text{Mn}(\text{H}_{\text{ph}}\text{SX}^*)-\text{OOH}$ (carboxylic acid dimer) | -69749.31 |
| $\text{Mn}(\text{H}_{\text{ph}}\text{SX}^*)-\text{OOH}$ (no carboxylic acid dimer) | -69704.88 |

acid functionalized complexes compared to when the acids are directly attached to the xanthene bridge (*vide supra*), where the two acids are too far apart to form an intramolecular dimer.

4.3.8. Acid-to-Metal Distance Effects

Chart 4.1

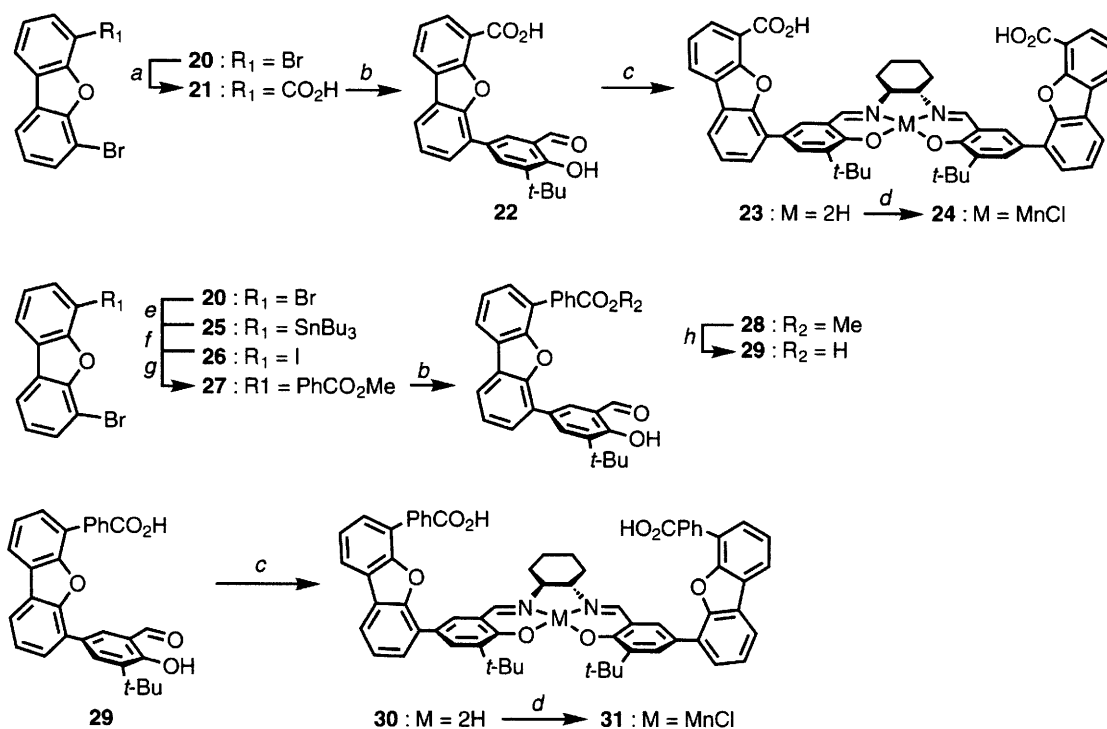


Although the HSX* framework displayed greater catalase activity than H_{ph}SX*, the correlation between reactivity and functional group distance can not be directly compared because of the carboxylic acid dimer formed in the latter. Therefore, we are unable to discern the effect of the acid distance from changes in the acid pK_a upon formation of the dimer. Because of the importance of the acid hanging groups in assembly of the hydrogen peroxide in the molecular cleft, we wanted to investigate this effect. To this end, we synthesized two additional Hangman ligands by replacing the xanthene scaffolds with dibenzofuran. The geometry of the dibenzofuran scaffold positions the functionality away from the metal center. By synthesizing the dibenzofuran manganese Hangman salen compounds functionalized with carboxylic acid Mn[HSD^{tBu}-COOH]Cl and benzoic acid Mn[H_{ph}SD^{tBu}-COOH]Cl (shown in Chart 4.1), we gain two additional complexes to study the effect of the acid distance on catalase activity.

4.3.9. Synthesis of Dibenzofuran Analogues of Manganese Hangman Salens

The Hangman salen compounds using the dibenzofuran scaffold were assembled according to the sequence described in Scheme 4.5. 4,6-Dibromodibenzofuran (**20**) was synthesized by dilithiation of the commercially available dibenzofuran using *sec*-butyllithium followed by bromination by elemental bromide.³⁸ To generate the carboxylic-acid-functionalized Hangman, 4,6-dibromodibenzofuran was monolithiated

Scheme 4.5



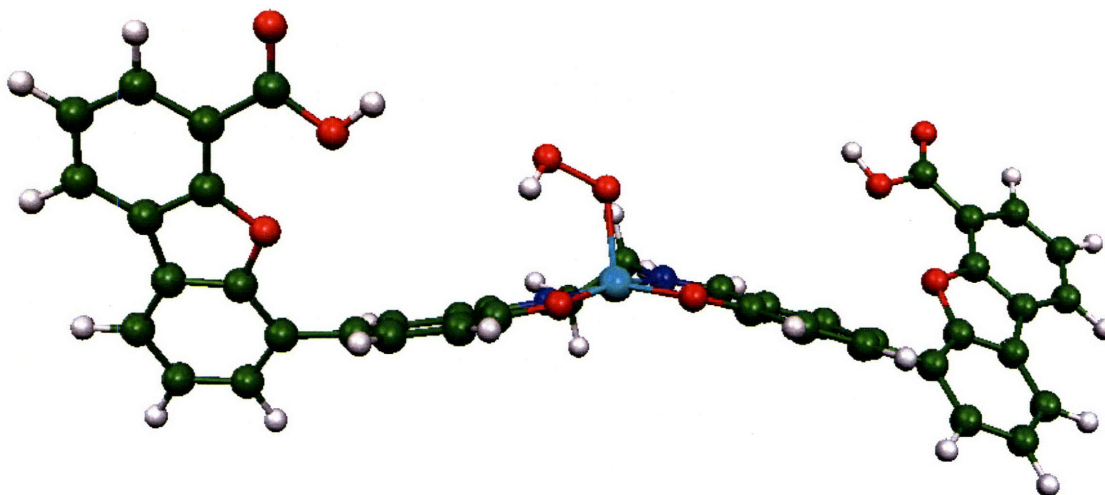
(a) (i) Phenyllithium, cyclohexane/THF, (ii) CO₂ gas (b) 3-*tert*-butyl-2-hydroxy-5-(4,4,5,5-tetramethyl-[1,3,2]dioxaborolan-2-yl)-benzaldehyde, Na₂CO₃, Pd(PPh₃)₄, DMF/H₂O, (c) (1*R*,2*R*)-(-)-1,2-diaminocyclohexane, EtOH, (d) (i) Mn(OAc)₂(H₂O)₄, EtOH, (ii) aq. NaCl, (e) (i) Phenyllithium, cyclohexane/THF, (ii) SnBu₃Cl, (f) I₂, CH₂Cl₂, (g) 4-methoxycarbonylphenylboronic acid, CsF, Pd(PPh₃)₄, dioxane, (h) BBr₃, CH₂Cl₂

using phenyllithium and carbon dioxide was bubbled through the solution to form 4-bromo-6-hydroxycarbonyldibenzofuran (**21**).³⁸ Palladium-catalyzed Suzuki coupling conditions with 3-*tert*-butyl-2-hydroxy-5-(4,4,5,5-tetramethyl-[1,3,2]dioxaborolan-2-yl)-benzaldehyde³¹ furnished the salen precursor **22**. Synthesis of the benzoic acid functionalized dibenzofuran required additional steps, similar to the multi-step procedure used to obtain the analogous xanthene derivative.¹ 4,6-Dibromo-dibenzofuran (**20**) was monolithiated using phenyllithium, followed by addition of tributyltin chloride to give **25**. Addition of elemental iodine to **25** gave 4-bromo-6-iododibenzofuran (**26**). The aryl-iodo position could be allowed to selectively react using palladium-catalyzed Suzuki cross-coupling conditions with 4-methoxycarbonylphenylboronic acid to give **27**. The deprotected benzoic acid derivative of **27** could not be isolated cleanly due to its

insolubility, but **27** can be coupled directly with 3-*tert*-butyl-2-hydroxy-5-(4,4,5,5-tetramethyl-[1,3,2]dioxaborolan-2-yl)-benzaldehyde to give the more soluble **28**. The methyl ester can then be easily deprotected using boron tribromide to give **29**. Ligand precursors **22** and **29** can be condensed with half an equivalent of (1*R*,2*R*)-(-)-1,2-diaminocyclohexane to give the ligands **23** and **30** in good yields. Manganese(III) chloride can be inserted by refluxing with manganese(II) acetate, followed by workup with an aqueous sodium chloride solution to give Mn[HSD*^tBu-COOH]Cl (**24**) and Mn[H_{ph}SD*^tBu-COOH]Cl (**31**).

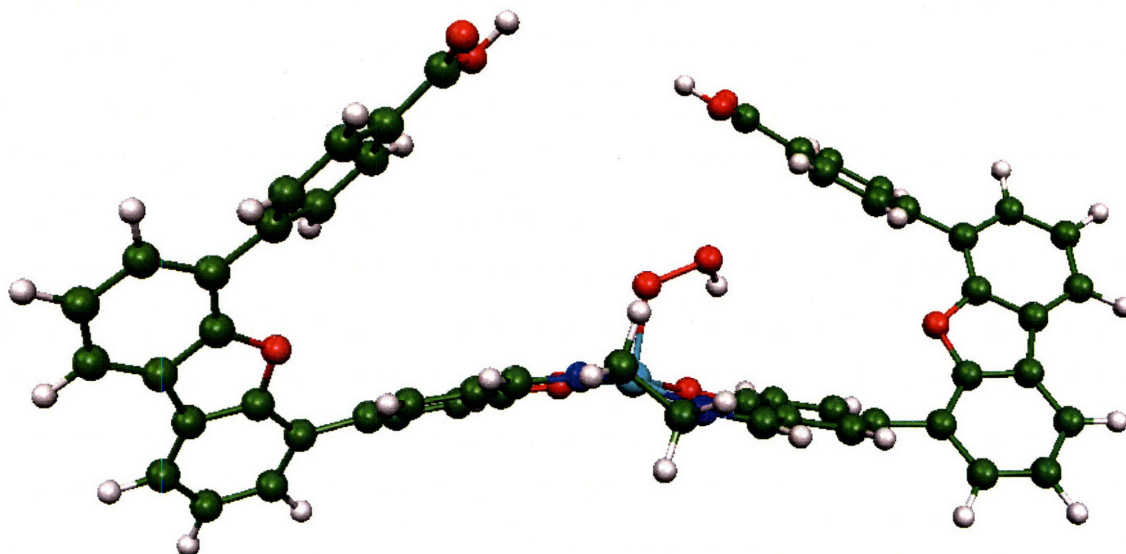
4.3.10. Density Functional Theory of Dibenzofuran Analogues of Manganese Hangman Salens

Figure 4.7. Energy-minimized structures obtained from DFT of the hydroperoxide complex Mn[HSD*^tBu]OOH.



We examined the geometric parameters of the two manganese Hangman compounds Mn[HSD*^tBu-COOH]Cl (**24**) and Mn[H_{ph}SD*^tBu-COOH]Cl (**31**), using the same geometry optimized energy-minimization calculations on the hydroperoxide bound species (replacing the chloride). Again, in order to simplify the calculations, we replaced the cyclohexanediamine bridge with ethylenediamine and did not include the *tert*-butyl and methyl groups. Selected bond and distance measurements for those two compounds as well as the xanthene analogues are shown in Table 4.4 (located at the end of the Chapter). For Mn[HSD*^tBu-COOH]Cl (**24**), we find that the dibenzofuran tilts the carboxylic acid functionalities appreciably away both vertically and laterally from the

Figure 4.8. Energy-minimized structures obtained from DFT of the hydroperoxide complex $\text{Mn}[\text{H}_{\text{ph}}\text{SD}^{\text{tBu}}]\text{OOH}$.



bound hydroperoxide, giving an average acid-to-metal distance of about 7.4 Å (see Figure 4.7). We expect this distance can increase slightly with some rotation about the dibenzofuran-salen bond. As shown in Figure 4.8 (bottom), when the scaffold is functionalized by a benzoic acid in Hangman complex **31**, the acid is moved closer to the metal along the salen macrocycle plane, but the tilt upwards forced by the dibenzofuran geometry also moves the acid further away vertically from the metal center, giving acid-to-metal distances of about 7.0 Å and 7.6 Å. In this structure, unlike the xanthene analogue, the carboxylic acids are not close enough to form an intermolecular carboxylic acid dimer.

4.3.11. Catalase Activity: Acid-to-Metal Distance Effects

The Hangman complexes $\text{Mn}[\text{HSD}^{\text{tBu}}\text{-COOH}]\text{Cl}$ (**24**) and $\text{Mn}[\text{H}_{\text{ph}}\text{SD}^{\text{tBu}}\text{-COOH}]\text{Cl}$ (**31**) were evaluated for their reactivity in catalyzing the disproportionation of hydrogen peroxide. The amount of O_2 evolved in turnover numbers (TON) for each catalyst is shown in Table 1. Of the two Hangman complexes with dibenzofuran scaffolds, the benzoic acid functionalized catalyst $[\text{H}_{\text{ph}}\text{SD}^{\text{tBu}}\text{-COOH}]\text{Cl}$ (**31**) demonstrated greater activity, averaging 2537 TON after one hour. The acid-functionalized $\text{Mn}[\text{HSD}^{\text{tBu}}\text{-COOH}]\text{Cl}$ (**24**), however, displays much lower activity, averaging only 767 TON an hour

Table 4.2. Observed Turnover Number (TON) for H₂O₂ Disproportionation by Manganese Hangman Catalysts over One Hour. ^a

| Catalyst | TON |
|---|------|
| Mn[HphSX* ^t Bu]Cl ^b | 2495 |
| Mn[HSX* ^t Bu]Cl ^b | 5328 |
| Mn[HphSD* ^t Bu]Cl | 2537 |
| Mn[HSD* ^t Bu]Cl | 838 |
| Mn[salen]Cl ^{b,c} | 164 |
| Mn[salen]Cl ^{b,d} | 182 |

^a In 2:1 dichloromethane: methanol at 25 °C.

^b Data taken from ref. 10.

^c salen = (1*R*,2*R*)-(-)-[(1,2-cyclohexanediamino-*N,N'*-bis(3,5-di-*tert*-butylsalicylidene))].

^d Two equivalents of benzoic acid.

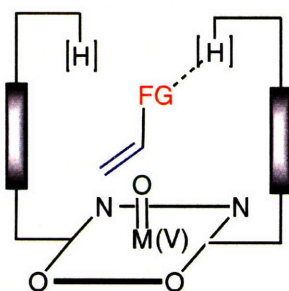
under the same conditions. For comparison, we have also included the average TON from our two previously studied xanthene based Hangman salen compounds. The acid functionalized xanthene Hangman Mn[HSX*^tBu]Cl demonstrates the best catalase activity, while the benzoic acid functionalized version Mn[H_{ph}SX*^tBu]Cl is slightly less active but similar to the dibenzofuran analogue [H_{ph}SD*^tBu-COOH]Cl (**31**).

Although the distances are similar, the ideal assembly of the second equivalent of hydrogen peroxide is thought to be roughly linear. This may explain why compound [H_{ph}SD*^tBu-COOH]Cl (**31**), where the increase in acid distance is primarily perpendicular from the metallosalen macrocycle, is a superior catalysts to Mn[HSD*^tBu-COOH]Cl (**24**), which moves shifts the acids both vertically and horizontally. While Mn[HSD*^tBu-COOH]Cl (**24**) is the poorest-performing Hangman salen compound studied thus far (shown in Table 4.2), it still outperforms the redox only manganese salen platform with the addition of two equivalents of benzoic acid. So while it provides less than ideal carboxylic acid distance for hydrogen peroxide, the structural Hangman framework that provides the hydrogen bonding environment over the metal center is better than the only having the proton source.

4.3.12. Epoxidation of Functionalized Olefins

In Chapter 3, we examined the manganese Hangman salens with xanthene scaffolds for their epoxidation activity. While they retained the ability to catalyze enantioselective oxygen atom transfer, analogous to their manganese salen counterparts lacking the Hangman framework, there was no appreciable enhancement in turnover number (TON). From these results and our stopped-flow studies using Hangman salophens (discussed in Chapter 2), the hanging group does not appear to facilitate the formation of the high valent Mn(V) oxo species using peroxide, hypochlorite, or iodosobenzene as the oxidant. However, we saw in this Chapter that the hanging group can assist hydrogen peroxide oxidation by pre-assembly in the molecular cleft, resulting in turnover numbers orders of magnitude over their unfunctionalized analogues. We sought to apply this principle to the epoxidation of olefins appended with a functional group capable of hydrogen-bonding,

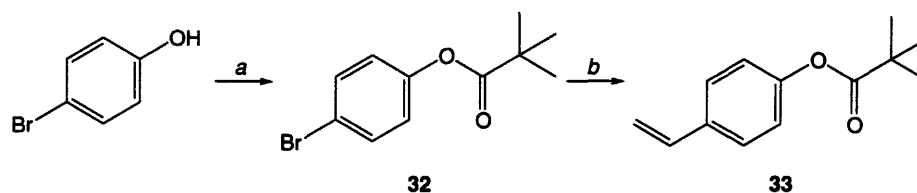
Scheme 4.6



thereby positioning the substrate for oxidation over the Mn(V) oxo, as shown in Scheme 4.6.

4-Acetoxystyrene was our initial substrate as it is well behaved in the GC-MS conditions we employed to determine turnover numbers. As the different acid-to-metal distances in our Hangman salens form molecular clefts of varying size, we examined the epoxidation activity for all of our acid functionalized complexes, $\text{Mn}[\text{H}_{\text{ph}}\text{SX}^t\text{Bu}]\text{Cl}$, $\text{Mn}[\text{HSX}^t\text{Bu}]\text{Cl}$, $\text{Mn}[\text{H}_{\text{ph}}\text{SD}^t\text{Bu}]\text{Cl}$, and $\text{Mn}[\text{HSD}^t\text{Bu}]\text{Cl}$ (listed from shortest to longest acid-to-metal distance). As a control, we also examined the TON for an unmodified manganese salen platform. Sodium hypochlorite was used as the oxidant. The results we obtained are shown in Table 4.3. Although there was improvement in the TON for some of the Hangman complexes, particularly $\text{Mn}[\text{H}_{\text{ph}}\text{SX}^t\text{Bu}]\text{Cl}$, the observed yield

Scheme 4.7



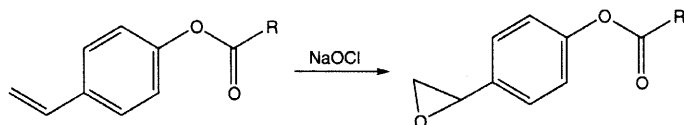
(a) pivaloyl chloride, pyridine, CH_2Cl_2 , (b) tributyl(vinyl)tin, $\text{Pd}(\text{PPh}_3)_4$, toluene

for the epoxidation product for this substrate was not very high. Instead, we saw a significant amount of α -mono- and di-chlorinated product, which was present in greater amounts for the Hangman catalysts.

To prevent the formation of this side product, we initially thought to use the trifluorinated analogue, but found during its synthesis that the trifluoroacetate appendage was extremely prone to hydrolysis, particularly in the presence of base.³⁹ Instead, we used the pivalic acid analogue, which was synthesized in two steps, shown in Scheme 4.7. 4-Bromophenol was treated with pivaloyl chloride in the presence of pyridine to give **32**,⁴⁰ which was coupled under Stille coupling conditions⁴¹ with tributyl(vinyl)tin to give the functionalized olefin product **33**.

This modified substrate prevents formation of the α -mono- and di-chlorinated side products discussed above; the epoxidized substrate is instead the major product. As shown in Table 4.3, the manganese Hangman salens with the functionalized xanthene scaffolds demonstrate better epoxidation activity than the unmodified salen platform. The dibenzofuran Hangman salen analogues show approximately the same activity as the control. Although thus far we have only examined the two substrates described above, we believe the enhanced TON we see with some of the Hangman complexes could be due to a modest substrate pre-assembly via the carboxylic acid functionalities. Epoxidation of functionalized olefins typically brings Sharpless' titanium tartrate catalyst to mind, which enforces allylic alcohol assembly through a covalent bond between the metal and alcohol group.⁴²⁻⁴⁴ In this case, we are using hydrogen-bonding interactions instead of covalent interactions to direct reactivity. Hydrogen-bond interactions, along with π -stacking, are thought to be important for the high regio- and stereoselective oxidation chemistry performed by monooxygenases,⁴⁵⁻⁴⁸ heme peroxidases,⁴⁹ and fatty acid desaturases.⁵⁰⁻⁵⁵

Table 4.3. Analysis of products and turnover numbers (TON) for epoxidation reactions as determined using GC/MS with 4-acetoxystyrene (R = H) and 2,2-dimethyl-propionic acid 4-vinyl-phenyl ester (R = *t*-Bu) over 1 and 3 hours, using sodium hypochlorite as the oxidant.



| | R = H, (TON) | | | | R = <i>t</i> -Bu, (TON) | |
|---|--------------|-------|----------|--------|-------------------------|-------|
| | products | | | | | |
| | epoxide | | monochl. | dichl. | epoxide (34) | |
| | 1 hrs | 3 hrs | 3 hrs | 3 hrs | 1 hrs | 3 hrs |
| Mn(salen)Cl ^a | 1 | 3 | 8 | 5 | 3 | 8 |
| Mn(H _{ph} SX* ^t Bu)Cl | 11 | 13 | 24 | 22 | 3 | 26 |
| Mn(HSX* ^t Bu)Cl | 5 | 10 | 25 | 23 | 7 | 16 |
| Mn(H _{ph} SD* ^t Bu)Cl | 9 | 7 | 26 | 20 | 7 | 8 |
| Mn(HSD* ^t Bu)Cl | 4 | 8 | 26 | 21 | 4 | 4 |

^a salen = (1*R*,2*R*)-(-)-[(1,2-cyclohexanediamino-*N,N'*-bis(3,5-di-*tert*-butylsalicylidene)]

The use of more labile non-covalent interactions plays an important role in facilitating substrate turnover and catalyst activity. Secondary environments that take advantage of this have already been successfully incorporated into synthetic catalysts to enforce substrate selectivity.⁵⁶⁻⁶¹ Although we have yet to demonstrate regioselectivity in our epoxidation reactions, the hydrogen-bonding interactions we are accessing in our Hangman framework are reminiscent of those found in enzymatic systems.

4.4. Concluding Remarks and Future Work

Comparison of the reactivity profiles and overall TON for H₂O₂ dismutation between Hangman salens with pendant acid and methyl ester groups establishes the importance of a hydrogen bonding group is in facilitating catalysis. Computational studies suggest that only one carboxylic acid is needed to promote the favored end-on hydrogen peroxide assembly with the metal oxo catalytic intermediate. When the functional group is extended with a phenylene spacer, the two carboxylic acids are sufficiently close to form

a $-(\text{COOH})_2-$ dimer, which reduces the propensity of the hanging group to promote substrate assembly; accordingly, lower catalytic activity is observed.

The activity of the oxo catalyst of Mn salen is enhanced by the positioning of an acid-base group over the salen that is modified with steric blocking groups at the 3 and 3' position of the macrocycle, as predicted by theoretical investigations into the mechanism. The hydrogen bonding network established by the Hangman scaffold and the steric blocking groups work in concert to promote the end-on assembly of the second equivalent of the hydrogen peroxide in conformation that productive for its subsequent oxidation by the manganyl oxo. These design principles should find utility for the construction of general Mn salen catalysts displaying enhanced ROS activity.

As the hydrogen-bonding functionalities on our Hangman ligands serve as a platform for facilitating hydrogen peroxide disproportionation, we would like to investigate their effect on the related ROS, the superoxide radical. This is a particularly important activity in the context of developing therapeutic agents against oxidative stress.⁶²⁻⁶⁹ As mentioned in the introduction, most manganese salens behave as superoxide dismutase (SOD) mimics as well as demonstrating high catalase activity.^{70,71} The two most effective are currently being tested in human studies.^{17,26} However, unlike catalase activity, the only methods for detecting SOD activity are indirect.⁷² Typically, superoxide is generated in low levels using xanthine/xanthine oxidase. The concentration of superoxide can be quantitatively tested spectroscopically using a reporter molecule, commonly ferricytochrome c, which is reduced by superoxide and produces a spectral shift.^{73,74} More accurate measurements of superoxide concentration can be made via spectroscopically observing the superoxide itself using stopped-flow⁷² or using pulse radiolysis.⁷⁵ Regardless of the method used to measure SOD activity, they all require the assay to be performed in aqueous solutions.

Synthesizing water-soluble versions of our Hangman complexes should be fairly straightforward; the assembly of appropriately functionalized precursors should follow a similar synthetic path we have already developed. Disulfonated xanthene derivatives are already commonly used in the synthesis of water-soluble ligand for hydroformulation catalysts⁷⁶ and photoinitiators.⁷⁷ The installation of sulfonate groups using fuming

sulfuric acid should be feasible for a xanthene dibromide precursor. Additionally, our chiral cyclohexane bridge is not necessary for this activity; therefore we can replace our diamine bridge with one that possesses water solubilizing functional groups.

Of all of the complexes studied using the Hangman framework (porphyrin, salophen, and salen), the Hangman salens are best suited to assay for SOD activity and potential use in biological systems. In the Hangman porphyrin system, it was the iron complex that displayed high catalase activity. Most of the interest in synthesizing a therapeutic drug has focused on manganese. The likely product of catalyst decomposition is the hydrated metal ion, and of the three metal ions used in the pursuit of SOD mimics, iron, copper and manganese, the latter is the least toxic.^{62,78} (Iron can also perform Fenton chemistry with hydrogen peroxide to form hydroxyl radicals). The Hangman salophens will likely be limited in their ability to serve as a therapeutic drug as well. Manganese salophens are active SOD mimics under laboratory conditions, but showed loss of activity when incubated in a cell culture, indicating instability under biological conditions.⁷⁹ Conversely, manganese salen compounds have demonstrated cytoprotective activity in vivo.¹⁹⁻²⁵ They are stable in bovine serum albumin (BSA) and in acidic conditions.^{10,80} This is particularly important as tissue in ischemic stress (lack of oxygen) can approach pH 5.^{81,82} All of these factors make the manganese Hangman salen system an ideal candidate for extending our studies of ROS neutralization activity.

4.5. Experimental Section

4.5.1. Materials

Silica gel 60 (70-230 and 230-400 mesh) was used for column chromatography. Analytical thin layer chromatography was performed using F254 silica gel (pre-coated sheets, 0.2 mm thick). Solvents for synthesis were for reagent grade or better and used as received or dried according to standard methods.⁸³ Boron tribromide (1M in dichloromethane), iodine, 5-bromosalicylaldehyde, phenylboronic acid, 4-bromophenol, pivaloyl chloride, pyridine, 4-acetoxystyrene, and (1*R*,2*R*)-(-)-1,2-diaminocyclohexane were used as received from Aldrich. Bis(pinacolato)diboron and 3-formyl-4-methoxyphenyl-boronic acid was used as received from Frontier Scientific. Tetrakis(triphenylphosphine)palladium, tri(*n*-butyl)tin chloride, dichloro[1,1'-

bis(diphenylphosphino)ferrocene]palladium(II) dichloromethane adduct, tributyl(vinyl)tin, sodium carbonate, cesium fluoride, and manganese(II) acetate tetrahydrate were used as received from Strem Chemicals. Phenyllithium (1.6-1.7 M in cyclohexane) and 30% aqueous solution of hydrogen peroxide were used as received from Alfa Aesar. The following compounds were obtained using published protocols and their purity confirmed by ^1H NMR: 4-methoxycarbonyl-5-bromo-2,7-di-*tert*-butyl-9,9-dimethylxanthene (1),³ 4-(5-bromo-2,7-di-*tert*-butyl-9,9-dimethyl-9H-xanthen-4-yl)-benzoic acid methyl ester (2),³ 4,6-dibromo-dibenzofuran (20),³⁸ 4-bromo-6-hydroxycarbonyldibenzofuran (21).³⁸ 3-*tert*-butyl-2-hydroxy-5-(4,4,5,5-tetramethyl-[1,3,2]dioxaborolan-2-yl)-benzaldehyde was synthesized as described in Chapter 3.

4.5.2. Physical measurements

^1H NMR and ^{13}C NMR spectra were collected in CDCl_3 or $\text{C}_4\text{D}_8\text{O}$ (Cambridge Isotope Laboratories) at the MIT Department of Chemistry Instrumentation Facility (DCIF) using an Inova 500 or Mercury 300 Spectrometer at 25 °C. All chemical shifts are reported using the standard δ notation in parts-per-million relative to tetramethylsilane and spectra have been internally calibrated to the monoprotio impurity of the deuterated solvent used. High-resolution mass spectral analyses were carried out by the MIT Department of Chemistry Instrumentation Facility on a Bruker APEXIV47e.FT-ICR-MS using an Apollo ESI source.

4.5.3. Synthesis

4.5.3.1. 2,7-Di-*tert*-butyl-5-(3-formyl-4-methoxy-phenyl)-9,9-dimethyl-9H-xanthene-4-carboxylic acid methyl ester (3)

Under nitrogen, a mixture of 4-methoxycarbonyl-5-bromo-2,7-di-*tert*-butyl-9,9-dimethylxanthene (1) (0.300 g, 0.653 mmol), 3-formyl-4-methoxyphenylboronic acid (0.130 g, 0.722 mmol), sodium carbonate (0.101 g, 0.981 mmol), tetrakis(triphenylphosphine)palladium (0.029 g, 0.040 mmol), DMF (9 mL), and deionized water (1 mL) was heated to 90 °C for 36 hours. Upon cooling, the mixture was extracted with 3 \times 75 mL of dichloromethane. The organic portions were combined and dried over MgSO_4 and the solvent removed by rotary evaporation. The crude solid was purified by column chromatography (silica gel, 3:7 hexane: dichloromethane) to elute the colorless product

(0.333 g, 99% yield). ¹H NMR (500 MHz, CDCl₃, δ): 10.54 (s, 1H), 8.01 (d, *J* = 2.5 Hz, 1H), 7.85 (dd, *J* = 8.5 Hz, 2.5 Hz, 1H), 7.57 (s, 2H), 7.43 (d, *J* = 2.5 Hz, 1H), 7.21 (d, *J* = 2.5 Hz, 1H), 7.10 (d, *J* = 8.5 Hz, 1H), 4.01 (s, 3H), 3.50 (s, 3H), 1.70 (s, 6H), 1.36 (s, 9H), 1.33 (s, 9H). ¹³C NMR (500 MHz, CDCl₃, δ): 190.0, 167.7, 160.9, 147.4, 146.1, 145.3, 145.2, 138.2, 131.4, 131.1, 130.2, 130.0, 127.9, 126.3, 126.2, 125.9, 124.5, 121.9, 119.7, 111.2, 56.0, 52.0, 35.0, 34.7, 34.6, 32.1, 31.7, 31.5. HRESI-MS ([M + Na]⁺) NaC₃₃H₃₈O₅ *m/z*, Calcd. 537.2611, Found 537.2601.

4.5.3.2. 4-[2,7-Di-*tert*-butyl-5-(3-formyl-4-methoxy-phenyl)-9,9-dimethyl-9H-xanthen-4-yl]-benzoic acid methyl ester (4)

Under nitrogen, a mixture of 4-(5-bromo-2,7-di-*tert*-butyl-9,9-dimethyl-9H-xanthen-4-yl)-benzoic acid methyl ester (2) (0.200 g, 0.374 mmol), 3-formyl-4-methoxyphenylboronic acid (0.074 g, 0.411 mmol), sodium carbonate (0.058 g, 0.563 mmol), tetrakis(triphenylphosphine)palladium (0.016 g, 0.022 mmol), DMF (9 mL), and deionized water (1 mL) was heated to 90 °C for 36 hours. Upon cooling, the mixture was extracted with 3 × 100 mL of dichloromethane. The organic portions were combined and dried over MgSO₄ and the solvent removed by rotary evaporation. The crude solid was purified by column chromatography (silica gel, dichloromethane) to elute the colorless product (0.219 g, 99% yield). ¹H NMR (500 MHz, CDCl₃, δ): 10.39 (s, 1H), 7.77 (d, *J* = 8.5 Hz, 2H), 7.74 (d, *J* = 2.5 Hz, 1H), 7.47 (d, *J* = 2.5 Hz, 1H), 7.44 (d, *J* = 2.5 Hz, 1H), 7.38 (dd, *J* = 8.5 Hz, 2.5 Hz, 1H), 7.31 (d, *J* = 8.5 Hz, 2H), 7.16 (m, 2H), 6.57 (2, *J* = 8.5 Hz, 1H), 3.97 (s, 3H), 3.89 (s, 3H), 1.74 (s, 6H), 1.36 (s, 9H), 1.35 (s, 9H). ¹³C NMR (500 MHz, CDCl₃, δ): 190.3, 167.8, 161.5, 146.5, 146.42, 146.40, 146.3, 144.0, 138.1, 131.4, 131.3, 131.1, 130.4, 130.0, 129.7, 128.9, 128.5, 128.4, 126.23, 126.17, 124.9, 123.0, 122.4, 111.5, 56.2, 52.7, 35.9, 35.3, 32.3, 32.2. HRESI-MS ([M + Na]⁺) C₃₉H₄₂O₅Na *m/z*, Calcd. 613.2924, Found 613.2920.

4.5.3.3. 2,7-Di-*tert*-butyl-5-(3-formyl-4-hydroxy-phenyl)-9,9-dimethyl-9H-xanthene-4-carboxylic acid methyl ester (5)

2,7-Di-*tert*-butyl-5-(3-formyl-4-methoxy-phenyl)-9,9-dimethyl-9H-xanthene-4-carboxylic acid methyl ester (3) (0.200 g, 0.389 mmol) was added to 8 mL of dichloromethane and cooled to 0 °C. A solution of boron tribromide (1.2 mL, 1.0 M in dichloromethane) was added and upon stirring for 1 hour, 4 mL of water was added. The

organic layer was separated, washed with 10 mL of water, and dried over MgSO₄. The solvent was evaporated and the residue was purified by column chromatography (silica gel, 99:1 dichloromethane: methanol) to elute the product (0.054 g, 28% yield). ¹H NMR (500 MHz, CDCl₃, δ): 11.12 (s, 1H), 10.07 (s, 1H), 7.96 (d, *J* = 2 Hz, 1H), 7.76 (dd, *J* = 8.5 Hz, 2 Hz, 1H), 7.58 (d, *J* = 2.5 Hz, 1H), 7.56 (d, *J* = 2 Hz, 1H), 7.45 (d, *J* = 2.5 Hz, 1H), 7.25 (d, *J* = 2 Hz, 1H), 7.09 (d, *J* = 8.5 Hz, 1H), 3.55 (s, 3H), 1.71 (s, 6H), 1.38 (s, 9H), 1.34 (s, 9H). ¹³C NMR (500 MHz, CDCl₃, δ): 197.8, 167.5, 160.8, 147.3, 146.3, 145.4, 145.3, 138.9, 135.9, 131.0, 130.3, 130.2, 127.6, 126.4, 126.0, 125.8, 122.2, 120.3, 119.8, 117.2, 52.3, 35.1, 34.8, 34.7, 32.3, 31.8, 31.6. HRESI-MS ([M + H]⁺) C₃₂H₃₇O₅ *m/z*, Calcd. 501.2636 Found 501.2625.

4.5.3.4. 4-[2,7-Di-*tert*-butyl-5-(3-formyl-4-hydroxy-phenyl)-9,9-dimethyl-9H-xanthen-4-yl]-benzoic acid methyl ester (6)

4-[2,7-Di-*tert*-butyl-5-(3-formyl-4-methoxy-phenyl)-9,9-dimethyl-9H-xanthen-4-yl]-benzoic acid methyl ester (4) (0.100 g, 0.169 mmol) was added to 8 mL of dichloromethane and cooled to 0 °C. A solution of boron tribromide (0.51 mL, 1.0 M in dichloromethane) was added and stirred for 1 hour. 4 mL of water was then added. The organic layer was separated, washed with 10 mL of water, and dried over MgSO₄. The solvent was evaporated and the residue was purified by column chromatography (silica gel, dichloromethane) to elute the product (0.076 g, 78% yield). ¹H NMR (500 MHz, CDCl₃, δ): 10.87 (s, 1H), 9.29 (s, 1H), 7.26 (d, *J* = 8.5 Hz, 2H), 7.49 (d, *J* = 2.5 Hz, 1H), 7.46 (m, 2H), 7.33 (m, 2H), 7.31 (s, 1H), 7.20 (d, *J* = 2 Hz, 1H), 7.17 (d, *J* = 2 Hz, 1H), 6.85 (d, *J* = 8.5 Hz, 1H), 4.00 (s, 3H), 1.76 (s, 6H), 1.37 (s, 18H). ¹³C NMR (500 MHz, CDCl₃, δ): 197.0, 167.4, 161.1, 146.5, 146.4, 146.1, 146.0, 143.6, 138.6, 135.8, 130.93, 130.91, 130.4, 130.3, 129.6, 129.1, 128.9, 128.1, 126.3, 126.0, 123.2, 122.7, 120.8, 117.8, 52.8, 35.8, 35.3, 32.7, 32.3. HRESI-MS ([M + Na]⁺) C₃₈H₄₀O₅Na *m/z*, Calcd. 599.2768, Found 599.2756.

4.5.3.5. H₂(HSX*-COOMe) (7)

A mixture of 2,7-di-*tert*-butyl-5-(3-formyl-4-hydroxy-phenyl)-9,9-dimethyl-9H-xanthene-4-carboxylic acid methyl ester (5) (0.050 g, 0.100 mmol) was combined with (1*R*,2*R*)-(-)-1,2-diaminocyclohexane (0.006 mg, 0.050 mmol) in 5 mL of absolute

ethanol and refluxed for 8 hours. Upon cooling the solvent was removed by rotary evaporation and the resulting solid was washed with 1 mL of cold methanol and dried under vacuum to yield the product as a yellow solid (0.053 g, 98%). ¹H NMR (500 MHz, CDCl₃, δ): 13.42 (bs, 2H), 8.46 (s, 2H), 7.55 (d, *J* = 2.5 Hz, 2H), 7.52 (d, *J* = 2.5 Hz, 2H), 7.56 (s, 2H), 7.45 (d, *J* = 2.5 Hz, 2H), 7.38 (d, *J* = 2.5 Hz, 2H), 7.16 (d, *J* = 2.5 Hz, 2H), 6.96 (d, *J* = 9 Hz, 2H), 3.45 (d, *J* = 9 Hz, 2H), 3.32 (s, 6H), 1.99 (d, *J* = 9 Hz, 2H), 1.92 (d, *J* = 9 Hz, 2H), 1.78 (d, *J* = 9 Hz, 2H), 1.69 (s, 6H), 1.67 (s, 6H), 1.53 (t, *J* = 9 Hz, 2H), 1.43 (s, 9H), 1.33 (s, 9H). ¹³C NMR (500 MHz, CDCl₃, δ): 168.2, 165.3, 160.3, 147.4, 146.0, 145.4, 145.2, 134.0, 133.2, 131.2, 130.1, 129.1, 128.6, 126.2, 126.1, 125.7, 121.4, 120.1, 118.3, 116.5, 72.9, 52.1, 35.1, 34.73, 34.70, 33.5, 32.1, 31.9, 31.7, 31.6, 24.4. HRESI-MS ([M + H]⁺) C₇₀H₈₃N₂O₈ *m/z*, Calcd. 1079.6144, Found 1079.6167.

4.5.3.6. H₂(H_{ph}SX*-COOMe) (8)

A mixture of 4-[2,7-di-*tert*-butyl-5-(3-formyl-4-hydroxy-phenyl)-9,9-dimethyl-9H-xanthen-4-yl]-benzoic acid methyl ester (6) (0.018 g, 0.031 mmol) was combined with (1*R*,2*R*)-(-)-1,2-diaminocyclohexane (0.002 g, 0.016 mmol) in 5 mL of absolute ethanol and refluxed for 8 hours. Upon cooling the solvent was removed by rotary evaporation and the resulting yellow solid was washed with 0.5 mL of cold methanol and dried under vacuum (0.019 mg, 98% yield). ¹H NMR (500 MHz, CDCl₃, δ): 13.09 (bs, 2H), 8.05 (s, 2H), 7.65 (d, *J* = 8 Hz, 2H), 7.61 (d, *J* = 8 Hz, 2H), 7.43 (d, *J* = 1.5 Hz, 2H), 7.35 (d, *J* = 2 Hz, 2H), 7.20 (m, 4H), 7.13 (d, *J* = 2 Hz, 2H), 7.09 (d, *J* = 1.5 Hz, 2H), 7.02 (m, 4H), 6.50 (d, *J* = 8 Hz, 2H), 4.37 (t, *J* = 11.5 Hz, 2H), 3.25 (bs, 2H), 2.97 (m, 4H), 1.72 (s, 6H), 1.67 (s, 6H), 1.53 (bs, 2H), 1.34 (s, 18H), 1.38 (s, 18H). ¹³C NMR (500 MHz, CDCl₃, δ): 167.1, 164.8, 160.3, 146.1, 145.9, 145.6, 142.9, 138.1, 135.3, 133.5, 132.8, 130.9, 130.43, 130.37, 129.6, 129.0, 128.8, 128.5, 128.1, 125.8, 125.6, 122.2, 121.2, 118.2, 116.3, 72.8, 52.1, 35.4, 34.8, 34.74, 34.68, 33.0, 32.14, 32.11, 31.7, 31.2, 29.91, 29.87, 29.6, 24.4. HRESI-MS ([M + H]⁺) C₈₂H₉₁N₂O₈ *m/z*, Calcd. 1231.6770, Found 1231.6799.

4.5.3.7. Mn(HSX*-COOMe)Cl (9)

H₂(HSX*-COOMe) (7) (0.020 g, 0.019 mmol) and manganese(II) acetate tetrahydrate (0.007 g, 0.029 mmol) was added to 4 mL of ethanol and refluxed for 2 hours in air.

Upon cooling 0.5 mL of an aqueous saturated sodium chloride solution was added and the mixture was extracted with 2 × 15 mL of dichloromethane. The combined organic portions were then washed with 15 mL of water and dried over MgSO₄. The solvent was removed by rotary evaporation to yield the brown product (0.021 g, 98% yield). HRESI-MS ([M - Cl]⁻) C₇₀H₈₀MnN₂O₈ *m/z*, Calcd. 1131.5290, Found 1131.5318. Anal. Calcd for C₇₀H₈₀ClMnN₂O₈: C, 72.00; H, 6.90; N, 2.40. Found: C, 71.82; H, 6.72 N, 2.48.

4.5.3.8. Mn(H_{ph}SX*-COOMe)Cl (10)

H₂(H_{ph}SX*-COOMe) (8) (0.010 g, 0.008 mmol) and manganese(II) acetate tetrahydrate (0.003 g, 0.012 mmol) was added to 3 mL of ethanol and refluxed for 4 hours in air. Upon cooling 0.5 mL of an aqueous saturated sodium chloride solution was added and the mixture was extracted with 2 × 15 mL of dichloromethane. The combined organic portions were then washed with 15 mL of water and dried over MgSO₄. The solvent was removed by rotary evaporation to yield the brown product (0.010 g, 93% yield). HRESI-MS ([M - Cl]⁻) C₈₂H₈₈MnN₂O₈ *m/z*, Calcd. 1283.5926, Found 1283.5857. Anal. Calcd for C₈₂H₈₈ClMnN₂O₈: C, 74.61; H, 6.72; N, 2.12. Found: C, 74.53; H, 6.60; N, 2.10.

4.5.3.9. 4-Hydroxy-biphenyl-3-carbaldehyde (11)

Under nitrogen, 5-bromosalicylaldehyde (1.00 g, 4.98 mmol), phenylboronic acid (0.910 g, 7.46 mmol), sodium carbonate (0.800 g, 7.46 mmol), dichloro[1,1'-bis(diphenylphosphino)ferrocene]palladium(II) dichloromethane adduct (0.109 g, 0.15 mmol) was added to degassed 1,2-dimethoxyethane (36 mL) and deionized water (12 mL) and heated to 80 °C for 24 hours. Upon cooling, 20 mL of deionized water was added, and the solution was extracted with 3 × 100 mL dichloromethane. The organic layers were combined and dried using MgSO₄ and the solvent was removed by rotary evaporation. The residue was purified by column chromatography (silica gel, 7: 3 pentane: dichloromethane) to elute the product (0.355 g, 36%). ¹H NMR (500 MHz, CDCl₃, δ): 11.02 (s, 1H), 10.00 (s, 1H), 7.28 (m, 2H), 7.56 (m, 2H), 7.47 (t, *J* = 7 Hz, 2H), 7.37 (t, *J* = 7 Hz, 1H), 7.10 (d, *J* = 8 Hz, 1H). ¹³C NMR (500 MHz, CDCl₃, δ): 196.89, 161.13, 135.93, 132.05, 129.175, 129.08, 128.66, 127.58, 126.80, 126.77, 118.31. HRESI-MS ([M + Na]⁺) NaC₁₃H₁₀O₂ *m/z*, Calcd. 221.0573, Found 221.0562.

4.5.3.9. (R,R)-N,N'-Bis(5-phenylsalicylidene)-1,2-cyclohexanediamine (12)

A mixture of 4-hydroxybiphenyl-3-carbaldehyde (**11**) (0.300 g, 1.51 mmol) was refluxed with (1*R*,2*R*)-(-)-1,2-diaminocyclohexane (0.086 g, 0.757 mmol) in 5 mL of absolute ethanol for 12 hours and then cooled to 0 °C and filtered. The precipitate was collected by vacuum filtration and washed with 2 × 5 mL of cold ethanol and dried in vacuo to yield 0.241g of the bright yellow product in 67% yield. ¹H NMR (500 MHz, CDCl₃, δ): 13.39 (bs, 2H), 8.35 (s, 2H), 7.50 (d, *J* = 2 Hz, 2H), 7.47 (m, 2H), 7.46 (s, 2H), 7.40 (s, 2H), 7.38 (m, 4H), 7.30 (s, 2H), 7.29 (s, 2H), 6.97 (d, *J* = 9 Hz, 2H), 3.38 (d, *J* = 9 Hz, 2H), 1.99 (m, 2H), 1.92 (d, *J* = 9 Hz, 2H), 1.78 (d, *J* = 9 Hz, 2H), 1.51 (t, *J* = 9 Hz, 2H). ¹³C NMR (500 MHz, CDCl₃, δ): 165.0, 160.7, 140.4, 132.1, 131.2, 130.1, 128.9, 126.9, 126.7, 118.9, 117.5, 72.9, 33.3, 24.3. HRESI-MS ([M + H]⁺) C₃₂H₃₁N₂O₂ *m/z*, Calcd. 475.2380, Found 475.2371.

4.5.3.10. Mn[(*R,R*)-*N,N'*-Bis(5-phenylsalicylidene)-1,2-cyclohexanediaminato]Cl (**13**)

(*R,R*)-*N,N'*-Bis(5-phenylsalicylidene)-1,2-cyclohexanediamine (**12**) (0.050 g, 0.105 mmol) and manganese(II) acetate tetrahydrate (0.039 g, 0.158 mmol) was added to 4 mL of ethanol and refluxed for 4 hours in air. Upon cooling 1 mL of an aqueous saturated sodium chloride solution was added and the mixture was extracted with 2 × 15 mL of dichloromethane. The combined organic portions were then washed with 15 mL of water and dried over MgSO₄. The solvent was removed by rotary evaporation to yield a brown product (0.050 g, 84% yield). HRESI-MS ([M - Cl]⁻) C₃₂H₂₈MnN₂O₂ *m/z*, Calcd. 527.1526, Found 527.1518. Anal. Calcd for C₃₂H₂₈ClMnN₂O₂: C, 68.27; H, 5.01; N, 4.98. Found: C, 68.20; H, 5.21.; N, 5.08.

4.5.3.11. 2,7-Di-*tert*-butyl-5-(3-*tert*-butyl-5-formyl-4-hydroxy-phenyl)-9,9-dimethyl-9H-xanthene-4-carboxylic acid methyl ester (**14**)

Under nitrogen, 4-methoxycarbonyl-5-bromo-2,7-di-*tert*-butyl-9,9-dimethylxanthene (**1**) (0.100 g, 0.218 mmol), 3-*tert*-butyl-2-hydroxy-5-(4,4,5,5-tetramethyl-[1,3,2]dioxaborolan-2-yl)-benzaldehyde (0.073 g, 0.239 mmol), sodium carbonate (0.034 g, 0.327 mmol), and tetrakis(triphenylphosphine)palladium(0) (0.015 g, 0.013 mmol) were added to 9 mL DMF and 1 mL deionized water. The mixture was heated to 90 °C for 24 hours. Upon cooling 10 mL of deionized water was added and the solution was

extracted with 3 × 20 mL of dichloromethane. The combined organic portions were washed with 10 mL of deionized water and dried over MgSO₄. The solvent was removed by rotary evaporation and the residue was purified by column chromatography (silica gel, 1:9 diethyl ether: pentane) to give the desired product (0.084 g, 69% yield). ¹H NMR (500 MHz, CDCl₃, 25 °C): δ = 11.87 (s, 1H), 10.03 (s, 1H), 7.78 (d, *J* = 2.5 Hz, 1H), 7.68 (d, *J* = 2.5 Hz, 1H), 7.57 (d, *J* = 2.5 Hz, 1H), 7.56 (d, *J* = 2.5 Hz, 1H), 7.44 (d, *J* = 2.5 Hz, 1H), 7.22 (d, *J* = 2.5 Hz, 1H), 3.46 (s, 3H), 1.71 (s, 9H), 1.49 (s, 9H), 1.38 (s, 9H), 1.33 (s, 9H). ¹³C NMR (500 MHz, CDCl₃, δ): 198.41, 198.12, 167.24, 160.40, 147.40, 146.11, 145.31, 145.28, 137.72, 136.22, 134.02, 130.92, 129.98, 129.46, 128.44, 126.50, 126.16, 125.81, 121.99, 120.30, 120.28, 119.65, 52.04, 35.14, 35.08, 34.78, 34.72, 32.47, 31.75, 31.58, 29.45. HRESI-MS ([M + Na]⁺) calcd for C₃₆H₄₄NaO₅ *m/z*, 579.2903, found 579.2911.

4.5.3.12. 4-[2,7-Di-*tert*-butyl-5-(3-*tert*-butyl-5-formyl-4-hydroxy-phenyl)-9,9-dimethyl-9H-xanthen-4-yl]-benzoic acid methyl ester (15)

The addition of 4-(5-bromo-2,7-di-*tert*-butyl-9,9-dimethyl-9H-xanthen-4yl)-benzoic acid methyl ester (**2**) (0.100 g, 0.187 mmol), 3-*tert*-butyl-2-hydroxy-5-(4,4,5,5-tetramethyl-[1,3,2]dioxaborolan-2-yl)-benzaldehyde (0.063 g, 0.205 mmol), sodium carbonate (0.029 g, 0.280 mmol), and tetrakis(triphenylphosphine)palladium(0) (0.013 g, 0.011 mmol) to 9 mL DMF and 1 mL deionized water was performed under N₂. The mixture was heated to 90 °C for 24 hours. Upon cooling 10 mL of deionized water was added and the solution was extracted with 3 × 20 mL of dichloromethane. The combined organic portions were washed with 10 mL of deionized water and dried over MgSO₄. The solvent was removed by rotary evaporation and the residue was purified by column chromatography (silica gel, 1:9 diethyl ether: pentane) to give the desired product (0.106 g, 90% yield). ¹H NMR (500 MHz, CDCl₃, 25 °C): δ = 11.66 (s, 1H), 9.29 (s, 1H), 7.67 (s, 1H), 7.65 (s, 1H), 7.49 (d, *J* = 2.5 Hz, 1H), 7.47 (dd, *J* = 2.5 Hz, 7 Hz, 2H), 7.27 (d, *J* = 2.5 Hz, 1H) 7.25 (s, 1H), 7.18 (m, 2H), 7.16 (d, *J* = 2.5 Hz, 1H), 3.98 (s, 3H), 1.76 (s, 6H), 1.42 (s, 9H), 1.39 (s, 9H). ¹³C NMR (500 MHz, CDCl₃, δ): 197.00, 196.93, 166.84, 160.27, 145.93, 145.87, 145.70, 142.88, 137.86, 135.39, 133.71, 130.64, 130.39, 129.63, 129.06, 128.92, 128.57, 128.40, 128.26, 125.76, 125.54, 122.64, 121.93, 120.35, 52.20, 35.38, 35.03, 34.79,

32.13, 31.78, 31.75, 29.43. HRESI-MS ($[M + Na]^+$) calcd for $C_{42}H_{48}O_5Na$ m/z , 655.3185, found 655.3196.

4.5.3.13. $H_2[HSX^*-'Bu-COOMe]$ (16)

2,7-Di-*tert*-butyl-5-(3-*tert*-butyl-5-formyl-4-hydroxyphenyl)-9,9-dimethyl-9H-xanthene-4-carboxylic acid methyl ester (14). (0.040 g, 0.072 mmol) was added to (1*R*,2*R*)-(-)-1,2-diaminocyclohexane (0.004 g, 0.036 mmol) in 4 mL of absolute ethanol and heated to reflux for 12 hours. Upon cooling, the solvent was removed by rotary evaporation and the residue was washed with 1 mL of cold deionized water and then dried under vacuum to give the bright yellow product (0.042 g, 98%). 1H NMR (500 MHz, $CDCl_3$, 25°C): δ = 13.92 (bs, 2H), 8.46 (s, 2H), 7.55 (d, J = 2.5 Hz, 2H) 7.51 (d, J = 2.5 Hz, 2H), 7.37 (m, 4H), 7.29 (d, J = 2 Hz, 2H), 7.15 (d, J = 2 Hz, 2H), 3.46 (d, J = 10 Hz, 2H), 3.18 (s, 6H), 2.02 (d, J = 7 Hz, 2H), 1.92 (d, J = 10 Hz, 2H), 1.80 (d, J = 7 Hz, 2H), 1.69 (s, 6H), 1.68 (s, 6H), 1.53 (m, 2H), 1.40 (s, 18H), 1.34 (s, 18H), 1.33 (s, 18H). HRESI-MS ($[M + H]^+$) calcd for $C_{78}H_{99}N_2O_8$ m/z , 1191.7396, found 1191.7342.

4.5.3.14. $H_2[H_{ph}SX^*-'Bu-COOMe]$ (17)

4-[2,7-Di-*tert*-butyl-5-(3-*tert*-butyl-5-formyl-4-hydroxyphenyl)-9,9-dimethyl-9H-xanthen-4-yl]-benzoic acid methyl ester (15) (0.050 g, 0.080 mmol) was added to (1*R*,2*R*)-(-)-1,2-diaminocyclohexane (0.004 g, 0.040 mmol) to 6 mL of absolute ethanol and the mixture was refluxed for 12 hours. Upon cooling, the solvent was removed by rotary evaporation and the residue was washed with 1 mL of cold deionized water and dried under vacuum to give the yellow product (0.053 g, 100%). 1H NMR (500 MHz, $CDCl_3$, 25 °C): δ = 13.71 (bs, 2H), 7.48 (d, J = 8 Hz, 4H), 7.42 (d, J = 2.5 Hz, 2H), 7.39 (d, J = 2.5 Hz, 2H), 7.09 (m, 6H), 7.02 (d, J = 2 Hz, 2H), 6.97 (d, J = 2 Hz, 2H), 6.87 (d, J = 2 Hz, 2H), 2.91 (s, 6H), 3.32 (J = 10 Hz, 2H), 2.07 (bs, 2H), 2.04 (bs, 2H), 1.97 (d, J = 10 Hz, 2H), 1.72 (s, 6H), 1.70 (s, 6H), 1.55 (m, 2H), 1.34 (s, 18H), 1.31 (s, 18H), 1.14 (s, 18H). HRESI-MS ($[M + H]^+$) calcd for $C_{90}H_{107}N_2O_8$ m/z , 1343.8022, found 1343.8016.

4.5.3.15. $Mn[HSX^*-'Bu-COOMe]Cl$ (18)

$H_2[HSX^*-'Bu-COOMe]$ (16) (0.020 g, 0.017 mmol) was added to manganese(II) acetate tetrahydrate (0.006 g, 0.025 mmol) in 4 mL of absolute ethanol and the solution was

refluxed in air for 2 hours. Upon cooling, 0.5 mL of an aqueous saturated sodium chloride solution was added and the mixture was stirred for 10 minutes and then extracted with 3×10 mL of dichloromethane. The organic layers were combined and washed with 10 mL of water and then dried over MgSO_4 . The solvent was removed by rotary evaporation to leave the brown product (0.021 g, 98%). HRESI-MS ($[\text{M} - \text{Cl}]^-$) calcd for $\text{C}_{78}\text{H}_{96}\text{MnN}_2\text{O}_8$ m/z , 1243.6542, found 1243.6582. Anal. Calcd for $\text{C}_{78}\text{H}_{96}\text{ClMnN}_2\text{O}_8$: C, 73.19; H, 7.56; N, 2.19. Found: C, 73.01; H, 7.76; N, 2.30.

4.5.3.16. $\text{Mn}[\text{H}_{\text{ph}}\text{SX}^*-\text{tBu-COOMe}]\text{Cl}$ (19)

$\text{H}_2[\text{H}_{\text{ph}}\text{SX}^*-\text{tBu-COOMe}]$ (17) (25 mg, 0.019 mmol) was combined with manganese(II) acetate tetrahydrate (6.8 mg, 0.028 mmol) in 4 mL of absolute ethanol and refluxed in air for 2 hours. Upon cooling, 0.5 mL of an aqueous saturated sodium chloride solution was added and the mixture was stirred for 10 minutes and then extracted with 3×10 mL of dichloromethane. The organic layers were combined and washed with 5 mL of water and dried over MgSO_4 . The solvent was removed by rotary evaporation to give the brown product (0.026 g, 98%). HRESI-MS ($[\text{M} - \text{Cl}]^+$) calcd for $\text{C}_{90}\text{H}_{104}\text{MnN}_2\text{O}_8$ m/z , 1395.7168, found 1395.7136. Anal. Calcd for $\text{C}_{90}\text{H}_{104}\text{ClMnN}_2\text{O}_8$: C, 75.48; H, 7.32; N, 1.96. Found: C, 75.34; H, 7.45; N, 2.03

4.5.3.17. 6-(3-*tert*-Butyl-5-formyl-4-hydroxyphenyl)-dibenzofuran-4-carboxylic acid (22).

Under nitrogen, a mixture of 4-bromo-6-hydroxycarbonyldibenzofuran (21) (0.200 g, 0.687 mmol), 3-*tert*-butyl-2-hydroxy-5-(4,4,5,5-tetramethyl-[1,3,2]dioxaborolan-2-yl)-benzaldehyde (0.230 g, 0.756 mmol), sodium carbonate (0.106 g, 1.03 mmol), and tetrakis(triphenylphosphine)palladium (0.048 g, 0.041 mmol) was added to 14.5 mL of DMF and 1.5 mL of deionized water and heated to 90 °C for 36 hours. Upon cooling, the reaction mixture was extracted with 3×20 mL of dichloromethane. The combined organic layers were then washed with 2×20 mL of water and dried over MgSO_4 , and the solvent was removed by rotary evaporation. The residue was purified by column chromatography (8: 2 pentane: ethyl acetate) to give the colorless product (0.125 g, 47 % yield). ^1H NMR (500 MHz, $\text{C}_4\text{D}_8\text{O}$, 25°C): δ = 12.08 (s, 1H), 10.06 (s, 1H), 8.40 (d, J = 2 Hz, 1H), 8.37 (d, J = 2 Hz, 1H), 8.29 (dd, J = 7.5 Hz, 1 Hz, 1H), 8.13 (dd, J = 7.5 Hz,

1 Hz, 1H), 8.03 (dd, $J = 7.5$ Hz, 1 Hz, 1H), 7.80 (dd, $J = 7.5$ Hz, 1 Hz, 1H), 7.47 (m, 2H), 1.56 (s, 9H). ^{13}C NMR (500 MHz, $\text{C}_4\text{H}_8\text{O}$, δ): 198.13, 164.97, 160.67, 154.99, 153.44, 137.98, 134.22, 132.49, 129.79, 127.10, 125.94, 125.76, 125.18, 124.38, 124.26, 123.79, 122.59, 121.28, 119.49, 116.25, 35.04, 28.93. HRESI-MS ($[\text{M} + \text{Na}]^+$) cacl'd for $\text{C}_{24}\text{H}_{20}\text{O}_5\text{Na}$ m/z , 411.1208, found 411.1202.

4.5.3.18. $\text{H}_2[\text{HSD}^*\text{Bu-COOH}]$ (23)

A mixture of 4-[6-(3-*tert*-butyl-5-formyl-4-hydroxy-phenyl)-dibenzofuran-4-yl]-benzoic acid methyl ester (22) (30.0 mg, .077 mmol) and (1*R*,2*R*)-(-)-1,2-diaminocyclohexane (4.4 mg, 0.039 mmol) was added to 6 mL of absolute ethanol. The solution was heated to reflux for 2 hours and upon cooling the solvent was removed by rotary evaporation. The yellow residue was washed with 0.3 mL cold methanol and dried under vacuum to give the product (30 mg, 91% yield). HRESI-MS ($[\text{M} + \text{H}]^+$) cacl'd for $\text{C}_{54}\text{H}_{51}\text{N}_2\text{O}_8$ m/z , 855.3640, found 855.3631. Anal. Calcd for $\text{C}_{54}\text{H}_{50}\text{N}_2\text{O}_8$: C, 75.86; H, 5.89; N, 3.28. Found: C, 75.73; H, 6.01; N, 2.45.

4.5.3.19. $\text{Mn}[\text{HSD}^*\text{Bu-COOH}]\text{Cl}$ (24)

A mixture of 23 (30.0 mg, 0.035 mmol) and manganese(II) acetate tetrahydrate (13.0 mg, 0.053 mmol) was added to 4 mL of absolute ethanol and heated to reflux for 2 hours. Upon cooling, 4 mL of saturated aqueous sodium chloride was added and the solution was stirred for 20 minutes and the solid was collected by filtration and washed with water. Upon drying, the brown solid was taken up in dichloromethane and filtered. The filtrate was reduced to give the brown product (14 mg, 42% yield). HRESI-MS ($[\text{M} - \text{Cl}]^+$) cacl'd for $\text{C}_{54}\text{H}_{48}\text{MnN}_2\text{O}_8$ m/z , 907.2792, found 907.2821. Anal. Calcd for $\text{C}_{54}\text{H}_{48}\text{ClMnN}_2\text{O}_8$: C, 68.75; H, 5.13; N, 2.97. Found: C, 68.66; H, 5.23 N, 2.85.

4.5.3.20. (6-Bromo-dibenzofuran-4-yl)-tributyl-stannane (25)

Under nitrogen, a solution of 4,6-dibromodibenzofuran (20) (0.500 g, 1.53 mmol) in 40 mL of dry THF was cooled in an acetone/dry ice bath. Phenyllithium (1.1 mL, 1.7 M solution in cyclohexane) was added and the resulting solution was stirred for 30 minutes and then warmed to room temperature and stirred for an additional 30 minutes before the addition of tri(*n*-butyl)tin chloride (0.549 g, 1.69 mmol). After 15 minutes, the solvent was removed by rotary evaporation to give an oily residue. 15 mL of pentane was added

and the solution was filtered. The filtrate was reduced back to an oil by rotary evaporation and purified by column chromatography (silica gel, pentane) to give the desired product as an oil at room temperature (0.592 g, 72% yield). ¹H NMR (500 MHz, CDCl₃, 25°C): δ = 7.94 (d, *J* = 8 Hz, 1H), 7.90 (d, *J* = 7.5 Hz, 1H), 7.66 (m, 2H), 7.43 (t, *J* = 8 Hz, 1H), 7.23 (t, *J* = 8 Hz, 1H), 1.76 (m, 6H), 1.48 (sextet, *J* = 7.5 Hz, 6H), 1.39 (t, *J* = 8 Hz, 6H), 1.00 (t, *J* = 7.5 Hz, 9H). ¹³C NMR (500 MHz, CDCl₃, δ): 162.21, 153.29, 135.69, 129.70, 126.35, 124.23, 123.66, 123.41, 122.16, 121.08, 119.73, 104.72, 29.41, 27.65, 13.98, 10.29.

4.5.3.21. 4-Bromo-6-iodo-dibenzofuran (26)

Iodine (0.280 g, 1.75 mmol) was slowly added to a rapidly stirring solution of (6-bromo-dibenzofuran-4-yl)-tributylstannane (**25**) (0.592 g, 1.10 mmol) dissolved in 10 mL of dichloromethane. After stirring for one hour, the solution was washed with a saturated aqueous sodium carbonate solution (2 × 10 mL) followed by 10 mL of deionized water. The organic portion was dried over MgSO₄ and the solvent was removed by rotary evaporation to give an oily solid which was purified by loading onto a short silica plug, flushing with pentane, followed by dichloromethane to elute the product as colorless solid (0.386 g, 94%). ¹H NMR (500 MHz, CDCl₃, 25°C): δ = 7.90 (d, *J* = 8 Hz, 1H), 7.87 (m, 2H), 7.66 (d, *J* = 8 Hz, 1H), 7.26 (dt, *J* = 8 Hz, 2.5 Hz, 1H), 7.15 (dt, *J* = 5.5 Hz, 2.5 Hz, 1H). ¹³C NMR (500 MHz, CDCl₃, δ): 153.06, 136.89, 130.88, 126.16, 125.08, 124.70, 124.57, 121.14, 120.32, 105.05, 75.82. HRESI-MS ([M + Na]⁺) caclcd for C₁₂H₆BrIONa *m/z*, 394.8539, found 394.8542.

4.5.3.22. 4-(6-Bromo-dibenzofuran-4-yl)-benzoic acid methyl ester (27)

Under nitrogen, a mixture of 4-bromo-6-iodo-dibenzofuran (**26**) (0.250 g, 0.670 mmol), 4-methoxycarbonylphenylboronic acid (0.133 g, 0.737 mmol), cesium fluoride (0.336 g, 2.21 mmol) and tetrakis(triphenylphosphine)palladium (0.077 g, 0.067 mmol) was added to 8 mL of 1,2-dimethoxyethane and heated to 90 °C for 24 hours. Upon cooling to room temperature, the solvent was removed under vacuum and the residue was taken up in 50 mL of dichloromethane and washed with 2 × 10 mL of deionized water. The organic portion was dried with MgSO₄ and the solvent was removed by rotary evaporation. The residue was purified by column chromatography (silica gel, 7: 3 dichloromethane:

pentane) to give the colorless product (0.235 g, 92%). ¹H NMR (500 MHz, CDCl₃, 25°C): δ = 8.21 (d, *J* = 8.5 Hz, 2H), 8.04 (d, *J* = 8.5 Hz, 2H), 7.90 (dd, *J* = 7.5 Hz, 1 Hz, 1H), 7.87 (dd, *J* = 7.5 Hz, 1 Hz, 1H), 7.66 (dd, *J* = 7.5 Hz, 1 Hz, 1H), 7.61 (dd, *J* = 7.5 Hz, 1 Hz, 1H), 7.43 (t, *J* = 7.5 Hz, 1H), 7.22 (t, *J* = 7.5 Hz, 1H), 3.98 (s, 3H). ¹³C NMR (500 MHz, CDCl₃, δ): 166.99, 153.29, 153.09, 140.40, 130.30, 130.01, 129.34, 128.59, 127.33, 125.38, 125.14, 124.80, 124.19, 123.84, 120.94, 119.72, 104.68, 52.23. HRESI-MS ([M + H]⁺) calcd. for C₂₀H₁₄BrO₂ *m/z*, 381.0121, found 381.0130.

4.5.3.23. 4-[6-(3-*tert*-Butyl-5-formyl-4-hydroxyphenyl)dibenzofuran-4-yl]-benzoic acid methyl ester (28)

Under nitrogen, a mixture of 4-(6-bromo-dibenzofuran-4-yl)-benzoic acid methyl ester (27) (0.250 g, 0.656 mmol), 3-*tert*-butyl-2-hydroxy-5-(4,4,5,5-tetramethyl-[1,3,2]dioxaborolan-2-yl)-benzaldehyde (0.219 g, 0.721 mmol), sodium carbonate (0.101 g, 0.984 mmol), and tetrakis(triphenylphosphine)palladium (0.045 g, 0.039 mmol) was added to 9 mL of DMF and 1 mL of deionized water and heated to 90 °C for 24 hours. Upon cooling, the reaction mixture was extracted with 3 × 20 mL of dichloromethane. The combined organic layers were then washed with 2 × 20 mL of water and dried over MgSO₄, and the solvent was removed by rotary evaporation. The residue was purified by column chromatography (7:3 dichloromethane: pentane) to give the colorless product (0.238 g, 76% yield). ¹H NMR (500 MHz, CDCl₃, 25°C): δ = 11.91 (s, 1H), 9.97 (s, 1H), 8.16 (d, *J* = 9 Hz, 2H), 8.10 (d, *J* = 2 Hz, 1H), 8.03 (dd, *J* = 9 Hz, 1 Hz, 1H), 7.97 (m, 4H), 7.68 (dd, *J* = 7.5 Hz, 1 Hz, 1H), 7.63 (dd, *J* = 7.5 Hz, 1 Hz, 1H), 7.49 (quartet, *J* = 7.5 Hz, 2H), 3.98 (s, 3H), 1.44 (s, 9H). ¹³C NMR (500 MHz, CDCl₃, δ): 197.47, 167.01, 161.10, 153.42, 141.03, 138.84, 134.81, 132.07, 130.08, 129.52, 128.86, 128.74, 127.52, 127.15, 126.47, 125.21, 125.02, 124.95, 124.88, 123.84, 123.75, 121.06, 121.02, 120.87, 119.97, 119.84, 52.44, 35.25, 29.32. HRESI-MS ([M + Na]⁺) calcd for C₃₁H₂₆O₅Na *m/z*, 501.1672, found 501.1678.

4.5.3.24. 4-[6-(3-*tert*-Butyl-5-formyl-4-hydroxyphenyl)dibenzofuran-4-yl]-benzoic acid (29)

Under nitrogen, 4-[6-(3-*tert*-butyl-5-formyl-4-hydroxyphenyl)dibenzofuran-4-yl]-benzoic acid methyl ester (28) (0.080 g, 0.167 mmol) was dissolved in 6 mL of dry dichloromethane and cooled to 0 °C in an ice bath. A solution of 1.0 M boron tribromide

(0.50 mL, 0.502 mmol) was added via syringe and the temperature of the reaction mixture was raised to room temperature. This was then stirred for 2 hours, upon which 10 mL of deionized water was added. The subsequent mixture was extracted with 3 × 20 mL of dichloromethane, and the combined organic layers was washed with 10 mL of fresh deionized water, and then dried over MgSO₄ and the solvent was removed by rotary evaporation. The residue was purified by column chromatography (99:1 dichloromethane: methanol) to give the colorless product (0.046 g, 59% yield). ¹H NMR (500 MHz, C₄D₈O, 25°C): δ = 12.10 (s, 1H), 11.48 (bs, 1H), 10.04 (s, 1H), 8.16 (m, 4H), 8.11 (dd, *J* = 7.5 Hz, 1 Hz, 1H), 8.06 (m, 3H), 7.77 (dd, *J* = 7.5 Hz, 1 Hz, 1H), 7.71 (dd, *J* = 7.5 Hz, 1 Hz, 1H), 7.50 (m, 2H), 1.44 (s, 9H). ¹³C NMR (500 MHz, C₄D₈O, δ): 198.96, 167.64, 161.68, 154.31, 154.18, 141.43, 139.10, 135.22, 133.14, 131.50, 131.04, 129.45, 128.53, 128.00, 127.40, 126.12, 125.90, 125.82, 124.73, 124.68, 122.31, 121.68, 120.70, 35.89, 29.75. HRESI-MS ([M + H]⁺) calcd for C₃₀H₂₅O₅ *m/z*, 465.1696, found 465.1691.

4.5.3.25. H₂[H_{ph}SD*^tBu-COOH] (30)

A mixture of 4-[6-(3-*tert*-butyl-5-formyl-4-hydroxyphenyl)dibenzofuran-4-yl]-benzoic acid (**29**) (42.0 mg, 0.090 mmol) and (1*R*,2*R*)-(-)-1,2-diaminocyclohexane (5.2 mg, 0.045 mmol) was added to 6 mL of absolute ethanol. The solution was heated to reflux for 2 hours and upon cooling the solvent was removed by rotary evaporation. The bright yellow residue was washed with 0.5 mL cold methanol and dried under vacuum to give the product (36 mg, 80% yield). HRESI-MS ([M + H]⁺) calcd for C₆₆H₅₉N₂O₈ *m/z*, 1007.4266, found 1007.6217. Anal. Calcd for C₆₆H₅₈N₂O₈: C, 78.71; H, 5.80; N, 2.78. Found: C, 78.52; H, 6.00 N, 2.85.

4.5.3.26. Mn[H_{ph}SD*^tBu-COOH]Cl (31)

A mixture of **30** (30.0 mg, 0.030 mmol) and manganese(II) acetate tetrahydrate (11.0 mg, .045 mmol) was added to 6 mL of absolute ethanol and heated to reflux for 2 hours. Upon cooling, 4 mL of saturated aqueous sodium chloride was added and the solution was stirred for 20 minutes and the solid was collected by filtration and washed with water. Upon drying, the brown solid was taken up in tetrahydrofuran and filtered. The filtrate was reduced to give the brown product (30 mg, 91% yield). HRESI-MS ([M –

Cl]⁺) calcd for C₆₆H₅₆MnN₂O₈ *m/z*, 1059.3423, found 1059.3457. Anal. Calcd for C₆₆H₅₆ClMnN₂O₈: C, 72.36; H, 5.15; N, 2.56. Found: C, 72.16; H, 5.26 N, 2.43.

4.5.3.27. 2,2-Dimethylpropionic acid 4-bromophenyl ester (32)

4-Bromophenol (1.00 g, 5.78 mmol) was dissolved in 20 mL of dry dichloromethane. Pyridine (0.93 mL, 11.56 mmol) was added via syringe, followed by pivaloyl chloride (1.42 mL, 11.56 mmol) and the reaction was stirred for 24 hours. 20 mL of deionized water was added to quench the reaction, and the separated aqueous layer was extracted with 2 × 20 mL of dichloromethane. The combined organic layers were dried using MgSO₄, and the solvent removed by rotary evaporation. The residue was purified by column chromatography (silica gel, 2: 8 pentane: dichloromethane to dichloromethane) to elude the product (1.40 g, 94% yield). ¹H NMR (500 MHz, CDCl₃, δ): 7.49 (dd, *J* = 9 Hz, 5Hz, 2H), 6.96 (dd, *J* = 9H, 1.5 Hz, 2H), 1.35 (s, 9H). HRESI-MS ([M + Na]⁺) calcd for NaC₁₃H₁₆O₂ *m/z*, 227.1043, found 227.1043.

4.5.3.28. 2,2-Dimethylpropionic acid 4-vinylphenyl ester (33)

Under nitrogen, 2,2-dimethylpropionic acid 4-bromophenyl ester (32) (0.500 g, 1.94 mmol), tri(*n*-butyl)vinyltin (0.762 g, 2.05 mmol), and tetrakis(triphenylphosphine)palladium (0.450 g, 0.39 mmol) was added to toluene (8 mL) and heated to 110° C in a sealed bomb for 12 hours. Upon cooling, 50 mL of dichloromethane was added, and the solution was washed with 2 × 10 mL of deionized water and dried using MgSO₄. The solvent was removed by rotary evaporation and the residue purified by column chromatography (silica gel, 9: 1 pentane: dichloromethane) to yield the colorless product (0.351 g, 88% yield). ¹H NMR (300 MHz, CDCl₃, δ): 7.45 (d, *J* = 8.4 Hz, 2 H), 7.07 (dd, *J* = 6.9 Hz, 1.8 Hz, 2H), 6.74 (dd, *J* = 17.8 Hz, 10.8 Hz, 1H), 5.75 (dd, *J* = 17.8 Hz, 0.6 Hz, 1H), 5.28 (dd, *J* = 17.8 Hz, 0.6 Hz, 1H), 1.42 (s, 9H). ¹³C NMR (500 MHz, CDCl₃, δ): 177.12, 150.78, 136.05, 135.22, 127.22, 121.92, 121.67, 113.96, 39.18, 27.25.

4.5.3.29. 2,2-Dimethylpropionic acid 4-oxiranylphenyl ester (34)

5 mL of a 0.05 M solution of Na₂HPO₄ was added to 12.5 mL of commercial bleach (Clorox). This was added to 2,2-dimethylpropionic acid 4-vinylphenyl ester (33) (0.150 g, 0.68 mmol) and manganese(salophen)chloride (25 mg, 0.04 mmol) in 10 mL of

dichloromethane and stirred for 3 hours. The solution was extracted with 3×10 mL of dichloromethane and the organic layers were combined and dried using MgSO_4 and the solvent removed by rotary evaporation and resulting residue purified by column chromatography (silica gel 3: 7 pentane: dichloromethane) to elude the product (0.45 g, 31% yield). ^1H NMR (500 MHz, CDCl_3 , δ): 7.29 (d, $J = 8.5$ Hz, 2H), 7.04 (d, $J = 8.5$, 2H), 3.87 (t, $J = 2$ Hz, 1H), 3.15 (dd, $J = 5$ Hz, 4 Hz, 1H), 2.78 (dd, $J = 5$ Hz, 2 Hz, 1H), 1.36 (s, 9H). ^{13}C NMR (500 MHz, CDCl_3 , δ): 177.26, 156.10, 135.11, 126.67, 121.85, 52.17, 52.49, 27.31. HRESI-MS ($[\text{M} + \text{Na}]^+$) calcd for $\text{NaC}_{13}\text{H}_{16}\text{O}_3$ m/z , 243.0992, found 243.0998.

4.5.4. Hydrogen Peroxide Disproportionation Reactions

Dismutation reactions were performed at room temperature in a sealed (PTFE septum) 20 mL reaction vial equipped with a magnetic stirbar and a capillary gas delivery tube linked to an inverted graduated burette filled with water. The reaction vial was charged with a stock solution of the corresponding catalyst in CH_2Cl_2 (1.0 mL). MeOH (0.5 mL) was added followed by H_2O_2 (790 μL , 8.22 mmol; 10.4 M (30%) aq. solution), and the reaction mixture was stirred vigorously. The time was set to zero immediately after addition of H_2O_2 . The conversion was monitored volumetrically, and the amount of O_2 (n) produced was calculated through the perfect gas equation $pV = nRT$, assuming that $p = 1$ atm. As a check on our experimental set-up, MnO_2 was employed to dismutate the hydrogen peroxide completely. Calibration runs show that the amount of oxygen collected matches the amount expected, given the concentration of the hydrogen peroxide solution.

The amount of catalyst used to obtain the turnover numbers for the catalase experiments: $\text{Mn}(\text{5-phsalen})\text{Cl}$ (**13**) (1.0 mL from a 5.3 mg into 10 mL CH_2Cl_2 solution or 0.00095 mmol) to give an average of 1.01 mL O_2 in 1 hour. $\text{Mn}(\text{5-phsalen})\text{Cl}$ (**13**) with 1 equivalent of benzoic acid (1.0 mL from a 2.7 mg $\text{Mn}(\text{5-phsalen})\text{Cl}$ and 0.6 mg benzoic acid into 5 mL CH_2Cl_2 solution or 0.00095 mmol of each) to give 3.21 mL O_2 in 1 hour. $\text{Mn}(\text{HSX}^*\text{-COOH})\text{Cl}$ (1.0 mL from a 5.6 mg into 5 mL CH_2Cl_2 solution or 0.00095 mmol) to give 35.91 mL O_2 in 1 hour. $\text{Mn}(\text{HSX}^*\text{-COOMe})\text{Cl}$ (**9**) (1.0 mL from a 5.54 mg into 5 mL CH_2Cl_2 solution or 0.00095 mmol) to give 1.61 mL O_2 in 1 hour.

Mn(H_{ph}SX*-COOH)Cl (1.0 mL from a 2.5 mg into 2 mL CH₂Cl₂ solution or 0.00095 mmol) to give 18.01 mL O₂ in 1 hour. Mn(H_{ph}SX*-COOMe)Cl (**10**) (1.0 mL from a 2.5 mg into 2 mL CH₂Cl₂ solution or 0.00095 mmol) to give 2.01 mL O₂ in 1 hour. (1*R*, 2*R*)-(–)-[1,2-Cyclohexanediamino-*N,N'*-bis(3,5-di-*tert*-butylsalicylidene)]manganese(III) chloride (1.0 mL from a 6.0 mg into 10 mL CH₂Cl₂ solution or 0.00095 mmol) to give an average of 3.7 mL O₂ in 1 hour. (1*R*, 2*R*)-(–)-[1,2-Cyclohexanediamino-*N,N'*-bis(3,5-di-*tert*-butylsalicylidene)] manganese (III) chloride with 2 equivalent of benzoic acid (1.0 mL from a 6.0 mg (1*R*, 2*R*)-(–)-[1,2-cyclohexanediamino-*N,N'*-bis(3,5-di-*tert*-butylsalicylidene)]manganese(III) chloride and 1.2 mg benzoic acid into 10 mL CH₂Cl₂ solution or 0.00095 mmol and 0.0019 mmol respectively) to give on average 4.2 mL O₂ in 1 hour. Mn(HSX*-'Bu-COOH)Cl (1.0 mL from a 3.0 mg into 5 mL CH₂Cl₂ solution or 0.000475 mmol) to give 60.7 mL O₂ in 1 hour. Mn(HSX*-'Bu-COOMe)Cl (**18**) (1.0 mL from a 2.4 mg into 2 mL CH₂Cl₂ solution or 0.00095 mmol) to give 1.4 mL O₂ in 1 hour. Mn(H_{ph}SX*-COOH)Cl (1.0 mL from a 1.3 mg into 2 mL CH₂Cl₂ solution or 0.00095 mmol) to give 56.9 mL O₂ in 1 hour. Mn(H_{ph}SX*-COOMe)Cl (**19**) (1.0 mL from a 2.7 mg into 2 mL CH₂Cl₂ solution or 0.00095 mmol) to give 27.5 mL O₂ in 1 hour. The standard deviations on the turnover number (TON) measurements over one hour are derived from at least three data points.

4.5.5. Epoxidation of Functionalized Olefins

The TON for epoxidation of 4-acetoxystyrene was determined as follows: 0.47 mM solutions of the catalyst (1*R*, 2*R*)-(–)-[1,2-cyclohexanediamino-*N,N'*-bis(3,5-di-*tert*-butylsalicylidene)]manganese(III) chloride (7.5 mg in 25 mL of dichloromethane), Mn[HSX*'Bu-COOH]Cl (5.9 mg in 10 mL of dichloromethane), [H_{ph}SX*'Bu-COOH]Cl (6.7 mg in 10 mL of dichloromethane), Mn[HSD*'Bu-COOH]Cl (2.2 mg in 10 mL of dichloromethane), [H_{ph}SD*'Bu-COOH]Cl (5.2 mg in 10 mL of dichloromethane) were prepared. A 47.5 mM solution of 4-acetoxystyrene and 23.75 mM dodecane (192.6 mg of 4-acetoxystyrene and 101.1 mg of dodecane in 25.00 mL) was prepared. For NaOCl as the oxidant, the oxidant solution was prepared by mixing 10 mL of 0.05 M NaHPO₄ and 25 mL of commercial bleach (Clorox) and 1.0 mL of 1 M NaOH solution and then cooled to 0 °C. 1.0 mL of this solution was added to 0.5 mL of each catalyst solution and 0.5 mL

of the 4-acetoxystyrene/dodecane solution, pre-cooled to 0 °C and stirred at room temperature.

The TON for epoxidation of 2,2-dimethylpropionic acid 4-bromophenyl ester was determined as follows: A 47.5 mM solution of 2,2-dimethylpropionic acid 4-bromophenyl ester and 23.75 mM dodecane (242.6 mg of 2,2-dimethylpropionic acid 4-bromophenyl ester and 101.1 mg of dodecane in 25 mL) was prepared. For each reaction, 0.5 mL of the catalyst solution (as prepared above) were added to 0.5 mL of the of 2,2-dimethylpropionic acid 4-bromophenyl ester/dodecane solution and cooled to 0 °C. 1.0 mL of the oxidant solution pre-cooled to 0 °C (as prepared above) was added to each reaction and stirred at room temperature.

The reactions were calibrated at time zero, and examined by GC/MS at $t = 1$ hour and 3 hours. The response factor of the substrate and epoxidation product relative to the internal standard of dodecane was determined and fitted with at least three points using a linear calibration curve. The calibration curve was used to determine the concentration of the substrate and epoxide product, and calculate the corresponding turnover numbers (TON) based on the concentration of the latter. The GC/MS spectra were taken on an Agilent Technologies 6890N Network housed at the MIT DCIF.

4.5.6. Density Functional Theory Calculations

Gas-phase density functional theoretical (DFT) calculations of the hydroperoxide complexes of $\text{Mn}(\text{HSX}^*-\text{COOH})$, $\text{Mn}(\text{H}_{\text{ph}}\text{SX}^*-\text{COOH})$, $\text{Mn}(\text{HSD}^*-\text{COOH})$, $\text{Mn}(\text{H}_{\text{ph}}\text{SD}^*-\text{COOH})$ were performed using the Amsterdam Density Functional (ADF2002.02)^{84,85} package on a home-built Linux cluster of sixty Intel processors running in parallel groups of twelve. To simplify the calculation, the *t*-butyl and methyl groups were removed from the xanthenes, as well as replacing the cyclohexyl backbone to ethylenediamine. The generalized gradient approximation (GGA) was implemented by use of Becke's 1988 exchange functional⁸⁶ and Perdew and Wang's 1991 correlation functional.⁸⁷ The basis set was of triple-zeta quality for manganese, oxygen, and nitrogen, with a double set of polarization functions for Mn and a single polarization set for O and N, and of double-zeta quality with single polarization set for carbon and hydrogen; the frozen core approximation was used for the 1s shell of C, N, and O and for the 1s, 2s, and

2p shells of Mn. Full geometry optimizations of the entire complexes were run at 0° K. All computations were carried out in the quintet spin state and the spin restriction was lifted. The molecular geometries and the spatial components of the resulting Kohn-Sham single-electron wavefunctions were visualized and analyzed using the software Molekel.^{88,89} The input (run) file and final geometry optimized output coordinates are located in Appendix C.

Table 4.3. Selected bond distance parameters from DFT calculated energy minimized structures of the hydroperoxide complexes of manganese Hangman salen compounds.

| Distance (Å) | Mn[HSX* ¹ Bu]OOH | Mn[H _{ph} SX* ¹ Bu]OOH | Mn[HSD* ¹ Bu]OOH | Mn[H _{ph} SD* ¹ Bu]OOH |
|---------------------|---|---|---|--|
| Mn-O | 1.89 Å | 1.85 Å | 1.968 Å | 1.961 Å |
| peroxide O-O | 1.46 Å | 1.46 Å | 1.447 Å | 1.452 Å |
| peroxide O-H | 0.99 | 0.99 Å | 0.986 Å | 0.986 Å |
| acid OH-Mn | 5.14 Å, 6.77 Å | 4.58 Å, 6.03 Å | 7.338 Å, 7.532 Å | 7.039 Å, 7.568 Å |
| peroxide-acid | peroxide H to acid OH : 1.94 Å | peroxide H to acid CO : 3.11 Å | peroxide H to acid OH : 5.05 Å | peroxide H to acid OH : 4.579 Å |

References

1. Liu, S.-Y.; Nocera, D. G. *J. Am. Chem. Soc.* **2005**, *127*, 5278-5279.
2. Liu, S.-Y.; Soper, J. D.; Yang, J. Y.; Rybak-Akimova, E. V.; Nocera, D. G. *Inorg. Chem.* **2006**, *45*, 7572-7574.
3. Chang, C. J.; Chng, L. L.; Nocera, D. G. *J. Am. Chem. Soc.* **2003**, *125*, 1866-1876.
4. Chng, L. L.; Chang, C. J.; Nocera, D. G. *Org. Lett.* **2003**, *5*, 2421-2424.
5. Chang, C. J.; Chang, M. C. Y.; Damrauer, N. H.; Nocera, D. G. *Biophys. Biochim. Acta* **2004**, *1655*, 13-28.
6. Stubbe, J.; Nocera, D. G.; Yee, C. S.; Chang, M. C. Y. *Chem. Rev.* **2003**, *103*, 2167-2202.
7. Cukier, R. I.; Nocera, D. G. *Annu. Rev. Phys. Chem.* **1998**, *49*, 337-369.
8. Dempsey, J. L.; Esswein, A. J.; Manke, D. R.; Rosenthal, J.; Soper, J. D.; Nocera, D. G. *Inorg. Chem.* **2005**, *44*, 6879-6892.
9. Nicholls, P.; Fita, I.; Loewen, P. C. *Adv. Inorg. Chem.* **2001**, *51*, 51-106.
10. Doctrow, S. R.; Adinolfi, C.; Baudry, M.; Huffman, K.; Malfroy, B.; Marcus, C. B.; Melov, S.; Pong, K.; Rong, Y.; Smart, J. L.; Tocco In *Critical Reviews of Oxidative Stress and Aging: Advances in Basic Science, Diagnostics, and Intervention*, Vol. 2; Cutler, R. G., Rodriguez, H., Eds.; World Scientific: New Jersey, 2003; pp. 1324-1343.
11. Halliwell, B.; Gutteridge, J. M. C. *Free Radicals in Biology and Medicine*, 2nd ed.; Clarendon Press: Oxford, 1989; pg 543.
12. Sies, H. *Angew. Chem. Int. Ed.* **1986**, *25*, 1058-1071.
13. Rice-Evans, C. A.; Diplock, A. T. *Free Radical Biol. Med.* **1993**, *15*, 77-96.
14. Riley, D. P.; Weiss, R. H. *J. Am. Chem. Soc.* **1994**, *116*, 387-388.
15. Salvemini, D.; Wang, Z. Q.; Zweier, J. L.; Samouilov, A.; Macarther, H.; Misko, T. P.; Currie, M. G.; Cuzzocrea, S.; Sikorski, J. A.; Riley, D. P. *Science* **2000**, *286*, 304-306.
16. Baudry, M.; Etienne, S.; Bruce, A.; Palucki, M.; Jacobsen, E. N.; Malfroy, B. *Biochem. Biophys. Res. Commun.* **1993**, *192*, 964-968.
17. Doctrow, S. R.; Huffman, K.; Marcus, C. B.; Musleh, W.; Bruce, A.; Baudry, M.; Malfroy, B. In *Antioxidants in Disease Mechanisms and Therapeutic Strategies*, Sies, H., Ed.; Advances in Pharmacology: Academic Press: New York, 1997; pp 247-270.
18. EUKARION, Inc. U. S. Patent US5696109, 1997. EUKARION, Inc. PCT Int. Appl. WO9640148. 1996. EUKARION, Inc. PCT Int. Appl. WO9640149. 1996. EUKARION, Inc. PCT Int. Appl. WO9413300, 1993.

19. Gonzalez, P. K.; Zhuang, J.; Doctrow, S. R.; Malfroy, B.; Benson, P. F.; Menconi, M. J.; Fink M. P. *J. Pharmacol. Exp. Ther.* **1995**, *275*, 798-806.
20. McDonald, M. C.; d'Emmanuele di Villa Bianca, R.; Wayman, N.S.; Pinto, A.; Sharpe, M. A.; Cuzzocrea, S.; Chatterjee, P. K.; Thiernemann, C. *Eur. J. Pharmacol.* **2003**, *466*, 181-189.
21. Olcott, A. P.; Tocco, G.; Tian, J.; Zekzer, D.; Fukuto, J.; Ignarro, L.; Kaufman, D. L. *Diabetes* **2004**, *53*, 2574-2579.
22. Baker, K.; Marcus, C. B.; Huffman, K.; Kruk, H.; Malfroy, B.; Doctrow, S. R. *J. Pharmacol. Exp. Ther.* **1998**, *284*, 215-221.
23. d'Emmanuele di Villa Bianca, Roberta; Wayman, N. S.; McDonald, M. C.; Pinto, A.; Sharpe, M. A.; Chatterjee, P. K.; Thiernemann, C. *Med. Sci. Monit.* **2002**, *8*, BR1-7.
24. Decraene, D.; Smaers, K.; Gan, D.; Mammone, T.; Matusi, M.; Maes, D.; Declercq, L.; Garmyn, M. *J. Invest. Derm.*, **2004**, *122(2)*, 484-491.
25. Melov, S.; Ravenscroft, J.; Malik, S.; Gill, M. S.; Walker, D. S.; Clayton, P. E.; Wallace, D. C.; Malfroy, B.; Doctrow, S. R.; Lithgow, G. J. *Science* **2000**, *289*, 1567-1569.
26. Proteome Systems, Therapeutics Division, Human Studies Information. <http://www.proteomesystems.com/Therapeutics/PharmaceuticalOverview.aspx> and <http://www.proteomesystems.com/Therapeutics/HumanStudies.aspx> (accessed February 2007)
27. Doctrow, S. R.; Huffman, K.; Marcus, C. B.; Tocco, G.; Malfroy, E.; Adinolfi, C. A.; Kruk, H.; Baker, K.; Lazarowych, N.; Mascarenhas, J. *J. Med. Chem.* **2002**, *45*, 4549-4558.
28. Abashkin, Y. G.; Burt, S. K. *J. Phys. Chem. B* **2004**, *108*, 2708-2711.
29. Abashkin, Y. G.; Burt, S. K. *Inorg. Chem.* **2005**, *44*, 1425-1432.
30. Ships, G., Jr.; Rebek, J., Jr. *Tetrahedron Lett.* **1994**, *35*, 6823-6825.
31. Miyaura, N.; Suzuki, A. *Chem. Rev.* **1995**, *95*, 2457-2483.
32. Kende, A. S.; Rizzi, J. P. *Tetrahedron Lett.* **1981**, *22*, 1779-1982
33. Brooks, P. R.; Wirtz, M. C.; Vetelino, M. G.; Rescek, D. M.; Woodworth, G. F.; Morgan, B. P.; Coe, J. W. *J. Org. Chem.* **1999**, *64*, 9719-9712.
34. Felix, A. M. *J. Org. Chem.* **1974**, *39*, 1427-1429.
35. Mate, M. J.; Murshudov, G.; Bravo, J.; Melik-Adamyan, W.; Loewen, P. C.; Fita, I. In *Handbook of Metalloproteins*; Messerschmidt, A., Huber, R., Ed.s; John Wiley: New York, 2001.
36. Nomura, Y.; Kubozono, T.; Hidaka, M.; Horibe, M.; Mizushima, N.; Yamamoto, N.; Takahashi, T.; Komiyama, M. *Bioorg. Chem.* **2004**, *32*, 26-37.

37. Chang, C. K.; Bag, N.; Guo, B.; Peng, S.-M. *Inorg. Chim. Acta* **2003**, *351*, 261-268.
38. Schwartz, E. B.; Knobler, C. B.; Cram, D. J. *J. Am. Chem. Soc.* **1992**, *114*, 10775-10784.
39. Kalman, J. R.; Pinhey, J. T.; Sternhell, S. *Tetrahedron Lett.* **1972**, *52*, 5369-5372.
40. Lee, J.; Lee, J.-H.; Kim, S. Y.; Perry, N. A.; Lewin, N. E.; Ayres, J. A.; Blumberg, P. M. *Bioorg. Med. Chem.* **2006**, *14*, 2022-2031.
41. Gomez-Lor, B.; Echavarren, A. M.; Santos, A. *Tetrahedron Lett.* **1997**, *38*, 5347-5350.
42. Katsuki, T.; Sharpless, K. B. *J. Am. Chem. Soc.* **1980**, *102*, 5974-5978.
43. Lin, G.-Q.; Li, Y.-M.; Chan, A. S. C. Asymmetric Oxidations. In *Principles and Applications of Asymmetric Synthesis*; Wiley-Interscience: New York, 2001, Chapter 4.
44. Johnson, R. A.; Sharpless, K. B. Catalytic Asymmetric Epoxidation of Allylic Alcohols. In *Catalytic Asymmetric Synthesis*, 1st Eds; Ojima, I; Wiley-VCH: New York, 1993; Chapter 4.1.
45. *Cytochrome P-450 Structure, Mechanism, and Biochemistry*; Ortiz de Montellano, P. R., Ed.; Plenum Press: New York, 1995.
46. Dawson, J. H.; Sono, M. *Chem Rev.* **1987**, *87*, 1255-1276.
47. *Metallo Porphyrins in Catalytic Oxidations*; Sheldon, R. A., Ed.; Dekker: New York, 1994.
48. De Visser, S. P.; Ogliaro, F.; Sharma, P.K.; Shaik, S. *Angew. Chem. Int. Ed.* **2002**, *41*, 1947-1951.
49. van Rantwijk, F.; Sheldon, R. A. *Curr. Opin. Biotech.* **2000**, *11*, 554-564.
50. Behrouzian, B.; Buist, P. H. *Prostaglandins Leukot. Essent. Fatty Acids* **2003**, *68*, 107-112.
51. van Beilen, J. B.; Kingma, J.; Witholt, B. *Enzyme Microbiol. Technol.* **1994**, *16*, 904-11.
52. Behrouzian, B.; Savile, C. K.; Dawson, B.; Bulst, P. H.; Shanklin, J. *J. Am. Chem. Soc.* **2002**, *124*, 3277-3283.
53. Moche, M.; Shanklin, J.; Ghoshal, A.; Lindqvist, Y. *J. Biol. Chem.* **2003**, *278*, 25072-25080.
54. Broadwater, J. A.; Whittle, E.; Shaklin, J. *J. Biol. Chem.* **2002**, *277*, 15613-15620.
55. Fox, B. G.; Lyle, K. S.; Rogge, C. E. *Acc. Chem. Res.* **2004**, *37*, 421-429.
56. Groves, J. T.; Neumann, R. *J. Am. Chem. Soc.* **1987**, *109*, 5045-5047.
57. Breslow, R.; Brown, A. B.; McCullough, R. D.; White, P. W. *J. Am. Chem. Soc.* **1989**, *111*, 4517-4518.

58. Breslow, R.; Huang, Y.; Zhang, X.; Yang, J. *Proc. Natl. Acad. Sci. U.S.A.* **1997**, *94*, 11156-11158.
59. Breslow, R.; Zhang, X.; Huang, Y. *J. Am. Chem. Soc.* **1997**, *119*, 4535-4536.
60. Yang, J.; Gabriele, B.; Belvedere, S.; Huang, Y.; Breslow, R. *J. Org. Chem.* **2002**, *67*, 5057-5067.
61. Das, S.; Incarvito, C. D.; Crabtree, R. H.; Brudvig, G. W. *Science* **2006**, *312*, 1941-1943.
62. Xhang, C. X.; Lippard, S. J. *Curr. Opin. Mol. Biol.* **2003**, *7*, 481-489.
63. Salvemini, D.; Riley, D. P.; Cuzzocrea, S. *Drug Discovery* **2002**, *1*, 367-374.
64. Henke, S. L. *Expert Opin. Ther. Patents* **1999**, *9*, 169-180.
65. Muscoli, C.; Cuzzocrea, S.; Riley, D. P.; Zweier, J. L.; Thiemermann, C.; Wang, Z.-Q.; Salvemini, D. *Br. J. Pharmacol.* **2003**, *140*, 445-460.
66. Naughton, D. P.; Fisher, A. E. *Chem. & Biol.* **2003**, *10*, 197-198.
67. Cuzzocrea, S.; Riley, D. P.; Caputi, A. P.; Salvemini, D. *Pharmacol. Rev.* **2001**, *53*, 135-159.
68. Salvemini, D.; Muscoli, C.; Riley, D. P.; Cuzzocrea. *Pul. Pharmacol. & Ther.* **2002**, *15*, 439-447.
69. Fridovich, I. *J. Biol. Chem.* **1997**, *272*, 18515-18517.
70. Baudry, M.; Etienne, S.; Bruce, A.; Palucki, M.; Jacobsen, E. N.; Malfroy, B. *Biochem. Biophys. Res. Commun.* **1993**, *192*, 964-968.
71. Puglisi, A.; Tabbi, G.; Vecchio, G. *J. Inorg. Biochem.* **2004**, *98*, 969-976.
72. Weise, R. H.; Flickinger, A. G.; Rivers, W. J.; Hardy, M. M.; Aston, K. W.; Ryan, U. S.; Riley, D. P. *J. Biol. Chem.* **1993**, *268*, 23049-23053.
73. McCord, J. M.; Fridovich, I. *J. Biol. Chem.* **1968**, *243*, 5753-5760.
74. Crapo, J. D.; McCord, J. M.; Fridovich, I. *Methods in Enzymology* **1978**, *53*, 382-293.
75. Riley, D. P.; Rivers, W. J.; Weiss, R. H. *Anal. Biochem.* **1991**, *196*, 344-349.
76. Goedheijt, M. S.; Kamer, P. C. J.; van Leewen, P. W. N. M. *J. Mol. Cat. A.* **1998**, *134*, 243-249.
77. Timpe, H.-J.; Kronfeld, K.-P.; Mahlow, R. *Eur. Polym. J.* **1991**, *27*, 69-75.
78. Riley, D. P. *Chem. Rev.* **1999**, *99*, 2573-2587.
79. Liu, Z. X.; Robinson, G. B.; Gregory, E. M. *Arch. Biochem. Biophys.* **1994**, *315*, 74-81.
80. Doctrow, S. R.; Huffman, K.; Marcus, C. B.; Malfroy, B. *Adv. Pharmacol.* **1997**, *38*, 247-269.

81. Kilgore, K. S.; Lucchesi, B. R. *Clin. Biochem.* **1993**, *26*, 259-370.
82. Floyd, R. A. *FASEB J.* **1990**, *4*, 2587-2597.
83. Armarego, W. L. F.; Perrin, D. D. *Purification of Laboratory Chemicals*; 4th ed.; Butterworth-Heinmann: Oxford, 1966.
84. te Velde, G.; Bickelhaupt, F. M.; van Gisbergen, A. J. A.; Fonseca Guerra, C.; Baerends, E. J.; Snijders, J. G.; Ziegler, T. J. *Comput. Chem.* **2001**, *22*, 931-967.
85. Fonseca Guerra, C.; Snijders, J. G.; te Velde, G.; Baerends, E. J. *Theor. Chem. Acc.* **1998**, *99*, 391-403.
86. Becke, A. D. *Phys. Rev. A* **1998**, *38*, 3098-3100.
87. Perdew, J. P.; Chevary, J. A.; Vosko, S. H.; Jackson, K. a.; Pederson, M. R.; Singh, D. J.; Fiolhais, C. *Phys. Rev. B* **1992**, *46*, 6671-6687
88. Molekel v. 4.2/3, Flükiger, P.; Lüthi, H. P.; Portmann, S.; Weber, J., Swiss Center for Scientific Computing, Manno, 2000-2002.
89. Portmann, S.; Lüthi, H. P. *Chimica* **2000**, *54*, 776-780.

Chapter 5

Synthesis of Amido-Imine Macrocyclic Ligands

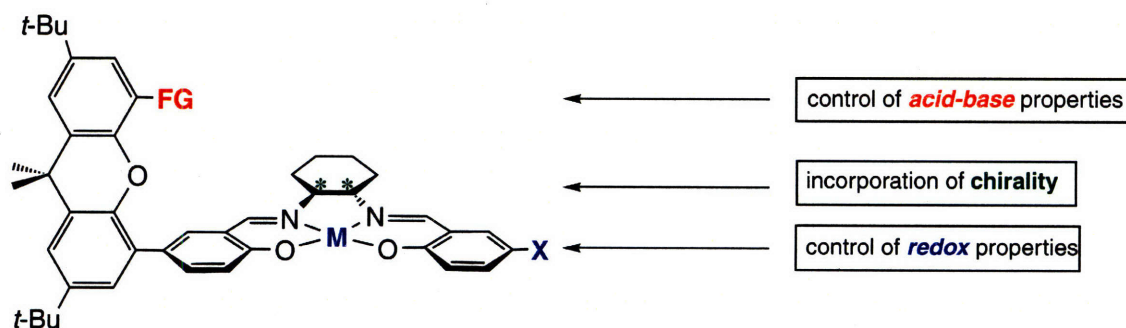
5.1. Motivation and Specific Aims

Several key catalyst design elements have been identified for managing oxidation and catalase chemistry promoted by Hangman salophen and Hangman salen architectures, such as redox properties and the presence of proximate acid-base functionalities. Incorporation of these features into one Hangman Schiff-base ligand is difficult owing to imine hydrolysis. This complication provided the impetus for the design of the amido-imine bisphenolic macrocycle described in this Chapter. The resulting Hangman ligand framework incorporates: (1) the chiral *trans*-cyclohexyldiamine bridge; (2) an open site for facile integration of electron-withdrawing/donating functionalities along the macrocycle; and, (3) the acid-base group over the reactive metal site. The resulting manganese complex is examined for its oxygen atom chemistry to ascertain whether the crucial catalyst profiles are maintained in a non-salen redox platform.

5.2. Background

The epoxidation studies described in Chapter 3 reveal that manganese salens bearing two functionalized xanthene scaffolds are capable of catalytically epoxidizing olefins enantioselectively.^{1,2} Chiral information is relayed to the substrate by the enantiopure cyclohexanediamine bridge and the redox properties of the salophen ring can be tuned with substituent modification.³ We were interested in retaining these properties upon removal of one of the Hangman scaffolds. The xanthene scaffold Hangman ligand architecture shown in Chart 5.1 is present to position an acid-base functionality in the secondary coordination sphere, and the cyclohexanediamine bridge incorporates the

Chart 5.1



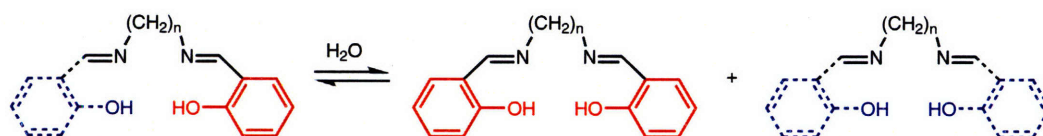
desired chiral function. The lack of a second xanthene pillar allows for greater flexibility in design by opening a site for the installation of various functional groups to tune the redox properties of the metal center, as demonstrated by the Hangman salen ligand of Chapter 2. With this ligand, we hope to integrate all of the productive elements of the previously described Hangman Schiff-base ligand constructs.

5.3. Results and Discussion

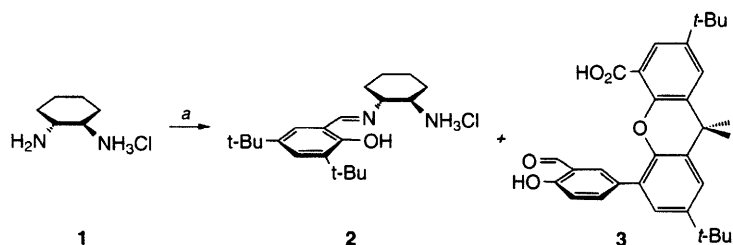
5.3.1. Synthetic Attempts towards a Hangman Salen Bearing a Single Functionalized Xanthene Scaffold

Isolated salen ligands that are asymmetric across their diamine bridge are rare,⁴⁻⁷ and in these cases, small amounts of symmetrical impurities are typically observed^{4,5} owing to facile hydrolysis of the imine bond (represented in Figure 5.1).⁸ The hydrolysis occurs even under very mild conditions.⁹ One of the more successful approaches for synthesizing a salen composed of two unique salicylaldehyde units involves a precursor with one amine protected by forming the hydrochloric acid salt (**2**),⁶ as shown in Scheme 5.1. This half-salen (**2**) can be synthesized in two steps. First, hydrochloric acid in diethyl ether is added dropwise to a solution of the diamine to give **1**, which is subsequently condensed with 3,5-di-*tert*-butyl salicylaldehyde to give **2**.⁶ The HCl can then be removed using triethylamine to expose the amine for condensation with the xanthene-functionalized-salicylaldehyde (**3**). However, the resulting product is a mixture of symmetric and asymmetric salens. An effort was made to separate the mixture, but attempts to isolate the desired ligand were frustrated by the reappearance of the symmetric ligand in solution. In an effort to avert hydrolysis of the imines, the condensation was performed under rigorously dry conditions over activated molecular

Figure 5.1. Equilibrium representing the exchange reaction that produces symmetric impurities when salens containing two unique phenolate arms undergo hydrolysis. The two unique salicylaldehyde components are represented in blue (dashed) and red (solid).



Scheme 5.1



(a) 3,5-di-*tert*-butyl salicylaldehyde, MeOH/EtOH, 4Å mol. sieves

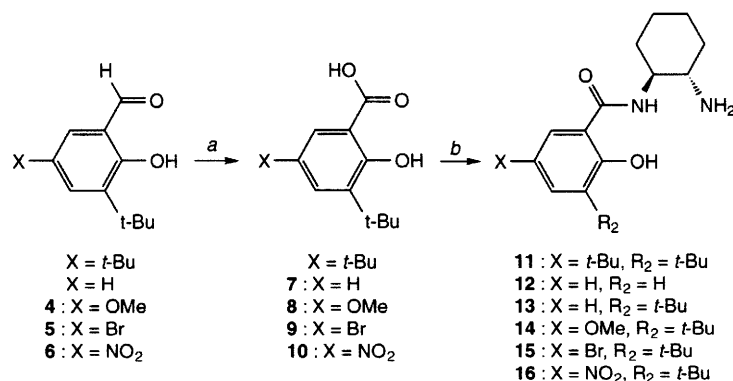
sieves. Notwithstanding, the reaction produces water and thus we were unable to prevent the disproportionation of the ligand. A re-design of the ligand was needed to circumvent the hydrolysis re-distribution.

5.3.2. Design and Synthesis of Amido-Imine Macrocycles and Manganese Complexes

To evade the problem presented by Figure 5.1 in the synthesis of an asymmetric salen, we decided to replace one of the imine bonds with an amido bond, which are less prone to hydrolysis. We targeted the synthesis of macrocyclic “half-units”, where a cyclohexanediamine could be singly condensed to form an amido bond, leaving the other amine available to form an imine bond.

The step-wise synthesis of the necessary precursors is described in Scheme 5.2. We

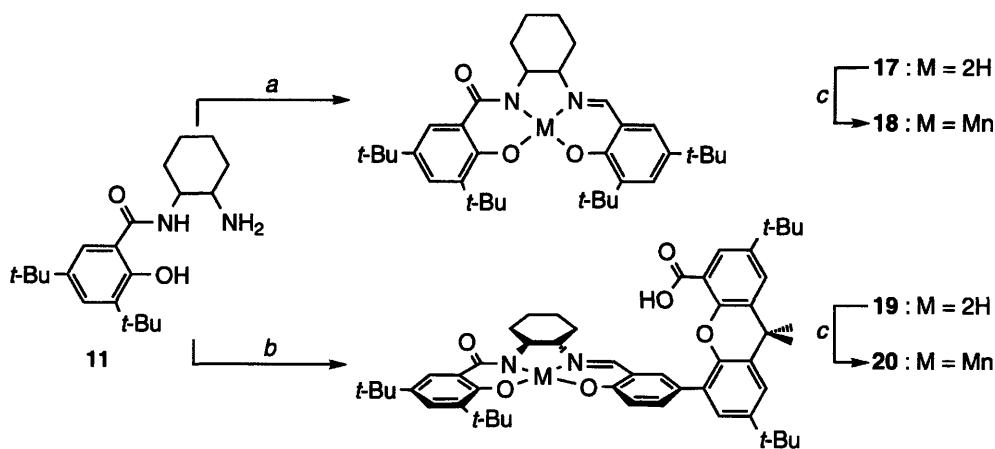
Scheme 5.2



(a) Ag₂O, 3M NaOH_{aq}, (b) (1*R*,2*R*)-(-)-1,2-diaminocyclohexane, N-methylmorpholine, 1-[3-(dimethylamino)propyl]-3-ethylcarbodiimine·HCl, CH₂Cl₂, or *i*) SOCl₂, *ii*) (1*R*,2*R*)-(-)-1,2-diaminocyclohexane, Et₃N, CH₂Cl₂

assembled a series of salicylaldehydes with various functionalities in the 5 position. 3,5-di-*tert*-butyl salicylaldehyde and 3-*tert*-butyl salicylaldehyde were obtained commercially. The methoxy,¹⁰ bromo,¹¹ and nitro¹² functionalized salicylaldehydes (**4** - **6**) could all be prepared in one step as described in the literature. The aldehydes were oxidized to the carboxylic acid by heating with silver(I) oxide in basic solution. Coupling proceeded with one equivalent of (1*R*,2*R*)-(-)-1,2-diaminocyclohexane using two methods to form the amide bond. **11** and **12** were synthesized in higher yields by allowing the acid and diamine to react with 1-[3-(dimethylamino)propyl]-3-ethylcarbodiimine·HCl and *N*-methylmorpholine. **13** - **16** were synthesized by allowing the acid to react with thionyl chloride to form the acetyl chloride in situ, followed by addition of the diamine. Both methods gave varying amounts of the symmetric diamide ligand impurity despite dilute reaction conditions. The symmetric ligand was separated from the desired products **11** - **16** by column chromatography. Macrocyclization is completed by condensation of the amine to the imine, furnishing the amido-imine macrocycles shown in Scheme 5.3.

Scheme 5.3



(a) 3,5-di-*tert*-butyl-2-hydroxybenzaldehyde, EtOH, (b) 2,7-di-*tert*-butyl-5-(3-formyl-4-hydroxy-phenyl)-9,9-dimethyl-9H-xanthene-4-carboxylic acid, EtOH, (c) Mn(OAc)₂(H₂O)₄, EtOH

11 was refluxed in ethanol with 3,5-di-*tert*-butyl salicylaldehyde to give the bright yellow macrocycle **17**. The Hangman-type ligand **19** was also synthesized by condensation of **11** with a salicylaldehyde attached to the carboxylic acid functionalized xanthene scaffold.

With **19**, we saw no evidence of any functional group exchange in solution. The distinct phenolic groups were maintained in the NMR spectrum. The manganese(III) ion can be inserted into the ligands **17** and **19** by refluxing with manganese(II) acetate tetrahydrate in ethanol in air to give **18** and **21**, respectively. The amido nitrogen is deprotonated during metallation to afford the neutral complex.¹³ The molecular weights of the ions (sodium adduct) obtained by high resolution mass spectrometry are consistent with this formulation for the complex. Unique amide (C=O) and imine (C=N) stretches are present in the infrared spectra. The C=O stretch is observed at 1628 cm⁻¹ in **17** and 1638 cm⁻¹ in **19**. In the manganese complexes, the stretching frequency shifts to 1624 cm⁻¹ in **18** and 1626 cm⁻¹ in **20**. The shift upon metallation is more dramatic for the imine bond; the stretching frequency at 1587 cm⁻¹ in **17** and 1588 cm⁻¹ in **19** shifts to 1535 cm⁻¹ and 1531 cm⁻¹ in their respective manganese complexes.

5.3.3. Epoxidation Activity of Manganese Complexes

We were interested in ascertaining how our substitution of an amido group for an imine in our ligand would affect the reactivity compared to its double-scaffold salen congeners. Particularly, we were interested in learning whether this ligand framework could support the type of oxidation chemistry observed in salens, and if the chirality of the ligand would be transferred effectively to substrate. To this end, we examined the manganese complex **20** towards the epoxidation of 1,2-dihydronaphthalene. Sodium hypochlorite was used as the external oxidant, under the same conditions previously used to study their salen counterparts.^{1,2} The complexes did catalytically perform the desired epoxidation chemistry with good yields, but the epoxide product was racemic. The lack of asymmetric induction by these ligands may be due to their geometry. In salens, the geometry of the macrocycle in the Mn(V) oxo species is believed to be roughly planar.¹⁴ However, the analogous diamido macrocycles are known to be more structurally flexible and they can deviate from a non-planar coordination.¹⁵⁻¹⁸ If such conformational changes perturb substrate approaches towards the oxidizing intermediate, then communication with the chiral cyclohexane bridge may be prevented.

5.4. Concluding Remarks

Although there was no chiral induction by the amido-imine ligands, they represent an interesting family of trianionic ligands. The oxygen atom transfer chemistry performed by the manganese complexes suggest they are capable of supporting high-valent metal oxidation states. This result is not too surprising as similar diamido diphenolic ligands have long been used to stabilize metals in high oxidation states.¹⁹⁻²⁴ Additionally, the synthetic method is extremely modular. Several variations of the “half-units” were rapidly synthesized with varying functionalities, permitting facile synthetic tuning of electronic and steric ligand properties.

5.5. Experimental Section

5.5.1. Materials

Silica gel 60 (70 - 230 and 230 - 400 mesh) was used for column chromatography. Analytical thin layer chromatography was performed using F254 silica gel (pre-coated sheets, 0.2 mm thick). Solvents for synthesis were reagent grade or better and used as received from Aldrich or dried according to standard methods.²⁵ 3,5-Di-*tert*-butyl-2-hydroxybenzaldehyde, 3-*tert*-butyl-2-hydroxybenzaldehyde, 3,5-di-*tert*-butylsalicylic acid, salicylic acid, 1-[3-dimethylamino)propyl]-3-ethylcarbodiimide hydrochloric acid, N-methylmorpholine, (1*R*,2*R*)-(-)-1,2-diaminocyclohexane, thionyl chloride, manganese (II) acetate tetrahydrate and 1,2-dihydronaphthalene were used as received from Aldrich. Silver(I) oxide was used as received from Strem Chemicals.

The following compounds were obtained using published protocols and their purity confirmed by ¹H NMR: (1*R*,2*R*)-(-)-1,2-diaminocyclohexane·HCl adduct (**1**),⁷ 2-[(2-aminocyclohexaneimino)-methyl]-4,6-di-*tert*-butyl-phenol·HCl adduct (**2**),⁷ 2,7-di-*tert*-butyl-5-(3-formyl-4-hydroxyphenyl)-9,9-dimethyl-9H-xanthene-4-carboxylic acid (**3**),¹ 3-*tert*-butyl-2-hydroxy-5-methoxybenzaldehyde (**4**),¹⁰ 5-bromo-3-*tert*-butyl-2-hydroxybenzaldehyde (**5**),¹¹ 3-*tert*-butyl-2-hydroxy-5-nitrobenzaldehyde (**6**).¹²

5.5.2. Physical Measurements

¹H NMR and ¹³C NMR spectra were performed in CDCl₃ (Cambridge Isotope Laboratories) at 25 °C unless otherwise noted. Spectra were taken on an Inova 500 or

Mercury 300 Spectrometer housed in the MIT Department of Chemistry Instrumentation Facility (DCIF). All chemical shifts are reported using the standard δ notation in parts-per-million relative to tetramethylsilane. The ^1H NMR and ^{13}C NMR spectra were internally calibrated to the monoprotio impurity of the deuterated solvent used. High-resolution mass spectral analyses were carried out by the MIT DCIF on a Bruker APEXIV47e.FT-ICR-MS using an Apollo ESI source.

5.5.3. Synthesis

5.5.3.1. 3-*tert*-Butyl-2-hydroxybenzoic acid (7)

3-*tert*-Butyl-2-hydroxybenzaldehyde (0.300 g, 1.68 mmol) and silver(I) oxide (0.234 g, 1.01 mmol) were added to 8 mL of 3 M aqueous NaOH solution and heated to 80 °C for 4 hours, followed by stirring at room temperature for an additional 12 hours. The solution was then neutralized using HCl and filtered. The white precipitate was washed with diethyl ether (20 mL) to leave the product (0.180 g, 46% yield). ^1H NMR (500 MHz, CDCl_3 , δ): 11.21 (s, 1H), 7.82 (dd, $J = 8$ Hz, 2 Hz, 1H), 7.54 (dd, $J = 8$ Hz, 2 Hz, 1H), 6.87 (t, $J = 8$ Hz, 1H), 1.44 (s, 9H).

5.5.3.2. 3-*tert*-Butyl-2-hydroxy-5-methoxy-benzoic acid (8)

3-*tert*-Butyl-2-hydroxy-5-methoxybenzaldehyde (4) (0.500 g, 2.40 mmol) and silver(I) oxide (0.557 g, 2.40 mmol) was added to 8 mL of 3 M aqueous NaOH solution and heated to 80 °C for 4 hours, followed by stirring at room temperature for 8 hours. The solution was then neutralized using HCl and filtered. The precipitate was washed with diethyl ether (10 mL) to leave the red product (0.131 g, 24% yield). ^1H NMR (500 MHz, CDCl_3 , δ): 10.90 (s, 1H), 7.23 (d, $J = 3$ Hz, 1H), 7.19 (d, $J = 3$ Hz, 1H), 3.81 (s, 3H), 1.43 (s, 9H). ^{13}C NMR (500 MHz, CDCl_3 , δ): 175.45, 157.08, 151.37, 140.08, 124.13, 110.57, 108.89, 55.89, 35.30, 29.40.

5.5.3.3. 5-Bromo-3-*tert*-butyl-2-hydroxybenzoic acid (9)

5-Bromo-3-*tert*-butyl-2-hydroxybenzaldehyde (5) (0.500 g, 1.95 mmol) and silver(I) oxide (0.270 g, 1.17 mmol) was added to 12 mL of 3M aqueous NaOH solution and heated to 80 °C for 4 hours, followed by stirring at room temperature for 10 hours. The solution was then filtered. The collected filtrate was neutralized using HCl and the

resulting precipitate was collected by filtration. The precipitate was washed with deionized water (20 mL) to give the orange product (0.171 g, 32% yield). ¹H NMR (500 MHz, CDCl₃, δ): 11.24 (bs, 1H), 7.91 (d, *J* = 2.5 Hz, 1H), 7.57 (d, *J* = 2.5 Hz, 1H), 1.41 (s, 9H). ¹³C NMR (500 MHz, CDCl₃, δ): 174.60, 161.02, 140.95, 137.04, 130.94, 129.41, 110.95, 35.45, 29.30.

5.5.3.4. 3-*tert*-Butyl-2-hydroxy-5-nitrobenzoic acid (10)

3-*tert*-Butyl-2-hydroxy-5-nitrobenzaldehyde (**6**) (0.300 g, 1.34 mmol) and silver(I) oxide (0.187 g, 0.81 mmol) were added to 5 mL of 3M aqueous NaOH and heated to 80 °C for 4 hours and then stirred at room temperature for 12 hours. The solution was then filtered over Celite. The collected filtrate was neutralized using HCl and refiltered to collect the resulting colorless precipitate. The filtrate was extracted with 2 × 10 mL of diethyl ether, and the organic portions combined with the previously collected precipitate and purified by column chromatograph (silica gel, 90:10 dichloromethane: methanol) to elute the product (0.276 g, 86% yield). ¹H NMR (500 MHz, CDCl₃, δ): 12.05 (bs, 1H), 8.77 (d, *J* = 3 Hz, 1H), 8.41 (s, 1H), 3.53 (bs, 1H), 1.47 (s, 9H).

5.5.3.5. *N*-(2-Aminocyclohexane)-3,5-di-*tert*-butyl-2-hydroxybenzamide (11)

3,5-Di-*tert*-butylsalicylic acid (1.80 g, 6.81 mmol) (0.460 g, 1.74 mmol), (1*R*,2*R*)-(-)-1,2-diaminocyclohexane, 1-[3-(dimethylamino)propyl]-3-ethylcarbodiimine hydrochloric acid (0.367 g, 1.91 mmol) and *N*-methylmorpholine (0.76 mL, 6.96 mmol) were added to 6 mL of dry dichloromethane and stirred at room temperature for 12 hours. The solution was washed with dilute NaOH, dried over MgSO₄, and the solvent removed by rotary evaporation. The residue was purified by column chromatography (silica gel, 5:5 pentane: dichloromethane, followed by dichloromethane, followed by 98:1:1 dichloromethane: methanol: triethylamine) to elute the product (0.239 g, 40% yield). ¹H NMR (500 MHz, CDCl₃, δ): 7.42 (d, *J* = 2 Hz, 1H), 7.32 (d, *J* = 2 Hz, 1H), 7.01 (bs, 1H), 3.62 (bs, 1H), 2.54 (bs, 1H), 1.97 (d, *J* = 2 Hz, 1H), 1.87 (bs, 1H), 1.62 (d, *J* = 6 Hz, 2H), 1.38 (s, 9H), 1.26 (s, 9H), 1.24 (m, 2H), 1.11 (t, *J* = 9 Hz, 2H). ¹³C NMR (500 MHz, CDCl₃, δ): 171.79, 158.88, 140.00, 138.16, 128.92, 119.61, 113.50, 56.10, 55.05, 35.53, 35.32, 34.47, 32.42, 31.65, 29.52, 25.12, 25.10.

5.5.3.6. *N*-(2-Aminocyclohexane)-2-hydroxybenzamide (12)

Salicylic acid (0.300 g, 2.17 mmol), (1*R*,2*R*)-(-)-1,2-diaminocyclohexane (0.250 g, 2.17 mmol), 1-[3-dimethylamino)propyl]-3-ethylcarbodiimide hydrochloric acid (0.458 g, 2.39 mmol), and *N*-methylmorpholine (0.96 mL, 8.68 mmol) were added to 12 mL of dry dichloromethane in an oven-dried flask and stirred for 36 hours. The reaction was then washed with a dilute aqueous sodium carbonate solution and the organic portion dried with MgSO₄. The solvent was removed by rotary evaporation and the residue was purified by column chromatography (silica gel, 98:1:1 dichloromethane: methanol: triethylamine followed by 89:10:1 dichloromethane: methanol: triethylamine) to elute the product (0.203 g, 40% yield). ¹H NMR (500 MHz, CDCl₃, δ): 7.52 (dd, *J* = 8 Hz, 1.5 Hz, 1H), 7.50 (bs, 1H), 7.36 (dt, *J* = 8 Hz, 1.5 Hz, 1H), 6.89 (dd, *J* = 8 Hz, 1 Hz, 1H), 6.85 (dt, *J* = 8 Hz, 1.5 Hz, 1H), 3.99 (bs, 1H), 3.68 (t, *J* = 4.5 Hz, 2H), 2.40 (bs, 2H), 2.27 (s, 2H), 2.24 (s, 1H), 1.85 (d, *J* = 6.5 Hz, 1H), 1.45 (m, 2H).

5.5.3.7. *N*-(2-Amino-cyclohexane)-3-*tert*-butyl-2-hydroxybenzamide (13)

3-*tert*-Butyl-2-hydroxybenzoic acid (7) (0.160 g, 0.824 mmol) was heated to 70 °C in neat thionyl chloride (2 mL) for about one hour, or when evolution of gas from the reaction ceased. The excess thionyl chloride was removed under reduced pressure and 100 mL of dry dichloromethane was added to the residue. A solution of (1*R*,2*R*)-(-)-1,2-diaminocyclohexane (0.114 g, 0.989 mmol) in 100 mL of dry dichloromethane was slowly added to the acyl chloride solution in 15 mL aliquots, followed by neat triethylamine (0.115 mL, 0.824 mmol). After stirring at room temperature for 12 hours, the solution was filtered and the filtrate was reduced by rotary evaporation to give the crude product, which was purified by column chromatography (silica gel, 98:1:1 dichloromethane: methanol: triethylamine) to give the product (0.091 g, 38% yield). ¹H NMR (500 MHz, CDCl₃, δ): 7.40 (t, *J* = 6.5 Hz, 1H), 6.78 (m, 2H), 3.80 (bs, 1H), 3.00 (bs, 1H), 3.07 (m, 2H), 2.75 (bs, 2H), 2.19 - 2.05 (m, 2H), 1.75 (d, *J* = 11 Hz, 2H), 1.42 (s, 9H). 171.52, 161.23, 138.95, 131.31, 123.88, 117.82, 114.24, 55.82, 55.05, 35.25, 35.17, 34.68, 32.46, 29.46, 25.06. ¹³C NMR (500 MHz, CDCl₃, δ): 171.52, 161.23, 138.95, 131.31, 123.88, 117.82, 114.24, 59.01, 55.82, 55.05, 45.98, 35.17, 32.46, 29.46, 25.06.

5.5.3.8. *N*-(2-Aminocyclohexane)-3-*tert*-butyl-2-hydroxy-5-methoxybenzamide (14)

3-*tert*-Butyl-2-hydroxy-5-methoxybenzoic acid (**8**) (0.100 g, 0.446 mmol) was heated to 70 °C in neat thionyl chloride (2 mL) for about one hour. The excess thionyl chloride was removed under reduced pressure and 100 mL of dry dichloromethane was added to the residue. A solution of (1*R*,2*R*)-(-)-1,2-diaminocyclohexane (0.061 g, 0.535 mmol) in 100 mL of dry dichloromethane was slowly added to the acyl chloride solution in 15 mL aliquots, followed by neat triethylamine (0.061 mL, 0.446 mmol). After stirring at room temperature for 12 hours, the solution was filtered and the filtrate was reduced by rotary evaporation to give the crude product, which was purified by column chromatography (silica gel, 98:1:1 dichloromethane: methanol: triethylamine followed by 89:10:1 dichloromethane: methanol: triethylamine) to give the product (0.061 g, 43% yield). ¹H NMR (500 MHz, CDCl₃, δ): 7.04 (t, *J* = 3 Hz, 1H), 6.97 (bs, 1H), 3.81 (s, 3H), 3.53 (bs, 1H), 3.34 (bs, 1H), 3.07 (m, 2H), 2.8 (bs, 1H), 2.40 (d, *J* = 12 Hz, 1H), 2.18 - 2.03 (m, 2H), 1.74 (d, *J* = 8.5 Hz, 2H), 1.40 (s, 9H). ¹³C NMR (500 MHz, CDCl₃, δ): 171.53, 155.58, 150.92, 140.22, 119.98, 113.77, 107.13, 56.21, 55.20, 54.26, 46.00, 35.29, 32.19, 29.38, 24.93, 24.75.

5.5.3.9. *N*-(2-Aminocyclohexane)-5-bromo-3-*tert*-butyl-2-hydroxybenzamide (**15**)

5-Bromo-3-*tert*-butyl-2-hydroxybenzoic acid (**6**) (0.120 g, 0.439 mmol) was heated to 70 °C in neat thionyl chloride (2 mL) for about one hour. The excess thionyl chloride was removed under reduced pressure and 100 mL of dry dichloromethane was added to the residue. A solution of (1*R*,2*R*)-(-)-1,2-diaminocyclohexane (0.061 g, 0.535 mmol) in 100 mL of dry dichloromethane was slowly added to the acyl chloride solution in 15 mL aliquots, followed by neat triethylamine (0.061 mL, 0.446 mmol). After stirring at room temperature for 12 hours, the solution was filtered and the filtrate was reduced by rotary evaporation to give the crude product, which was purified by column chromatography (silica gel, 98:1:1 dichloromethane: methanol: triethylamine followed by 89:10:1 dichloromethane: methanol: triethylamine) to give the product (0.078 g, 48% yield). ¹H NMR (500 MHz, CDCl₃, δ): 7.64 (d, *J* = 2.5 Hz, 1H), 7.42 (d, *J* = 2.5 Hz, 1H), 7.02 (bs, 1H), 3.70 (bs, 1H), 3.51 (m, 2H), 2.72 (m, 2H), 2.67 (bs, 1H), 2.09 (bs, 1H), 2.00 (bs, 1H), 1.74 (m, 2H), 1.35 (s, 9H). ¹³C NMR (500 MHz, CDCl₃, δ): 170.53, 160.31, 141.06, 133.96, 127.33, 115.86, 109.91, 55.22, 53.93, 52.93, 35.35, 32.12, 29.26, 24.86, 24.82.

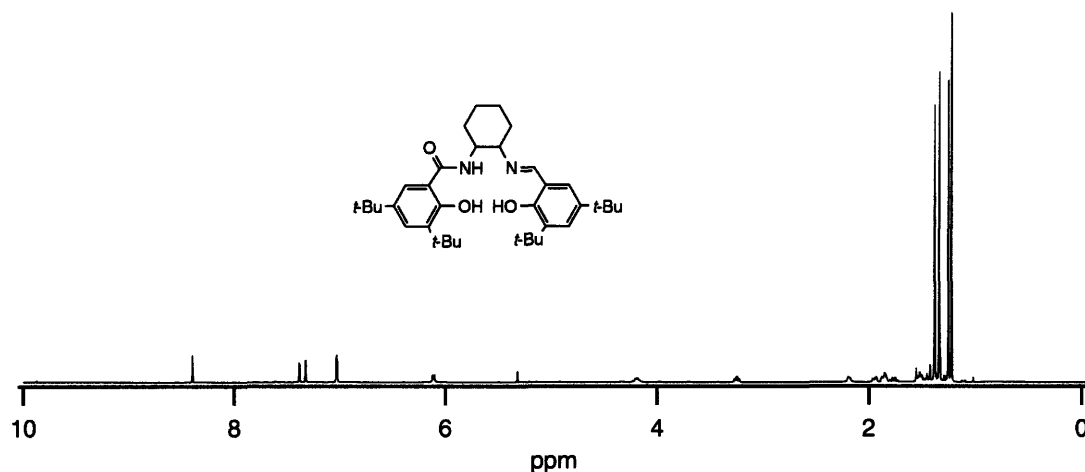
5.5.3.10. *N*-(2-Aminocyclohexane)-3-*tert*-butyl-2-hydroxy-5-nitrobenzamide (**16**)

3-*tert*-Butyl-2-hydroxy-5-nitrobenzoic acid (**10**) (0.040 g, 0.167 mmol) was heated to 70 °C in neat thionyl chloride (2 mL) for about one hour. The excess thionyl chloride was removed under reduced pressure and 50 mL of dry dichloromethane was added to the residue. A solution of (1*R*,2*R*)-(-)-1,2-diaminocyclohexane (0.023 g, 0.201 mmol) in 50 mL of dry dichloromethane was slowly added to the acyl chloride solution in 15 mL aliquots, followed by neat triethylamine (0.023 mL, 0.167 mmol). After stirring at room temperature for 12 hours, the solution was filtered and the filtrate was reduced by rotary evaporation to give the crude product, which was purified by column chromatography (silica gel, 89:10:1 dichloromethane: methanol: triethylamine) to give the product (0.013 g, 23% yield). ¹H NMR (500 MHz, CDCl₃, δ): 8.98 (s, 1H), 8.11 (s, 1H), 4.12 (bs, 1H), 3.80 (bs, 1H), 3.25 (m, 1H), 2.35 (d, *J* = 12 Hz, 1H), 2.15 (d, *J* = 9 Hz, 1H), 1.96 (m, 2H), 1.88 (d, *J* = 7 Hz, 1H), 1.75 (bs, 2H), 1.39 (s, 9H).

5.5.3.11. 3,5-Di-*tert*-butyl-*N*-{2-[(3,5-di-*tert*-butyl-2-hydroxybenzylidene)amino]-cyclohexane}-2-hydroxybenzamide (**17**)

N-(2-Aminocyclohexane)-3,5-di-*tert*-butyl-2-hydroxybenzamide (**11**) (0.250 g, 0.721 mmol) and 3,5-di-*tert*-butyl-2-hydroxybenzaldehyde (0.169 g, 234.23 mmol) were added to 6 mL of ethanol and heated to reflux for 12 hours. The reaction was then cooled to 0 °C and filtered. The bright yellow precipitate was washed with cold ethanol (2 mL) to give the product (0.300 g, 74% yield). IR (KBr) ν_{\max} : 1628 cm⁻¹ (C=O), 1587 cm⁻¹ (C=N). ¹H NMR (500 MHz, CDCl₃, δ): 13.42 (s, 1H), 12.54 (s, 1H), 8.40 (s, 1H), 7.38 (d, *J* = 2.5 Hz, 1H), 7.32 (d, *J* = 2.5 Hz, 1H), 7.03 (m, 2H), 6.11 (d, *J* = 7.5 Hz, 1H), 4.19 (bs, 1H), 3.25 (dt, *J* = 10.5 Hz, 4 Hz, 1H), 2.19 (bs, 1H), 1.96 - 1.73 (m, 4H), 1.55 - 1.50 (m, 3H), 1.38 (s, 9H), 1.34 (s, 9H), 1.25 (s, 9H), 1.22 (s, 9H). ¹³C NMR (500 MHz, CDCl₃, δ): 171.16, 165.60, 158.74, 158.26, 140.25, 139.83, 138.28, 137.10, 128.81, 127.50, 126.01, 119.05, 117.75, 113.79, 54.06, 35.34, 35.22, 34.35, 34.29, 33.84, 31.66, 31.58, 31.53, 31.31, 29.62, 29.53, 24.85, 24.33. HRESI-MS ([M + H]⁺) C₃₆H₅₄N₂O₃ *m/z*, Calcd. 563.4207 Found 563.4202.

Figure 5.2. ^1H NMR of compound 17.



5.5.3.12. Mn[3,5-di-*tert*-butyl-*N*-{2-[(3,5-di-*tert*-butyl-2-hydroxybenzylidene)amino]cyclohexane}-2-hydroxybenzamide] (18)

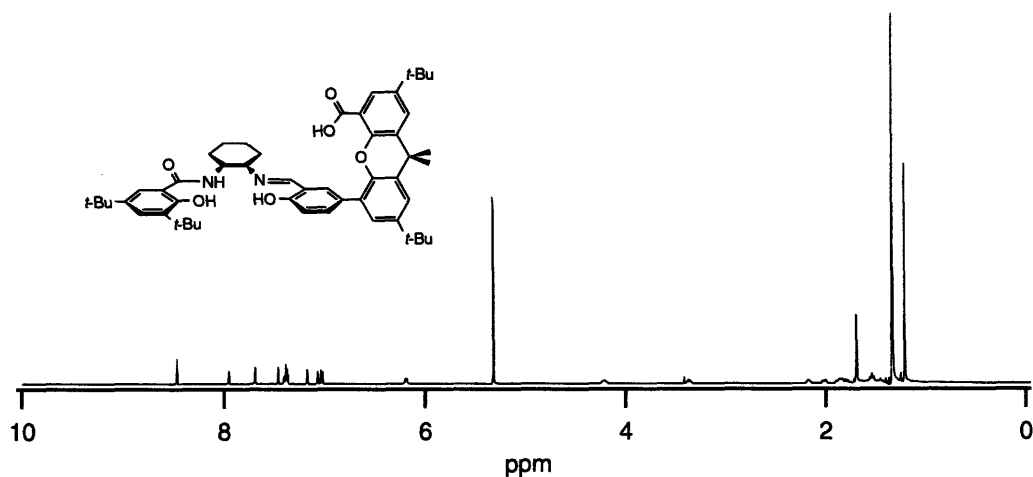
The ligand 3,5-di-*tert*-butyl-*N*-{2-[(3,5-di-*tert*-butyl-2-hydroxybenzylidene)amino]cyclohexane}-2-hydroxybenzamide (17) (15.0 mg, 0.027 mmol) was added to manganese(II) acetate tetrahydrate (6.5 mg, 0.027 mmol) in 2 mL of ethanol and refluxed in air for 4 hours. Upon cooling, the solvent was removed under reduced pressure. The residue was washed with methanol and the insoluble portion dissolved in dichloromethane and washed with 2 \times 10 mL of deionized water. The organic portion was dried with MgSO_4 and the solvent removed by rotary evaporation to give the brown product (8.0 mg, 49% yield). IR (KBr) ν_{max} : 1624 cm^{-1} (C=O), 1535 cm^{-1} (C=N). HRESI-MS ($[\text{M} + \text{Na}]^+$) $\text{NaC}_{36}\text{H}_{51}\text{MnN}_2\text{O}_3$ m/z , Calcd. 637.3178 Found 637.3204.

5.5.3.13. 2,7-Di-*tert*-butyl-5-(3-{[2-(3,5-di-*tert*-butyl-2-hydroxybenzoylamino)cyclohexaneimino]methyl}-4-hydroxyphenyl)-9,9-dimethyl-9H-xanthene-4-carboxylic acid (19)

N-(2-Aminocyclohexane)-3,5-di-*tert*-butyl-2-hydroxybenzamide (11) (25.0 mg, 0.072 mmol) was added to 2,7-di-*tert*-butyl-5-(3-formyl-4-hydroxyphenyl)-9,9-dimethyl-9H-xanthene-4-carboxylic acid (35.1 mg, 0.072 mmol) in 3 mL of methanol. The mixture was refluxed for 12 hours and then cooled to 0 $^\circ\text{C}$ and filtered. The precipitate was washed with 4 mL of cold methanol to leave the bright yellow product (26 mg, 44% yield). IR (KBr) ν_{max} : 1638 cm^{-1} (C=O), 1588 cm^{-1} (C=N). ^1H NMR (500 MHz, CDCl_3 ,

δ): 8.45 (s, 1H), 7.95 (d, $J = 2.5$ Hz, 1h), 7.69 (d, $J = 2.5$ Hz, 1H), 7.46 (d, $J = 2.5$ Hz, 1H), 7.39 (m, 2H), 7.17 (d, $J = 2.5$ Hz, 1H), 7.07 (d, $J = 2.5$ Hz, 1H), 7.03 (d, $J = 9$ Hz, 1H), 6.19 (d, $J = 9$ Hz, 1H), 4.22 (d, $J = 6$ Hz, 1H), 3.42 (s, 1H), 3.37 (dt, $J = 11.5$ Hz, 4.5 Hz, 1H), 2.18 (bs, 1H), 2.01 (d, $J = 13.5$ Hz, 1H), 1.89 - 1.76 (m, 3H), 1.54 - 1.48 (m, 2H), 1.34 (s, 9H), 1.21 (s, 9H). ^{13}C NMR (500 MHz, CDCl_3 , δ): 171.47, 160.92, 159.00, 146.06, 145.64, 145.13, 139.99, 137.81, 130.33, 128.75, 128.57, 128.40, 128.02, 126.08, 125.85, 124.62, 124.47, 124.32, 124.15, 121.77, 121.58, 120.64, 120.47, 118.35, 117.13, 116.90, 113.88, 69.9, 53.93, 53.70, 50.74, 50.57, 44.26, 35.30, 35.05, 34.68, 31.74, 31.65, 31.60, 31.51, 29.63, 29.55, 29.51. HRESI-MS ($[\text{M} + \text{H}]^+$) $\text{C}_{52}\text{H}_{66}\text{N}_2\text{O}_6$ m/z , Calcd. 815.4994 Found 815.5028.

Figure 5.3. ^1H NMR spectra of compound **19**.



5.5.3.14. Mn[2,7-di-*tert*-butyl-5-(3-{[2-(3,5-di-*tert*-butyl-2-hydroxybenzoylamino)-cyclohexaneimino]methyl}-4-hydroxyphenyl)-9,9-dimethyl-9H-xanthene-4-carboxylic acid] (20)

2,7-Di-*tert*-butyl-5-(3-{[2-(3,5-di-*tert*-butyl-2-hydroxybenzoylamino)cyclohexaneimino]-methyl}-4-hydroxyphenyl)-9,9-dimethyl-9H-xanthene-4-carboxylic acid (**19**) (26.0 mg, 0.032 mmol) was added to manganese(II) acetate tetrahydrate (7.8 mg, 0.032 mmol) in 2 mL of ethanol and refluxed in air for 4 hours. Upon cooling, the solvent was removed under reduced pressure, and the residue was washed with methanol. The insoluble portion was dissolved in dichloromethane and washed with 2×10 mL of deionized water. The organic portions were dried with MgSO_4 and the solvent was removed by rotary

evaporation to leave the product (14 mg, 52% yield). IR (KBr) ν_{max} : 1626 cm^{-1} (C=O), 1531 cm^{-1} (C=N). ESI-MS ($[\text{M} + \text{Na}]^+$) $\text{NaC}_{52}\text{H}_{63}\text{MnN}_2\text{O}_6$ m/z , Calcd. 889.40 Found 889.56.

5.5.4. Epoxidation Measurements

The epoxidation measurement was performed as follows: 0.75 mL of 0.05 M Na_2HPO_4 was added to 2 mL of commercial bleach (Clorox) and cooled to 0 °C. This solution of oxidant was added to a solution of Mn[2,7-di-*tert*-butyl-5-(3-{[2-(3,5-di-*tert*-butyl-2-hydroxybenzoylamino)-cyclohexaneimino]methyl}-4-hydroxyphenyl)-9,9-dimethyl-9H-xanthene-4-carboxylic acid] (**20**) (6.7 mg, 0.008 mmol) and 1,2-dihydronaphthalene (100 mg, 0.768 mmol) in 1 mL of dichloromethane, also cooled to 0 °C. Upon stirring for 12 hours, the layers were separated and the aqueous layer was extracted with 2 × 6 mL of dichloromethane. The combined organic layers were washed with 10 mL of water and 10 mL of a saturated sodium chloride solution and dried over MgSO_4 . After solvent removal by rotary evaporation the crude product was purified to by column chromatography (silica gel, 98:2 petane: ethyl acetate) to yield the epoxide product (36 mg, 32% yield). The *ee* of 0% was determined by use of a chiral GC calibrated using a pure racemic epoxide sample. The *ee* measurements were performed using a chiral GC housed in Professor Gregory Fu's laboratory by Shih-Yuan Liu.

References

1. Yang, J. Y.; Bachmann, J.; Nocera, D. G. *J. Org. Chem.* **2006**, *71*, 8706-8714.
2. Yang, J. Y.; Nocera, D. G. *J. Am. Chem. Soc.* 2007, *accepted for publication*.
3. Liu, S.-Y.; Nocera, D. G. *J. Am. Chem. Soc.* **2005**, *127*, 5278-5279.
4. Sasaki, I.; Pujol, D.; Gaudemer, A. *Inorg. Chim. Acta* **1987**, *134*, 53-57.
5. Daly, A. M.; Dalton, C. T.; Renehan, M. F.; Gilheany, D. G. *Tetrahedron Lett.* **2003**, *44*, 6445-6448.
6. Lopez, J.; Liang, S.; Bu, X. R. *Tetrahedron Lett.* **1998**, *39*, 4199-4202.
7. Campbell, E. J.; Nguyen, S.-B. T. *Tetrahedron Lett.* **2001**, *42*, 1221-1225.
8. Koehler, K.; Sandstrom, W.; Cordes, E. H. *J. Am. Chem. Soc.* **1964**, *86*, 2413-2419.
9. Akine, S.; Taniguchi, T.; Dong, W.; Masubuchi, S.; Nabeshima, T. *J. Org. Chem.* **2005**, *70*, 1704-1711.
10. Larrow, J. F.; Jacobsen, E. N.; Gao, Y.; Hong, Y.; Nie, X.; Zepp, C. M. *J. Org. Chem.* **1994**, *59*, 1939-1942.
11. Cavazzini, M.; Manfredi, A.; Montanari, F.; Quici, S.; Pozzi, G. *Eur. J. Org. Chem.* **2001**, 4639-4649.
12. Braud, M.; Fleischer, R.; Mai, B.; Schneider, M.-A.; Lachenicht, S. *Adv. Synth. Catal.* **2004**, *346*, 474-482.
13. Costes, J.-P.; Daha, F.; Donnadiou, B.; Douton, M.-J. R.; Garcia, M.-I. F.; Bousseksou, A.; Tuchagues, J.-P. *Inorg. Chem.* **2004**, *43*, 2736-2744.
14. Jacobsen, E. N.; Wu, M. H. Epoxidation of Alkenes other than Allylic Alcohols. In *Comprehensive Asymmetric Catalysis*, Vol 2; Pfaltz, A.; Jacobsen, E. N.; Yamamoto H.; Springer: Berlin, Heidelberg, New York, 1999: Chapter 18.2 and references therein.
15. Collins, T. J.; Coots, R. J.; Furutani, T.T.; Keech, J. T.; Peake, G. T.; Santarsiero, B. D. *J. Am. Chem. Soc.* **1986**, *108*, 5333-5339.
16. Barner, C. J.; Collins, T. J.; Mapes, B. E.; Santarsiero, B. D. *Inorg. Chem.* **1986**, *25*, 4323-4325.
17. Collins, T. J.; Lai, T.; Peake, G. T. *Inorg. Chem.* **1987**, *26*, 1674-1677.
18. Collins, T. J.; Keech, J. T. *J. Am. Chem. Soc.* **1988**, *110*, 1162-1167.
19. Anson, F. C.; Christie, J. A.; Collins, T. J.; Coots, R. J.; Furutani, T. T.; Gipson, S. L.; Keech, J. T.; Krafft, T. E.; Santarsiero, B. D.; Spies, G. H. *J. Am. Chem. Soc.* **1984**, *106*, 4460-4472.
20. Anson, F. C.; Collins, T. J.; Coots, R. J.; Gipson, S. L.; Richmond, T. G. *J. Am. Chem. Soc.* **1984**, *106*, 5037-5038.

21. Anson, F. C.; Collins, T. J.; Richmond, T. G.; Santarsiero, B. D.; Toth, J. E.; Treco, B. G. R. T. *J. Am. Chem. Soc.* **1987**, *109*, 2974-2979.
22. Kochi, J. K.; Koola, J. D. *J. Org. Chem.* **1987**, *52*, 4545-4553.
23. Anson, F. C.; Collins, T. J.; Gipson, S. L.; Keech, J. T.; Krafft, T. E. *Inorg. Chem.* **1987**, *26*, 1157-1160.
24. Bertocello, K.; Fallon, G. D.; Murray, K. S. *Inorg. Chim. Acta* **1990**, *174*, 57-60.
25. Armarego, W. L. F.; Perrin, D. D. *Purification of Laboratory Chemicals*; 4th ed.; Butterworth-Heinmann: Oxford, 1966.

Chapter 6

Synthesis of Cofacial Pacman Salen Architectures and Their Iron Complexes

6.1. Motivation and Specific Aims

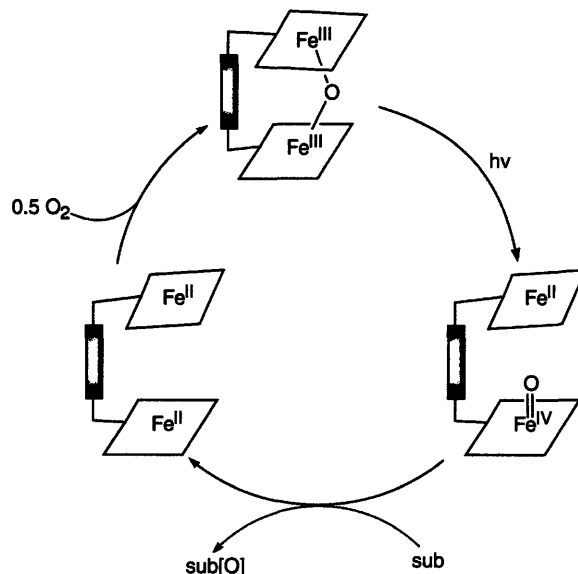
Our interest in multi-electron reactivity has led us to synthesize a series of bimetallic cofacial Pacman salen architectures with different inter-metal distances. A general synthetic methodology is developed for the construction of the ligands with two different pillars, which can be assembled and isolated in the absence of a metal ion template. This Chapter focuses on the synthesis of diferric, diferrous, and the μ -oxo diferric salen Pacman complexes and their reactivity; the ensuing Chapter captures the diversity of metal Pacman complexes that can be made from the ligands described here. We attempt to photolytically activate the μ -oxo bond in an attempt to expose a high-valent iron oxo that can perform enantioselective oxygen atom transfer chemistry to electron rich substrates, as displayed in the diiron Pacman porphyrin analogues.

6.2. Background

The design of ligand architectures capable of arranging two metal sites in a cofacial fashion has been explored with a variety of porphyrin¹⁻²⁶ and other macrocyclic²⁷⁻⁵² frameworks for a variety of reasons, including modeling enzymatic active sites, exploring multi-electron reactivity, and studying host-guest chemistry. Schiff-base macrocycles have been used in several of these architectures as they can support a wide range of transition metals in many oxidation states. The facile incorporation of enantioselective features into the salen macrocycles makes them interesting templates for assembling bimetallic ligands that form a chiral cleft between the metal centers. Moreover, Lewis-acid-assisted epoxide ring opening reactions are catalyzed by metallosalens and the mechanism is believed to involve a bimetallic intermediate. Therefore, a cofacial disalen construct that can pre-organize the transition state is a logical approach to improve catalytic activity through ligand design (this will be discussed further in Chapter 7).

The features of oxidative stability and construction of a chiral cleft are the primary motivations in extending the chemistry that has been performed with cofacial “Pacman” ligands. One of the intriguing reactions performed by the diiron μ -oxo bonded complexes is photocatalytic oxidation of electron rich substrates.^{22-26,53-55} The overall catalytic cycle is shown in Scheme 5.1. The μ -oxo bonds, formed upon oxidation of the diferrous

Scheme 6.1



species with molecular oxygen, is thermally unreactive. However, transient absorption spectroscopy has shown that the Fe—O bond can be photolytically cleaved, generating an iron(IV) oxo capable of performing oxygen atom transfer (OAT) chemistry.²⁴ These studies reveal that the geometrically splayed dibenzofuran pillar directs substrate approach to the oxidizing intermediate, favoring oxidation of substrate instead of the reverse reaction, re-clamping to reform the μ -oxo bond. Additionally, functionalizing the porphyrins with electron-withdrawing groups shifts the excitation wavelength into the visible and increases the electrophilicity of the iron(IV) oxo intermediate sufficiently to oxidize more challenging substrates such as hydrocarbons.^{25,26}

We were motivated to extend this photocatalytic oxidation chemistry using molecular oxygen as the oxidant to Pacman salen architectures. Using these architectures, we could potentially expand the utility of this reaction to the oxidation of prochiral substrates. Although no efforts that we are aware of have been made to photoactivate a diiron salen μ -oxo bond, there is chemical precedent for the last two steps of the catalytic cycle. Firstly, iron salens have shown catalytic oxygen atom transfer to olefins⁵⁶ and sulfides⁵⁷ using the oxidants sodium hypochlorite and iodosylbenzene, respectively, although the nature of the oxidizing iron intermediate is still under debate.⁵⁸⁻⁶⁰ The subsequent reaction of the diferrous species with molecular oxygen to oxidize the metals by one electron and reform the μ -oxo bridge is also well known in the iron salen literature.⁶¹⁻⁷² Therefore, a

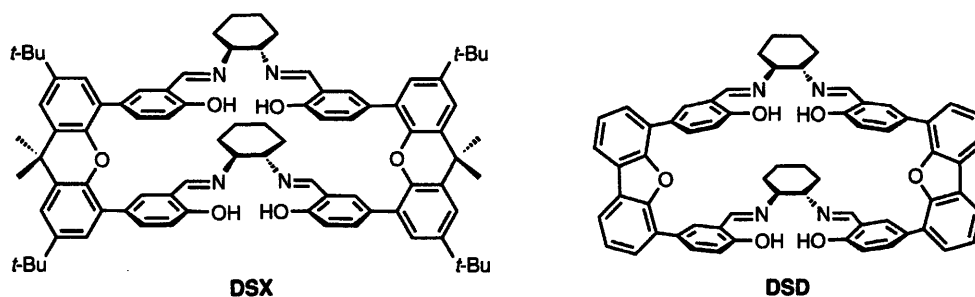
catalytic cycle using diiron Pacman salens may be constructed provided that the Fe—O bond may be cleaved photolytically.

The synthesis of cofacial salens has been demonstrated in the literature using a variety of linkers, such as naphthalene,⁴⁷ methylene,^{50,51} 1,2-ethanediol,^{50,51} and 9,9-dimethylxanthene.⁴⁸ The cofacial geometry is enforced by bridging the salens on both ends of the phenolic arms via the synthetically accessible 3 and 3' or 5 and 5' positions. In all of these examples, the complexes were synthesized in the presence of a metal ion^{46,48,50,51} or boric acid,⁵² which is believed to be critical in templating the formation of the ligand. This requirement complicates the synthesis of other bimetallic complexes; only M²⁺ ions (specifically Mn, Ni, and Zn) have successfully been used as templates for ligand assembly. Consequently, in our synthesis of diiron and diiron μ -oxo Pacman salen complexes, we sought to synthesize and isolate the free ligands in the absence of a templating agent.

6.3. Results and Discussion

6.3.1. Ligand Design

Chart 6.1



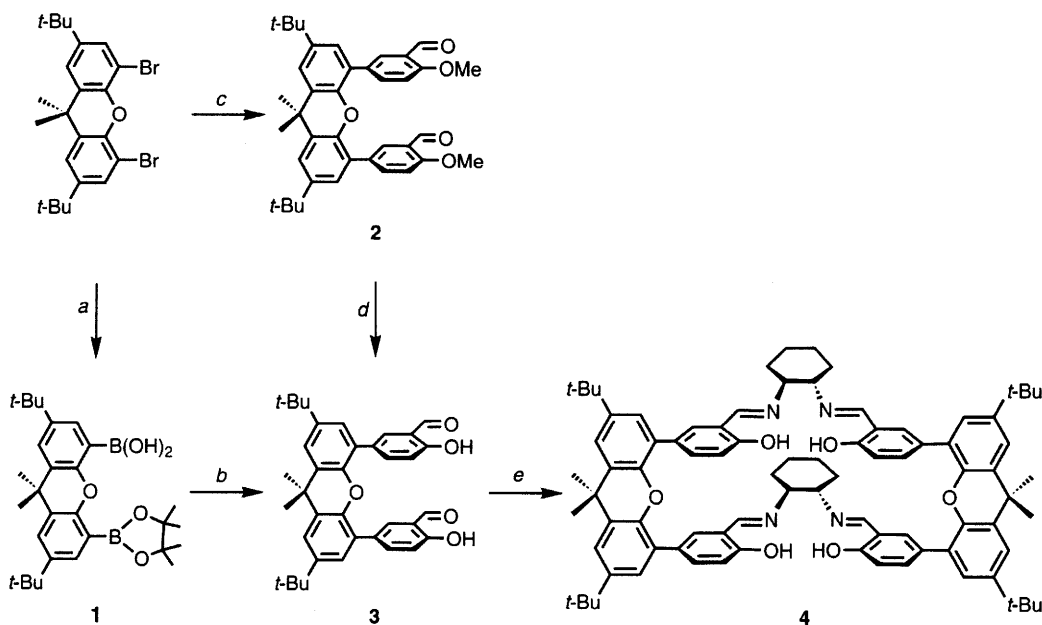
Xanthene and dibenzofuran were used as the rigid pillars to bridge the two macrocycles to form the ligands DSX and DSD, respectively, shown in Chart 5.1. Because the imine bonds on the salen macrocycle are easily hydrolyzed,⁷³⁻⁷⁶ resulting in exchange,⁷⁷ salens with unique salicylaldehydes are difficult to isolate and extremely sensitive to water. To avoid this issue, we once again turned to using two pillars to form salen macrocycles that were symmetric across the diamine bridge. The (1*R*,2*R*)-(-)-1,2-diaminocyclohexane enantiomer was used as the diamine bridge for complexes that we hoped to effect

enantioselective chemistry; the racemic version was used for the other Pacman complexes. The xanthenes are expected to hold the salens roughly parallel, whereas the dibenzofuran pillars enforces a more splayed geometry, as they do in the porphyrin Pacman complexes. Thus, the two pillars provide geometric endpoints for molecular cleft sizes of Pacman salens.

6.3.2. Synthesis of DiSalen Xanthene Ligand (DSX)

The synthesis of the DSX ligand is outlined in Scheme 6.1. The formation of the xanthene-to-salicylaldehyde aryl-aryl bonds of ligand **4** required the precursor 4,5-di(5-salicylaldehyde)-2,7-di-*tert*-butyl-9,9-dimethylxanthene (**3**), which was approached from two different synthetic pathways. In the first, 7-di-*tert*-butyl-9,9-dimethyl-4-dihydroxyborane-5-(4,4,5,5-tetramethyl-[1,3,2]dioxaborolan-2-yl)-9H-xanthene (**1**) was synthesized from Rebek's xanthene dibromide (procedure described in Chapter 3). Suzuki coupling of **1** directly with 5-bromosalicylaldehyde gave **3**, with an overall yield of 13%. Alternatively, the xanthene dibromide is already equipped with the electrophilic

Scheme 6.1



(a) bis(pinacolato)diboron, Pd(dppf)Cl₂, KOAc, DMSO, (b) 5-bromosalicylaldehyde, Na₂CO₃, Pd(dppf)Cl₂, DME: H₂O (3:1) (c) 3-formyl-4-methoxyphenylboronic acid, Na₂CO₃, Pd(dppf)Cl₂, DME: H₂O (3:1), (d) BBr₃, CH₂Cl₂, (e) 1,2-diaminocyclohexane, EtOH

aryl carbons necessary for palladium catalyzed coupling. Under Suzuki coupling conditions, the commercially available 3-formyl-4-methoxyphenylboronic acid was joined to the xanthene dibromide to furnish 4,5-di-(3-formyl-4-methoxyphenyl)-2,7-di-*tert*-butyl-9,9-dimethylxanthene (**2**). The methyl ether was then deprotected using boron tribromide to give **3** in 53% overall yield. Both pathways to **3** require two steps from the xanthene starting material. The modest yield is limited by the consecutive application of two palladium catalyzed cross-coupling steps, which are typically low yielding.

The precursor 4,5-di(5-salicylaldehyde)-2,7-di-*tert*-butyl-9,9-dimethylxanthene (**3**) was refluxed with one equivalent of 1,2-diaminocyclohexane to give the DSX ligand (**4**). Unlike previous attempts by other groups to synthesize a disalen ligand, we were able to isolate the ligand **4** without using a metal ion template. The isolated ligand was characterized by high-resolution mass spectrometry and elemental analysis was used to determine purity. The ¹H NMR spectra at room temperature of **4** was poorly resolved and broad (see Figure 6.1). The spectra of different isomers were resolved at lower temperatures. Head-to-head or head-to-tail orientations will be obtained with rotation of the salen macrocycles about the bond connecting the macrocycle to the xanthene.

Insight into the geometry disposition of the cofacial macrocycles was provided from the X-ray analysis. Single crystals of **4** suitable for X-ray diffraction were grown from the slow evaporation of a pentane-dichloromethane solution. The structure, shown in Figure 6.2 indicates considerable flexibility of the ligand salen macrocycle. They can twist along the aliphatic diamine bridge to break the square planar ligand arrangement and form the bent orientation observed in the crystal structure. We believe that insertion of a metal ion is expected to enforce the planar orientation of the ligand and provides the cofacial parallel construction desired of this architecture.

The DSX ligand was also characterized by infrared spectroscopy. The most notable feature is the imine bond stretch, found at 1589 cm⁻¹. This is a useful diagnostic in characterizing the subsequent DSX complexes as it blue shifted when coordinated to a metal.

Figure 6.1. Variable temperature ^1H NMR spectra of DiSalen Xanthene ligand (**4**) from room temperature (20 °C) to -60 °C, taken in 10 °C intervals.

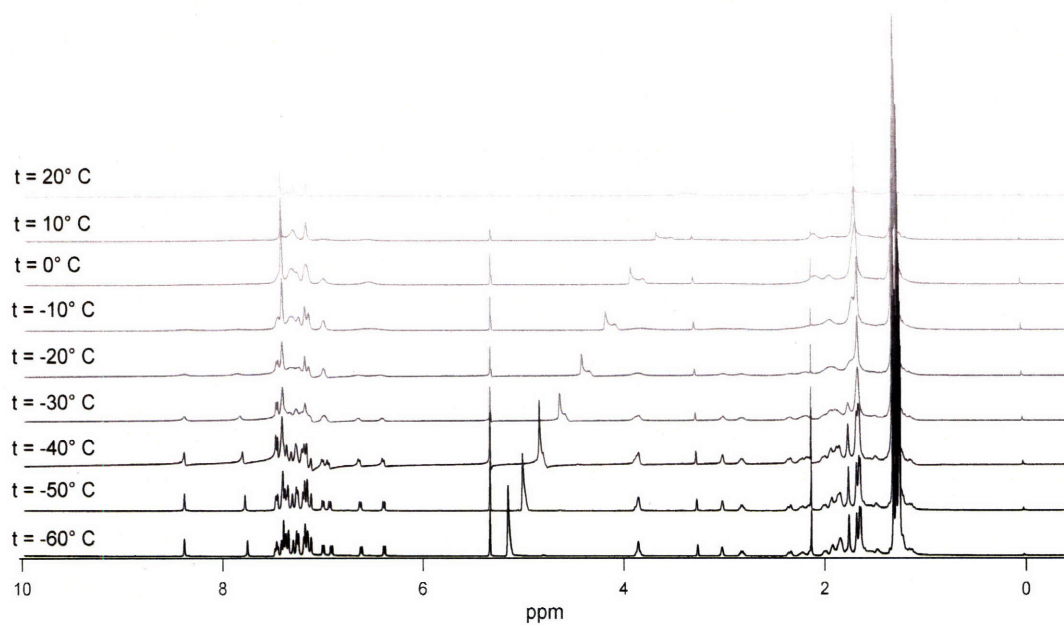
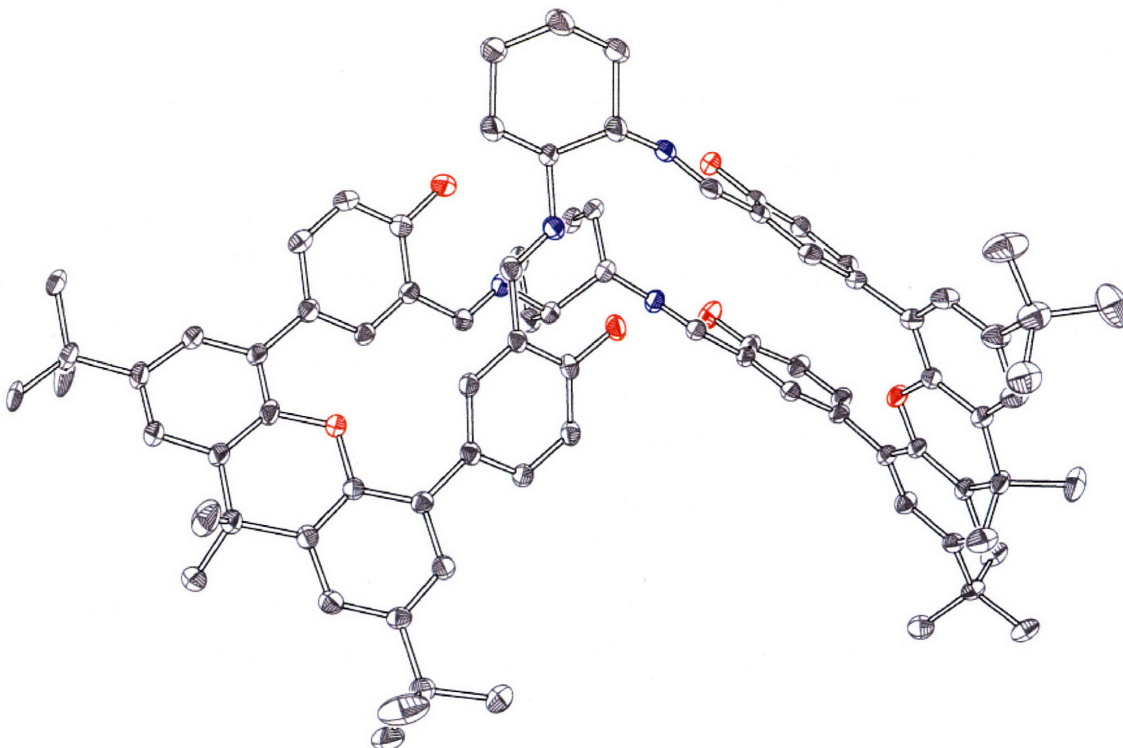
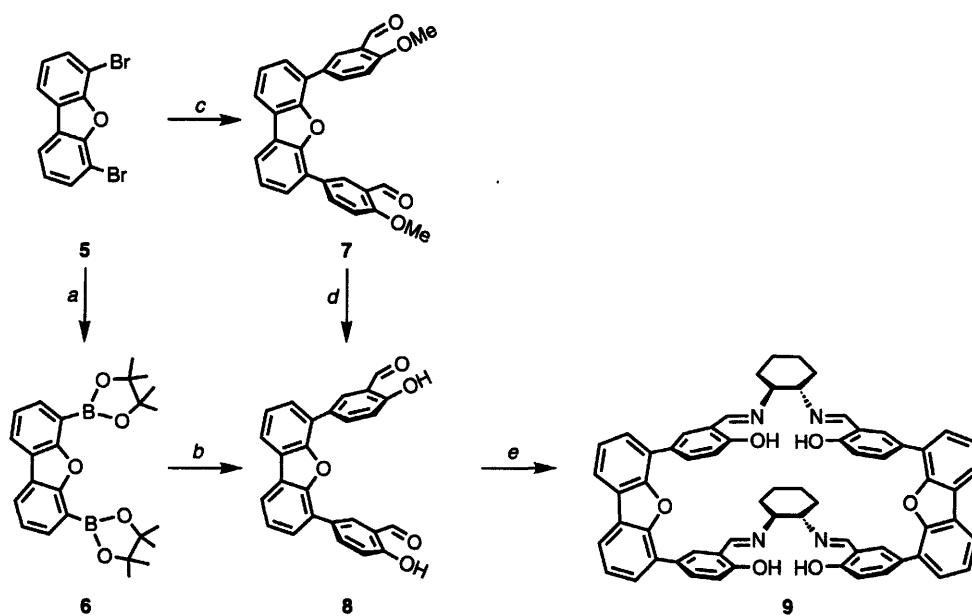


Figure 6.2. X-Ray crystal structure of DiSalen Xanthene (**4**). Crystals were grown from slow evaporation of a pentane-dichloromethane solution. Carbons are depicted as gray, oxygens as red, and nitrogens as blue. H atoms are omitted for clarity.



6.3.3. Synthesis of DiSalen Dibenzofuran Ligand (DSD)

Scheme 6.2



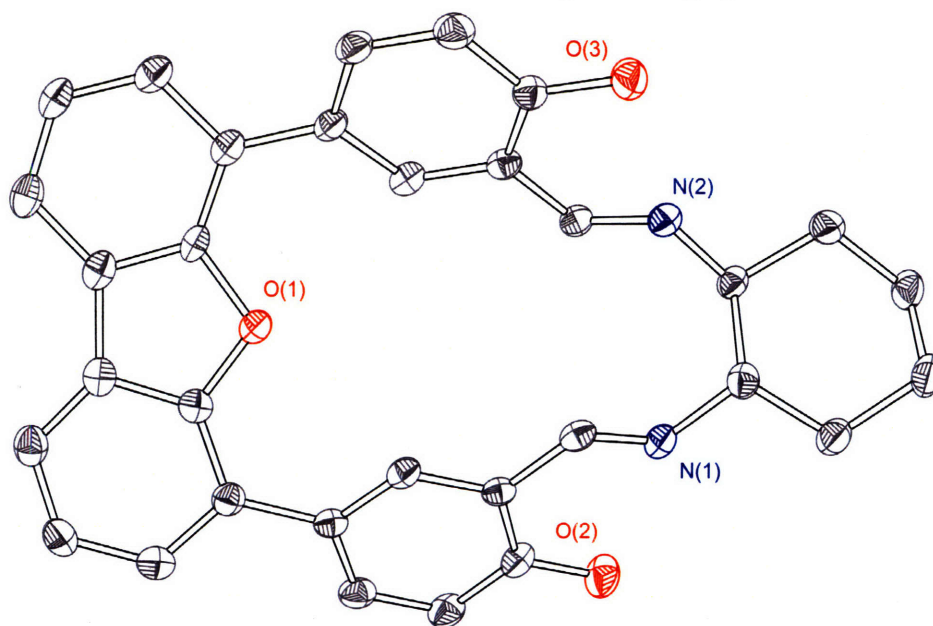
(a) bis(pinacolato)diboron, Pd(dppf)Cl₂, KOAc, DMSO, (b) BBr₃, CH₂Cl₂, (c) 3-formyl-4-methoxyphenylboronic acid, Na₂CO₃, Pd(dppf)Cl₂, DME: H₂O (3: 1), (d) 5-bromosalicylaldehyde, Na₂CO₃, Pd(dppf)Cl₂, DME: H₂O (3: 1) (e) 1,2-diaminocyclohexane, EtOH

The synthesis of the disalen dibenzofuran ligand (DSD) is outlined in Scheme 5.2. Dibenzofuran (5) is not commercially available but can be produced in a one-pot synthesis by treating dibenzofuran successively with *sec*-butyllithium, followed by elemental bromine. We initially synthesized the diboronate (6) using palladium catalyzed cross-coupling conditions with bis(pinacolato)diboron, followed by its reaction with 5-bromosalicylaldehyde under Suzuki coupling conditions to give the desired precursor 8. The low overall yield along this path led us to synthesize 2-hydroxy-5-(4,4,5,5-tetramethyl-[1,3,2]dioxaborolan-2-yl)-benzaldehyde as a precursor, but this was also met with disappointing yields (this synthesis is presented in Appendix B2). A few years into this work, 3-formyl-4-methoxyphenylboronic acid became commercially available, which can be coupled directly to dibromodibenzofuran (5). Attempted Suzuki coupling conditions resulted in the monocatenated product (also discussed in Appendix B2), but

proper conditions were eventually found to give **7** in good yields. The methyl ethers were deprotected using boron tribromide to give **8** in 62% overall yield.

The DSD ligand (**9**) is produced upon refluxing **8** with one equivalent of 1,2-diaminocyclohexane. Unlike the DSX ligand, the ^1H NMR spectrum of DSD is well resolved; the splayed pillar may strain the salens enough to prevent rotation in solution. The product was analyzed using high-resolution mass spectrometry and elemental analysis. The infrared spectra of the ligand contained a peak at 1586 cm^{-1} , assigned to the imine bond stretch. X-ray quality crystals grown from pentane-dichloromethane solutions gave the surprising structure shown in Figure 6.3. Diamine couples to the salicylaldehydes on the same dibenzofuran spacers instead of bridging between two dibenzofurans. The ^1H NMR clearly shows the existence of only one isomer in solution, and the mass spectrum proves it to be the heavier disalen dibenzofuran (DSD) ligand. Because the imine bonds in salen ligands are in equilibrium with their hydrolysis products, we believe that impurity shown in Figure 6.3 is formed in small concentrations from the fluxional nature of the imine bonds in our ligand. Solutions left under conditions for crystallization typically form large single crystals of the impurity, which is less soluble. The impurity appears to be in equilibrium with the disalen. When the crystals are

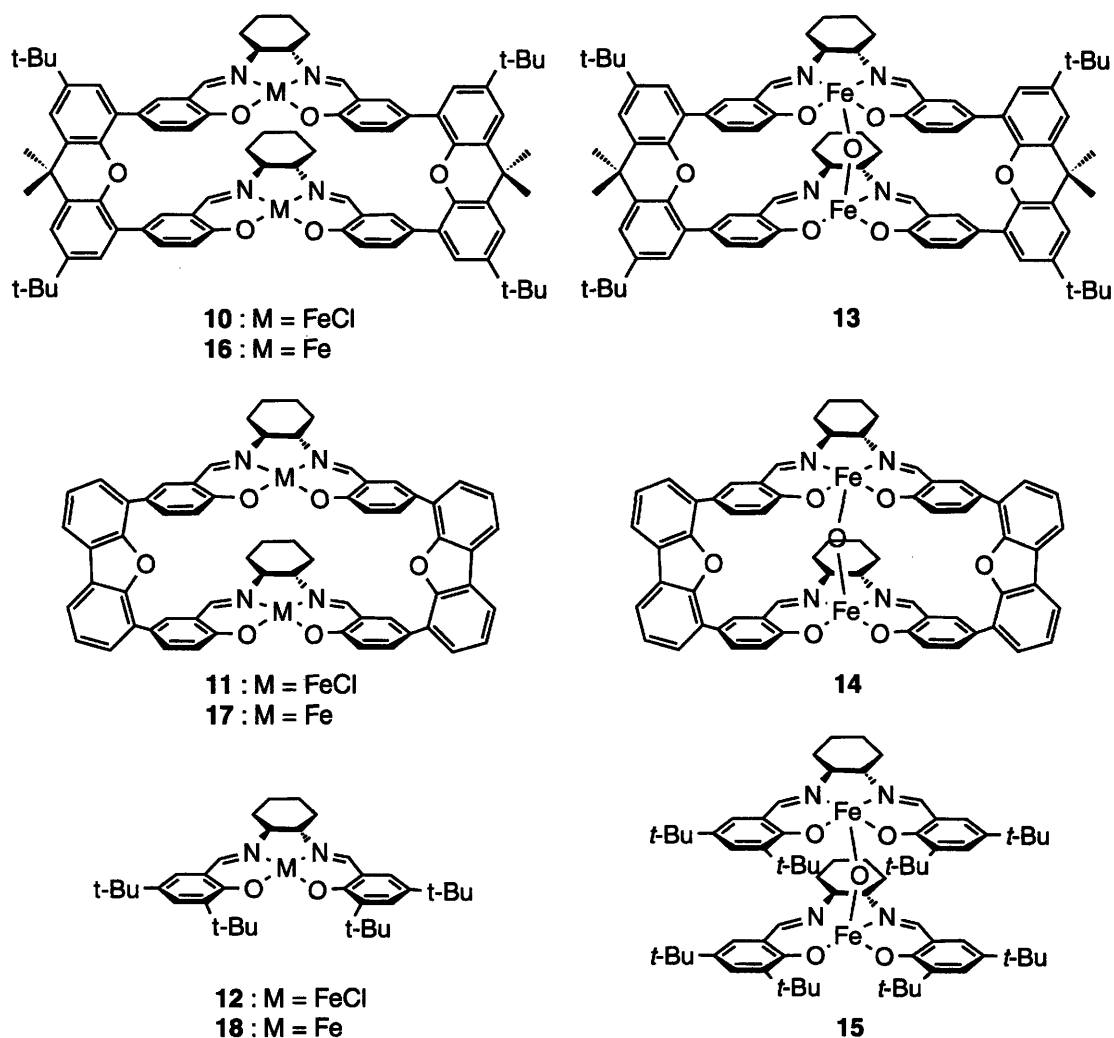
Figure 6.3. X-Ray crystal structure of DSD impurity. Crystals were grown out of a pentane-dichloromethane solution. Carbons are depicted as gray.



isolated and redissolved into solution, their mass spectrum is again composed primarily of the disalen dibenzofuran ligand. Therefore we believe the desired product DSD is the major component of our condensation reaction, and the impurity crystallizes out of solution as a minor product. As the impurity is less soluble, crystallizing conditions drives the equilibrium to the undesired product. Although present in small amounts in solutions of the ligand, metalation of the salen prevents hydrolysis and thus stabilizes the formation of the disalen ligand; the impurity may easily be separated from the metallated ligand. We have not observed an analogous impurity in the synthesis of disalen xanthene (DSX). The aldehydes are likely too close to bridge a cyclohexanediamine bridge.

5.3.4. Synthesis of Ferric Chloride Complexes

Chart 6.2



The iron salen and Pacman salen complexes shown in Chart 6.2 were prepared. Iron(III) insertion into the Pacman ligands was achieved by the reaction of two equivalents of ferric chloride in ethanol; the procedure is analogous to the preparation of monomeric iron salen compounds.⁷⁸ Anhydrous reactions conditions and workup were required to prevent the formation of μ -oxo-bridged impurities.^{79,80} This is particularly important as elemental analysis is not sensitive enough to distinguish between a partially aquated species and μ -oxo bridged impurities. This metalation method was also successful in producing the iron salen complex monomer **12** cleanly and in good yield. The purity of the ferric complexes **10** - **12** was determined by elemental analysis and their molecular formula by mass spectrometry. The infrared spectrum of the Pacman complexes also possessed the blue-shifted imine peaks of 1540 cm^{-1} for **10** and 1538 cm^{-1} for **11** (compared to the free ligand), diagnostic of metal coordination.

5.3.5. Synthesis of Diiron μ -Oxo Complexes

The diiron μ -oxo complexes **13** - **15** (as shown in Chart 6.2) were prepared using a method similar to a procedure used for other salen ligands.^{81,82} Ferric chloride hexahydrate was added to the ligand, followed by slow addition of excess triethylamine. The iron(III) centers are expected to be paramagnetic, but coupling through the μ -oxo can result in ferromagnetic or antiferromagnetic coupling, depending on the angle of the Fe—O—Fe bond. A crystal of the unpillared **15** was grown out of a tetrahydrofuran solution

Figure 6.4. X-Ray crystal structure of the unpillared $\text{Fe}_2(\text{salen})_2\text{O}$ (**15**). Crystals were grown from a pentane-dichloromethane solution. The angle of the Fe—O—Fe bond is $165.2(7)^\circ$, and the salens are by rotated 124.5° with respect to each other.

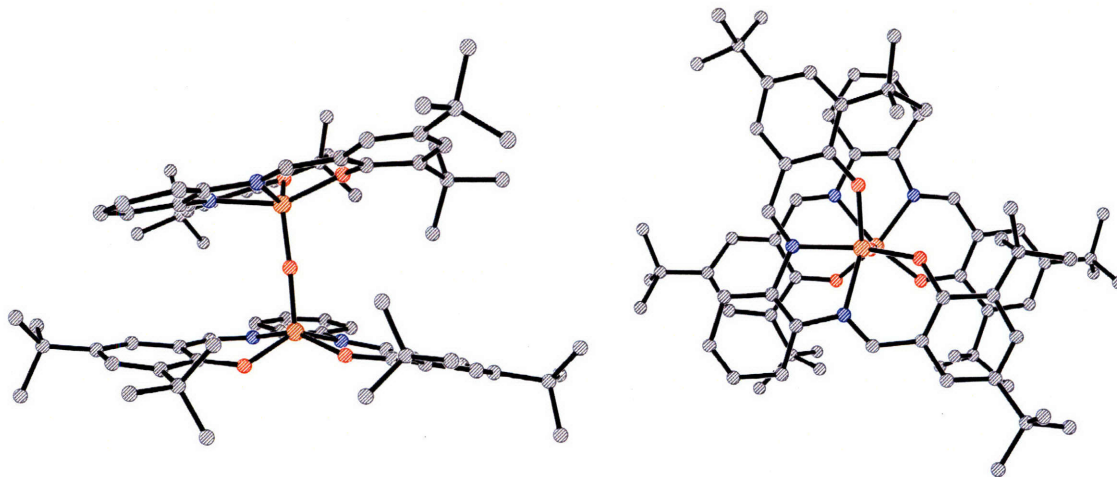
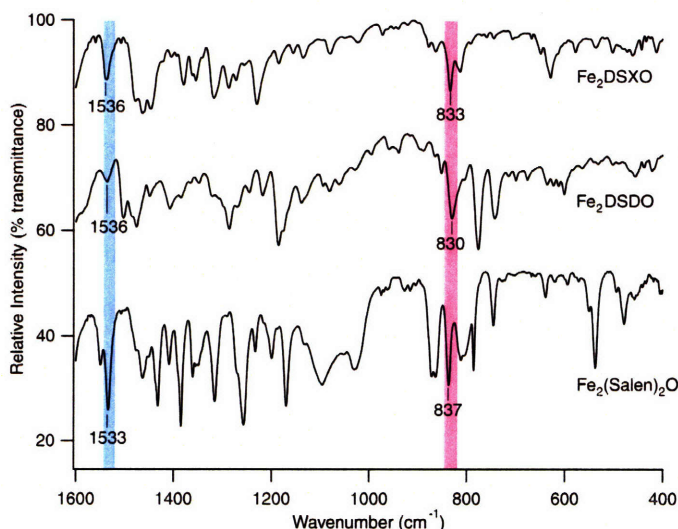


Figure 6.5. Infrared spectra displaying the fingerprint region of Fe₂DSXO (**13**), Fe₂DSDO (**14**), and Fe₂(salen)₂O (**15**), highlighting the imine (C=N, blue) and Fe—O—Fe bond (purple) stretch.



and the structure is shown in Figure 6.4. The Fe—O—Fe bond of 165° (it should be noted that the quality of the crystal data was poor). The structure is shown in Figure 5.4. This observed angle is more linear than the related diiron μ -oxo bis(disalicylaethylenediamine) complex, which displays an Fe—O—Fe of 144.6(7)°,⁸³ but within the 139°-175° range expected with a variety for four-coordinate macrocycles. The more linear geometry may indicate more π -bonding character in the Fe—O—Fe.⁷² Additionally, the Fe—O bond distances of 1.773(9) and 1.754(9) are expected for a diiron μ -oxo bridge, as opposed to the longer distances indicative of a hydroxyl bridged species. We expect the restricted geometry of the Pacman complexes to alter the angle of the diiron μ -oxo coordination, although we have yet to determine this parameter using crystallographically. The imine stretch was again diagnostic of metal coordination in the infrared spectra, coming in at 1536 cm⁻¹ for both **13** and **14** and 1533 cm⁻¹ for **15**. The Fe—O—Fe asymmetric bond stretch was also identified (based on published literature values), coming in at 833 cm⁻¹, 830 cm⁻¹ and 837 cm⁻¹ for **13**, **14** and **15**, respectively (see Figure 6.5). In addition to ¹H NMR spectroscopy, the compounds were characterized by mass spectroscopy and their purity determined by elemental analysis.

5.3.6. Synthesis of Ferrous Complexes

Previous preparations of iron(II) salen compounds have used ferrous acetate to insert the metal ion in dimethylformamide.⁶² We found the air-sensitive ferrous complexes **16** - **18** could be cleanly synthesized with this starting material using tetrahydrofuran instead, which is more convenient to remove during product isolation. The purity of the products was determined by elemental analysis.

6.3.7. ⁵⁷Fe Mössbauer Spectroscopy of Iron Complexes

⁵⁷Fe Mossbauer spectra were recorded for all of the iron compounds **10** - **18** in the solid state at 4.2K. The parameters from the data fit are given in Table 6.1. The data for the iron salen compounds, along with the fit, are shown in Figures 6.6, 6.7 and 6.8, and a summary of the parameters found is listed in Table 6.1.

The Fe(III) chloride salen complexes (Figure 6.6) have similar isomer shifts (δ) (0.428, 0.435, and 0.447 mm/s for **10**, **11**, and **12** respectively), indicating that the chemical environment around the irons are comparable. These values fall within the range of an Fe(III) high spin $S = 5/2$ species, typically listed as between 0.25 and 0.60 mm/s.⁸⁴⁻⁸⁶ This

Figure 6.6. Fitted ⁵⁷Fe Mössbauer spectra of (a) Fe₂DSXCl₂ (**10**), (b) Fe₂DSDCl₂ (**11**), (c) Fe(salen)Cl (**12**) at 4.2 K. Gray dots represent the experimental data points and the black solid line represents the fit. The vertical axis is an arbitrary transmission scale.

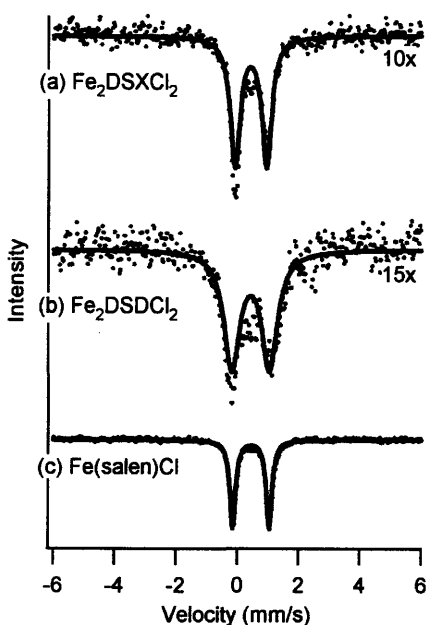


Figure 6.7. Fitted ^{57}Fe Mössbauer spectra of (a) Fe_2DSXO (**13**), (b) Fe_2DSDO (**14**), (c) $\text{Fe}_2(\text{salen})_2\text{O}$ (**15**) at 4.2 K. Gray dots represent the experimental data points and the black solid line represents the fit. The vertical axis is an arbitrary transmission scale.

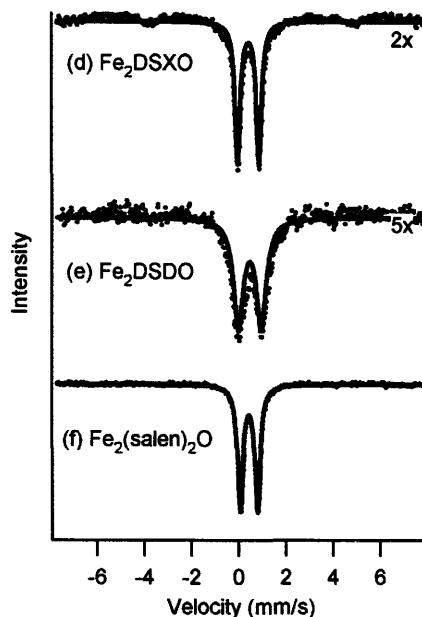
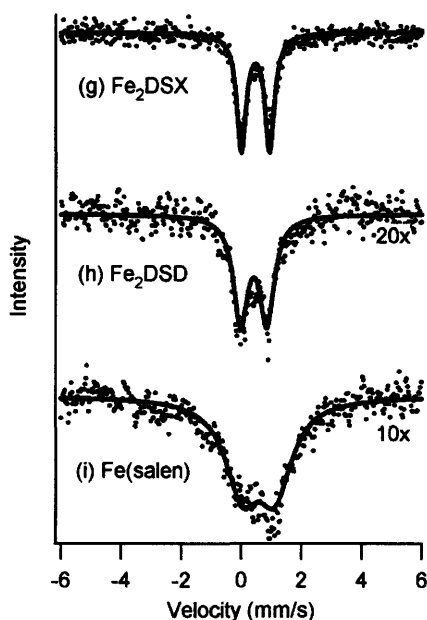


Table 6.1. Summary of Mössbauer parameters for compounds **10** - **18** recorded at 4.2 K. δ is relative to elemental iron. All samples were measured in the solid state (powdered). Γ is the half-width at half-maximum of the peaks, and the value presented is the same for both peaks.

| Complex | δ (mm/s) | ΔE_Q (mm/s) | Γ |
|--|-----------------|---------------------|----------|
| $\text{Fe}_2\text{DSXCl}_2$ (10) | 0.428 | 1.03 | 0.387 |
| $\text{Fe}_2(\text{DSD})\text{Cl}_2$ (11) | 0.435 | 1.23 | 0.617 |
| $\text{Fe}(\text{salen})\text{Cl}$ (12) ^a | 0.447 | 1.18 | 0.219 |
| $\text{Fe}_2(\text{DSX})\text{O}$ (13) | 0.439 | 0.90 | 0.259 |
| $\text{Fe}_2(\text{DSD})\text{O}$ (14) | 0.490 | 0.97 | 0.498 |
| $\text{Fe}_2(\text{salen})_2\text{O}$ (15) ^a | 0.441 | 0.73 | 0.275 |
| $\text{Fe}_2(\text{DSX})$ (16) | 0.472 | 0.94 | 0.372 |
| $\text{Fe}_2(\text{DSD})$ (17) | 0.416 | 0.87 | 0.581 |
| $\text{Fe}(\text{salen})$ (18) ^a | 0.578 | 1.08 | 1.362 |

^a salen = (1*R*, 2*R*)-(–)-[1,2-cyclohexanediamino-*N,N'*-bis(3,5-di-*tert*-butylsalicylidene)].

Figure 6.8. Fitted ^{57}Fe Mössbauer spectra of (a) Fe_2DSX (**16**), (b) Fe_2DSD (**17**), (c) $\text{Fe}(\text{salen})$ (**18**) at 4.2 K. Gray dots represent the experimental data points and the solid black line represents the fit. The vertical axis is an arbitrary transmission scale.



spin state is supported by magnetic data on the related $\text{Fe}(\text{salen})\text{Cl}$ compounds (with ethylenediamine and phenylenediamine bridges) in the literature.^{78,79} The similar quadrupole splitting value ΔE_Q of the diiron Pacman complexes (1.03 for **13** and 1.23 for **14**) compared to the monomeric compound **12** ($\Delta E_Q = 1.18$ mm/s) suggests the tetradentate salen ligand geometry is probably not distorted from its normal square planar geometry by incorporation in the Pacman framework. The Γ values are the same for both peaks.

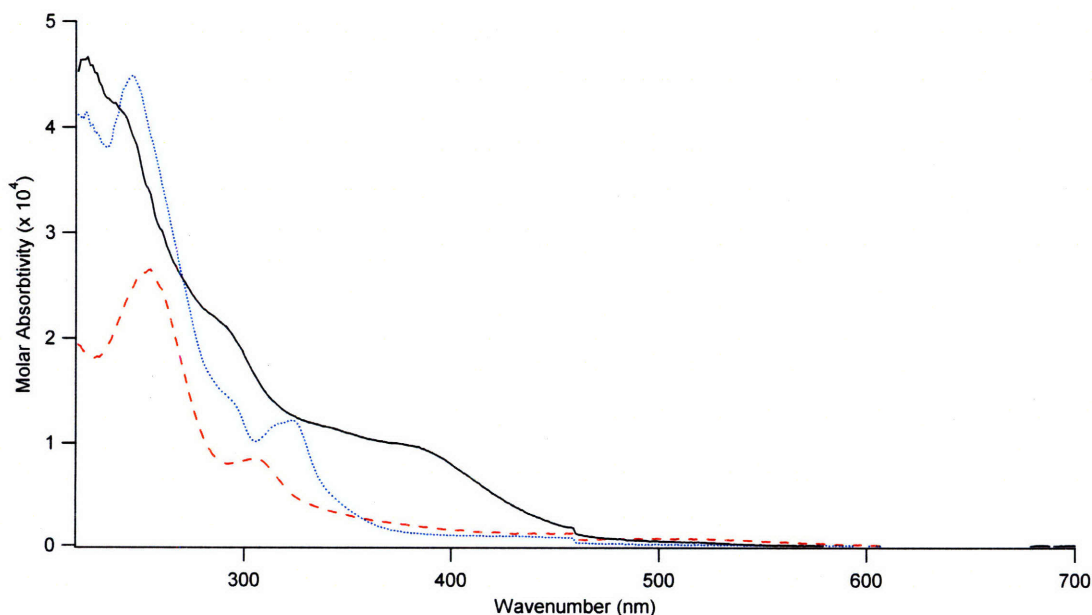
The diiron μ -oxo-bridged species (data shown in Figure 6.7) have δ values of 0.439, 0.490, and 0.447 mm/s for **13**, **14** and **15**, respectively. These values are consistent with other unbound $\text{Fe}(\text{III})$ μ -oxo bridged salen complexes, which display isomer shifts of 0.47 to 0.56 mm/s (at 77 K).^{72,87-90} The slightly higher quadrupole splitting (ΔE_Q) seen in the Pacman complexes (0.90 and 0.97 mm/s for the Pacmans **13** and **14** compared to 0.73 mm/s for the monomer **15**) could be due to a more acute $\text{Fe}-\text{O}-\text{Fe}$ angle due to ligand constraints, although this is a tentative conclusion in the absence of more structural evidence.

The Fe(II) salen complexes (Figure 6.8) display isomer shifts (δ) of 0.472, 0.416, and 0.578 mm/s for **16**, **17** and **18** respectively. These shifts for **16** and **17** are consistent with a low spin Fe(II) environment. As mentioned previously, the ferrous compounds are subject to oxidation in the presence of air. Although the samples were prepared under an inert atmosphere, and brought to the instrument immersed in liquid nitrogen, they may have been exposed to air during the manipulation into the sample holder. This may explain the poor data quality of **18**, and δ values that are on the high end for low-spin Fe(II) complexes (approaching the range observed for high-spin Fe(III) complexes). However, the isomer shifts we measured are below the range expected for high spin Fe(II) complexes, which generally fall between $\delta = 0.8 - 1.5$ mm/s.⁸⁶

6.3.8. Photolysis Studies of Iron Complexes

The diiron μ -oxo salen photo-oxidation studies were performed under conditions similar to those used in the analogous porphyrin systems. We examined the Pacman complexes bridged with xanthene (**13**), dibenzofuran (**14**), and the species lacking a pillar, **15**. Dimethyl sulfide and dibutyl sulfide used as OAT substrates, and dodecane was used as the internal standard for product analysis via GC/MS. Excess substrate was used (10

Figure 6.9. UV-vis absorption profiles of 30 μ mol solutions of Fe₂DSXCl₂ (**13**) (---), Fe₂DSDCl₂ (**14**) (···), and Fe₂(salen)₂O (**15**) (—) in acetonitrile. The spectra is scaled to molar absorptivity.



equivalents) and the reactions were photolyzed for 20 hours; the wavelength was tailored using long-wavelength-pass filters. Unlike the porphyrin complexes, the diiron μ -oxo salens do not absorb strongly above 300 nm. In the Pacman salen complexes **13** and **14**, there is only a tail above 350 nm that extends into the visible, as shown in Figure 6.9. The disalen complex **15** exhibits a broad shoulder at about 380 nm. Photolysis using $\lambda_{\text{exc}} > 400$ nm gave no oxidation products. When λ_{exc} was shifted into the ultraviolet (295 nm and 324 nm), there were no sulfoxide or sulfone products obtained above the background level, as determined by control experiments in the absence of catalysts. (Trace oxidation of sulfides occurs upon aerobic photolysis with ultraviolet light). In the context of the previous studies with the Pacman porphyrin catalytic cycle we can make a few observations about the lack of reactivity from the diiron μ -oxo salens. Transient absorption spectroscopy of the Pacman porphyrins shows that photon absorption results in cleavage of the Fe—O bond to give the ferrous and ferryl oxo species. Oxidation of substrate competes with reclamping to reform the μ -oxo diiron bridge. The double-pillared structure of the Pacman salens would appear to facilitate the reclamping and prevent exposure of any photolytically generated ferryl oxo. However, the unbridged complex also does not display any oxidation chemistry. This leads us to believe that the lack of photocatalytic activity is likely due to the low absorptive qualities of the diiron μ -oxo complexes. The Pacman porphyrin complexes are excited in the LMCT ($\lambda = 360$ nm, $\epsilon \sim 10^5$). The salen compounds, however, lack any pronounced absorption peaks in $\lambda > 350$ with lower molar absorptivity. In an effort to elucidate the LMCT bands, the absorption spectra was taken in solvents of varying dielectric constants⁹¹ (specifically benzene, acetonitrile, and propylene carbonate), but no notable changes were observed.

6.4. Concluding Remarks

We have developed a synthetic methodology to synthesize cofacial salen ligands using dibenzofuran and xanthene pillars in the absence of a templating agent. As a result, we were able to isolate and characterize the unmetallated ligands, and easily synthesize several diiron compounds. We tested the μ -oxo diiron complexes for the same photocatalytic oxidation chemistry that is observed in the porphyrin analogues, but did not see any activity. This is likely due to the lack of prominent absorption features that are present in the porphyrin complexes.

6.5. Experimental Section

6.5.1. Materials

Silica gel 60 (70 - 230 and 230 - 400 mesh) was used for column chromatography. Analytical thin layer chromatography was performed using F254 silica gel (pre-coated sheets, 0.2 mm thick). Solvents for synthesis were reagent grade or better and used as received from Aldrich or dried according to standard methods.⁹² 4,5-Dibromo-2,7-di-*tert*-butyl-9,9-dimethylxanthene, boron tribromide, (1*R*,2*R*)-(-)-1,2-diaminocyclohexane, triethylamine, and (1*R*, 2*R*)-(-)-(1,2-cyclohexanediamino-*N,N'*-bis(3,5-di-*tert*-butylsalicylidene)] were also used as received from Aldrich. Bis(pinacolato)diboron and 3-formyl-4-methoxyphenylboronic acid were used as received from Frontier Scientific. Sodium carbonate, potassium acetate, anhydrous iron(III) chloride, iron(III) chloride hexahydrate, anhydrous iron(II) acetate, and dichloro[1,1'-bis(diphenylphosphino)ferrocene]palladium(II) dichloromethane adduct were used as received from Strem Chemicals. The following compound was obtained using published protocols and its purity confirmed by ¹H NMR: 4,6-dibromodibenzofuran (**5**). The synthesis for 2,7-di-*tert*-butyl-9,9-dimethyl-4-dihydroxyborane-5-(4,4,5,5-tetramethyl-[1,3,2]dioxaborolan-2-yl)-9*H*-xanthene (**1**) was presented in Chapter 3 (as compound **13**). The synthesis of 4,5-di(5-salicylaldehyde)-2,7-di-*tert*-butyl-9,9-dimethylxanthene (**3**) via (**1**) can be found in Appendix B2.

6.5.2. Physical Measurements

¹H NMR and ¹³C NMR spectra were collected in CDCl₃ (Cambridge Isotope Laboratories) at the MIT Department of Chemistry Instrumentation Facility (DCIF) using an Inova 500 Spectrometer at 25 °C. All chemical shifts are reported using the standard δ notation in parts-per-million relative to tetramethylsilane and spectra have been internally calibrated to the monoprotio impurity of the deuterated solvent used. High-resolution mass spectral analyses were carried out by the MIT Department of Chemistry Instrumentation Facility on a Bruker APEXIV47e.FT-ICR-MS using an Apollo ESI source. Infrared spectrum were taken on a Perkin-Elmer Model 2000 FTIR using KBr pellets prepared using a high pressure press. Mössbauer absorption data were recorded at

4.2 K on an MS1 spectrometer (WEB Research Co.) equipped with a ^{57}Co source and a Janus cryostat, and referenced to elemental iron. UV-visible absorption spectra were recorded on a Spectral Instruments 440 spectrophotometer. Molar absorptivity coefficients were determined on solutions of sub-mM concentrations of the respective compounds.

6.5.3. Synthesis

6.5.3.1. 4,5-Di-(3-formyl-4-methoxyphenyl)-2,7-di-*tert*-butyl-9,9-dimethylxanthene (2)

Under nitrogen, a mixture of 4,5-dibromo-2,7-di-*tert*-butyl-9,9-dimethylxanthene (2.00 g, 4.17 mmol), 3-formyl-4-methoxyphenylboronic acid (1.65 g, 9.17 mmol), sodium carbonate (1.33 g, 12.5 mmol), dichloro[1,1'-bis(diphenylphosphino)ferrocene]-palladium(II) dichloromethane adduct (0.367 g, 0.500 mmol), 1,2-dimethoxyethane (45 mL), and deionized water (15 mL) was heated to 90 °C for 48 hours. Upon cooling, the mixture was extracted with 4 × 100 mL of dichloromethane. The organic portions were combined and dried over MgSO_4 and the solvent removed by rotary evaporation. The crude solid was purified by column chromatography (silica gel, 2: 8 hexane: dichloromethane) to elute the colorless product (1.671 g, 69 % yield). ^1H NMR (500 MHz, CDCl_3 , δ): 10.35 (s, 2H), 7.73 (d, $J = 2.5$ Hz, 2H), 7.44 (d, $J = 2.5$ Hz, 2H), 7.39 (dd, $J = 8.5$ Hz, 2 Hz, 2H), 7.13 (d, $J = 2$ Hz, 2H), 6.61 (d, $J = 8.5$ Hz, 2H), 3.94 (s, 6H), 1.74 (s, 6H), 1.35 (s, 18H). ^{13}C NMR (500 MHz, CDCl_3 , δ): 189.53, 160.46, 145.71, 137.57, 131.12, 130.37, 129.97, 127.81, 125.54, 124.28, 122.07, 121.93, 111.95, 55.68, 35.26, 34.71, 32.03, 31.72. HRESI-MS ($[\text{M} + \text{Na}]^+$) $\text{NaC}_{39}\text{H}_{42}\text{O}_5$ m/z , Calcd. 613.2924 Found 613.2925.

6.5.3.2. 4,5-Di(5-salicylaldehyde)-2,7-di-*tert*-butyl-9,9-dimethylxanthene (3)

4,5-Di-(3-formyl-4-methoxyphenyl)-2,7-di-*tert*-butyl-9,9-dimethylxanthene (2) (1.01 g, 1.63 mmol) was added to 55 mL of dry dichloromethane and cooled to 0 °C. A solution of boron tribromide (7.0 mL, 1.0 M in dichloromethane) was added and upon stirring for 3 hours, 40 mL of water was added. The aqueous layer was separated and extracted with 3 × 50 mL of dichloromethane. The combined organic layers were washed with 25 mL of water, and dried over MgSO_4 . The solvent was evaporated and the residue was eluted

by column chromatography (silica gel, dichloromethane) and further purified by recrystallization in hot ethanol (0.748 g, 77% yield). ^1H NMR (500 MHz, CDCl_3 , δ): 10.86 (s, 2H), 9.38 (s, 2H), 7.50 (d, $J = 3$ Hz, 2H), 7.47 (t, $J = 3$ Hz, 2H), 7.40 (d, $J = 2.5$ Hz, 2H), 7.17 (d, $J = 2.5$ Hz, 2H) 6.84 (d, $J = 8.5$ Hz, 2H), 1.76 (s, 6H), 1.37 (s, 18). ^{13}C NMR (500 MHz, CDCl_3 , δ): 195.84, 160.47, 146.07, 145.27, 145.26. 138.01, 135.35, 130.01, 127.38, 125.60, 122.53, 122.40, 120.20, 117.35, 35.24, 34.81, 32.56, 31.76. HRESI-MS ($[\text{M} + \text{Na}]^+$) $\text{NaC}_{37}\text{H}_{38}\text{O}_5$ m/z , Calcd. 585.2617 Found 585.2605.

6.5.3.4. DSX (4)

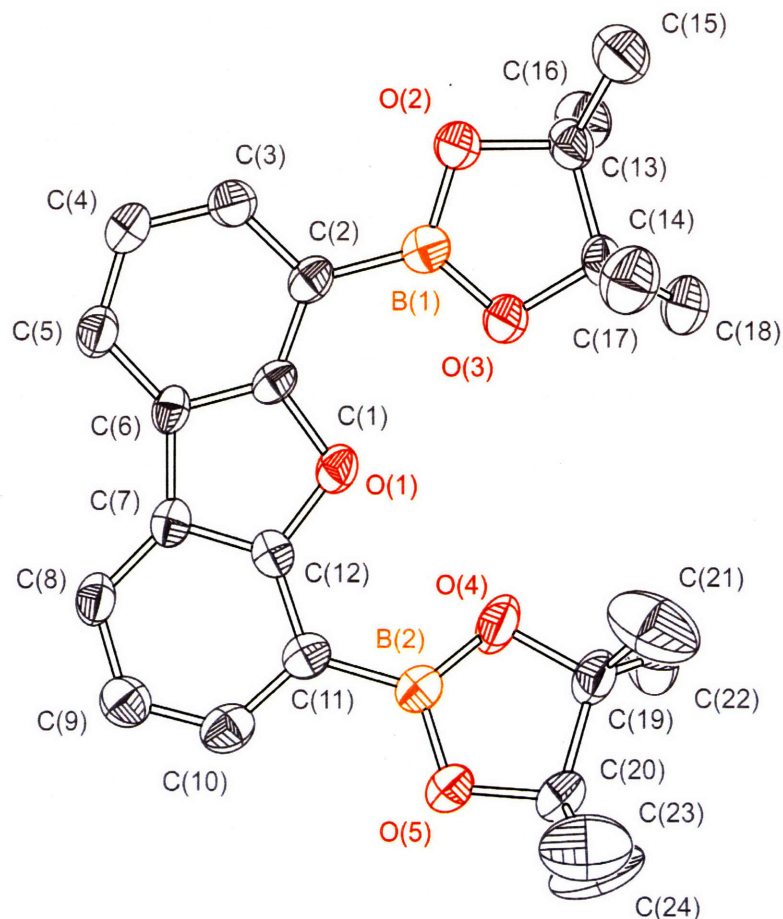
4,5-Di(5-salicylaldehyde)-2,7-di-*tert*-butyl-9,9-dimethylxanthene (3) (500 mg, 0.841 mmol) and (1*R*,2*R*)-(-)-1,2-diaminocyclohexane (96 mg, 0.841 mmol) was added to 8 mL of anhydrous ethanol and heated to reflux overnight. The solution was then cooled in a freezer and filtered. The bright yellow solid collected was washed with an additional 4 mL of cold ethanol to give the product (504 mg, 94% yield). X-Ray quality crystals were grown from slow evaporation of a pentane-dichloromethane solution. IR (KBr) ν_{max} : 1589 cm^{-1} (C=N). HRESI-MS ($[\text{M} + \text{H}]^+$) $\text{C}_{86}\text{H}_{96}\text{N}_4\text{O}_6$ m/z , Calcd. 1281.7403 Found 1281.7405. UV-vis (CH_2Cl_2) λ_{max} , nm (ϵ): 307 (31,924), 336 (14,984). Anal. Calcd for $\text{C}_{86}\text{H}_{96}\text{N}_4\text{O}_6$: C, 80.59; H, 7.55; N, 4.37. Found: C, 80.65; H, 7.38; N, 4.29.

6.5.3.5. 4,6-(4,4,5,5-Tetramethyl-[1,3,2]dioxaborolan-2-yl)-dibenzofuran (6)

Under nitrogen, a mixture of 4,6-dibromodibenzofuran (5) (2.00 g, 6.14 mmol), bis(pinacolato)diboron (4.67 g, 18.4 mmol), potassium acetate (4.22 g, 43.0 mmol), dichloro[1,1'-bis(diphenylphosphino)ferrocene]palladium(II) dichloromethane adduct (0.450 g., 0.613 mmol), dimethyl sulfoxide (30 mL), was heated to 90 °C for 48 hours. Upon cooling, the mixture was extracted with 4 \times 200 mL of dichloromethane. The organic portions were combined and washed with 5 \times 100 mL of water and dried over MgSO_4 and the solvent removed by rotary evaporation. 2 \times 500 mL of hexanes was stirred into the residue and filtered. The filtrate was reduced by rotary evaporation to give a crude solid, which was recrystallized by hot ethanol to give the colorless product (2.253 g, 87 % yield). Subsequent synthetic procedure to produce 8 from 6 is presented in Appendix B2. ^1H NMR (500 MHz, CDCl_3 , δ): 8.02 (d, $J = 7.5$ Hz, 2H), 7.85 (d, $J = 7.5$ Hz, 2H), 7.32 (t, $J = 7.5$ Hz, 2H), 1.46 (s, 12H). ^{13}C NMR (500 MHz, CDCl_3 , δ): 160.83,

134.00, 123.58, 123.39, 122.16, 122.16, 120.05, 83.94, 83.62, 25.25, 25.16, 25.09.
HRESI-MS ($[M + Na]^+$) $NaC_{24}H_{30}B_2O_5$ m/z , Calcd. 443.2195 Found 443.2192.

Figure 6.10. X-Ray crystal structure of 4,6-(4,4,5,5-Tetramethyl-[1,3,2]dioxaborolan-2-yl)-dibenzofuran (**6**).



6.5.3.6. 4,6-Di(3-formyl-4-methoxyphenyl)-dibenzofuran (**7**)

Under nitrogen, a mixture of 4,6-dibromodibenzofuran (**5**) (1.00 g, 3.07 mmol), 3-formyl-4-methoxyphenylboronic acid (1.22 g, 6.75 mmol), sodium carbonate (0.948 g, 9.20 mmol), tetrakis(triphenylphosphine)palladium (0.425 g, 0.368 mmol), dimethylformamide (27 mL), and deionized water (3 mL) was heated to 90 °C for 48 hours. Upon cooling, the mixture was extracted with 4 × 100 mL of dichloromethane. The organic portions were combined and dried over $MgSO_4$ and the solvent removed by rotary evaporation. The crude solid was purified by column chromatography (silica gel, dichloromethane) to elute the colorless product (1.02 g, 76% yield). 1H NMR (500 MHz,

CDCl₃, δ): 10.58 (s, 2H), 8.48 (d, *J* = 2.5 Hz, 2H), 8.28 (d, *J* = 7.5 Hz, 2H), 7.97 (dd, *J* = 2.5 Hz, 1 Hz, 2H), 7.68 (dd, *J* = 7.5 Hz, 1 Hz, 2H), 7.25 (m, 4H), 4.04 (s, 6H).

6.5.3.7. 4,6-Di(5-salicylaldehyde)dibenzofuran (8)

4,6-Di(3-formyl-4-methoxyphenyl)dibenzofuran (7) (1.02 g, 2.34 mmol) was added to 50 mL of dry dichloromethane and cooled to 0 °C. A solution of boron tribromide (10 mL, 1.0 M in dichloromethane) was added and upon stirring for 3 hours, 30 mL of water was added. The aqueous layer was separated and extracted with 3 × 50 mL of dichloromethane. The combined organic layers were washed with 25 mL of water, and dried over MgSO₄. The solvent was evaporated and the residue was eluted by column chromatography (silica gel, dichloromethane) and further purified by recrystallization in hot ethanol (0.773 g, 81% yield). ¹H NMR (500 MHz, CDCl₃, δ): 11.11 (s, 2H), 9.97 (s, 2H), 8.17 (m, 4H), 8.01 (dd, *J* = 7.5 Hz, 1 Hz, 2H), 7.66 (dd, *J* = 2.5 Hz, 1 Hz, 2H), 7.51 (d, *J* = 7.5 Hz, 1H), 7.15 (d, *J* = 7.5 Hz, 2H). ¹³C NMR (500 MHz, CDCl₃, δ): 196.73, 161.20, 153.14, 137.18, 135.35, 133.78, 131.73, 128.36, 126.31, 125.14, 123.93, 120.97, 120.21. HRESI-MS ([M + Na]⁺) NaC₂₆H₁₆O₅ *m/z*, Calcd. 431.0890 Found 431.0893.

6.5.3.8. DSD (9)

4,6-Di(5-salicylaldehyde)dibenzofuran (8) (0.400 g, 0.980 mmol) and (1*R*,2*R*)-(-)-1,2-diaminocyclohexane (0.112 g, 0.980 mmol) was added to 12 ml of anhydrous ethanol and heated to reflux overnight. The solution was then cooled in a freezer and filtered. The bright yellow solid collected was washed with an additional 8 mL of cold ethanol to give the product (0.416 g, 87% yield). ¹H NMR (500 MHz, CDCl₃, δ): 13.96 (s, 4H), 8.20 (s, 4H), 8.17 (d, *J* = 2.5 Hz, 4H), 7.92 (dd, *J* = 7.5 Hz, 1 Hz, 4H), 7.71 (dd, *J* = 8 Hz, 1H, 4H), 7.63 (dd, *J* = 8.5 Hz, 2 Hz, 4H), 7.56 (t, *J* = 8 Hz, 4H), 7.14 (d, *J* = 8.5 Hz, 4H), 3.24 (m, 4H), 2.35 (d, *J* = 10.5 Hz, 4H), 1.93 (m, 8H), 1.50 (m, 4H). ¹³C NMR (500 MHz, CDCl₃, δ): IR (KBr) *v*_{max} : 1586 cm⁻¹ (C=N). HRESI-MS ([M + H]⁺) C₆₄H₅₃N₄O₆ *m/z*, Calcd. 943.3960 Found 973.3957. UV-vis (CH₂Cl₂) *λ*_{max}, nm (ε): 297 (sh, 37,096), 318 (sh, 30,396), 327 (sh, 32,334). Anal. Calcd for C₆₄H₅₂N₄O₆: C, 78.99; H, 5.39; N, 5.76. Found: C, 78.76; H, 5.26; N, 5.68.

6.5.3.9. Fe₂(DSX)Cl₂ (10)

Under a nitrogen atmosphere, anhydrous ferric chloride (7.6 mg, 0.047 mmol) was added to 5 mL of anhydrous ethanol. The ligand DSX (**4**) (30.0 mg, 0.023 mmol) was added and the solution turned reddish-brown with precipitate. Upon stirring for 18 hours the now purple-red solution was filtered, and the precipitate was washed with an additional 10 mL of ethanol. The combined filtrates were reduced under vacuum and the resulting residue was recrystallized from hot acetone to give the dark purple product (27 mg, 82% yield). IR (KBr) ν_{\max} : 1540 cm^{-1} (C=N). ESI-MS ($[\text{M} - \text{Cl}]^-$) $\text{C}_{86}\text{H}_{92}\text{N}_4\text{O}_6\text{ClFe}_2$ m/z , Calcd. 1423.53 Found 1423.61. Anal. Calcd for $\text{C}_{86}\text{H}_{92}\text{Cl}_2\text{Fe}_2\text{N}_4\text{O}_6$: C, 70.73; H, 6.35; N, 3.84. Found: C, 70.63; H, 6.39; N, 3.88.

6.5.3.10. $\text{Fe}_2(\text{DSD})\text{Cl}_2$ (**11**)

Under a nitrogen atmosphere, anhydrous ferric chloride (55.6 mg, 0.206) was added to 10 mL of anhydrous methanol. The ligand DSD (**9**) was added and the solution was heated to reflux overnight. Upon cooling, the green solution was cooled in an ice bath and filtered. The precipitate was washed with 1 mL of cold methanol to give the dark purple product (45 mg, 75% yield). IR (KBr) ν_{\max} : 1538 cm^{-1} (C=N). HRESI-MS ($[\text{M} - \text{Cl}]^-$) $\text{C}_{64}\text{H}_{48}\text{N}_4\text{O}_6\text{ClFe}_2$ m/z , Calcd. 1115.1976 Found 1115.1973. Anal. Calcd for $\text{C}_{64}\text{H}_{48}\text{N}_4\text{O}_6\text{Cl}_2\text{Fe}_2$: C, 66.74; H, 4.20; N, 4.86. Found: C, 66.68; H, 4.28; N, 4.81.

6.5.3.11. $\text{Fe}[(1R, 2R)\text{-}(-)\text{-}(1,2\text{-cyclohexanediamino-}N,N'\text{-bis}(3,5\text{-di-}i\text{-tert-butylsalicylidene))]\text{Cl}$ (**12**)

This compound has previously been prepared using different reagents and conditions.^{58,93} Under a nitrogen atmosphere, anhydrous ferric chloride (14.8 mg, 0.091 mmol) was added to (1*R*, 2*R*)-(-)-(1,2-cyclohexanediamino-*N,N'*-bis(3,5-di-*tert*-butylsalicylidene)) (50.0 mg, 0.091 mmol) in 4 mL of anhydrous ethanol. Upon stirring at room temperature for 12 hours, the reaction was filtered and the precipitate was washed with cold ethanol and recrystallized from hot acetone to give (42 mg, 72 % yield). HRESI-MS ($[\text{M} - \text{Cl}]^-$) $\text{C}_{36}\text{H}_{52}\text{N}_2\text{O}_2\text{Fe}$ m/z , Calcd. 600.3378 Found 600.3379. Anal. Calcd for $\text{C}_{36}\text{H}_{52}\text{ClFeN}_2\text{O}_2$: C, 67.97; H, 8.24; N, 4.40. Found: C, 67.75; H, 8.05; N, 4.46.

6.5.3.12. $\mu\text{-oxo-(Fe}_2\text{DSX)}$ (**13**)

Ferric chloride hexahydrate (84.5 mg, 0.312 mmol) was slowly added to the ligand DSX (**4**) (200.0 mg, 0.156 mmol) in 8 mL of methanol. After 5 minutes, triethylamine (0.44

mL, 3.12 mmol) was added dropwise to the dark red solution and precipitate formed. The mixture was stirred for an additional 3 hours, then cooled in an ice bath and filtered. The precipitate was taken up in dichloromethane and filtered through a 0.45 μm polypropylene syringe filter. The filtrate was reduced by rotary evaporation to leave the reddish-brown product (173 mg, 80% yield). IR (KBr) ν_{max} : 1536 cm^{-1} (C=N), 834 cm^{-1} (Fe—O—Fe). ESI-MS ($[\text{M} + \text{H}]^+$) $\text{C}_{86}\text{H}_{93}\text{N}_4\text{O}_7\text{Fe}_2$ m/z , Calcd. 1405.57 Found 1405.61. Anal. Calcd for $\text{C}_{86}\text{H}_{92}\text{Fe}_2\text{N}_4\text{O}_7$: C, 73.50; H, 6.60; N, 3.99. Found: C, 73.42; H, 6.62; N, 4.06.

6.5.3.13. μ -oxo-(Fe₂DSD) (14)

Ferric trichloride hexahydrate (44.4 mg, 0.164 mmol) was added slowly to a solution of the ligand DSD (9) (80.0 mg, 0.082 mmol) in 2 mL of methanol, which turned dark olive green. After 10 minutes, triethylamine 0.23 mL, 1.64 mmol) was added dropwise and the solution was stirred for an additional 2 hours, then cooled in an ice bath. The red mixture was filtered using 0.22 μm polypropylene filter paper, and the precipitate was washed with 20 mL of methanol. The solid was then taken up in dichloromethane and filtered. The dark red filtrate was reduced by rotary evaporation to leave the reddish- orange product (53 mg, 59% yield). IR (KBr) ν_{max} : 1536 cm^{-1} (C=N), 830 cm^{-1} (Fe—O—Fe). Anal. Calcd for $\text{C}_{64}\text{H}_{48}\text{Fe}_2\text{N}_4\text{O}_7$: C, 70.09; H, 4.41; N, 5.11. Found: C, 69.84; H, 4.30; N, 4.96.

6.5.3.14. μ -oxo-[Fe(1R, 2R)-(-)-(1,2-cyclohexanediamino-*N,N'*-bis(3,5-di-*tert*-butyl salicylidene))]₂ (15)

Ferric trichloride hexahydrate (24.7 mg, 0.091 mmol) was added slowly to a solution of (1R, 2R)-(-)-[1,2-cyclohexanediamino-*N,N'*-bis(3,5-di-*tert*-butylsalicylidene)] (50.0 mg, 0.091 mmol) in 4 mL of methanol. After 5 minutes, triethylamine (0.13 mL, 0.914 mmol) was added dropwise to the purplish brown solution, which turned orange with precipitate. This was stirred for an additional 3 hours, then filtered washed with 2 mL of methanol. The precipitate was then taken up in dichloromethane and refiltered. The filtrate was reduced by rotary evaporation to leave the orange product (35 mg, 64% yield). X-Ray quality crystals were grown from a pentane-dichloromethane solution. IR (KBr) ν_{max} : 1533 cm^{-1} (C=N), 837 cm^{-1} . HRESI-MS ($[\text{M} + \text{H}]^+$) $\text{C}_{72}\text{H}_{105}\text{N}_4\text{O}_5\text{Fe}_2$ m/z , Calcd.

1217.6872 Found 1217.6902. Anal. Calcd for $C_{72}H_{104}Fe_2N_4O_5$: C, 71.04; H, 8.61; N, 4.60. Found: C, 71.15; H, 8.40; N, 4.55.

6.5.3.15. $Fe_2(DSX)$ (16)

Under a nitrogen atmosphere, ferrous acetate (27.2 mg, 0.156 mmol) was added to the ligand DSX (4) (50.0 mg, 0.078) in 6 mL of anhydrous tetrahydrofuran. The solution went from red to dark purple upon stirring for 24 hours. The solvent was removed under reduced pressure and the residue was washed with 2 mL of anhydrous ether to leave the dark purple product (100 mg, 92% yield). Anal. Calcd for $C_{86}H_{92}Fe_2N_4O_6$: C, 74.34; H, 6.67; N, 4.03. Found: C, 74.26; H, 6.74; N, 3.91.

6.5.3.16. $Fe_2(DSD)$ (17)

Under a nitrogen atmosphere, ferrous acetate (18.0 mg, 0.103 mmol) was added to the ligand DSD (9) (50.0 mg, 0.051 mmol) in 10 mL of anhydrous tetrahydrofuran. The solution turned red and was stirred for 24 hours. The solvent was removed under reduced pressure and the remaining residue was washed with 4 mL of anhydrous ether to leave the reddish-purple product (48 mg, 88% yield). Anal. Calcd for $C_{64}H_{48}Fe_2N_4O_6$: C, 71.12; H, 4.48; N, 5.18. Found: C, 70.94; H, 4.58; N, 5.08.

6.5.3.17. $Fe[(1R, 2R)-(-)-[1,2-cyclohexanediamino-*N,N'*-bis(3,5-di-*tert*-butylsalicylidene)]]$ (18)

Under a nitrogen atmosphere, ferrous acetate (31.8 mg, 0.183 mmol) was added to (1*R*, 2*R*)-(-)-[1,2-cyclohexanediamino-*N,N'*-bis(3,5-di-*tert*-butylsalicylidene)] (100.0 mg, 0.183 mmol) in 10 mL of anhydrous tetrahydrofuran and stirred at room temperature for 24 hours. The solvent was removed under reduced pressure and the remaining residue was washed with 2 mL of anhydrous ether to give the purple product (72.5 mg, 66% yield). Anal. Calcd for $C_{36}H_{52}FeN_2O_2$: C, 71.99; H, 8.73; N, 4.66. Found: C, 69.55; H, 8.46; N, 3.88.

6.5.4. Photolysis Studies

Representative Procedure. 100 mL of a 3.13 mM substrate (dibutyl sulfide or methyl sulfide) and 74.9 mM dodecane solution of acetonitrile or benzene was prepared. 4.0 mL

of this solution was added to separate matching cells containing 5.4 mg of Fe₂DSXO (**13**), 2.1 mg of Fe₂DSDO (**14**), 2.4 mg of Fe₂(salen)₂O (**15**), or no catalyst. Each of these reactions was then photolyzed for 20 hours and the solutions were then analyzed using GC/MS. Using light through a 400 nm long wavelength pass (LWP) filter, there were no oxidation products observed. Using light through a 295 nm and 324 nm LWP there were trace amounts of sulfoxide and sulfone produced, all in quantities similar to that observed for the control solution with no catalyst.

6.5.5. X-Ray Crystal Data Collection and Refinement Parameters

Data collection and reduction

Crystals were coated with Paratone N oil and mounted on a glass fiber. X-ray diffraction data were collected at -80 °C on a Siemens three-circle diffractometer equipped with a CCD detector, using the Mo K α radiation, selected by a graphite monochromator. The data were integrated to *hkl*-intensity and the final unit cell calculated using the SAINT v.4.050 program from Siemens. Solution and refinement were performed with the SHELXTL v.5.03 suite of programs developed by G. M. Sheldrick and Siemens Industrial Automation, 1995. No absorption correction was performed. The structure was solved by direct methods; the least-squares refinement converged normally (with hydrogen atoms placed at calculated positions using a standard riding model and refined isotropically).

Table 6.2 Crystal data and structure refinement for DSX (4).

| | |
|-----------------------------------|--|
| Identification code | c05035_ortho |
| Empirical formula | C ₉₆ H ₁₁₉ N ₄ O ₆ |
| Formula weight | 1424.95 |
| Temperature | 100(2) K |
| Wavelength | 0.71073 |
| Crystal system | Orthorhombic |
| Space group | P2(1)2(1)2(1) |
| Unit cell dimensions | a = 16.2351(5) Å b = 18.8877(6) Å c = 28.0461(8) Å |
| Volume | 8600.2(5) Å ³ |
| Z | 4 |
| Density (calculated) | 1.101 Mg/m ³ |
| Absorption coefficient | 0.068 mm ⁻¹ |
| F(000) | 3084 |
| Crystal size | 0.30 x 0.18 x 0.12 mm ³ |
| Theta range for data collection | 1.65 to 23.26°. |
| Index ranges | -16<=h<=18, -20<=k<=20, - 27<=l<=31 |
| Reflections collected | 41819 |
| Independent reflections | 12323 [R(int) = 0.0502] |
| Completeness to theta = 23.26° | 99.8 % |
| Absorption correction | None |
| Max. and min. transmission | 0.9919 and 0.9800 |
| Refinement method | Full-matrix least-squares on F ² |
| Data / restraints / parameters | 12323 / 2 / 1001 |
| Goodness-of-fit on F ² | 1.059 |
| Final R indices [I>2sigma(I)] | R1 = 0.0473, wR2 = 0.1160 |

Table 6.3 Crystal data and structure refinement for 4,6-(4,4,5,5-Tetramethyl-[1,3,2]dioxaborolan-2-yl)-dibenzofuran (**6**).

| | | |
|-----------------------------------|---|--------------------------------|
| Identification code | 002220m | |
| Empirical formula | C ₂₄ H ₃₀ B ₂ O ₅ | |
| Formula weight | 420.10 | |
| Temperature | 193(2) K | |
| Wavelength | 0.71073 Å | |
| Crystal system | Monoclinic | |
| Space group | P2(1)/c | |
| Unit cell dimensions | a = 23.2735(18) Å | $\beta = 100.3650(10)^\circ$. |
| | b = 8.2995(7) Å | |
| | c = 12.2614(10) Å | |
| Volume | 2329.7(3) Å ³ | |
| Z | 4 | |
| Density (calculated) | 1.198 Mg/m ³ | |
| Absorption coefficient | 0.081 mm ⁻¹ | |
| F(000) | 896 | |
| Crystal size | 0.48 × 0.31 × 0.07 mm ³ | |
| Theta range for data collection | 2.61 to 20.00°. | |
| Index ranges | -22 ≤ h ≤ 22, -7 ≤ k ≤ 7, -6 ≤ l ≤ 11 | |
| Reflections collected | 6450 | |
| Independent reflections | 2157 [R(int) = 0.0555] | |
| Completeness to theta = 20.00° | 99.6 % | |
| Absorption correction | None | |
| Refinement method | Full-matrix least-squares on F ² | |
| Data / restraints / parameters | 2157 / 0 / 289 | |
| Goodness-of-fit on F ² | 1.077 | |
| Final R indices [I > 2σ(I)] | R1 = 0.0551, wR2 = 0.1321 | |
| R indices (all data) | R1 = 0.0584, wR2 = 0.1345 | |

Table 6.4. Crystal data and structure refinement for structure shown in Figure 6.3.

| | |
|---------------------------------|---|
| Identification code | c04085m |
| Empirical formula | C ₃₂ H ₂₆ N ₂ O ₃ |
| Formula weight | 486.55 |
| Temperature | 150(2) K |
| Wavelength | 0.71073 |
| Crystal system | Orthorhombic |
| Space group | P2 ₁ 2 ₁ 2 ₁ |
| Unit cell dimensions | a = 11.269(3) Å b = 13.507(3) Å c = 16.031(4) Å |
| Volume | 2440.2(11) Å ³ |
| Z | 4 |
| Density (calculated) | 1.324 Mg/m ³ |
| Absorption coefficient | 0.085 mm ⁻¹ |
| F(000) | 1024 |
| Crystal size | 0.09 × 0.07 × 0.07 mm ³ |
| Theta range for data collection | 1.97 to 23.34°. |
| Index ranges | -12 ≤ h ≤ 12, -14 ≤ k ≤ 15, -17 ≤ l ≤ 13 |
| Reflections collected | 11313 |
| Independent reflections | 3528 [R(int) = 0.0624] |
| Completeness to theta = 23.34° | 99.8 % |
| Absorption correction | None |
| Refinement method | Full-matrix least-squares on F ² |
| Data / restraints / parameters | 3528 / 0 / 341 |
| Goodness-of-fit on F2 | 1.044 |
| Final R indices [I > 2σ(I)] | R1 = 0.0413, wR2 = 0.0922 |
| R indices (all data) | R1 = 0.0517, wR2 = 0.0982 |

Table 6.5. Crystal data and structure refinement for structure shown in Figure 6.4.

| | | |
|---------------------------------|--|------------------------------|
| Identification code | C04060 | |
| Empirical formula | $C_{36}H_{52}Fe_2N_4O_5$ | |
| Formula weight | 732.52 | |
| Temperature | 150(2) K | |
| Wavelength | 0.71073 Å | |
| Crystal system | Triclinic | |
| Space group | P-1 | |
| Unit cell dimensions | $a = 13.75(3)$ Å | $\alpha = 105.76(3)^\circ$. |
| | $b = 17.69(3)$ Å | $\beta = 102.39(3)^\circ$. |
| | $c = 17.73(4)$ Å | $\gamma = 107.99(4)^\circ$. |
| Volume | $3731(13)$ Å ³ | |
| Z | 4 | |
| Density (calculated) | 1.304 Mg/m ³ | |
| Absorption coefficient | 0.822 mm ⁻¹ | |
| F(000) | 1552 | |
| Crystal size | $0.16 \times 0.10 \times 0.10$ mm ³ | |
| Theta range for data collection | 1.26 to 20.00°. | |
| Index ranges | $-12 \leq h \leq 13$, $-15 \leq k \leq 17$, - $15 \leq l \leq 17$ | |
| Reflections collected | 7468 | |
| Independent reflections | 5781 [R(int) = 0.0389] | |
| Completeness to theta = 20.00° | 83.2 % | |
| Absorption correction | None | |
| Refinement method | Full-matrix least-squares on F ² | |
| Data / restraints / parameters | 5781 / 1321 / 1034 | |
| Goodness-of-fit on F2 | 2.956 | |
| Final R indices [I > 2sigma(I)] | R1 = 0.2492, wR2 = 0.5434 | |
| R indices (all data) | R1 = 0.2760, wR2 = 0.5732 | |

References

1. Collman, J. P.; Wagenknecht, P. S. Hutchinson, J. E. *Angew. Chem. Int. Ed. Engl.* **1994**, *33*, 1537-1554 and references therein.
2. Harriman, A.; Sauvage, J. P. *Chem. Soc. Rev.* **1996**, *25*, 41-49 and references therein.
3. Anderson, S.; Anderson, H. L.; Sanders, J. K. M. *Acc. Chem. Res.* **1993**, *26*, 469-475 and references therein.
4. Collman, J. P.; Fish, H. T. *Inorg. Chem.* **1996**, *35*, 7922-7923.
5. Guildard, R.; Brandes, S.; Tabard, A.; Bouhmaida, N.; LeComte, C.; Richard, P.; Latour, J. M. *J. Am. Chem. Soc.* **1994**, *116*, 10202-10211.
6. Guildard, R.; Brandes, S.; Tardieuz, C.; Tabard, A.; L'Her, M.; Miry, C.; Gouerac, P.; Knop, Y.; Collman, J. P. *J. Am. Chem. Soc.* **1995**, *117*, 11721-11729.
7. Ichihara, K.; Naruta, Y. *Chem. Lett.* **1998**, 185-186.
8. Naruta, Y.; Sasayama, M.; *Chem. Commun.* **1994**, 2667-2668.
9. Naruta, Y.; Sasayama, M. *Chem. Lett.* **1994**, 2411-2414.
10. Naruta, Y.; Sawada, N.; Tadokoro, M. *Chem. Lett.* **1994**, 1713-1716.
11. Naruta, Y.; Sasayama, M.; Sasaki, T. *Angew. Chem. Int. Ed. Engl.* **1994**, *33*, 1839-1841.
12. Naruta, Y.; Sasayama, M.; Ichihara, K. *J. Mol. Cat. A* **1997**, *117*, 115-121.
13. Deng, Y.; Chang, C. J.; Nocera, D. G. *J. Am. Chem. Soc.* **2000**, *122*, 410-411.
14. Chang, C. J.; Deng, Y.; Shi, C.; Chang, C. K.; Anson, F. C.; Nocera, D. G. *Chem. Commun.* **2000**, 1355-1356.
15. Chang, C. J.; Deng, Y.; Heyduk, A. F.; Chang, C. K.; Nocera, D. G. *Inorg. Chem.* **2000**, *39*, 959-966.
16. Loh, Z.-H.; Miller, S. E.; Chang, C. J.; Carpenter, S. D.; Nocera, D. G. *J. Phys. Chem. A* **2002**, *106*, 11700-11708.
17. Chang, C. J.; Deng, Y.; Peng, S.-M.; Lee, G.-H.; Yeh, C.-Y.; Nocera, D. G. *Inorg. Chem.* **2002**, *41*, 3008-3016.
18. Chang, C. J.; Yeh, C.-Y.; Nocera, D. G. *J. Org. Chem.* **2002**, *67*, 1403-1406.
19. Chang, C. J.; Loh, Z.-H.; Shi, C.; Anson, F. C.; Nocera, D. G. *J. Am. Chem. Soc.* **2004**, *126*, 10013-10020.
20. Chng, L. L.; Chang, C. J.; Nocera, D. G. *J. Org. Chem.* **2003**, *68*, 4075-4078.
21. Chang, C. J.; Loh, Z.-H.; Deng, Y.; Nocera, D. G. *Inorg. Chem.* **2003**, *42*, 8262-8269.
22. Pistorio, B. J.; Chang, C. J.; Nocera, D. G. *J. Am. Chem. Soc.* **2002**, *124*, 7884-7885.

23. Chang, C. J.; Baker, E. A.; Pistorio, B. J.; Deng, Y.; Loh, Z.-H.; Miller, S. E.; Carpenter, S. D.; Nocera, D. G. *Inorg. Chem.* **2003**, *41*, 3102-3109.
24. Hodgkiss, J. M.; Chang, C. J.; Pistorio, B. J.; Nocera, D. G. *Inorg. Chem.* **2003**, *42*, 8270-8277.
25. Rosenthal, J.; Pistorio, B. J.; Chng, L. L.; Nocera, D. G. *J. Org. Chem.* **2005**, *70*, 1885-1888.
26. Rosenthal, J.; Lockett, T. D.; Hodgkiss, J. M.; Nocera, D. G. *J. Am. Chem. Soc.* **2006**, *128*, 6546-6547.
27. Gavriolva, A. L.; Bosnich, B. *Chem. Rev.* **2004**, *104*, 349-383 and references therein.
28. Fenton, D.E. *Chem. Soc. Rev.* **1999**, *28*, 159-168 and references therein.
29. Sabater, L.; Guillot, R.; Aukauloo, A. *Tetrahedron Lett.* **2005**, *46*, 2923-2926.
30. Maverick, A. W.; Klavetter, F. E. *Inorg. Chem.* **1984**, *23*, 4129-4130.
31. He, C.; Lippard, S. J. *Tetrahedron*, **2000**, *56*, 8245-8252.
32. He, C.; Lippard, S. J. *Inorg. Chem.* **2001**, *40*, 1414-1420.
33. He, C.; Barrios, A. M.; Lee, D.; Kuzelka, J.; Davydov, R. M.; Lippard, S. J. *J. Am. Chem. Soc.* **2000**, *122*, 12683-12690.
34. Coughlin, P. K.; Martin, A. E.; Dewan, J. C.; Watanabe, E.-I.; Bulkowski, J. E.; Lehn, J.-M.; Lippard, S. J. *Inorg. Chem.* **1984**, *23*, 1004-1009.
35. Nelson, S. M.; Escho, F.; Lavery, A.; Drew, M. G. B. *J. Am. Chem. Soc.* **1983**, *105*, 5693-5695.
36. Tei, L.; Blake, A. J.; Devillanova, F. A.; Garau, A.; Lippolis, V.; Wilson, C.; Schröder, M. *Chem. Commun.* **2001**, 2582-2583.
37. Herron, N.; Schammel, W. P.; Jackels, S. C.; Grzybowski, J. J.; Zimmer, L. L.; Busch, D. H. *Inorg. Chem.* **1983**, *22*, 1433-1440.
38. Beletskaya, R. P.; Averin, A. D.; Bessmertnykh, A. G.; Denat, F.; Guillard, R. *Tetrahedron Lett.* **2002**, *43*, 1193-1196.
39. Malinak, S. M.; Coucouvanis, D. *Inorg. Chem.* **1996**, *35*, 4810-4811.
40. Busch, D. H.; Christoph, G. G.; Zimmer, L. L.; Jackels, S. C.; Grzybowski, J. J.; Callahan, R. W.; Kojima, M.; Holter, K. A.; Mocak, J.; Herron, N.; Chavan, M.; Schammel, W. P. *J. Am. Chem. Soc.* **1981**, *103*, 5107-5114.
41. Mtekaitis, R. J.; Martell, A. E.; Dietrich, B.; Lehn, J.-M. *Inorg. Chem.* **1984**, *23*, 1588-1591.
42. Bradbury, J. R.; Hampton, J. L.; Martone, D. P.; Maverick, A. W. *Inorg. Chem.* **1989**, *28*, 2392-2399.
43. Maverick, A. W.; Buckingham, S. C.; Bradbury, J. R.; Yao, Q.; Stanley, G. G. *J. Am. Chem. Soc.* **1986**, *108*, 7430-7431.

44. del Rosario Benites, M.; Fronczek, F. R.; Hammer, R. P.; Maverick, A. W. *Inorg. Chem.* **1997**, *36*, 5826-5831.
45. Kaiwara, T.; Yamaguchi, T.; Kido, H.; Kawabata, S.; Kuroda, R.; Ito, T. *Inorg. Chem.* **1993**, *32*, 4990-4991.
46. van Veggel, F. C. J. M.; Bos, M.; Harkema, S.; van de Bovenkamp, H.; Verboom, W.; Reedijk, J.; Reinhoudt, D. N. *J. Org. Chem.* **1991**, *56*, 225-235.
47. Watkinson, M.; Whiting, A.; McAuliffe, C. A. *Chem. Commun.* **1994**, 2141-2142.
48. Hirotsu, M.; Ohno, N.; Nakajima, T.; Ueno, K. *Chemistry Letters* **2005**, *34*, 848-849.
49. Gianneschi, N. C.; Bertin, P. A.; Nguyen, S. T.; Mirkin, C. A.; Zakharov, L. N.; Rheingold, A. L. *J. Am. Chem. Soc.* **2003**, *125*, 10508-10509.
50. Li, Z.; Jablonski, C. *Chem. Commun.* **1999**, 1531-1532.
51. Li, Z.; Jablonski, C. *Inorg. Chem.* **2000**, *39*, 2456-2461.
52. Shimakoshi, H.; Takemoto, H.; Aritome, I.; Hisaeda, Y. *Tetrahedron Lett.* **2002**, *43*, 2809-2812.
53. Peterson, M. W.; Rivers, D. S.; Richman, R. M. *J. Am. Chem. Soc.* **1985**, *107*, 2907-2915.
54. Weber, L.; Hommel, R.; Behling, J.; Haufe, G.; Henning, H. *J. Am. Chem. Soc.* **1994**, *116*, 2400-2408.
55. Hennig, H.; Lupp, D. *J. Prakt. Chem.* **1999**, *341*, 757-767.
56. Shyu, H.-L.; Wei, H.-H.; Lee, G.-H.; Wang, Y. *J. Chem. Soc., Dalton Trans.* **2000**, 915-918.
57. Sivasubramanian, V. K.; Ganesan, M.; Rajagopal, S.; Ramaraj, R. *J. Org. Chem.* **2002**, *67*, 1506-1514.
58. Bryliakov, K. P.; Talsi, E. P. *Angew. Chem. Int. Ed.* **2004**, *43*, 5228-5230.
59. Kurashashi, T.; Kobayashi, Y.; Nagatomo, S.; Tosha, T.; Kitagawa, T.; Fujii, H. *Inorg. Chem.* **2005**, *44*, 8156-9166.
60. Venkataramanan, N. S.; Kuppuraj, G.; Rajagopal, S. *Coord. Chem. Rev.* **2005**, *249*, 1249-1268.
61. Niswander, R. H.; Martell, A. E. *Inorg. Chem.* **1978**, *17*, 2341-2344.
62. Calderazzo, F.; Floriani, C.; Henzi, R.; L'Eplattenier, F. *J. Chem. Soc. A* **1969**, 1378-1386.
63. Earnshaw, A.; King, E. A.; Larkworthy, L. F. *J. Chem. Soc. A* **1968**, 1048-1052.
64. Corazza, F.; Floriani, F. *J. Chem. Soc., Dalton Trans.* **1987**, 709-714.
65. Floriani, C.; Calderazzo, F. *J. Chem. Soc. A* **1971**, 3665-3669.

66. Fochi, G.; Floriani, C. *J. Chem. Soc., Dalton Trans.* **1984**, 2577-2580.
67. Earnshaw, A.; King, E. A.; Larkworthy, L. F. *J. Chem. Soc. A* **1969**, 2459-2463.
68. Coggon, P.; McPhail, A. T.; Mabbs, F. E.; McLachlan, V. N. *J. Chem. Soc. A* **1971**, 1014-1019.
69. Lewis, J.; Mabbs, F. E.; Richards, A. *J. Chem. Soc. A* **1967**, 1014-1018.
70. Wollman, R. G.; Hendrickson, D. N. *Inorg. Chem.* **1977**, *16*, 723-733.
71. Oyaizu, K.; Dewi, E. L.; Tsuchida, E. *Inorg. Chim. Acta* **2001**, *321*, 205-208.
72. Murray, K. S. *Coord. Chem. Rev.* **1974**, *12*, 1-35.
73. Koehler, K.; Sandstrom, W.; Cordes, E. H. *J. Am. Chem. Soc.* **1964**, *86*, 2413-2419.
74. Toth, G.; Pinter, I.; Messmer, A. *Tetrahedron Lett.* **1974**, 735-738.
75. Layer, R. W. *Chem. Rev.* **1963**, *63*, 489-510.
76. Rowan, S. J.; Cantrill, S. J.; Cousins, G. R. L.; Sanders, J. K. M.; Stoddart, J. F. *Angew. Chemie. Int. Ed.* **2002**, *41*, 898-952.
77. Akin, S.; Taniguchi, T.; Dong, W.; Masubuchi, S.; Naebeshima, T. *J. Org. Chem.* **2005**, *70*, 1704-1711.
78. Gerlock, M.; Lewis, J.; Mabbs, Fe. E.; Richards, A. *J. Chem. Soc. A* **1968**, 112-116.
79. Gullotti, M.; Casella, L.; Pasini, A.; Ugo, R. *J. Chem. Soc. A* **1977**, 339-345.
80. Kennedy, B. J.; McGrath, A. C.; Murray, K. S.; Skelton, B. W.; White, A. H. *Inorg. Chem.* **1987**, *26*, 483-495.
81. Leung, W.-H.; Chan, E. Y. Y.; Chow, E. K. F.; Williams, I. D.; Peng, S.-M. *J. Chem. Soc., Dalton Trans.* **1996**, 1229-1236.
82. Edulji, S. K.; Nguyen, S. T. *Organometallics* **2001**, *20*, 5171-5176.
83. Davies, J. E.; Gatehouse, B. M. *Acta Crstallograpr., Sect. B: Struct. Crystallogr. Cryst. Chem.* **1973**, *B29*, 1934.
84. Kessel, S. L.; Hendrickson, D. N. *Inorg. Chem.* **1978**, *17*, 2630-2636.
85. Gütlich, P. Chapter 2: Mössbauer Spectroscopy in Chemistry. In *Topics in Applied Physics, Vol 5*; Gonser, U.; Springer-Verlag: New York, 1974; page 53-96.
86. Gibb, T. C. *Principles of Mössbauer Spectrscopy*; Chapman & Hall Ltd.: London, 1971.
87. Reiff, W. M.; Baker, Jr., W. A.; Erickson, N. E. *J. Am. Chem. Soc.* **1968**, *90*, 4794-4800.
88. Okamura, M. Y.; Klotz, I. M.; Johnson, C. E; Winter, M. R. C.; Williams, R. J. P. *Biochemistry*, **1969**, *8*, 1951-1958
89. Berrett, R. R.; Fitzsimmons, B. R.; Owusu, A. A. *J. Chem. Soc. A* **1968**, 1575-1579.

90. Bancroft, G. M.; Maddock, A. G.; Randl, R. P. *J. Chem. Soc. A* **1968**, 2939-2944.
91. Chen, P.; Meyer, T. J. *Chem. Rev.* **1998**, *98*, 1439-1477.
92. Armarego, W. L. F.; Perrin, D. D. *Purification of Laboratory Chemicals*; 4th ed.; Butterworth-Heinmann: Oxford, 1966.
93. Fürstner, A.; Leitner, A.; Méndez, M.; Krause, H. *J. Am. Chem. Soc.* **2002**, *124*, 13856-13863.

Chapter 7

Synthesis of Bimetallic Cofacial Pacman

Salens

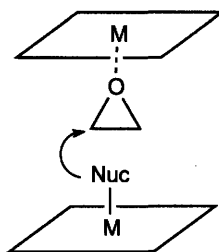
7.1. Motivation and Specific Aims

The untemplated synthesis of cofacial Pacman ligands using the rigid pillars xanthene (DSX) and dibenzofuran (DSD) was presented in Chapter 6. In many cases, metalation can proceed under conditions similar to those established for monomeric salens, allowing easy synthetic access to a diverse metallosalen library of complexes. This metalation chemistry is explored here to generate bimetallic complexes of copper, chromium, manganese, cobalt, and zinc. Initial studies into catalytic Lewis-acid assisted epoxide ring-opening chemistry is also explored.

7.2. Background

An avenue of reactivity we sought to explore with our Pacman salens was the ring-opening of epoxides. The intrinsic ring-strain of epoxides can be coupled with coordination of the oxygen to a Lewis acid to induce ring opening. This reaction has been catalyzed with a variety of chiral metallosalens with a host of nucleophiles.¹⁻²⁵ The ring opening reactions are significant because of their high selectivity; this reaction produces two adjacent stereocenters from an achiral precursor. Additionally, several of the catalysts (notably the chromium-azide nucleophile and cobalt/water nucleophile systems) are able to efficiently kinetically resolve racemic mixtures of epoxides, an important strategy in asymmetric synthesis.²⁶

Scheme 7.1



The mechanism of epoxide ring-opening reaction is believed to involve two metals; one metal is utilized for epoxide coordination while the second metal poisons the nucleophile for attack at the α -carbon, as shown in Scheme 7.1.²³⁻²⁵ Non-rigid oligomeric multinuclear salens exhibit marked improvements in reaction rates as compared to their

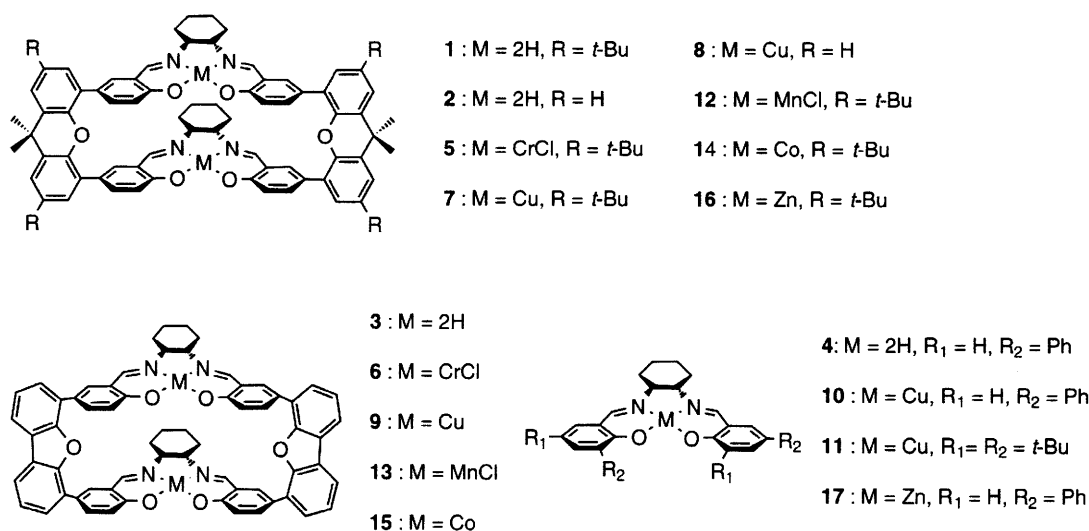
monomeric counterparts for the asymmetric ring opening (e.g., chromium/azide system),¹¹ as well as the hydrolytic kinetic resolution of epoxides (e.g., dicobalt).²⁷⁻³¹ We set out to explore whether analogous reactivity enhancements would be achieved with the more rigid cofacial Pacman architectures.

7.3. Results and Discussion

7.3.1. Ligand Characteristics and Synthesis

Metallo complexes of the DSX ligand **1** were prone to oil in crystallization attempts. We therefore synthesized the DSX ligand lacking the *tert*-butyl functionalities on the xanthene pillar to produce the slightly less soluble **2** (shown in Chart 7.1). This ligand was prepared in similar fashion to **1**, as discussed in Chapter 6. Other complexes of note in this Chapter are also listed in Chart 7.1.

Chart 7.1



7.3.2. Synthesis of Chromium Pacman Salen Complexes

Dichromium Pacman complexes Cr₂DSXC1₂ (**5**) and Cr₂DSDCl₂ (**6**) were synthesized by procedures adapted from the literature.⁹ The divalent metal ions were inserted by stirring two equivalents of anhydrous chromium(II) chloride in dry tetrahydrofuran under an inert atmosphere. Upon exposure to air, the metal was oxidized to chromium(III); addition of ammonium chloride forms the chloride salt. The yield was quantitative for DSX but only 11% for DSD, possibly due to its lower solubility in tetrahydrofuran. The compounds

were characterized by mass spectrometry and their purity was established by elemental analysis. Small hexagonal crystals of $\text{Cr}_2\text{DSXCl}_2$ could be grown from the evaporation of concentrated tetrahydrofuran solutions, but none diffracted well enough for X-ray crystallographic analysis. In an effort to improve the diffraction intensity, an attempt was made to synthesize the bromide salt of $[\text{Cr}_2\text{DSX}]^{2+}$, but the Pacman complex could not be obtained cleanly.

7.3.3. Epoxide Ring Opening Reactivity with Chromium Pacman Complexes

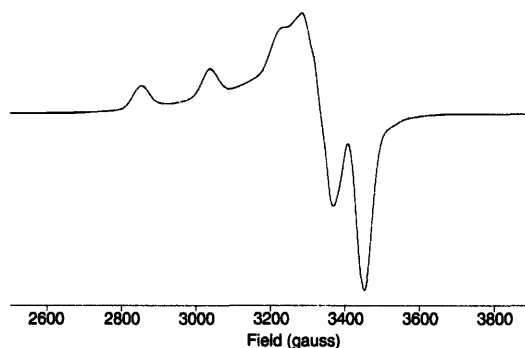
The chromium Pacman complexes were explored for their activity towards the catalytic ring-opening of cyclohexene oxide. The conditions used were similar to those described as successful for $\text{Cr}(\text{salen})\text{Cl}$ and meso-epoxide substrates.⁹ $\text{Cr}_2\text{DSDCl}_2$ (**6**) was not sufficiently soluble in diethyl ether, so the study was only performed with $\text{Cr}_2\text{DSXCl}_2$ (**5**) and $\text{Cr}(\text{salen})\text{Cl}$ was employed as the control. Trimethylsilyl azide was used to deliver the nucleophile in diethyl ether. The reaction was monitored using GC/MS (with dodecane as the internal standard). The amount of substrate consumed per equivalent of catalyst was found to be the same for both compounds.

7.3.4. Synthesis of Cu Pacman Salen Complexes

The copper(II) Pacman salen complexes were synthesized using a procedure similar to that described for the monomeric salens.³² The disalen ligands DSX (**1**), DSX[^] (**2**) and DSD (**3**) were refluxed with two equivalents of copper(II) acetate hydrate in ethanol for 1 - 2 hours. (Another method used to metallate salen monomers using aqueous sodium hydroxide to deprotonate the salens followed by addition of copper(II) nitrate trihydrate did not give any product). The yields ranged from 36 - 93% for the various Pacman ligands. The copper salen monomers **10** and **11** were also synthesized using sodium hydroxide and the copper nitrate salt as described above.

The **7** - **11** compounds were characterized by mass spectrometry and elemental analysis was used to determine the purity. We had hoped it would be easier to grow crystals of the xanthene Pacman lacking the di-*tert*-butyl groups on the pillar, $\text{Cu}_2\text{DSX}^{\wedge}$ (**8**), since this

Figure 7.1 EPR spectra of compound **11** taken a chloroform-ethanol frozen solution at 4.5 K.



was the case for the analogous porphyrin Pacman complexes. But we found that this was not the case. With Cu_2DSX (**7**), small needle-like crystals could be grown, but none were large or high quality enough for X-ray structural determination. The EPR spectrum of the copper complex **11** was taken in a frozen chloroform-ethanol solution (Figure 7.1). The g -values of, $g_{\parallel} = 2.283$ and $g_{\perp} = 2.094$ are within a range that is observed for monomeric copper salens.³³⁻³⁸ Frozen solutions of **7** - **11** were also recorded, but the spectra was poorly resolved and the g values were not obtained.

7.3.5. Synthesis of Manganese, Cobalt, and Zinc Pacman Salen Complexes

Manganese Pacman salens **12** and **13** were synthesized under conditions similar to that used to prepare manganese salen monomeric compounds. The ligands were refluxed in ethanol with manganese(II) acetate tetrahydrate in air and worked up with aqueous sodium chloride to give the chloride compounds. The compounds were analyzed by mass spectrometry.

The air-sensitive dicobalt(II) Pacman salens **14** and **15** were synthesized by adding a solution of the ligand in dichloromethane to a solution of cobalt(II) acetate tetrahydrate in methanol under an inert atmosphere. The product was isolated by collecting the bright red (**14**) or orange (**15**) product that precipitates. $\text{Co}_2(\text{DSX})$ (**14**) was identified as the positive ion in the high resolution mass spectra, suggesting some of the sample may have been singly oxidized to Co(III) during data collection. This does not appear to be an issue with the obtained product; $\text{Co}_2(\text{DSX})$ (**14**) was analytically pure by elemental analysis. The

Co₂DSD (**15**) product was also identified in the high resolution mass spectra and analyzed for purity.

Preparation of the zinc Pacman salens was pursued on several fronts. Metal ion incorporation was attempted by refluxing the ligand with: (i) refluxing zinc(II) chloride and triethylamine; (ii) diethylzinc in tetrahydrofuran; and (iii) refluxing with zinc acetate in ethanol. For the DSX (**1**) and (*R,R*)-*N,N'*-bis(5-phenylsalicylidene)-1,2-cyclohexanediamine (**4**) ligand, the latter reaction showed the desired compound in the mass spectra. But the isolated product was not analytically pure, and a suitable solvent for recrystallization could not be found. The zinc complexes of the DSD (**3**) ligand escaped preparation.

7.4. Concluding Remarks and Future Work

We were able to establish the generality of the Pacman salen ligands by synthesis of a variety of metallocomplexes. For most of the Pacman complexes, particularly DSX, synthetic procedures for the introduction of the metal into the macrocycle follows from those typically used for metallosalen monomers. From these established methods we were able to cleanly prepare the copper, manganese, and cobalt (DSX only) Pacman salens. A preliminary study was done on the catalytic ring-opening of cyclohexene oxide by the Cr₂DSXCl₂, although no enhancement of activity was observed. Zinc Pacman salens, and could not be prepared in a straightforward manner and we were unable to isolate pure products.

7.5. Experimental Section

7.5.1. Materials

Solvents for synthesis were reagent grade or better and used as received from Aldrich or dried according to standard methods.³⁹ (*1R,2R*)-(-)-1,2-diaminocyclohexane, and manganese acetate tetrahydrate, and cyclohexene oxide were also used as received from Aldrich. Copper(II) acetate monohydrate, anhydrous chromium(II) chloride, cobalt(II) acetate tetrahydrate, and zinc(II) acetate dihydrate were used as received from Strem Chemicals. Tetramethylsilyl azide was used as received from Alfa Aesar. The following

compound was obtained using published protocols and its purity confirmed by ^1H NMR: 4,5-di(5-salicylaldehyde)-9,9-dimethylxanthene (**5**).⁴⁰ The following compounds were obtained as described previously: DiSalen Xanthene (DSX), compound **4** in Chapter 6; DiSalen Dibenzofuran (DSD), compound, compound **9** in Chapter 6; (*R,R*)-*N,N'*-bis(5-phenylsalicylidene)-1,2-cyclohexanediamine, compound **12** in Chapter 4.

7.5.2. Physical Measurements

^1H NMR spectra were collected in CDCl_3 (Cambridge Isotope Laboratories) at the MIT Department of Chemistry Instrumentation Facility (DCIF) using an Inova 500 Spectrometer at 25 °C. All chemical shifts are reported using the standard δ notation in parts-per-million relative to tetramethylsilane and spectra have been internally calibrated to the monoprotio impurity of the deuterated solvent used. High-resolution mass spectral analyses were carried out by the MIT Department of Chemistry Instrumentation Facility on a Bruker APEXIV47e.FT-ICR-MS using an Apollo ESI source. Infrared spectrum were taken on a Perkin-Elmer Model 2000 FTIR using KBr pellets prepared using a high pressure press. UV-visible absorption spectra were recorded on a Spectral Instruments 440 spectrophotometer. X-band EPR measurements were carried out on frozen chloroform-ethanol solutions on a Bruker EMX spectrometer; the cavity was maintained at 4.5 K by an Oxford liquid helium cryostat. The spectrum was not fitted and the g values presented in the text correspond to zeros of the first or second derivative of the signal with respect to the field.

7.5.3. Synthesis

7.5.3.1. DSX[^] (**2**)

4,5-Di(5-salicylaldehyde)-9,9-dimethylxanthene (**5**) (250 mg, 0.56 mmol) and (1*R*,2*R*)-(-)-1,2-diaminocyclohexane (63 mg, 0.56 mmol) were added to 9 mL of anhydrous ethanol and heated to reflux overnight. The solution was then cooled in a freezer and filtered. The bright yellow solid collected was washed with an additional 2 mL of cold ethanol to give the product (266 mg, 88% yield). HRESI-MS ($[\text{M} + \text{H}]^+$) $\text{C}_{70}\text{H}_{65}\text{N}_4\text{O}_6$ m/z , Calcd. 1057.4899 Found 1057.4903.

7.5.3.2. Cr(DSX)Cl₂ (**5**)

In an inert atmosphere, the ligand DSX (**8**) (250.0 mg, 0.195 mmol) was dissolved in 6 mL of dry tetrahydrofuran. Anhydrous chromium(II) chloride (72.0 mg, 0.586 mmol) was added and the solution rapidly turned greenish-brown. Upon stirring overnight, the reaction was exposed to air and 6 mL of aqueous saturated ammonium chloride was added. After stirring in air for 6 hours, the organic layer was washed with 6 mL of additional aqueous saturated ammonium chloride, followed by 2 × 6 mL of aqueous saturated sodium chloride. The organic layer was dried with MgSO₄ and the solvent reduced by rotary evaporation to leave the brown product in quantitative yield (293 mg). HRESI-MS ([M – Cl]⁺) C₈₆H₉₂Cr₂N₄O₆ *m/z*, Calcd. 1411.5621 Found 1411.5668. Anal. Calcd for C₈₆H₉₂Cl₂Cr₂N₄O₆: C, 71.11; H, 6.38; N, 3.86. Found: C, 71.18; H, 6.44; N, 3.78.

7.5.3.3. Cr(DSD)Cl₂ (**6**)

In an inert atmosphere, the ligand DSD (**13**) (100.0 mg, 0.103 mmol) was dissolved in 4 mL of dry tetrahydrofuran. Anhydrous chromium(II) chloride (38.0 mg, 0.308 mmol) was added. Upon stirring overnight, the olive green solution was exposed to air and 2 mL of aqueous saturated ammonium chloride was added. After stirring in air for 6 hours, the organic layer was washed with 2 mL of additional aqueous saturated ammonium chloride, followed by 2 × 2 mL of aqueous saturated sodium chloride. The organic layer was dried with MgSO₄ and the solvent reduced by rotary evaporation to leave the green product (14 mg, 11% yield). Anal. Calcd for C₆₄H₄₈Cl₂Cr₂N₄O₆: C, 67.19; H, 4.23; N, 4.90. Found: C, 67.38; H, 4.25; N, 4.78.

7.5.3.4. Cu₂(DSX) (**7**)

The disalen xanthene (DSX) ligand (**8**) (145 mg, 0.113 mmol) was added to copper(II) acetate monohydrate (45.2 mg, 0.226 mmol) and 10 mL of ethanol was added. The mixture was heated to reflux for 1 hour, during which the solution turned rose red with precipitate. The reaction was then cooled to 0 °C, filtered, and the solid washed with cold ethanol and deionized water. The precipitate was taken up in dichloromethane and filtered through a 0.45 μm polypropylene syringe filter. The solvent was removed from the filtrate using rotary evaporation to give the dark purple product (139 mg, 87% yield). HRESI-MS ([M + H]⁺) C₈₆H₉₃Cu₂N₄O₆ *m/z*, Calcd. 1403.5682 Found 1403.5598. UV-vis

(CH₂Cl₂) λ_{\max} , nm (ϵ): 310 (96,170), 379 (26,210), 553 (2178). Anal. Calcd for C₈₆H₉₂Cu₂N₄O₆: C, 73.48; H, 6.67; N, 3.99. Found: C, 73.41; H, 6.68; N, 3.87.

7.5.3.5. Cu₂(DSX[^]) (8)

The ligand **7** (50.0 mg, 0.047 mmol) was added to copper(II) acetate monohydrate (19.0 mg, 0.095 mmol) and 4 mL of ethanol was added. The mixture was heated to reflux for 1 hour and then cooled to 0 °C and filtered. The precipitate was taken up in dichloromethane and filtered. The solvent was removed from the filtrate under reduced pressure to reveal the light reddish-purple product (20 mg, 36% yield). HRESI-MS ([M + H]⁺) C₇₀H₆₁Cu₂N₄O₆ *m/z*, Calcd. 1179.3178 Found 1179.3153.

7.5.3.6. Cu₂(DSD) (9)

The disalen dibenzofuran (DSD) ligand (**13**) (50.0 mg, 0.051 mmol) was added to copper(II) acetate monohydrate (20.4 mg, 0.102 mmol) and 4 mL of ethanol was added. The mixture was heated to reflux for 2 hours, during which the solution turned into a rust brown suspension. Upon cooling to 0 °C, the mixture was filtered, and washed with cold ethanol. The precipitate was taken up in dichloromethane and filtered through a 0.45 μ m polypropylene syringe filter. The solvent was removed by rotary evaporation to give the dark red product (35 mg, 62% yield). HRESI-MS ([M + H]⁺) C₆₄H₄₉Cu₂N₄O₆ *m/z*, Calcd. 1095.2444 Found 1095.1977. UV-vis (CH₂Cl₂) λ_{\max} , nm (ϵ): 330 (55,960), 387 (20,130), 474 (sh, 2,667).

7.5.4.7. Cu(5-phsalen) (10)

The ligand (*R,R*)-*N,N'*-bis(5-phenylsalicylidene)-1,2-cyclohexanediamine (50.0 mg, 0.105 mmol) was added to 5 mL of ethanol and 0.211 mL of an aqueous sodium hydroxide solution (0.9967 M). This was stirred until the ligand dissolved completely, about 5 minutes. Copper(II) nitrate trihydrate was then added, and the solution heated to reflux for 2 hours, during which the solution turned rust colored with precipitate. Upon cooling to 0 °C, the solution was filtered and the precipitate was washed with cold ethanol. The precipitate was then taken up in dichloromethane and filtered. The solvent was removed from the filtrate under vacuum to give the dark purple product (53.0 mg, 93% yield). This compound can also be synthesized using copper(II) acetate hydrate as the precursor, analogous to the procedure described above for the copper Pacman

complexes. IR (KBr) ν_{\max} : 1540 cm^{-1} (C=N). HRESI-MS ($[\text{M} + \text{H}]^+$) $\text{C}_{32}\text{H}_{29}\text{CuN}_2\text{O}_2$ m/z , Calcd. 536.1520 Found 536.1539. UV-vis (CH_2Cl_2) λ_{\max} , nm (ϵ): 381 (20,075), 564 (1,098). Anal. Calcd for $\text{C}_{32}\text{H}_{28}\text{CuN}_2\text{O}_2$: C, 71.69; H, 5.26; N, 5.23. Found: C, 71.66; H, 5.38; N, 5.17.

7.5.3.8. $\text{Mn}_2(\text{DSX})\text{Cl}_2$ (12)

The ligand DSX (**8**) (50.0 mg, 0.039 mmol) was added to manganese(II) acetate tetrahydrate (28.7 mg, 0.117 mmol) in 4 mL of ethanol and heated to reflux for 2 hours and cooled to room temperature. 1 mL of aqueous saturated sodium chloride solution was added and stirred for 1 minute. The mixture was extracted with 3×4 mL of dichloromethane, and the organic layers were combined and washed with 10 mL of deionized water, followed by drying using MgSO_4 . The solvent was removed by rotary evaporation to leave the brown product in quantitative yield (57 mg). ESI-MS ($[\text{M} - \text{Cl}]^-$) $\text{C}_{86}\text{H}_{92}\text{ClMn}_2\text{N}_4\text{O}_6$ m/z , Calcd. 1421.55 Found 1421.57.

7.5.3.9. $\text{Mn}_2(\text{DSD})\text{Cl}_2$ (13)

The ligand DSD (**13**) (50.0 mg, 0.051 mmol) was added to manganese(II) acetate tetrahydrate (37.8 mg, 0.154 mmol) in 4 mL of ethanol and then heated to reflux for 2 hours. Upon cooling, 1 mL of aqueous saturated sodium chloride solution was added and stirred for 1 minute. The mixture was extracted with 3×25 mL of dichloromethane, and the organic layers were combined and washed with 10 mL of deionized water, followed by drying using MgSO_4 . The solvent was removed by rotary evaporation to leave the brown product (48 mg, 81% yield). HRESI-MS ($[\text{M} - \text{Cl}]^-$) $\text{C}_{64}\text{H}_{48}\text{ClMn}_2\text{N}_4\text{O}_6$ m/z , Calcd. 1113.20 Found 1113.20.

7.5.3.10. Co_2DSX (14)

Under nitrogen, the ligand DSX (**8**) (60.0 mg, 0.047 mmol) was dissolved in 8 mL of degassed dichloromethane. Cobalt(II) acetate tetrahydrate (28.0 mg, 0.112 mmol) was dissolved in 6 mL of degassed methanol and this solution was added dropwise to the dichloromethane DSX solution, which turned orange. After stirring for about 1 hour under nitrogen, the solution turned red with precipitate. The solvent was removed under reduced pressure, and the residue was washed with cold methanol to leave the bright red

product (21 mg, 78% yield). HRESI-MS ($[M]^+$) $C_{86}H_{92}Co_2N_4O_6$ m/z , Calcd. 1394.5675 Found 1394.5668. Anal. Calcd for $C_{86}H_{92}Co_2N_4O_6$: C, 74.04; H, 6.61; N, 4.02. Found: C, 73.88; H, 6.73; N, 3.88.

7.5.3.11. Co_2 DSD (15)

Under nitrogen, the ligand DSD (60.0 mg, 0.062 mmol) was dissolved in 8 mL of degassed dichloromethane. Cobalt(II) acetate tetrahydrate was dissolved in 8 mL of degassed methanol, which was added dropwise to the dichloromethane DSD solution. After stirring for about 1 hour, the solution was reddish-brown with precipitate. The solvent was removed under reduced pressure, and the residue was washed with cold methanol to give the brown crude product (63 mg). HRESI-MS ($[M + H]^+$) $C_{64}H_{49}Co_2N_4O_6$ m/z , Calcd. 1087.2311 Found 1087.2322. Anal. Calcd for $C_{64}H_{48}Co_2N_4O_6 \cdot (H_2O)_5$: C, 65.31; H, 4.93; N, 4.76. Found: C, 65.04; H, 4.87; N, 4.36.

7.5.3.12. Zn_2 DSX (16)

The ligand DSX (8) (50.0 mg, 0.039 mmol) was added to zinc(II) acetate dihydrate (17.2 mg, 0.078 mmol) and 8 mL of ethanol and refluxed for 6 hours. Upon cooling, the solvent was removed by rotary evaporation, and the residue was washed with deionized water to leave the bright yellow crude product (48 mg). IR (KBr) ν_{max} : 1540 cm^{-1} (C=N). ESI-MS ($[M + H]^+$) $C_{86}H_{93}Zn_2N_4O_6$ m/z , Calcd. 1405.57 Found 1409.58.

7.5.3.13. $Zn(5\text{-phsalen})$ (17)

(*R,R*)-*N,N'*-Bis(5-phenylsalicylidene)-1,2-cyclohexanediamine (50.0 mg, 0.105 mmol) was added to zinc(II) acetate dihydrate (23.1 mg, 0.105 mmol) in 8 mL of ethanol and refluxed for 8 hours. Upon cooling, the solvent was removed by rotary evaporation, and the residue was washed with deionized water to leave the bright yellow crude product (52 mg). ESI-MS ($[M + H]^+$) $C_{32}H_{29}ZnN_2O_2$ m/z , Calcd. 537.15 Found 537.15.

7.5.4. Epoxide Ring Opening Studies

The following procedures were used to study the catalytic ring-opening of an epoxide by Cr_2DSXCl_2 (**5**) and $Cr(\text{salen})Cl$. A solution of Cr_2DSXCl_2 (**5**) (12.0 mg, 0.008 mmol) and

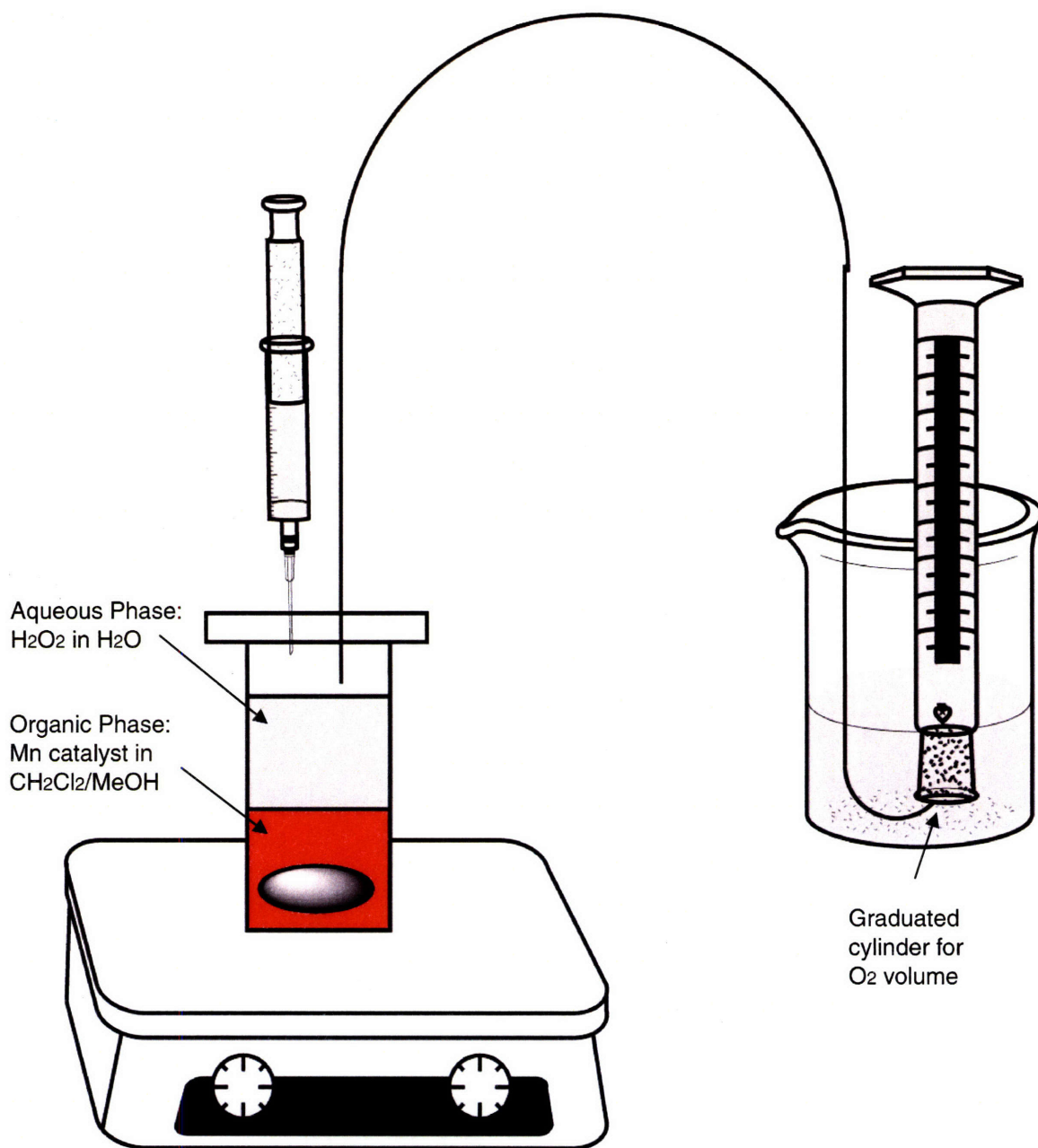
substrate cyclohexene oxide (95.4 mg, 0.756 mmol), and 1 mL of diethyl ether was prepared. As the control, a solution of chromium (1*R*, 2*R*)-(-)-[1,2-cyclohexanediamino-*N,N'*-bis(3,5-di-*tert*-butylsalicylidene) chloride (5.2 mg, 0.008 mmol), cyclohexene oxide (96.2 mg, 0.762 mmol), and 1 mL of diethyl ether was also prepared. To each solution, triethylsilyl azide (457 μ L, 5.6 mmol) and dodecane the internal standard was added. The solutions were sampled after 26 hours of stirring at room temperature. The concentration of substrate and product produced was determined using GC/MS and compared to the initial solutions.

References

1. Wu, J.; Hou, X.-L.; Dai, L.-X.; Xia, L.-J.; Tang, M.-H. *Tetrahedron Asymmetry*, **1998**, *9*, 3431-3436.
2. Wu, M. H.; Jacobsen, E. N. *J. Org. Chem.* **1998**, *63*, 5252-5254.
3. Bartoli, G.; Bosco, M.; Carlone, A.; Locatelli, M.; Massaccesi, M.; Melchiorre, P.; Sambri, L. *Org. Lett.* **2004**, *6*, 2173-2176.
4. Jacobsen, E. N.; Kakiuchi, F.; Konsler, R. G.; Larrow, J. F.; Tokunaga, M. *Tetrahedron Lett.* **1997**, *38*, 773-776.
5. Darensbourg, D. J.; Rodgers, J. L.; Fang, C. C. *Inorg. Chem.* **2003**, *42*, 4498-4450.
6. Darensbourg, D. J.; Mackiewicz, R. M.; Rodgers, J. L.; Fang, C. C.; Billodeaux, D. R.; Reibenspies, J. H. *Inorg. Chem.* **2004**, *43*, 6024-6034.
7. Schon, E.; Zhang, X.; Zhou, Z.; Chisholm, M. H.; Chen, P. *Inorg. Chem.* **2004**, *43*, 7278-7280.
8. Paddock, R. L.; Nguyen, S. T. *J. Am. Chem. Soc.* **2001**, *123*, 11498-11499.
9. Martinez, L. E.; Leighton, J. L.; Carsten, D. H.; Jacobsen, E. N. *J. Am. Chem. Soc.* **1995**, *117*, 5897-5898.
10. Larrow, J. F.; Schaus, S. E.; Jacobsen, E. N. *J. Am. Chem. Soc.* **1995**, *117*, 7420-7421.
11. Konsler, R. G.; Karl, J.; Jacobsen, E. N. *J. Am. Chem. Soc.* **1998**, *120*, 10780-10781.
12. Li, W.; Thakur, S. S.; Chen, S.-W.; Shin, C.-K.; Kawthekar, R. B.; Kim, G.-J. *Tetrahedron Lett.* **2006**, *47*, 3453-3457.
13. Chen, S.-W.; Thakur, S. S.; Li, W.; Shin, C.-K.; Kawthekar, R. B.; Kim, G.-J. *J. Mol. Cat. A.* **2006**, *259*, 116-120.
14. Ready, J. M.; Jacobsen, E. N. *J. Am. Chem. Soc.* **1999**, *121*, 6086-6087.
15. Peukert, S.; Jacobsen, E. N. *Org. Lett.* **1999**, *1*, 1245-1248.
16. Shen, Y.-M.; Duan, W.-L.; Shi, M. *J. Org. Chem.* **2003**, *68*, 1559-1562.
17. Annis, D. A.; Jacobsen, E. N. *J. Am. Chem. Soc.* **1999**, *121*, 4147-4154.
18. Tokunaga, M.; Larrow, J. F.; Kakiuchi, F.; Jacobsen, E. N. *Science* **1997**, *277*, 936-938.
19. Schaus, S. E.; Brandes, B. D.; Larrow, J. F.; Tokunaga, M.; Hansen, K. B.; Gould, A. E.; Furrow, M. E.; Jacobsen, E. N. *J. Am. Chem. Soc.* **2002**, *124*, 1307-1315.
20. Nielsen, L. P. C.; Stevenson, C. P.; Blackmond, D. G.; Jacobsen, E. N. *J. Am. Chem. Soc.* **2004**, *126*, 1360-1362.

21. Thakur, S. S.; Chen, S.-W.; Li, W.; Shin, C.-K. *Synth. Commun.* **2006**, *36*, 2371-2383.
22. Shin, C.-K.; Kim, S.-J.; Kim, G.-J. *Tetrahedron Lett.* **2004**, *45*, 7429-7433.
23. Jacobsen, E. N.; Wu, M. H. Ring Opening of Epoxides and Related Reactions. In *Comprehensive Asymmetric Catalysis*, Vol 2; Pfaltz, A.; Jacobsen, E. N.; Yamamoto H.; Springer: Berlin, Heidelberg, New York, 1999: Chapter 35.
24. Jacobsen, E. N. *Acc. Chem. Res.* **2000**, *33*, 421-431.
25. Larrow, J. F.; Jacobsen, E. N. *Topics Organomet. Chem.* **2004**, *6*, 123-152.
26. Kagan, H. B.; Fiaud, J. C. Kinetic Resolution; In *Topics in Stereochemistry*; Eliel, E. L.; Wilen, S. H.; Wiley: New York, 1987: pg 249.
27. Konsler, R.G.; Karl, J.; Jacobsen, E.N. *J. Am. Chem. Soc.* **1998**, *120*, 10780-10781.
28. Breinbauer, R.; Jacobsen, E. N. *Angew. Chem. Int. Ed.* **2000**, *39*, 3604-3607.
29. Ready, J. M.; Jacobsen, E. N. *J. Am. Chem. Soc.* **2001**, *123*, 2687-2688.
30. Ready, J. R.; Jacobsen, E. N. *Angew. Chem. Int. Ed.* **2002**, *41*, 1374-1377
31. White, D. E.; Jacobsen, E. N. *Tetrahedron: Asymm.*, **2003**, *14*, 3633-3638.
32. Pasini, A.; Bernini, E.; Scaglia, M. *Polyhedron* **1996**, *15*, 4461-4467.
33. Böttcher, A.; Elias, H.; Jäger, E.-G.; Langfelderova, H.; Mazur, M.; Müller, L.; Paulus, H.; Pelikan, P.; Rudolph, M.; Valko, M. *Inorg. Chem.* **1993**, *32*, 4131-4138.
34. Bhadbhade, M. M.; Srinivas, D. *Inorg. Chem.* **1993**, *32*, 6122-6130.
35. Valko, M.; Klement, R.; Pelikán, P.; Boča, R.; Dlháň, L.; Böttcher, A.; Elias, H.; Müller, L. *J. Phys. Chem.* **1995**, *99*, 137-143.
36. Valko, M.; Boča, R.; Klement, R.; Kožíšek, J.; Mazúr, M.; Pelikán, P.; Morris, H.; Elias, H.; Müller, L. *Polyhedron* **1997**, *16*, 903-908.
37. Klement, R.; Stock, F.; Elias, H.; Paulus, H.; Pelikán, P.; Valko, M.; Mazúr, M. *Polyhedron* **1999**, *18*, 3617-3628.
38. Koner, S. *J. Chem. Soc., Chem. Commun.* **1998**, 593-594.
39. Armarego, W. L. F.; Perrin, D. D. *Purification of Laboratory Chemicals*; 4th ed.; Butterworth-Heinmann: Oxford, 1966.
40. Hirotsu, M.; Ohno, N.; Nakajima, T.; Ueno, K. *Chem. Lett.* **2005**, *34*, 848-849.

Appendix

Figure A.1. Reaction setup for measuring catalase activity.

Appendix B.1: Alternate Synthetic Pathways from Chapter 3**2,7-Di-*tert*-butyl-5-(3-formyl-4-hydroxyphenyl)-9,9-dimethyl-9H-xanthene-4-carboxylic acid methyl ester (4) from (3), as shown in Scheme 3.1**

Under nitrogen, 2,7-di-*tert*-butyl-5-(3-formyl-4-hydroxy-phenyl)-9,9-dimethyl-9H-xanthene-4-carboxylic acid methyl ester (3) (0.250 g, 0.590 mmol), 5-bromosalicylaldehyde (0.119 g, 0.590 mmol), sodium carbonate (0.092 g, 0.884 mmol), dichloro[1,1'-bis(diphenylphosphino)ferrocene]palladium(II) dichloromethane adduct (0.026 g, 0.035 mmol), 14 mL of 1,2-dimethoxyethane, and 6 mL of deionized water and heated to 90 °C for 48 hours. Upon cooling, 25 mL of dichloromethane was added and the solution was washed with 2 × 25 mL of deionized water. The aqueous portions were extracted with 10 mL of dichloromethane. The combined organic portions were dried under MgSO₄ and the solvent was removed by rotary evaporation; the resulting residue was purified by column chromatography (silica gel, 99:1 dichloromethane: methanol) to elute the product as a colorless solid (0.118 g, 40% yield). Characterization data is provided in Chapter 4.5.3.1.

2,7-Di-*tert*-butyl-5-(3-formyl-4-hydroxyphenyl)-9,9-dimethyl-9H-xanthene-4-carboxylic acid (5) via deprotection of (4), as shown in Scheme 3.1

2,7-Di-*tert*-butyl-5-(3-formyl-4-hydroxyphenyl)-9,9-dimethyl-9H-xanthene-4-carboxylic acid methyl ester (4) (0.050 g, 0.10 mmol) was added to 8 mL of dichloromethane and cooled to 0 °C. A solution of boron tribromide (1.2 mL, 1.0 M in dichloromethane) was added and the reaction was warmed to room temperature and stirred for 4 hours, after which 4 mL of water was added. The organic layer was separated, washed with 10 mL of water, and dried over MgSO₄. The solvent was evaporated and the residue was purified by column chromatography (silica gel, 99:5 dichloromethane: methanol) to elute the product (0.014 g, 28 % yield). Characterization data is provided in Chapter 3.5.3.6.

2,7-Di-*tert*-butyl-5-(3-formyl-4-hydroxyphenyl)-9,9-dimethyl-9H-xanthene-4-carboxylic acid (5) via deprotection of (8), as shown in Scheme 3.2

Under nitrogen, 2,7-di-*tert*-butyl-5-(3-formyl-4-hydroxyphenyl)-9,9-dimethyl-9H-xanthene-4-carboxylic acid benzyl ester (8) (0.100 g, 0.174 mmol) was added to 20 mL of ethyl acetate and palladium (5% on activated carbon, 0.015 g) and placed under a hydrogen balloon overnight at room temperature. The mixture was then filtered over

Celite and the filtrate was reduced by rotary evaporation and the residue purified by column chromatography (silica gel, 95:5 dichloromethane: methanol) to elute the desired product (0.061 g, 72%) yield. Characterization data is provided in Chapter 3.5.3.6.

4-[2,7-Di-*tert*-butyl-5-(3-formyl-4-hydroxyphenyl)-9,9-dimethyl-9H-xanthen-4-yl]-benzoic acid methyl ester (17) via (16), as shown in Scheme 3.4.

Under nitrogen, 5-(5-bromo-2,7-di-*tert*-butyl-9,9-dimethyl-9H-xanthen-4-yl)-2-hydroxybenzaldehyde (16) (0.37 g, 0.071 mmol), 4-methoxycarbonylphenylboronic acid (0.013 g, 0.071 mmol), sodium carbonate (0.012 g, 0.112 mmol), and dichloro[1,1'-bis(diphenylphosphino)ferrocene]palladium(II) dichloromethane adduct (0.002 g, 0.002 mmol), and 6 mL of 1,2-dimethoxyethane and 2 mL of deionized water. This was heated to 90 °C for 24 hours and upon cooling, the solution was extracted with 2 × 50 mL of dichloromethane. The organic layers were combined and washed with water and dried using MgSO₄. The solvent was removed by rotary evaporation and purified by column chromatography (silica gel, dichloromethane) to give the product (0.025 g, 61% yield). Characterization data are provided in Chapter 4.5.3.4.

Appendix B.2: Alternate Synthetic Pathways from Chapter 5.**4,5-Di(5-salicylaldehyde)-2,7-di-*tert*-butyl-9,9-dimethylxanthene (3) via (1) as shown in Scheme 6.1**

Under nitrogen, 2,7-di-*tert*-butyl-9,9-dimethyl-4-dihydroxyborane-5-(4,4,5,5-tetramethyl-[1,3,2]dioxaborolan-2-yl)-9H-xanthene (1) (0.600 g, 1.22 mmol), 5-bromosalicylaldehyde (0.490 g, 2.44 mmol), sodium carbonate (0.377 g, 3.66 mmol), dichloro[1,1'-bis(diphenylphosphino)ferrocene]palladium(II) dichloromethane adduct (0.107 g, 0.146 mmol), 1,2-dimethoxyethane (12 mL), and deionized water (4 mL) was heated to 90 °C for 48 hours. Upon cooling, the mixture was extracted with 3 × 50 mL of dichloromethane. The organic portions were combined dried over MgSO₄ and the solvent removed by rotary evaporation. The residue was purified by column chromatography (silica gel, dichloromethane) and recrystallized in hot ethanol to obtain the colorless product (0.310 g, 43%). Characterization data are provided in Chapter 6.5.3.2.

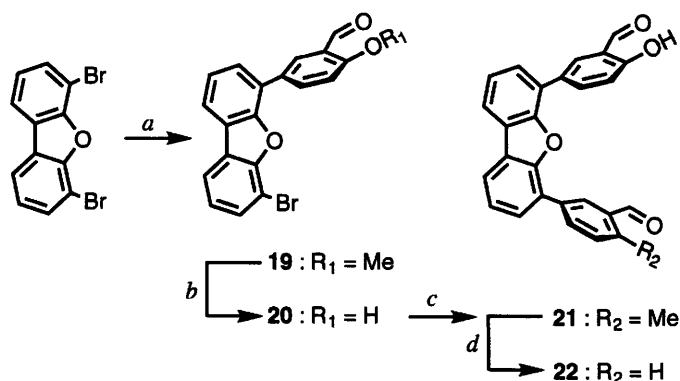
4,6-di(5-salicylaldehyde)-dibenzofuran (8) via (6) as shown in Scheme 6.2

Under nitrogen, 4,6-(4,4,5,5-tetramethyl-[1,3,2]dioxaborolan-2-yl)-dibenzofuran (10) (0.750 g, 1.78 mmol), 5-iodosalicylaldehyde (0.885 g, 3.57 mmol), sodium carbonate (0.551 g, 5.35 mmol), dichloro[1,1'-bis(diphenylphosphino)ferrocene]palladium(II) dichloromethane adduct (0.157 g, 0.214 mmol), dimethoxyethane (9 mL), and deionized water (3 mL) was heated to 90 °C for 48 hours. Upon cooling, the mixture was extracted with 3 × 100 mL of dichloromethane. The organic portions were combined dried over MgSO₄ and the solvent removed by rotary evaporation. The residue was purified by column chromatography (silica gel, dichloromethane) and recrystallized in hot ethanol to obtain the colorless product (0.206 g, 28%). Characterization data are provided in Chapter 6.5.3.5.

Synthetic Procedures as shown in Scheme B2.1**5-(6-Bromo-dibenzofuran-4-yl)-2-methoxy-benzaldehyde (19)**

Under nitrogen, 4,6-dibromodibenzofuran (5) (0.500 g, 1.54 mmol), 3-formyl-4-methoxyphenylboronic acid (0.611 g, 3.40 mmol), sodium carbonate (0.477 g, 4.63 mmol), and dichloro[1,1'-bis(diphenylphosphino)ferrocene]palladium(II) dichloromethane adduct (0.226 g, 0.39 mmol) was added to 9 mL of degassed 1,2-

Scheme B2.1



(a) 3-formyl-4-methoxyphenylboronic acid, Na_2CO_3 , $\text{Pd}(\text{dppf})\text{Cl}_2$, DME: H_2O (3: 1),
 (b) BBr_3 , CH_2Cl_2 , (c) 3-formyl-4-methoxyphenylboronic acid, Na_2CO_3 , $\text{Pd}(\text{PPh}_3)_4$,
 DMF: H_2O (9: 1), (d) BBr_3 , CH_2Cl_2 .

dimethoxyethane and 3 mL of deionized water and heated to 90 °C for 24 hours. Upon cooling, the reaction mixture was extracted with 3 × 20 mL of dichloromethane. The organic portions were combined and dried over MgSO_4 , the solvent removed by rotary evaporation and the residue was purified via column chromatography (silica gel, 5: 5 pentane: dichloromethane) to give the product (0.481 g, 82 % yield). ^1H NMR (500 MHz, CDCl_3 , δ): 10.58 (s, 1H), 8.40 (d, $J = 2.5$ Hz, 1H), 8.34 (dd, $J = 9$ Hz, 2.5 Hz, 1H), 7.92 (dt, $J = 7.5$ Hz, 1 Hz, 2H), 7.70 (dd, $J = 7.5$ Hz, 1 Hz, 1H), 7.64 (dd, $J = 7.5$ Hz, 1 Hz, 1H), 7.46 (t, $J = 8$ Hz, 1H), 7.26 (t, $J = 8$ Hz, 1H), 7.22 (d, $J = 9$ Hz, 1H), 4.05 (s, 3H). ^{13}C NMR (500 MHz, CDCl_3 , δ): 189.91, 189.87, 161.67, 153.48, 153.18, 136.41, 130.37, 128.75, 128.72, 127.01, 125.74, 125.22, 124.59, 124.35, 124.09, 120.29, 119.94, 112.28, 104.87, 56.12. HRESI-MS ($[\text{M} + \text{Na}]^+$) $\text{NaC}_{20}\text{H}_{13}\text{BrO}_3$ m/z , Calcd. 402.9940 Found 402.9946.

5-(6-Bromodibenzofuran-4-yl)-2-hydroxybenzaldehyde (20)

5-(6-Bromo-dibenzofuran-4-yl)-2-methoxybenzaldehyde (19) (0.481 g, 1.26 mmol) was added to 30 mL of dry dichloromethane and cooled in an acetone/dry ice bath and boron tribromide was added via syringe (6.0 mL of 1.0 M in dichloromethane). The reaction was warmed to room temperature and stirred for 2 hours. 20 mL of deionized water was added and the mixture extracted with 2 × 30 mL of dichloromethane. The organic portions were combined dried over MgSO_4 , the solvent removed by rotary evaporation and the residue eluted via column chromatography (silica gel, 3: 7 hexane:

dichloromethane) to give the product (0.400 g, 87% yield). ^1H NMR (500 MHz, CDCl_3 , δ): 11.13 (s, 1H), 10.05 (s, 1H), 8.28 (d, $J = 2.5$ Hz, 1H), 8.13 (dd, $J = 7.5$ Hz, 3 Hz, 1H), 7.92 (t, $J = 7.5$ Hz, 2H), 7.65 (d, $J = 8$ Hz, 2H), 7.46 (t, $J = 7.5$ Hz, 1H), 7.28 (t, $J = 3$ Hz, 1H), 7.18 (d, $J = 8$ Hz, 1H). ^{13}C NMR (500 MHz, CDCl_3 , δ): 197.09, 197.03, 161.51, 153.45, 153.09, 137.13, 134.18, 130.49, 128.03, 126.76, 124.47, 124.28, 124.16, 120.40, 120.02, 118.38, 104.85.

(21)

Under nitrogen, 5-(6-bromo-dibenzofuran-4-yl)-2-hydroxybenzaldehyde (**15**) (0.300 g, 0.82 mmol), 3-formyl-4-methoxyphenylboronic acid (0.176 g, 0.98 mmol), sodium carbonate (0.126 g, 1.22 mmol), and (triphenylphosphine)palladium (0.057 g, 0.049 mmol) were added to 9 mL of degassed dimethylformamide and 1 mL of deionized water and heated to 90 °C for 24 hours. Upon cooling, the mixture was extracted with 2 \times 30 mL of dichloromethane. The organic portions were combined dried over MgSO_4 , the solvent removed by rotary evaporation and the residue purified via column chromatography (silica gel, 2: 8 hexane: dichloromethane) to elute the product (0.275 g, 80% yield). ^1H NMR (500 MHz, CDCl_3 , δ): 11.15 (s, 1H), 10.59 (s, 1H), 10.00 (s, 1H), 8.51 (d, $J = 2.5$ Hz, 1H), 8.22 (d, $J = 2$ Hz, 1H), 8.15 (dd, $J = 9$ Hz, 2 Hz, 1H), 8.10 (dd, $J = 8.5$ Hz, 2.5 Hz, 1H), 7.99 (dd, $J = 2$ Hz, 1.5 Hz, 1H), 7.97 (dd, $J = 2$ Hz, 1.5 Hz, 1H), 7.65 (dd, $J = 3.5$ Hz, 1 Hz, 1H), 7.63 (dd, $J = 3.5$ Hz, 1 Hz), 7.47 (m, 2H), 7.19 (d, $J = 8.5$ Hz, 1H), 7.12 (d, $J = 8.5$ Hz, 1H).

4,6-di(5-salicylaldehyde)-dibenzofuran (22)

(**16**) (0.361 g, 0.85 mmol) was dissolved in 50 mL of dry dichloromethane cooled in an ice water bath. After boron tribromide (2 mL, 1.0 M in dichloromethane) was added via syringe, the solution was warmed to room temperature and stirred for 3 hours. 20 mL of deionized water was added and the mixture was extracted with 3 \times 25 mL of dichloromethane. The organic portions were combined dried over MgSO_4 , the solvent removed by rotary evaporation and the residue purified via column chromatography (silica gel, dichloromethane) to elute the product (0.319 g, 92 %yield). Characterization data are provided in Chapter 6.5.3.7.

Appendix C.1. Input File for the hydroperoxide complex of Mn(HSX*)

```

#!/bin/csh
$ADFBIN/adf -n12 << eor
TITLE Jenny's DPX pacman MnOOH
MAXMEMORYUSAGE 512
GEOMETRY
GO
Iterations 400
END
OCCUPATIONS KeepOrbitals 100
SCF
Iterations 1000
END
XC
GGA Becke PW91c
END
UNRESTRICTED
CHARGE 0 4

ATOMS
C 10.581210 -3.430240 -3.355240
C 9.725230 -2.665780 -2.563120
C 8.347830 -2.771270 -2.766220
C 7.812850 -3.638630 -3.738880
C 8.709320 -4.391440 -4.507120
C 10.081570 -4.294210 -4.324620
O 7.457180 -2.031580 -1.994730
C 7.913340 -0.931240 -1.272500
C 9.273180 -0.752590 -1.020600
C 10.266530 -1.786790 -1.470090
C 6.944120 -0.047350 -0.769220
C 7.394000 1.049590 -0.023320
C 8.748170 1.264210 0.214990
C 9.680120 0.361610 -0.283890
C 5.484320 -0.232080 -0.945340
C 4.857720 -0.194750 -2.212370
C 3.485760 -0.247540 -2.349740
C 2.624240 -0.341690 -1.226150
C 3.272009 -0.426770 0.066080
C 4.676359 -0.351890 0.175500
O 1.333210 -0.344740 -1.376430
Mn -0.133390 -0.886810 -0.190950
O -0.614281 -2.577590 0.377280
O -1.999151 -3.001679 0.271980
C 2.450379 -0.582370 1.201720
N 1.129731 -0.796132 1.382537
C 0.403721 -0.811071 2.661647
C -0.697689 0.238309 2.560427
N -1.389039 0.055509 1.275786
C -2.697689 0.316937 1.071853
C -3.483009 0.115707 -0.103617
C -2.894748 -0.293243 -1.347807
C -3.756078 -0.462473 -2.451497

```

| | | | |
|---|------------|-----------|-----------|
| C | -5.124598 | -0.300783 | -2.322648 |
| C | -5.712188 | 0.040578 | -1.091138 |
| C | -4.876199 | 0.274638 | -0.012048 |
| O | -1.373512 | -0.496915 | -1.552018 |
| C | -7.203888 | 0.116678 | -0.958719 |
| C | -7.953678 | 0.960398 | -1.783809 |
| C | -9.344938 | 0.993828 | -1.706920 |
| C | -10.003459 | 0.178788 | -0.790810 |
| C | -9.288049 | -0.665142 | 0.061320 |
| C | -7.896759 | -0.688542 | -0.032419 |
| O | -7.123790 | -1.506112 | 0.766422 |
| C | -7.699340 | -2.538532 | 1.461532 |
| C | -9.088591 | -2.612432 | 1.624281 |
| C | -9.978600 | -1.520311 | 1.088290 |
| C | -6.853641 | -3.525172 | 2.017752 |
| C | -7.444852 | -4.576262 | 2.729292 |
| C | -8.820092 | -4.667702 | 2.886251 |
| C | -9.632971 | -3.685361 | 2.327780 |
| C | -5.356401 | -3.606803 | 1.908193 |
| O | -4.781290 | -2.548463 | 1.299633 |
| C | 6.348870 | -3.856760 | -4.053790 |
| O | 5.432940 | -3.261980 | -3.259950 |
| O | -4.735112 | -4.565693 | 2.342444 |
| O | 6.002080 | -4.555090 | -4.985560 |
| H | -3.811620 | -2.741873 | 1.209664 |
| H | 5.885800 | -2.725180 | -2.569500 |
| H | 8.277440 | -5.054320 | -5.256110 |
| H | 10.760480 | -4.892280 | -4.932860 |
| H | 11.657750 | -3.349640 | -3.192370 |
| H | 10.540340 | -2.418650 | -0.603000 |
| H | 11.188020 | -1.291600 | -1.813710 |
| H | 10.745030 | 0.506400 | -0.092870 |
| H | 9.073070 | 2.134570 | 0.785910 |
| H | 6.649400 | 1.754100 | 0.350380 |
| H | -6.773132 | -5.327252 | 3.143492 |
| H | -9.256953 | -5.499641 | 3.438901 |
| H | -10.717101 | -3.739551 | 2.445410 |
| H | -11.092839 | 0.199259 | -0.721801 |
| H | -9.913147 | 1.660418 | -2.356500 |
| H | -7.424587 | 1.605268 | -2.487589 |
| H | -10.884540 | -1.967741 | 0.648510 |
| H | -10.308460 | -0.880511 | 1.929340 |
| H | -3.306667 | -0.705898 | -3.416220 |
| H | -5.768888 | -0.475752 | -3.187218 |
| H | -5.292579 | 0.556648 | 0.954092 |
| H | 3.021960 | -0.214450 | -3.336590 |
| H | 5.476390 | -0.100201 | -3.107110 |
| H | 5.126119 | -0.403030 | 1.168040 |
| H | 1.087734 | -0.600591 | 3.496055 |
| H | -0.035929 | -1.813904 | 2.775416 |
| H | -0.279480 | 1.259101 | 2.593446 |
| H | -1.408601 | 0.114588 | 3.390619 |
| H | -2.121011 | -3.076139 | -0.704260 |
| H | 2.897574 | -0.647606 | 2.192518 |

```
H -3.180732 0.586810 2.009808  
END
```

```
BASIS
```

```
C $ADFRESOURCES/DZP/C.1s
```

```
O $ADFRESOURCES/TZP/O.1s
```

```
N $ADFRESOURCES/TZP/N.1s
```

```
H $ADFRESOURCES/DZP/H
```

```
Mn $ADFRESOURCES/TZ2P/Mn.2p
```

```
END
```

```
END INPUT
```

```
eor
```

Table C.1. Cartesian coordinates from the DFT calculated energy minimized structure of the hydroperoxide complex of Mn(HSX*). The structure is shown in Figure 4.4.

| | x | y | z |
|-------|----------|----------|----------|
| 1.C | 10.54703 | -3.38522 | -3.3624 |
| 2.C | 9.68632 | -2.64592 | -2.55441 |
| 3.C | 8.311687 | -2.76836 | -2.75099 |
| 4.C | 7.783106 | -3.63145 | -3.72707 |
| 5.C | 8.682754 | -4.36068 | -4.51001 |
| 6.C | 10.05356 | -4.24241 | -4.33893 |
| 7.O | 7.416122 | -2.0485 | -1.96717 |
| 8.C | 7.862076 | -0.94236 | -1.24597 |
| 9.C | 9.218721 | -0.75202 | -0.9971 |
| 10.C | 10.21893 | -1.77446 | -1.45312 |
| 11.C | 6.884345 | -0.0688 | -0.7487 |
| 12.C | 7.324951 | 1.027343 | 0.001137 |
| 13.C | 8.675675 | 1.254335 | 0.240083 |
| 14.C | 9.615952 | 0.364363 | -0.26163 |
| 15.C | 5.427121 | -0.25561 | -0.94458 |
| 16.C | 4.814239 | -0.16331 | -2.2162 |
| 17.C | 3.44543 | -0.20198 | -2.36716 |
| 18.C | 2.57427 | -0.34933 | -1.24733 |
| 19.C | 3.203745 | -0.47449 | 0.049393 |
| 20.C | 4.608608 | -0.41023 | 0.159554 |
| 21.O | 1.287077 | -0.34475 | -1.42562 |
| 22.Mn | -0.16069 | -0.86555 | -0.23384 |
| 23.O | -0.6646 | -2.5896 | 0.3577 |
| 24.O | -2.07419 | -2.96625 | 0.295007 |
| 25.C | 2.429979 | -0.60886 | 1.24072 |
| 26.N | 1.137132 | -0.75186 | 1.294269 |
| 27.C | 0.434907 | -0.76124 | 2.575628 |
| 28.C | -0.67066 | 0.304545 | 2.506114 |
| 29.N | -1.35727 | 0.138633 | 1.233124 |
| 30.C | -2.63639 | 0.283297 | 1.136077 |
| 31.C | -3.39444 | 0.07964 | -0.06945 |
| 32.C | -2.80265 | -0.30302 | -1.316 |
| 33.C | -3.66507 | -0.45679 | -2.42489 |
| 34.C | -5.03447 | -0.30466 | -2.30187 |
| 35.C | -5.62856 | 0.015866 | -1.0648 |
| 36.C | -4.79101 | 0.222814 | 0.020031 |
| 37.O | -1.51506 | -0.5233 | -1.49761 |
| 38.C | -7.09904 | 0.10156 | -0.94635 |
| 39.C | -7.83231 | 0.931162 | -1.80171 |
| 40.C | -9.22335 | 0.979313 | -1.7475 |
| 41.C | -9.90188 | 0.188831 | -0.82458 |
| 42.C | -9.20428 | -0.64331 | 0.053971 |
| 43.C | -7.81255 | -0.67904 | -0.01552 |
| 44.O | -7.0592 | -1.48972 | 0.813131 |
| 45.C | -7.65478 | -2.53137 | 1.48274 |
| 46.C | -9.04792 | -2.58636 | 1.623098 |
| 47.C | -9.91558 | -1.47852 | 1.081779 |
| 48.C | -6.83248 | -3.54502 | 2.033475 |
| 49.C | -7.45473 | -4.59552 | 2.719975 |
| 50.C | -8.8336 | -4.66286 | 2.858963 |

| | | | |
|------|----------|----------|----------|
| 51.C | -9.62136 | -3.65903 | 2.303248 |
| 52.C | -5.33755 | -3.66437 | 1.922399 |
| 53.O | -4.73639 | -2.61443 | 1.329674 |
| 54.C | 6.320222 | -3.86776 | -4.03141 |
| 55.O | 5.401275 | -3.2661 | -3.24738 |
| 56.O | -4.73514 | -4.64188 | 2.338189 |
| 57.O | 5.975872 | -4.58544 | -4.94947 |
| 58.H | -3.77078 | -2.82908 | 1.23245 |
| 59.H | 5.849483 | -2.71298 | -2.56649 |
| 60.H | 8.254883 | -5.0207 | -5.26105 |
| 61.H | 10.73623 | -4.81956 | -4.95944 |
| 62.H | 11.62155 | -3.29034 | -3.20684 |
| 63.H | 10.49567 | -2.41122 | -0.59286 |
| 64.H | 11.13619 | -1.27075 | -1.78935 |
| 65.H | 10.67786 | 0.520843 | -0.07428 |
| 66.H | 8.991218 | 2.126241 | 0.809769 |
| 67.H | 6.575785 | 1.725685 | 0.37136 |
| 68.H | -6.8036 | -5.36913 | 3.125449 |
| 69.H | -9.29376 | -5.49536 | 3.391576 |
| 70.H | -10.7081 | -3.69612 | 2.401853 |
| 71.H | -10.992 | 0.218998 | -0.77225 |
| 72.H | -9.77516 | 1.637244 | -2.41979 |
| 73.H | -7.28691 | 1.557318 | -2.5098 |
| 74.H | -10.8272 | -1.91062 | 0.638539 |
| 75.H | -10.2388 | -0.82912 | 1.918061 |
| 76.H | -3.2148 | -0.72904 | -3.38048 |
| 77.H | -5.6749 | -0.47482 | -3.1698 |
| 78.H | -5.22411 | 0.485137 | 0.985485 |
| 79.H | 2.988855 | -0.11889 | -3.3517 |
| 80.H | 5.442582 | -0.03236 | -3.09736 |
| 81.H | 5.059577 | -0.49095 | 1.149005 |
| 82.H | 1.121107 | -0.55949 | 3.414924 |
| 83.H | -0.02263 | -1.75599 | 2.701444 |
| 84.H | -0.20891 | 1.308071 | 2.529538 |
| 85.H | -1.35302 | 0.208945 | 3.369173 |
| 86.H | -2.1853 | -3.16188 | -0.66379 |
| 87.H | 2.982576 | -0.57186 | 2.192149 |
| 88.H | -3.22249 | 0.563181 | 2.027737 |

Appendix C.2. Input File for the hydroperoxide complex of Mn(H_{ph}SX*) with carboxylic acid dimers.

```

#!/bin/csh
$ADFBIN/adf -n12 << eor
TITLE Jenny's DPX-Ph pacman MnOOH w/ H-bonds to the -OOH
MAXMEMORYUSAGE 512
GEOMETRY
GO
Iterations 400
END
OCCUPATIONS KeepOrbitals 100
SCF
Iterations 1000
END
XC
GGA Becke PW91c
END
UNRESTRICTED
CHARGE 0 4

```

```

ATOMS
C 0.206290 5.777170 15.541860
C -1.104080 5.319360 15.735900
C -1.865980 4.961720 14.618090
C -1.334450 5.073740 13.335840
C -0.026700 5.535250 13.144920
C 0.736430 5.892040 14.262000
C -1.693370 5.327640 17.096570
C -2.154200 4.163720 17.732940
C -2.713520 4.197960 19.011450
C -2.803290 5.425240 19.670840
C -2.353810 6.595120 19.064790
C -1.804320 6.539740 17.785760
C -3.236710 2.925260 19.622910
C -2.596850 1.705240 19.013080
C -2.029390 1.788060 17.742070
O -2.019210 2.979730 17.034940
C -1.488590 0.662590 17.092390
C -1.538190 -0.565770 17.765610
C -2.090929 -0.667250 19.039680
C -2.607310 0.467440 19.658580
C -0.906400 0.750041 15.737530
C 0.051870 1.727791 15.400190
C 0.599670 1.799971 14.133270
C 0.216530 0.901201 13.114170
C -0.745400 -0.113499 13.453780
C -1.273380 -0.165110 14.758590
C -1.164180 -1.084019 12.494760
N -0.935319 -1.115507 11.164673
C -1.442799 -2.138447 10.241113
C -1.850569 -1.427837 8.958562
N -0.709569 -0.573297 8.571822
C 0.000764 -0.668447 7.427762

```


| | | | |
|----|-----------|-----------|-----------|
| C | 1.174154 | -0.081617 | 6.933682 |
| C | 1.926223 | 0.733124 | 7.855342 |
| C | 3.053693 | 1.409224 | 7.311782 |
| C | 3.431333 | 1.211994 | 5.992312 |
| C | 2.755494 | 0.322624 | 5.120842 |
| C | 1.613774 | -0.295277 | 5.610822 |
| C | 3.340704 | 0.034794 | 3.792322 |
| C | 2.591734 | -0.250637 | 2.631332 |
| C | 3.202994 | -0.553176 | 1.415072 |
| C | 4.593584 | -0.528146 | 1.331333 |
| C | 5.363334 | -0.241576 | 2.451163 |
| C | 4.738124 | 0.018484 | 3.663023 |
| C | 2.368355 | -0.960707 | 0.231722 |
| C | 0.938464 | -0.520177 | 0.358292 |
| C | 0.431924 | -0.179337 | 1.607942 |
| O | 1.215234 | -0.225607 | 2.747472 |
| C | -0.914536 | 0.176862 | 1.786582 |
| C | -1.750396 | 0.161952 | 0.668662 |
| C | -1.262276 | -0.165968 | -0.591598 |
| C | 0.079685 | -0.494777 | -0.740408 |
| C | -1.443896 | 0.567362 | 3.109322 |
| C | -0.816357 | 1.570013 | 3.859202 |
| C | -1.290137 | 1.910373 | 5.118601 |
| C | -2.404097 | 1.256673 | 5.650701 |
| C | -3.069926 | 0.291782 | 4.887051 |
| C | -2.593616 | -0.049028 | 3.626202 |
| O | 1.619843 | 0.870374 | 9.112622 |
| Mn | -0.001377 | 0.536423 | 10.120382 |
| O | 0.821803 | 1.002764 | 11.750552 |
| C | -2.809707 | 1.467073 | 7.067671 |
| O | -2.036198 | 2.378623 | 7.686791 |
| C | 0.578760 | 5.747020 | 11.785090 |
| O | 0.112480 | 4.979680 | 10.770690 |
| O | -1.622607 | 1.560253 | 10.212212 |
| O | -1.550957 | 2.714084 | 11.113801 |
| O | -3.694447 | 0.817203 | 7.616641 |
| O | 1.440020 | 6.581890 | 11.588970 |
| H | -2.790946 | 0.456212 | 0.797252 |
| H | -1.925426 | -0.155478 | -1.454258 |
| H | 0.472705 | -0.756798 | -1.722138 |
| H | 2.397395 | -2.061977 | 0.139013 |
| H | 2.803275 | -0.548747 | -0.689928 |
| H | 5.070174 | -0.758896 | 0.379363 |
| H | 6.449574 | -0.240816 | 2.388243 |
| H | 5.344194 | 0.184514 | 4.550723 |
| H | -1.466590 | 7.450810 | 17.288990 |
| H | -2.439230 | 7.551110 | 19.581810 |
| H | -3.243860 | 5.458840 | 20.669210 |
| H | -3.048020 | 0.396600 | 20.655170 |
| H | -2.111569 | -1.628740 | 19.553280 |
| H | -1.103090 | -1.441830 | 17.283520 |
| H | -3.062550 | 2.934350 | 20.710270 |
| H | -4.332660 | 2.873080 | 19.470270 |
| H | 1.342470 | 2.559691 | 13.888310 |

| | | | |
|---|-----------|-----------|-----------|
| H | 0.377160 | 2.438841 | 16.159100 |
| H | -2.015640 | -0.933060 | 14.977440 |
| H | 3.598633 | 2.094174 | 7.961962 |
| H | 4.282903 | 1.774524 | 5.613982 |
| H | 1.034104 | -0.968577 | 4.988322 |
| H | -2.087217 | -2.132363 | 8.149534 |
| H | -2.715443 | -0.772082 | 9.135154 |
| H | -0.633719 | -2.858757 | 10.035213 |
| H | -2.293609 | -2.669127 | 10.691613 |
| H | -1.817437 | 2.315334 | 11.973352 |
| H | -2.106988 | 2.223033 | 8.677811 |
| H | -3.090286 | -0.829058 | 3.046482 |
| H | -3.943766 | -0.201338 | 5.313341 |
| H | 0.062153 | 2.074203 | 3.455602 |
| H | -0.775078 | 2.666823 | 5.708621 |
| H | -0.432770 | 4.220970 | 11.090030 |
| H | -1.970190 | 4.856350 | 12.476960 |
| H | -2.896740 | 4.632870 | 14.755020 |
| H | 0.807630 | 6.055880 | 16.410440 |
| H | 1.743770 | 6.279520 | 14.104250 |
| H | -1.883381 | -1.851984 | 12.775652 |
| H | -0.599671 | -1.310130 | 6.784612 |

END

BASIS

C \$ADFRESOURCES/DZP/C.1s

O \$ADFRESOURCES/TZP/O.1s

N \$ADFRESOURCES/TZP/N.1s

H \$ADFRESOURCES/DZP/H

Mn \$ADFRESOURCES/TZ2P/Mn.2p

END

END INPUT

eor

Table C.2. Cartesian coordinates from the DFT calculated energy minimized structure of the hydroperoxide complex of Mn(H_{ph}SX*) with the xanthenes oriented so the carboxylic acids can form a hydrogen bonded dimer. The structure is shown in Figure 4.5.

| | x | y | z |
|------|----------|----------|----------|
| 1.C | -3.75165 | 4.546489 | 14.31793 |
| 2.C | -3.38406 | 3.626824 | 15.30982 |
| 3.C | -2.8434 | 2.395334 | 14.92456 |
| 4.C | -2.68628 | 2.083854 | 13.58282 |
| 5.C | -3.06025 | 3.004904 | 12.59827 |
| 6.C | -3.58758 | 4.242615 | 12.97275 |
| 7.C | -3.60206 | 3.958867 | 16.73365 |
| 8.C | -2.56721 | 3.891009 | 17.68142 |
| 9.C | -2.77102 | 4.23596 | 19.01614 |
| 10.C | -4.04147 | 4.653395 | 19.41208 |
| 11.C | -5.08914 | 4.71473 | 18.49963 |
| 12.C | -4.86443 | 4.370164 | 17.17086 |
| 13.C | -1.63375 | 4.113736 | 19.99311 |
| 14.C | -0.29351 | 4.125105 | 19.30752 |
| 15.C | -0.20586 | 3.78953 | 17.95878 |
| 16.O | -1.33477 | 3.477823 | 17.22283 |
| 17.C | 1.021914 | 3.710811 | 17.27923 |
| 18.C | 2.176114 | 3.978908 | 18.02141 |
| 19.C | 2.115825 | 4.326536 | 19.3671 |
| 20.C | 0.882194 | 4.40687 | 20.00279 |
| 21.C | 1.11115 | 3.36242 | 15.84516 |
| 22.C | 0.330315 | 4.025557 | 14.87198 |
| 23.C | 0.413865 | 3.706708 | 13.53512 |
| 24.C | 1.281166 | 2.691984 | 13.06558 |
| 25.C | 2.13297 | 2.065424 | 14.03725 |
| 26.C | 2.009736 | 2.405781 | 15.40133 |
| 27.C | 3.137512 | 1.125374 | 13.65775 |
| 28.N | 3.331359 | 0.699528 | 12.44032 |
| 29.C | 4.394219 | -0.26124 | 12.15586 |
| 30.C | 3.868309 | -1.22721 | 11.08788 |
| 31.N | 3.242431 | -0.423 | 10.04361 |
| 32.C | 3.509082 | -0.6284 | 8.784802 |
| 33.C | 3.007294 | 0.125546 | 7.684865 |
| 34.C | 2.209732 | 1.311089 | 7.875835 |
| 35.C | 1.736861 | 1.958986 | 6.698018 |
| 36.C | 2.071322 | 1.513461 | 5.438487 |
| 37.C | 2.928479 | 0.399599 | 5.246521 |
| 38.C | 3.364036 | -0.27635 | 6.374625 |
| 39.C | 3.459637 | 0.040274 | 3.909948 |
| 40.C | 2.648788 | -0.24499 | 2.794942 |
| 41.C | 3.186567 | -0.58831 | 1.553547 |
| 42.C | 4.57522 | -0.60557 | 1.405997 |
| 43.C | 5.406733 | -0.31751 | 2.483065 |
| 44.C | 4.846457 | -0.00795 | 3.720003 |
| 45.C | 2.279383 | -0.99611 | 0.421165 |
| 46.C | 0.856353 | -0.55775 | 0.641278 |
| 47.C | 0.431035 | -0.20078 | 1.921345 |
| 48.O | 1.284142 | -0.19645 | 3.002532 |
| 49.C | -0.89868 | 0.185909 | 2.177049 |

| | | | |
|-------|----------|----------|----------|
| 50.C | -1.79941 | 0.201045 | 1.107698 |
| 51.C | -1.39444 | -0.15816 | -0.17648 |
| 52.C | -0.07203 | -0.5304 | -0.40197 |
| 53.C | -1.31587 | 0.571328 | 3.542132 |
| 54.C | -1.92146 | 1.812961 | 3.783046 |
| 55.C | -2.25587 | 2.200459 | 5.077877 |
| 56.C | -1.98531 | 1.343799 | 6.154086 |
| 57.C | -1.41963 | 0.086463 | 5.90944 |
| 58.C | -1.09142 | -0.29527 | 4.619417 |
| 59.O | 1.932871 | 1.80829 | 9.040583 |
| 60.Mn | 2.017818 | 0.941913 | 10.83467 |
| 61.O | 1.273912 | 2.407007 | 11.78954 |
| 62.C | -2.24824 | 1.724205 | 7.56468 |
| 63.O | -2.774 | 2.917394 | 7.745202 |
| 64.C | -2.88906 | 2.675209 | 11.16074 |
| 65.O | -2.53684 | 1.425547 | 10.95134 |
| 66.O | 0.535003 | -0.20666 | 11.02656 |
| 67.O | 0.250044 | -0.84851 | 9.744538 |
| 68.O | -1.96951 | 0.937607 | 8.494387 |
| 69.O | -3.06877 | 3.51929 | 10.25959 |
| 70.H | -2.83754 | 0.474442 | 1.302656 |
| 71.H | -2.11176 | -0.15753 | -0.99779 |
| 72.H | 0.252183 | -0.81884 | -1.40393 |
| 73.H | 2.306334 | -2.09848 | 0.319297 |
| 74.H | 2.655165 | -0.57658 | -0.52584 |
| 75.H | 5.000639 | -0.85511 | 0.432238 |
| 76.H | 6.4899 | -0.31843 | 2.358736 |
| 76.H | 6.4899 | -0.31843 | 2.358736 |
| 77.H | 5.487723 | 0.252168 | 4.563406 |
| 78.H | -5.67994 | 4.39356 | 16.44961 |
| 79.H | -6.08157 | 5.022087 | 18.8235 |
| 80.H | -4.20853 | 4.91942 | 20.45552 |
| 81.H | 0.822128 | 4.681388 | 21.05555 |
| 82.H | 3.03054 | 4.549584 | 19.91288 |
| 83.H | 3.136077 | 3.953563 | 17.50816 |
| 84.H | -1.68326 | 4.932077 | 20.72549 |
| 85.H | -1.74167 | 3.168577 | 20.55642 |
| 86.H | -0.19761 | 4.225949 | 12.79949 |
| 87.H | -0.35209 | 4.813256 | 15.18598 |
| 88.H | 2.633856 | 1.880058 | 16.12387 |
| 89.H | 1.111855 | 2.843248 | 6.830108 |
| 90.H | 1.697964 | 2.051326 | 4.565478 |
| 91.H | 3.999387 | -1.15685 | 6.253866 |
| 92.H | 4.684173 | -1.8534 | 10.68829 |
| 93.H | 3.095807 | -1.88001 | 11.53033 |
| 94.H | 5.264114 | 0.286524 | 11.75112 |
| 95.H | 4.711448 | -0.81151 | 13.059 |
| 96.H | -0.41679 | -0.22796 | 9.366585 |
| 97.H | -2.88509 | 3.120288 | 8.762245 |
| 98.H | -0.6426 | -1.2716 | 4.439241 |
| 99.H | -1.23114 | -0.58331 | 6.745625 |
| 100.H | -2.0949 | 2.494781 | 2.94807 |
| 101.H | -2.70507 | 3.176113 | 5.260958 |
| 102.H | -2.34413 | 1.271822 | 9.951154 |

| | | | |
|-------|----------|----------|----------|
| 103.H | -2.26015 | 1.128916 | 13.28726 |
| 104.H | -2.54897 | 1.674658 | 15.68419 |
| 105.H | -4.15206 | 5.516006 | 14.61272 |
| 106.H | -3.86272 | 4.958224 | 12.20067 |
| 107.H | 4.190518 | -1.45728 | 8.5362 |
| 108.H | 3.779046 | 0.736605 | 14.46404 |

Appendix C.3. Input File for the hydroperoxide complex of Mn(HSD*).

```

#!/bin/csh
$ADFBIN/adf -n12 << eor
TITLE Jenny's HSD, no phenyl,
MAXMEMORYUSAGE 512
GEOMETRY
GO
Iterations 400
END
OCCUPATIONS KeepOrbitals 100
SCF
Iterations 1000
END
XC
GGA Becke PW91c
END
UNRESTRICTED
CHARGE 0 4

ATOMS
C 1.372400 4.336910 -12.351861
C 0.975270 5.543420 -11.777121
C 0.567690 6.667260 -12.511201
C 0.532130 6.596010 -13.904851
C 0.913570 5.404000 -14.511341
C 1.326340 4.304700 -13.752591
O 0.945420 5.789520 -10.424451
C 0.509640 7.092370 -10.285101
C 0.265380 7.685390 -11.530611
C -0.180180 9.006830 -11.585691
C -0.375050 9.673530 -10.381911
C -0.137401 9.048520 -9.150501
C 0.318840 7.726990 -9.058711
C 0.635940 7.083380 -7.773371
C -0.179941 7.241030 -6.629171
C 0.179179 6.720770 -5.390821
C 1.415439 6.004579 -5.222381
C 2.206999 5.804839 -6.404410
C 1.793679 6.341259 -7.636741
C 3.454799 5.120939 -6.380580
N 4.050639 4.671469 -5.315729
Mn 3.409979 4.747139 -3.460570
O 3.076319 2.817999 -3.568699
O 3.343189 2.000131 -2.398729
O 1.760019 5.574599 -4.045881
C 1.777750 3.156620 -11.567391
C 5.340839 3.988739 -5.407769
C 6.220399 4.565900 -4.301479
N 5.396789 4.653639 -3.091149
C 5.959439 4.587610 -1.922659
C 5.273419 4.668470 -0.667879
C 3.855269 4.854559 -0.570689
C 3.280229 4.887250 0.727900

```

| | | | |
|---|-----------|-----------|------------|
| C | 4.058588 | 4.696580 | 1.848841 |
| C | 5.448508 | 4.468650 | 1.759791 |
| C | 6.034029 | 4.485910 | 0.506841 |
| C | 6.215948 | 4.086770 | 2.964171 |
| C | 5.799538 | 3.008700 | 3.747160 |
| C | 6.438548 | 2.586879 | 4.920030 |
| C | 7.592278 | 3.258950 | 5.340070 |
| C | 8.055988 | 4.318301 | 4.564131 |
| C | 7.381298 | 4.726130 | 3.402781 |
| C | 5.648118 | 1.481569 | 5.412120 |
| C | 4.619978 | 1.315570 | 4.474770 |
| O | 4.696458 | 2.238670 | 3.460650 |
| C | 5.711288 | 0.617419 | 6.512770 |
| C | 4.742698 | -0.378941 | 6.633270 |
| C | 3.728988 | -0.516471 | 5.676440 |
| C | 3.644478 | 0.322610 | 4.558040 |
| C | 2.621288 | 0.127740 | 3.514950 |
| O | 3.060699 | 4.961411 | -1.611159 |
| H | 1.579650 | 3.373460 | -14.256031 |
| H | 0.877450 | 5.313730 | -15.595281 |
| H | 0.207550 | 7.445590 | -14.502140 |
| H | -0.363470 | 9.502280 | -12.536811 |
| H | -0.707260 | 10.712280 | -10.388771 |
| H | -0.268231 | 9.616820 | -8.230361 |
| H | 3.004238 | -1.326351 | 5.770749 |
| H | 4.776558 | -1.064671 | 7.480030 |
| H | 6.502468 | 0.716909 | 7.257370 |
| H | 8.115248 | 2.966560 | 6.250861 |
| H | 8.951608 | 4.858891 | 4.872901 |
| H | 7.748477 | 5.584990 | 2.838421 |
| H | 2.205129 | 5.048429 | 0.803510 |
| H | 3.587048 | 4.693070 | 2.832671 |
| H | 7.102089 | 4.276140 | 0.413171 |
| H | -0.460691 | 6.839110 | -4.516481 |
| H | -1.127350 | 7.770840 | -6.722301 |
| H | 2.443949 | 6.200779 | -8.497001 |
| H | 5.802559 | 4.127500 | -6.399519 |
| H | 5.166720 | 2.915489 | -5.226419 |
| H | 6.547309 | 5.583250 | -4.581539 |
| H | 7.112129 | 3.937909 | -4.138859 |
| H | 3.027659 | 2.585191 | -1.670199 |
| H | 7.050279 | 4.450520 | -1.872159 |
| H | 3.954130 | 4.978459 | -7.346879 |
| O | 1.788809 | -0.756036 | 3.634607 |
| O | 1.732898 | 1.163984 | 3.203567 |
| H | 1.142217 | 0.878896 | 2.516310 |
| O | 2.114113 | 2.131625 | -12.137168 |
| O | 2.869011 | 3.237589 | -10.694125 |
| H | 2.997173 | 2.397870 | -10.268749 |

END

BASIS

C \$ADFRESOURCES/DZP/C.ls

O \$ADFRESOURCES/TZP/O.ls

```
N $ADFRESOURCES/TZP/N.1s  
H $ADFRESOURCES/DZP/H  
Mn $ADFRESOURCES/TZ2P/Mn.2p  
END  
END INPUT  
eor
```


Table C.3. Cartesian coordinates from the DFT calculated energy minimized structure of the hydroperoxide complex of Mn(HSD*). The structure is shown in Figure 4.7.

| | x | y | z |
|-------|----------|----------|----------|
| 1.C | 1.3724 | 4.33691 | -12.3519 |
| 2.C | 0.97527 | 5.54342 | -11.7771 |
| 3.C | 0.56769 | 6.66726 | -12.5112 |
| 4.C | 0.53213 | 6.59601 | -13.9049 |
| 5.C | 0.91357 | 5.404 | -14.5113 |
| 6.C | 1.32634 | 4.3047 | -13.7526 |
| 7.O | 0.94542 | 5.78952 | -10.4245 |
| 8.C | 0.50964 | 7.09237 | -10.2851 |
| 9.C | 0.26538 | 7.68539 | -11.5306 |
| 10.C | -0.18018 | 9.00683 | -11.5857 |
| 11.C | -0.37505 | 9.67353 | -10.3819 |
| 12.C | -0.1374 | 9.04852 | -9.1505 |
| 13.C | 0.31884 | 7.72699 | -9.05871 |
| 14.C | 0.63594 | 7.08338 | -7.77337 |
| 15.C | -0.17994 | 7.24103 | -6.62917 |
| 16.C | 0.179179 | 6.72077 | -5.39082 |
| 17.C | 1.415439 | 6.004579 | -5.22238 |
| 18.C | 2.206999 | 5.804839 | -6.40441 |
| 19.C | 1.793679 | 6.341259 | -7.63674 |
| 20.C | 3.454799 | 5.120939 | -6.38058 |
| 21.N | 4.050639 | 4.671469 | -5.31573 |
| 22.Mn | 3.409979 | 4.747139 | -3.46057 |
| 23.O | 3.076319 | 2.817999 | -3.5687 |
| 24.O | 3.343189 | 2.000131 | -2.39873 |
| 25.O | 1.760019 | 5.574599 | -4.04588 |
| 26.C | 1.77775 | 3.15662 | -11.5674 |
| 27.C | 5.340839 | 3.988739 | -5.40777 |
| 28.C | 6.220399 | 4.5659 | -4.30148 |
| 29.N | 5.396789 | 4.653639 | -3.09115 |
| 30.C | 5.959439 | 4.58761 | -1.92266 |
| 31.C | 5.273419 | 4.66847 | -0.66788 |
| 32.C | 3.855269 | 4.854559 | -0.57069 |
| 33.C | 3.280229 | 4.88725 | 0.7279 |
| 34.C | 4.058588 | 4.69658 | 1.848841 |
| 35.C | 5.448508 | 4.46865 | 1.759791 |
| 36.C | 6.034029 | 4.48591 | 0.506841 |
| 37.C | 6.215948 | 4.08677 | 2.964171 |
| 38.C | 5.799538 | 3.0087 | 3.74716 |
| 39.C | 6.438548 | 2.586879 | 4.92003 |
| 40.C | 7.592278 | 3.25895 | 5.34007 |
| 41.C | 8.055988 | 4.318301 | 4.564131 |
| 42.C | 7.381298 | 4.72613 | 3.402781 |
| 43.C | 5.648118 | 1.481569 | 5.41212 |
| 44.C | 4.619978 | 1.31557 | 4.47477 |
| 45.O | 4.696458 | 2.23867 | 3.46065 |
| 46.C | 5.711288 | 0.617419 | 6.51277 |
| 47.C | 4.742698 | -0.37894 | 6.63327 |
| 48.C | 3.728988 | -0.51647 | 5.67644 |
| 49.C | 3.644478 | 0.32261 | 4.55804 |
| 50.C | 2.621288 | 0.12774 | 3.51495 |

| | | | |
|------|----------|----------|----------|
| 51.O | 3.060699 | 4.961411 | -1.61116 |
| 52.H | 1.57965 | 3.37346 | -14.256 |
| 53.H | 0.87745 | 5.31373 | -15.5953 |
| 54.H | 0.20755 | 7.44559 | -14.5021 |
| 55.H | -0.36347 | 9.50228 | -12.5368 |
| 56.H | -0.70726 | 10.71228 | -10.3888 |
| 57.H | -0.26823 | 9.61682 | -8.23036 |
| 58.H | 3.004238 | -1.32635 | 5.770749 |
| 59.H | 4.776558 | -1.06467 | 7.48003 |
| 60.H | 6.502468 | 0.716909 | 7.25737 |
| 61.H | 8.115248 | 2.96656 | 6.250861 |
| 62.H | 8.951608 | 4.858891 | 4.872901 |
| 63.H | 7.748477 | 5.58499 | 2.838421 |
| 64.H | 2.205129 | 5.048429 | 0.80351 |
| 65.H | 3.587048 | 4.69307 | 2.832671 |
| 66.H | 7.102089 | 4.27614 | 0.413171 |
| 67.H | -0.46069 | 6.83911 | -4.51648 |
| 68.H | -1.12735 | 7.77084 | -6.7223 |
| 69.H | 2.443949 | 6.200779 | -8.497 |
| 70.H | 5.802559 | 4.1275 | -6.39952 |
| 71.H | 5.16672 | 2.915489 | -5.22642 |
| 72.H | 6.547309 | 5.58325 | -4.58154 |
| 73.H | 7.112129 | 3.937909 | -4.13886 |
| 74.H | 3.027659 | 2.585191 | -1.6702 |
| 75.H | 7.050279 | 4.45052 | -1.87216 |
| 76.H | 3.95413 | 4.978459 | -7.34688 |
| 77.O | 1.788809 | -0.75604 | 3.634607 |
| 78.O | 1.732898 | 1.163984 | 3.203567 |
| 79.H | 1.142217 | 0.878896 | 2.51631 |
| 80.O | 2.114113 | 2.131625 | -12.1372 |
| 81.O | 2.869011 | 3.237589 | -10.6941 |
| 82.H | 2.997173 | 2.39787 | -10.2687 |

Appendix C.4. Input File for the hydroperoxide complex of Mn(H_{ph}SD*).

```

#!/bin/csh
$ADFBIN/adf -n12 << eor
TITLE Jenny's HSD-phenyl
MAXMEMORYUSAGE 512
GEOMETRY
GO
Iterations 400
END
OCCUPATIONS KeepOrbitals 100
SCF
Iterations 1000
END
XC
GGA Becke PW91c
END
UNRESTRICTED
CHARGE 0 4

ATOMS
C      2.772680  2.341637 -11.875520
C      1.700776  3.143507 -11.469912
C      0.968351  2.783937 -10.333078
C      1.256879  1.605939 -9.657334
C      2.294132  0.788380 -10.101660
C      3.068625  1.172155 -11.194318
C      1.298681  4.292929 -12.279070
C      0.898427  5.499096 -11.722027
C      0.443153  6.590979 -12.476720
C      0.364369  6.480682 -13.866474
C      0.781361  5.289507 -14.450917
C      1.238532  4.220208 -13.673757
O      0.928713  5.785636 -10.385300
C      0.502843  7.084786 -10.263797
C      0.188083  7.634276 -11.515263
C      -0.257046  8.955417 -11.582581
C      -0.375004  9.675093 -10.395516
C      -0.052161  9.096591 -9.163969
C      0.397850  7.775551 -9.058544
C      0.781332  7.185010 -7.777349
C      0.067199  7.469518 -6.589414
C      0.466381  6.982032 -5.379842
C      1.614825  6.195159 -5.242150
C      2.339450  5.885073 -6.436386
C      1.894614  6.371328 -7.676882
C      3.546784  5.143674 -6.394659
N      4.135893  4.751744 -5.307648
Mn     3.514344  4.879692 -3.492018
O      3.126305  2.993078 -3.636416
O      3.206992  2.240128 -2.442159
O      1.972671  5.775985 -4.068477
C      2.588769 -0.513190 -9.470311
O      3.509677 -1.237816 -9.802316

```

| | | | |
|---|-----------|-----------|------------|
| C | 5.366884 | 3.990932 | -5.388663 |
| C | 6.255640 | 4.528230 | -4.285478 |
| N | 5.419889 | 4.628461 | -3.098036 |
| C | 5.968316 | 4.461600 | -1.939333 |
| C | 5.292476 | 4.554108 | -0.687374 |
| C | 3.898498 | 4.817591 | -0.608719 |
| C | 3.302241 | 4.859133 | 0.669181 |
| C | 4.043721 | 4.621593 | 1.804460 |
| C | 5.423573 | 4.357628 | 1.731412 |
| C | 6.027011 | 4.338141 | 0.490142 |
| C | 6.162573 | 4.040898 | 2.955941 |
| C | 5.713463 | 3.013718 | 3.771624 |
| C | 6.298710 | 2.656338 | 4.992567 |
| C | 7.427155 | 3.353583 | 5.417466 |
| C | 7.922034 | 4.368538 | 4.604762 |
| C | 7.300473 | 4.712547 | 3.397462 |
| C | 5.503469 | 1.556699 | 5.486011 |
| C | 4.527304 | 1.341079 | 4.503478 |
| O | 4.645901 | 2.221848 | 3.469161 |
| C | 3.543170 | 0.370151 | 4.581407 |
| C | 3.550125 | -0.411601 | 5.735401 |
| C | 4.506678 | -0.229118 | 6.734450 |
| C | 5.489493 | 0.755435 | 6.624989 |
| C | 2.603438 | 0.131829 | 3.491289 |
| C | 1.261449 | -0.145528 | 3.761738 |
| C | 0.403917 | -0.499319 | 2.734980 |
| C | 0.883450 | -0.575524 | 1.428766 |
| C | 2.207488 | -0.251766 | 1.143935 |
| C | 3.061553 | 0.108577 | 2.172043 |
| C | -0.043787 | -1.031682 | 0.378116 |
| O | -1.213508 | -1.305295 | 0.565653 |
| O | 3.135146 | 4.959578 | -1.668069 |
| O | 1.726388 | -0.822133 | -8.506941 |
| O | 0.551181 | -1.138428 | -0.828262 |
| H | 1.502867 | 3.273077 | -14.154098 |
| H | 0.733903 | 5.175208 | -15.537157 |
| H | 0.005285 | 7.314814 | -14.477332 |
| H | -0.500036 | 9.420945 | -12.541718 |
| H | -0.701602 | 10.717725 | -10.424339 |
| H | -0.096901 | 9.703324 | -8.253566 |
| H | 2.813765 | -1.214775 | 5.824825 |
| H | 4.480444 | -0.862295 | 7.624377 |
| H | 6.229306 | 0.896301 | 7.417384 |
| H | 7.917899 | 3.112437 | 6.364136 |
| H | 8.806830 | 4.927507 | 4.921346 |
| H | 7.680389 | 5.548990 | 2.802351 |
| H | 2.233607 | 5.077586 | 0.720168 |
| H | 3.564387 | 4.638246 | 2.787983 |
| H | 7.093782 | 4.095692 | 0.416439 |
| H | -0.103933 | 7.189405 | -4.472617 |
| H | -0.847663 | 8.068558 | -6.657725 |
| H | 2.468827 | 6.128270 | -8.577976 |
| H | 5.840460 | 4.085477 | -6.382270 |
| H | 5.116246 | 2.934044 | -5.177534 |

```
H 6.598291 5.545448 -4.555149
H 7.129489 3.875520 -4.111608
H 3.023492 2.945328 -1.753894
H 2.024401 -1.716263 -8.173067
H 3.383123 2.657563 -12.727341
H 3.892447 0.518518 -11.496886
H 0.138517 3.418734 -10.005155
H 0.660010 1.300357 -8.791693
H -0.175829 -1.447521 -1.438926
H 2.564894 -0.299433 0.111480
H 4.108292 0.346398 1.962759
H 0.893879 -0.056742 4.787997
H -0.651054 -0.727417 2.913311
H 7.047206 4.232872 -1.894439
H 4.019066 4.906830 -7.363068
END
```

BASIS

```
C $ADFRESOURCES/DZP/C.1s
O $ADFRESOURCES/TZP/O.1s
N $ADFRESOURCES/TZP/N.1s
H $ADFRESOURCES/DZP/H
Mn $ADFRESOURCES/TZ2P/Mn.2p
END
END INPUT
eor
```

Table C.4. Cartesian coordinates from the DFT calculated energy minimized structure of the hydroperoxide complex of Mn(H_{ph}SD*). The structure is shown in Figure 4.8.

| | x | y | z |
|------|----------|----------|----------|
| 1.C | 2.77268 | 2.341637 | -11.8755 |
| 2.C | 1.700776 | 3.143507 | -11.4699 |
| 3.C | 0.968351 | 2.783937 | -10.3331 |
| 4.C | 1.256879 | 1.605939 | -9.65733 |
| 5.C | 2.294132 | 0.78838 | -10.1017 |
| 6.C | 3.068625 | 1.172155 | -11.1943 |
| 7.C | 1.298681 | 4.292929 | -12.2791 |
| 8.C | 0.898427 | 5.499096 | -11.722 |
| 9.C | 0.443153 | 6.590979 | -12.4767 |
| 10.C | 0.364369 | 6.480682 | -13.8665 |
| 11.C | 0.781361 | 5.289507 | -14.4509 |
| 12.C | 1.238532 | 4.220208 | -13.6738 |
| 13.O | 0.928713 | 5.785636 | -10.3853 |
| 14.C | 0.502843 | 7.084786 | -10.2638 |
| 15.C | 0.188083 | 7.634276 | -11.5153 |
| 16.C | -0.25705 | 8.955417 | -11.5826 |
| 17.C | -0.375 | 9.675093 | -10.3955 |
| 18.C | -0.05216 | 9.096591 | -9.16397 |
| 19.C | 0.39785 | 7.775551 | -9.05854 |
| 20.C | 0.781332 | 7.18501 | -7.77735 |
| 21.C | 0.067199 | 7.469518 | -6.58941 |
| 22.C | 0.466381 | 6.982032 | -5.37984 |
| 23.C | 1.614825 | 6.195159 | -5.24215 |
| 24.C | 2.33945 | 5.885073 | -6.43639 |
| 25.C | 1.894614 | 6.371328 | -7.67688 |
| 26.C | 3.546784 | 5.143674 | -6.39466 |
| 27.N | 4.135893 | 4.751744 | -5.30765 |
| 28.M | 3.514344 | 4.879692 | -3.49202 |
| 29.O | 3.126305 | 2.993078 | -3.63642 |
| 30.O | 3.206992 | 2.240128 | -2.44216 |
| 31.O | 1.972671 | 5.775985 | -4.06848 |
| 32.C | 2.588769 | -0.51319 | -9.47031 |
| 33.O | 3.509677 | -1.23782 | -9.80232 |
| 34.C | 5.366884 | 3.990932 | -5.38866 |
| 35.C | 6.25564 | 4.52823 | -4.28548 |
| 36.N | 5.419889 | 4.628461 | -3.09804 |
| 37.C | 5.968316 | 4.4616 | -1.93933 |
| 38.C | 5.292476 | 4.554108 | -0.68737 |
| 39.C | 3.898498 | 4.817591 | -0.60872 |
| 40.C | 3.302241 | 4.859133 | 0.669181 |
| 41.C | 4.043721 | 4.621593 | 1.80446 |
| 42.C | 5.423573 | 4.357628 | 1.731412 |
| 43.C | 6.027011 | 4.338141 | 0.490142 |
| 44.C | 6.162573 | 4.040898 | 2.955941 |
| 45.C | 5.713463 | 3.013718 | 3.771624 |
| 46.C | 6.29871 | 2.656338 | 4.992567 |
| 47.C | 7.427155 | 3.353583 | 5.417466 |
| 48.C | 7.922034 | 4.368538 | 4.604762 |
| 49.C | 7.300473 | 4.712547 | 3.397462 |
| 50.C | 5.503469 | 1.556699 | 5.486011 |
| 51.C | 4.527304 | 1.341079 | 4.503478 |
| 52.O | 4.645901 | 2.221848 | 3.469161 |

| | | | |
|-------|----------|----------|----------|
| 53.C | 3.54317 | 0.370151 | 4.581407 |
| 54.C | 3.550125 | -0.4116 | 5.735401 |
| 55.C | 4.506678 | -0.22912 | 6.73445 |
| 56.C | 5.489493 | 0.755435 | 6.624989 |
| 57.C | 2.603438 | 0.131829 | 3.491289 |
| 58.C | 1.261449 | -0.14553 | 3.761738 |
| 59.C | 0.403917 | -0.49932 | 2.73498 |
| 60.C | 0.88345 | -0.57552 | 1.428766 |
| 61.C | 2.207488 | -0.25177 | 1.143935 |
| 62.C | 3.061553 | 0.108577 | 2.172043 |
| 63.C | -0.04379 | -1.03168 | 0.378116 |
| 64.O | -1.21351 | -1.3053 | 0.565653 |
| 65.O | 3.135146 | 4.959578 | -1.66807 |
| 66.O | 1.726388 | -0.82213 | -8.50694 |
| 67.O | 0.551181 | -1.13843 | -0.82826 |
| 68.H | 1.502867 | 3.273077 | -14.1541 |
| 69.H | 0.733903 | 5.175208 | -15.5372 |
| 70.H | 0.005285 | 7.314814 | -14.4773 |
| 71.H | -0.50004 | 9.420945 | -12.5417 |
| 72.H | -0.7016 | 10.71773 | -10.4243 |
| 73.H | -0.0969 | 9.703324 | -8.25357 |
| 74.H | 2.813765 | -1.21478 | 5.824825 |
| 75.H | 4.480444 | -0.8623 | 7.624377 |
| 76.H | 6.229306 | 0.896301 | 7.417384 |
| 77.H | 7.917899 | 3.112437 | 6.364136 |
| 78.H | 8.80683 | 4.927507 | 4.921346 |
| 79.H | 7.680389 | 5.54899 | 2.802351 |
| 80.H | 2.233607 | 5.077586 | 0.720168 |
| 81.H | 3.564387 | 4.638246 | 2.787983 |
| 82.H | 7.093782 | 4.095692 | 0.416439 |
| 83.H | -0.10393 | 7.189405 | -4.47262 |
| 84.H | -0.84766 | 8.068558 | -6.65773 |
| 85.H | 2.468827 | 6.12827 | -8.57798 |
| 86.H | 5.84046 | 4.085477 | -6.38227 |
| 87.H | 5.116246 | 2.934044 | -5.17753 |
| 88.H | 6.598291 | 5.545448 | -4.55515 |
| 89.H | 7.129489 | 3.87552 | -4.11161 |
| 90.H | 3.023492 | 2.945328 | -1.75389 |
| 91.H | 2.024401 | -1.71626 | -8.17307 |
| 92.H | 3.383123 | 2.657563 | -12.7273 |
| 93.H | 3.892447 | 0.518518 | -11.4969 |
| 94.H | 0.138517 | 3.418734 | -10.0052 |
| 95.H | 0.66001 | 1.300357 | -8.79169 |
| 96.H | -0.17583 | -1.44752 | -1.43893 |
| 97.H | 2.564894 | -0.29943 | 0.11148 |
| 98.H | 4.108292 | 0.346398 | 1.962759 |
| 99.H | 0.893879 | -0.05674 | 4.787997 |
| 100.H | -0.65105 | -0.72742 | 2.913311 |
| 101.H | 7.047206 | 4.232872 | -1.89444 |
| 102.H | 4.019066 | 4.90683 | -7.36307 |

Acknowledgements

This is the part of my thesis that I've looked forward to writing the most. There are an abundance of people that have helped me get through grad school. To start, my first few years were shaped by the friendship and advice of more senior members of the lab. Jeff Hirsch, my first bay mate for giving me perspective when I was transitioning into lab. Leng Leng Chng for always giving me synthetic help. Chris Chang for helping me get my bench set up. Adam Veige for always being up for watching hockey and drinking beer. Most of my most entertaining memories from grad school involve Bart Bartlett. Er, enough said. Aetna Wun was always great for girl-talk and restaurant recommendations. Dave Manke, thanks for serving the role of 'crisis counselor' so well for so many years. Steve Reece, it's been good times sharing a bay with you for 5 years, you've provided much needed reason and balance to my life, and for being there whenever I was going through a tough time. Arthur Q. Esswein, thanks for drinks at the B-Side, trips to the Cape, and making sure I always stand corrected. Becky, thanks for being a great listener and an understanding friend. Liz, it's been great playing hockey with you and hanging out in non-chemistry settings. It was so awesome to have the perfect partner-in-crime for so many fun things in labs, conferences, sporting events and out around town. I think the lab will be a lot quieter without the possibility of us being in the same room. DJEmilyM, I'll keep listening to your show, thanks for all the shout-outs, and yummy baked goods. I'm really glad I got to know you since we only overlapped a year. Tim, your drawings are awesome, and I'll keep checking your site out for new stuff and t-shirts. Montana, good luck with everything- thanks for the music on itunes. To my classmates- the other members of J-Crew- Justin, master of prank emails/phone calls, Joel, who kept me updated on all that was new and happening in Mets baseball. Julien, I owe a lot to you- you were encouraging when I was down, patient when explaining the complicated, and always willing to spend your time to help me with both my computational and laboratory experiments, and helping me get ready for exams and orals. The postdocs have always been a great crowd in our lab; Jake (squeaky) Soper and the laugh (which we changed), Nils Damrauer, the angry vegetarian (by the way, I am very proud that the infamous GRC video was filmed on my camera), Preston Snee and the inappropriate comments. Um, Grohol, for all the great stories; birthdays haven't been the same since you left. Thomas, for the always willing to discuss all things computational with me. Shih-yuan Liu- you, taught me a lot about how to do synthesis and methodical science. Ted Betley, I'll miss the singing and the maniacal laughter. Matt Kanan, I don't think I've ever met someone as good at distilling matters into just the facts. Dino Villagram, thanks for the \$5 when Cal beat A&M and the good chemistry gossip. Matt Shores, you were a mentor to me when I was an undergrad and a grad student, and are still my

favorite person to celebrate the little things in life with a glass of good scotch. Amy Prieto, you were a real beacon of positivity (is that a word?) and I have always appreciate your sound advice and sympathy. We've had some great undergrads in our lab too; although most have been quite memorable, I have to give special thanks to Jillian, Z-Loh, T.D., and H-Loh for contributions scientific (and social).

Of course I need to really thank the person who did the most to shape my graduate school experience and taught me the most about becoming a scientist. Dan, I'll thank you now- even though I forgot to in my fourth year talk. You really look out for your graduate students and their development as researchers and do everything you can to make sure everyone reaches their full potential. I will always appreciate (and find useful) how much you taught us and involved us in the logistics of doing research, like grant-writing, paper-writing, and giving talks. It's nice to know I'll always have your support and I hope I don't disappoint you (too much).

I also need to thank my undergrad advisor at Berkeley, Prof. Jeff Long- you were the first person to get me really interested in doing research and encouraged me to go to grad school. Knowing that I've have your support has really helped me a lot during the tough times. I've always appreciated your advice and discussions when I am facing cross-roads and making tough decisions in my life and career. I always look forward to seeing you when I get the chance.

Outside of chemistry and MIT I have also had a ton of support. My fellow hockey players; Moz, Pete, Curtis, Ben, Todd, and Josh and the rest of the IM team. Thank goodness for the women's team too! I have never met such an amazing collection of smart, athletic, and otherwise awesome women, I can't name everyone I've played with, but everybody has been great to me and supportive through all the trials of grad school. Alicia and Stos, thanks for dragging me out of Cambridge and the lab once in a while, and being my 'sponsor' on trips to the Cape and all over New England (and all the home cooked dinners too, yum!). I don't think I would have ever gotten into disc, running, skiing, grillin' or biking if it weren't for you guys. Alicia, you are pretty much my role model in life. Kiley, thanks for all the rides and girl talk, and, I'll always have the Kiley-dance on video. Also, for keeping me updated on all the news after I'm gone. Melissa, Elissa, Maryann, Nic, Jennie (Young), Taylor, Valerie, AJ, Hatsy, Michelle, hope to play with you girls again at tournaments. Shuley, thanks for the great sushi recommendations and discussions about the red sox and bruins. Ana you are one of my favorite drinking buddies. Speaking of drinking, thanks to the coaches; Reggie, Super-Dave, Marcel, and Luke. Disc people; well, you've all been tons of fun, especially Wally, Lucy, Mike (one more person I have to thank for rides), Dylan, Karen, Matt, Ciralo, and Luke (again). Dave, you've been involved in the disc, the hockey, *and* the chemistry; thanks for all the big things- support and encouragement throughout- and all the of the little things as well- the rides, watching me play

hockey, teaching me how to ride a bike again, helping me with my taxes, grocery shopping, making me home-brew, and more.

Lastly, I'd like to thank the most important people in my life; my family. To my parents, I can't really give enough thanks or for everything; being supportive, taking care of me, and doing everything they can to ensure a good future for me. I know I can always count on you at every stage of my life. Allis, you always seem to know when to give me a nice supportive call when I am feeling down. Gloria, somehow you never seem to forget an important date or milestone. If only I could be that organized. Thanks for always thinking of me and keeping me updated about all the family comings and goings; it was nice to stay in the loop about what's been going and has made me feel less homesick during grad school. To my niece Katie, you'll be too young to read this for a while, but you've been my 'happy thought' the last few years. Having your baby pics up on my desktop and all over my desk has always made me smile and laugh. Nothing makes me happier than hearing you giggle and call me ai-yi over the phone. To my grandparents- what you went through in your lives and the decisions you made to ensure future generations could have all the opportunities possible (and so that I could be as fortunate as I am today) humbles any achievement that I have ever made, and that I ever will make. My aunts, uncles, cousins, and family friends- everyone has always been so generous to me and welcomed me into their homes and given support; what a great network of people I know I can always rely on.

Biographical Note

The author was born almost three months premature on August 9, 1979 in Northridge, California to Steve and Julia Yang. She was raised in Chatsworth, California with her two older sisters, Gloria and Allis. As a child she took piano lessons and went to Chinese school, but she became passionate about science in high school, where she has many fond memories of spending Saturday mornings in the chemistry laboratory doing experiments. She attended college at the University of California, Berkeley where she was encouraged by her freshman Chemistry teaching assistant to start doing undergraduate research. She had the opportunity to work in a geochemistry laboratory the summer after her freshman year at the Lawrence Berkeley National Laboratory. The following year she entered Professor Jeffrey Long's lab. After an internship at the National Renewable Energy Lab the following summer, she continued to work in the Long lab until she graduated with a B.S. in 2001. The following Fall she entered the Massachusetts Institute of Technology for graduate school, joining the lab of Professor Daniel Nocera. Upon finishing her doctorate, she will be joining Dr. Daniel Dubois at the Pacific Northwest National Laboratory as a postdoctoral associate. She enjoys playing hockey and ultimate frisbee, running, biking, and watching baseball.

Jenny Y Yang

Department of Chemistry
Massachusetts Institute of Technology
Cambridge, MA 02139

Fax: (617) 253-7670
Phone: (617) 281-5844
jyy@mit.edu

EDUCATION & RESEARCH EXPERIENCE

2001 – present **Doctoral Candidate, Inorganic Chemistry, Massachusetts Institute of Technology**

Anticipated Graduation Date: April, 2007
under the direction of Professor Daniel G. Nocera

1997 – 2001 **B.S. College of Chemistry, University of California, Berkeley**
Chemistry

1999 – 2001 **Undergraduate Research Assistant, University of California, Berkeley**
Synthesis of high-nuclearity metal-cyanide clusters and their magnetic and inclusion properties under the direction of Professor Jeffrey R. Long

2000 **Undergraduate Summer Institutes in Applied Science, Lawrence Livermore National Laboratory- Livermore, CA**
Construction and use of single-walled carbon nanotubes as atomic force microscope tips under the direction of Dr. Aleksandr Noy

1999 **Department of Energy Research Undergraduate Laboratory Fellowship, National Renewable Energy Laboratory- Boulder, CO**
Synthesis and characterization of single-walled carbon nanotubes and their reversible hydrogen storage capabilities under the direction of Dr. Michael Heben

1998 **Department of Energy Research Undergraduate Laboratory Fellowship, Lawrence Berkeley National Laboratory- Berkeley, CA**
Sorption of sodium kaolinite clay on the air-water interface under the direction of Dr. Jiamin Wan

TEACHING EXPERIENCE

2000 Teaching Assistant, General Chemistry A, University of California, Berkeley

2001 Teaching Assistant, General Chemistry B, University of California, Berkeley

2001 Graduate Teaching Assistant, Advanced Chemistry Laboratory, Massachusetts Institute of Technology

2002 Graduate Teaching Assistant, General Chemistry Laboratory, Massachusetts Institute of Technology

PUBLICATIONS

“Catalase and Epoxidation Activity of Manganese Salen Complexes Bearing Two Xanthene Scaffolds”, Jenny Y. Yang and Daniel G. Nocera, *J. Am. Chem. Soc.* **2007**, accepted for publication.

“Hangman Salen Platforms Containing Two Xanthene Scaffolds”, Jenny Y Yang, Julien Bachmann, and Daniel G. Nocera, *J. Org. Chem.* **2006**, *71*, 8706-8714.

“Mechanistic Studies of Hangman Salophen-Mediated Activation of O—O Bonds”, Shih-Yuan Liu, Jake D. Soper, Jenny Y. Yang, Elena V. Rybak-Akimova, and Daniel G. Nocera, *Inorg. Chem.* **2006**, *45*, 7572-7574.

“High-Nuclearity Metal-Cyanide Clusters: Synthesis, Magnetic Properties, and Inclusion Behavior of Open-Cage Species Incorporating [(tach)M(CN)₃] (M = Cr, Fe, Co) Complexes”, (*cover article*), Jenny Y. Yang, Matthew P. Shores, Jennifer J. Sokol, Jeffrey R. Long, *Inorg. Chem.* **2003**, *42*, 1403-1419.

PRESENTATIONS

Yang, J. Y.; Nocera, D. G. “Functionalized Manganese Salen Complexes and Their Catalase Activity”, Chemistry Department Seminar Series, National Taiwan Normal University, 2007.

Yang, J. Y.; Nocera, D. G. "Synthesis of Bimetallic Salen Complexes for Oxidation Chemistry" at 232nd ACS National Meeting, San Francisco, CA, 2006.

Yang, J. Y.; Nocera, D. G. "Catalase Activity of Manganese Salen Platforms with Functionalized Xanthene Scaffolds" at Strem Chemicals, Newburyport, MA, *invited*, 2006.

Yang, J. Y.; Nocera, D. G. "Hangman Salens" at 231th ACS National Meeting, Atlanta, GA, 2006.

Yang, J. Y.; Nocera, D. G. "Hangman and Pacman Salens", Chemistry Department Seminar Series, Massachusetts Institute of Technology, 2005.

AWARDS

- | | |
|------------|--|
| 2001 | Presidential Fellowship , Massachusetts Institute of Technology |
| 2000, 2001 | National Science Foundation Graduate Competition, Honorable Mention |
| 2001 | Hypercube Scholar , University of California, Berkeley |
| 2000 | Undergraduate Summer Institutes in Applied Science Scholarship , Lawrence Livermore National Laboratory |
| 1999 | Department of Energy Research Undergraduate Laboratory Fellowship , National Renewable Energy Laboratory |
| 1998 | Department of Energy Research Undergraduate Laboratory Fellowship , Lawrence Berkeley National Laboratory |
| 1997 | Advanced Placement Scholar with Distinction , College Board |
| 1997 | MCI International Scholar , MCI, Inc. |
| 1997 | National Merit Honorary Scholar , National Merit Scholarship Corporation |

PROFESSIONAL AFFILIATIONS

- | | |
|----------------|--|
| 2001 – present | American Chemical Society , division of Inorganic Chemistry |
| 2001 – present | Women In Chemistry , Massachusetts Institute of Technology (Chair, 2002-2003) |
| 2002 – 2004 | Chemistry Graduate Student Council , Massachusetts Institute of Technology |